HAL
open science

Implication des aquaporines dans le fonctionnement hydraulique foliaire in planta

David Lopez

To cite this version:

David Lopez. Implication des aquaporines dans le fonctionnement hydraulique foliaire in planta. Biologie végétale. Université Blaise Pascal - Clermont-Ferrand II, 2012. Français. NNT : 2012CLF22323 . tel-01913507

HAL Id: tel-01913507

https://theses.hal.science/tel-01913507

Submitted on 6 Nov 2018

HAL is a multi-disciplinary open access archive for the deposit and dissemination of scientific research documents, whether they are published or not. The documents may come from teaching and research institutions in France or abroad, or from public or private research centers.

L'archive ouverte pluridisciplinaire **HAL**, est destinée au dépôt et à la diffusion de documents scientifiques de niveau recherche, publiés ou non, émanant des établissements d'enseignement et de recherche français ou étrangers, des laboratoires publics ou privés.

UNIVERSITE BLAISE PASCAL CLERMONT UNIVERSITE

N° D.U. : 2323 Année 2012

Ecole Doctorale Sciences de la vie, Santé, Agronomie, Environnement

N° d'ordre : 598

Thèse

Présentée à l'Université Blaise Pascal Pour l'obtention du grade de

DOCTEUR D'UNIVERSITE

(Spécialité : Physiologie et Biologie Moléculaire Végétales)

Soutenue le 17 décembre 2012

David LOPEZ

IMPLICATION DES AQUAPORINES DANS LE FONCTIONNEMENT HYDRAULIQUE FOLIAIRE *IN PLANTA*

Jury

Rapporteurs :

Dr. Raphaël MORILLON, CIRAD, IVIA, Valence

Dr. Thierry SIMONNEAU, UMR LEPSE-INRA Supagro, Montpellier

Examinateurs :

Pr. Marie-Pascale PRUD'HOMME, UMR 950 EVA, Université CBN, Caen

Pr. Jean-Louis JULIEN, UMR 547 PIAF, Université Blaise Pascal, Aubière (directeur de thèse)

Dr. Jean-Stéphane VENISSE, UMR 547 PIAF, Université Blaise Pascal, Aubière

Dr. Aurélie GOUSSET-DUPONT, UMR 547 PIAF, Université Blaise Pascal, Aubière

Centre de Recherches de Clermont-Ferrand-Theix

Université Blaise Pascal

U.M.R. PIAF

Ce manuscrit de thèse constitue pour moi l'aboutissement mon Cursus Universitaire. Au moment d'écrire ces dernières lignes, je repense au chemin parcouru avec émotion mais j'attends également la suite avec beaucoup d'impatience. D'ailleurs, n'est-ce pas l'attrait de la découverte, de la nouveauté et de l'innovation qui anime les chercheurs ? Ainsi la recherche s'appuie sur l'existant pour générer du progrès ; aussi, il convient de bien savoir d'où nous venons pour savoir ou aller.

Je ne pense pas que je serais là où j'en suis aujourd'hui si je n'avais pas été si bien entouré.

Je dédie cette thèse à mes parents Jean-Paul et Josette LOPEZ, qui m'ont donné la chance de faire des études, ainsi qu'à ma femme Qian WANG, qui a toujours été mon moteur, ma motivation.

Remerciements

A monsieur le Professeur Jean-Louis JULIEN, directeur de ma thèse mais qui bien avant cela, a été mon tout premier professeur à l'Université. Je ressens une grande fierté et beaucoup de reconnaissance à l'idée terminer sous votre direction, des études de biologie entreprises notamment par l'intérêt que vous aviez fait susciter en moi. Merci de m'avoir fait confiance et donné l'opportunité de faire ma thèse au sein de votre laboratoire.

Aux Docteurs Aurélie GOUSSET-DUPONT et Jean-Stéphane VENISSE, mes encadrants bienveillants. La décision de participer à ce sujet de thèse a été largement influencée par le fait que vous l'encadriez. Vous ne m'avez jamais fait défaut, j'espère en avoir fait autant. Sachez que je n'aurais su imaginer un meilleur encadrement que celui que vous m'avez prodigué. J'espère être à mon tour un aussi bon encadrant. Je souhaite également que mon humble contribution à vos travaux vous aura été utile.
Notre collaboration restera parmi les meilleures expériences de ma vie.

A Hervé COCHARD, Erwin DREYER, Bernard GENTY et Christophe MAUREL, membres de mon comité de thèse. Merci pour vos avis éclairés et vos conseils pour orienter au mieux ma thèse. Un grand merci à Christophe MAUREL pour m'avoir invité à l'école thématique sur les aquaporines à Montpellier en 2011 où j'ai eu l'occasion de rencontrer les acteurs actuels et futurs de la recherche sur les aquaporines et d'entamer de nouvelles collaborations.

Je remercie tout spécialement les membres actuels et passés de l'équipe HYDRO, vous m'avez apporté bien souvent votre aide directe mais également transmit votre savoir-faire. Un grand merci à Nicole BRUNEL, qui a beaucoup exercé sa patience avec mes expérirences d'hybridation *in situ*. J'ai trouvé dans l'ensemble des personnels du PIAF, des personnes toujours très disposées à apporter leur aide. Je ne pourrai pas tous les citer, mais je les remercie sincèrement tous. J'estime avoir eu beaucoup de chance de les connaître.

Résumé

Les modèles actuels de changements climatiques prédisent une réduction globale des précipitations, limitant ainsi la disponibilité en eau des plantes et induisant une augmentation de la fréquence des stress hydriques. Un stress hydrique modéré peut conduire à la fermeture des stomates ce qui diminue l'activité photosynthétique des plantes, et dans les cas les plus extrêmes, induit l'embolie du xylème causée par la rupture de la colonne d'eau. Afin de limiter ces effets délétères, les plantes ajustent en permanence leurs résistances hydrauliques. Les feuilles sont considérées comme la principale résistance aux flux d'eau. La compréhension des mécanismes de régulation de la résistance hydraulique foliaire est donc un enjeu fondamental. Parmi les facteurs influençant potentiellement la résistance hydraulique foliaire, les aquaporines (AQPs) pourraient jouer un rôle prépondérant. Les membres de la famille des PIP (Plasma membrane Intrinsic Protein) sont des AQPs agissant comme des pores permettant un passage sélectif de l'eau au travers du plasmalemme. Ce travail visait à caractériser la conductance hydraulique foliaire (K_{leaf} l'inverse de la résistance) et à étudier la contribution potentielle des PIP dans cinq espèces tempérées ainsi que chez l'arbre modèle: le peuplier. Les espèces pionnières ont des valeurs de K_{leaf} élevées, mais l'augmentation de K_{leaf} en réponse à la lumière est beaucoup plus faible que chez les espèces non-pionnières. Chez le Noyer (*Juglans regia*), la lumière bleue est responsable de la plupart de l'augmentation de K_{leaf} et de la modulation transcriptionnelle des PIP. En situation de disponibilité en eau et de lumière non limitante, la K_{leaf} du peuplier augmente au cours de la journée pour atteindre son maximum à midi. Cette augmentation de K_{leaf} se produit simultanément avec la transcription et l'accumulation de protéines PIP en réponse à l'éclairement. Cependant, l'expression des gènes PIP est en partie sous influence d'une régulation endogène circadienne. L'influence des AQPs dans la valeur élevée de K_{leaf} est démontrée par son inhibition en présence d'$HgCl_2$.

Abstract

Climate changes models predict a global reduction of rainfalls hence limiting plants water availability and increase water stress occurrence. A moderate water stress can lead to stomata closure thereby decreasing the plants photosynthetic activity and in extreme cases, xylem embolism due to the water column breakage. In order to limit such detrimental effects, plants permanently adjust their hydraulic resistances. Leaves are considered as the main bottleneck in plants water fluxes, thus understanding leaf resistance to water flux regulation is fundamental. Within known factors that can potentially influence leaf hydraulic resistance, the aquaporins (AQPs) might have a central role. Plasma membrane Intrinsic Protein (PIP) family members are AQPs acting as pores that selectively allow water to flow through cell membranes. This work aimed at characterizing leaf hydraulic conductance (K_{leaf} the inverse of resistance) and investigate the potential contribution of PIPs in five temperate tree species and in tree model: Poplar. Pioneer species have high K_{leaf} values, but the K_{leaf} increase in response to light is much lower than for non-pioneer ones. In walnut (*Juglans regia*) blue light is responsible of most of the K_{leaf} increase and PIP transcript modulation. Under non-limiting light and water availability, poplar leaf hydraulic conductance increases diurnally with a maximum reached at midday. This increase of K_{leaf} occurs in parallel with PIP transcript and protein accumulation in response to high irradiance. PIP gene expression is also under endogenous circadian regulation to some extent. The involvement of AQPs is demonstrated by the reduction of K_{leaf} using $HgCl_2$.

Sommaire

	Page
Liste des abréviations	5
Contexte de l'étude	7
Synthèse bibliographique	11
1. Introduction	12
1.1 Plant-level regulation	13
1.2 Leaf-level regulation	16
2. Leaf hydraulic conductance methodologies	16
2.1 High Pressure Flow Metter (HPFM)	16
2.2 Evaporative Flux Method (EFM)	17
2.3 Rehydration Kinetic Method (RKM)	18
2.4 Vacuum Pump Method (VPM)	18
2.5 Pressure probes	19
2.6 Leaf water status	19
3. Diurnal regulation	21
3.1 Light effect	21
3.2 Circadian regulation	23
4. Physiological implications	24
4.1 Water stress	24
4.2 Water use Efficiency	26
5. ABA and aquaporins, molecular actors of K_{leaf}	27
6. Conclusions and future prospects	31
Objectifs de la thèse	32
Resultats	35
Chapitre 1 : Modulation par la lumière de K_{leaf} et contribution des *PIP1* et des *PIP2* chez cinq espèces d'arbres.	36
Chapitre 2 : Implication des aquaporines dans la conductance hydraulique foliaire chez le peuplier.	53
Discussion générale et perspectives	73
Bibliographie	80
Annexes	108
Annexe 1 : Expression précoce de gènes lors de la stimulation lumineuse de la conductance hydraulique foliaire chez le noyer.	109
Annexe 2 : Les aquaporines XIP chez le peuplier, expansion évolutive, fonctionnalité et régulation en réponse à des facteurs environnementaux.	123
Annexe 3 : Modulation de la survie du bourgeon chez *Populus nigra* en réponse à l'embolie induite par le stress hydrique.	142

Liste des abréviations

A: Assimilation (µmol.m^{-2}.s^{-1})
ABA: Acide abscissique
ADN: Acide désoxyribonucléique
AFLP: Amplified fragment length polymorphism
AQP: Aquaporine
ARF: ADP-ribosylation factor 1
ARN: Acide ribonucléique
ATP: Adenosine triPhosphate
AUX: Auxin response factor-like protein
BLAST: Basic Local Alignment Tool
BSC: Cellule de la gaine périvasculaire
BSE: Extension de la gaine périvasculaire
BTB-Taz: Broad complex, Tramtrack and Bric-a-brac / Transcriptionnal adaptor zing finger
cDNA: ADN complémentaire
***C*leaf**: Capacitance hydraulique de la feuille
***C*root**: Capacitance hydraulique racinaire
***C*stem**: Capacitance hydraulique de la tige
CaBP: Calcium binding protein
CAM: Calmodulin
CDMD: Continuous darkness until midday
CDPK: Ca^{2+}-dependant protein kinase
CIPK: Calcineurin interacting protein kinase
CHX: Cycloheximide
CO_2: Dioxyde de carbone
***d*S**: Substitution synonyme
***d*N**: Substitution non-synonyme
DMSO: Dimethyl sulfoxide
DREB: Dehydration responsive element binding protein
E: Transpiration (µmol.m^{-2}.s^{-1})
EST: Expressed sequence tag
EFM: Evaporative flux method
FAR7: FAR1-related sequence 7
F: Flux (mmol.s^{-1})
***g*s**: Conductance stomatique (µmol.m^{-2}.s^{-1})
H_2O: Eau
HIS: Hybridation *in situ*
$HgCl_2$: Chlorure de mercure
HPFM: High pressure flow meter
HR: Humidité relative (%) ou **RH**
HRP: Horse radish peroxydase
HSP: Heat Shock protein
INRA: Institut Nationala de la Recherche Agronomique
JGI: Join Genom Institute
JTT: Jones-Taylor-Thornton matrix
***K*leaf**: Conductance hydraulique foliaire (µmol.m^{-2}.s^{-1}.MPa^{-1})
***K*root**: Conductance hydraulique racinaire
***K*Plant**: Conductance hydraulique de la plante entière
Kb: kilo base
KDa: kilo Dalton
$LaCl_3$: Chlorure de lanthanum (III)
LA: Leaf area (m^2)
MAPK: Mitogen activated protein kinase
MD: Midday
MIP: Major intrinsic protein
NCBI: National Center for Biotechnology Information
NIP: Nodulin 26-like intrinsic protein
NIRS: Near infrared spectroscopy

Liste des abréviations

ORF: Open reading frame
p: Probabilité
P: Pression (Mpa)
***P*50**: Pression du xylème induisant 50% de perte de conductance
PCR: Polymerase chain reaction
PD: Predawn
PhyML: Phylogeny maximum likelihood
PIAF: Physique et physiologie Intégratives de l'Arbre Fruitier et forestier
PK: Protein kinase
PIP: Plasma membrane intrinsic protein
PLACE: Plant Cis-acting regulatory element
***Ψ*leaf**: Potentiel hydrique foliaire
***Ψ*min**: Potentiel hydrique foliaire minimum ou Ψ_{md}
***Ψ*pd**: Potentiel hydrique foliaire de base
***Ψ*soil**: Potentiel hydrique du sol
RAV: AP2 domain transcription factor
RING: RING-finger copine like protein
RKM: Rehydration kinetic method
ROS: Reactive oxygen species
***R*leaf**: Résistance de la feuille au transport de l'eau
***R*non vascular**: Résistance extra-vasculaire de la feuille au transport de l'eau
***R*vascular**: Résistance vasculaire de la feuille au transport de l'eau
RT-qPCR: Reverse-transcription quantitative PCR
RubisCO: Ribulose 1,5 bisPhosphate carboxylase oxygenase
SE: Standard error
SIP: Small basic intrinsic protein
SYP121: Syntaxin type 121
TDF: Trancripts derivated fragments
TIP: Tonoplast intrinsic protein
VPD: Vapour pressure deficit
UAE: Ultrasound acoustic emission
Ub ligase: Ubiquitine ligase
VAC: Vascular associated cells
VPM: Vacuum pump method
WAK: Wall associated kinase
WRKY: WRKY-type transcription factor
WUE: Water use efficiency
XIP: X intrinsic protein

Contexte de l’étude

L'eau est une ressource essentielle pour les végétaux terrestres qui quotidiennement en libèrent dans l'atmosphère de grandes quantités par transpiration, afin de dissiper l'énergie thermique générée au niveau des feuilles par l'interception de la lumière et permettre simultanément l'entrée du dioxyde de carbone atmosphérique au niveau des stomates. Les plantes terrestres ont des besoins importants de prélèvement d'eau douce afin de maintenir une continuité du flux hydraulique en vue de maintenir une transpiration et une assimilation efficaces tout en évitant une rupture de la colonne d'eau. Paradoxalement, l'eau est également une ressource dont la disponibilité décroit sensiblement. Afin de soutenir le développement des productions forestière et agricole destinée à l'alimentation, il apparaît essentiel d'identifier les mécanismes de régulation des flux hydriques chez les plantes ainsi que ceux responsables de la tolérance au déficit hydrique.

Les travaux entrepris dans le cadre de cette thèse ont été réalisés au sein de l'UMR 547 PIAF « Physique et Physiologie Intégratives de l'Arbre Fruitier et Forestier » INRA-Université Blaise Pascal de Clermont-Ferrand dans l'équipe HYDRO. L'objectif principal de cette équipe est de modéliser l'architecture hydraulique et la tolérance à la sècheresse chez les arbres. L'essentiel de son activité s'organise autour de deux axes :

(i) La vulnérabilité à la cavitation et l'impact de l'embolie du xylème

(ii) L'étude de la conductance hydraulique foliaire et l'implication des aquaporines

L'organisation autour de ces deux axes trouve son origine dans le fait que des travaux antérieurs ont mis en avant un contrôle foliaire (stomatique) de l'embolie du xylème (Cochard *et al.* 1996 et 2002). La conductance hydraulique foliaire, ou la perméabilité de la feuille vis-à-vis de l'eau, apparait comme un élément majeur de la régulation des flux hydrauliques chez les plantes (Sack et Holbrook 2006).

L'étude de la conductance hydraulique foliaire a été initiée il y a environ une dizaine d'années au sein de l'équipe avec pour modèles d'étude le laurier (*Laurus nobilis* L.) et le noyer (*Juglans regia* L.) (Hervé Cochard *et al.* 2002 et 2004). Il a ainsi été mis en évidence une contribution importante du compartiment extravasculaire dans la résistance hydraulique foliaire (l'inverse de la conductance) de ces deux espèces.

L'analyse poussée de la conductance hydraulique foliaire du noyer a permis de démontrer que *(i)* celle ci augmentait en réponse à la lumière, *(ii)* que cette augmentation était indépendante de l'ouverture stomatique, et *(iii)* que cette augmentation était corrélée aux profils d'expression contrastée de deux aquaporines de type PIP2 (*JrPIP2.1* et *JrPIP2.2* Cochard *et al.* 2007) identifiées antéireurement pour leur implication dans la réparation de l'embolie chez cette même espèce (Sakr *et al.* 2003).

Les travaux menés sur la conductance hydraulique foliaire chez le noyer ont été poursuivis dans le cadre de la thèse de Khaoula Ben Bâaziz (2007-2011) à laquelle j'ai participé. Les approches mises en œuvre dans le cadre de sa thèse ont couvert les domaines de la biologie moléculaire et de l'écophysiologie. Dans un premier temps, Ben Bâaziz *et al.* (2012b, **annexe 1**) ont isolé 187 fragments de gènes différentiellement exprimés en réponse à la lumière par cDNA-AFLP (cDNA-amplified fragment length polymorphism). Parmi ces gènes, 93 avaient une fonction putative prédite : certains dans la transduction du signal lié au calcium, différentes kinases dont les WAK (Wall-Associated Kinase), ainsi que des protéines intervenant dans le trafic vésiculaire (Syntaxin 121, ARF1). Comme perspective à ce premier travail, l'utilisation d'inhibiteurs de la voie calcique et du trafic vésiculaire fut proposée afin de valider l'implication des partenaires moléculaires dans la modulation de la conductance foliaire. L'étude des éléments régulateurs des promoteurs des PIP identifiées a également été présentée comme perspective.

Si le noyer est un très bon modèle présentant des réponses de conductance hydraulique foliaire remarquables, l'absence de données génomiques consistantes limite les perspectives à l'échelle moléculaire. De même, des données ont été générées sur d'autres espèces en utilisant des amorces PCR génériques, cependant l'information reste partielle et les mêmes verrous méthodologiques que pour le cas du noyer subsistent. Ainsi, la décision d'orienter nos expériences sur le peuplier a été adoptée car le génôme de cette espèce était séquencé depuis peu et le genre *Populus* était déjà le support de plusieurs thématiques de recherche dans l'équipe HYDRO.

Appartenant à la famille des *Salicaceae,* le genre *Populus* compte environ 35 espèces ainsi que de nombreux hybrides commerciaux et naturels. Les peupliers sont des espèces dioïques et diploïdes (2n=38) à la croissance rapide et bien représentées dans les régions tempérées. Les espèces de peupliers présentent un caractère pionnier avec une préférence écologique pour les ripisylves et les zones humides et lumineuses. La culture du peuplier est

importante en France puisqu'elle représente environ 240 000 ha pour 1,5 millions de m^3 produits par an ; ce qui la place au premier rang européen et au second rang mondial derrière la Chine (Conseil National du peuplier). Le peuplier est une essence majeure utilisée par l'industrie de l'emballage et de la papeterie, et les filières « bois énergie ». Les principaux thèmes des programmes d'amélioration des espèces concernent la productivité et la résistance aux rouilles et aux insectes.

Depuis 2006, le génome de *Populus Trichocarpa* Torr & Gray est disponible, ce qui fait du peuplier le premier arbre séquencé. Choisi pour son petit génome (485 Mb), sa culture et sa multiplication aisées en font un modèle de prédilection pour la plupart des études biologiques menées sur les arbres. Enfin, la transformation génétique du peuplier est possible pour de nombreuses espèces et hybrides, atout majeur pour procéder à de la validation fonctionnelle de gènes candidats.

Les résultats principaux de cette thèse sont exposés en deux chapitres introduits par une synthèse et trois annexes. La synthèse bibliographique est rédigée en langue anglaise car il s'agit d'un projet de revue qui sera prochainement soumis et dont le thème abordé est « la conductance hydraulique foliaire chez les arbres et les ligneux, caractérisation, régulations et rôles». Les aspects méthodologiques ainsi que les rôles physiologiques sont traités et discutés, cependant, certains aspects tels la conductance hydraulique racinaire ou le rôle plus large des aquaporines chez des plantes non ligneuses n'y figurent pas. Ces aspects, trop déconnectés de la thématique de cette revue ne sont traités que dans les introductions des articles. A l'issue de cette synthèse bibliographique, les objectifs de la thèse sont présentés ainsi que les moyens mis en œuvre.

Synthèse bibliographique

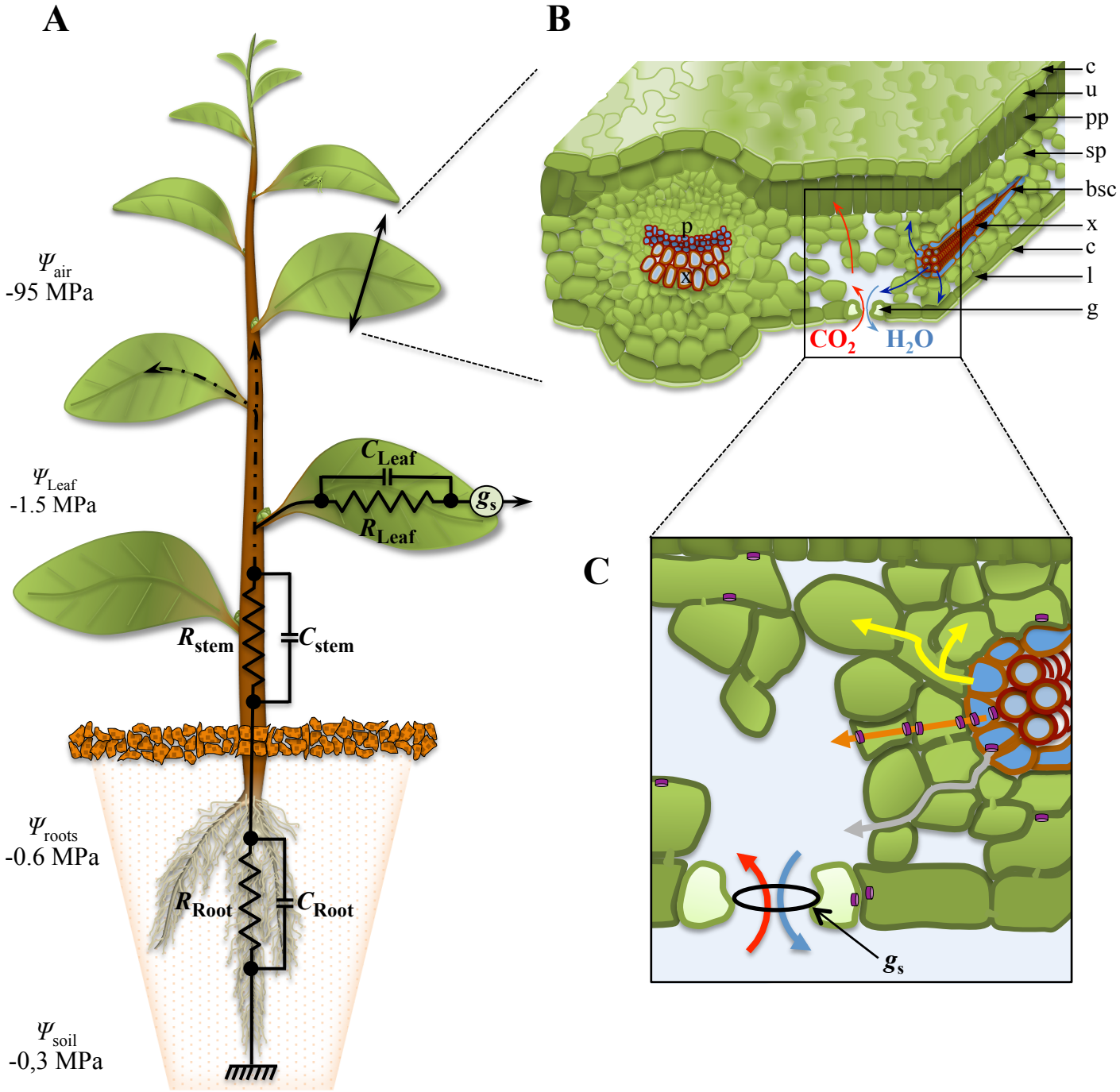

Figure 1 A Whole plant hydraulic resistance symbolized with the electrical analogue as resistances in root (R_{root}), stem (R_{stem}) and leaf (R_{leaf}) acting in series. Organs corresponding capacitances are shown (C_{root}, C_{stem}, C_{leaf}). Water potentials (Ψ) are provided as example to show the water potential gradient within the plant but they can vary greatly. Stomatal conductance (g_s) constricts gaz exchange . **B** Leaf cross section showing the midrib stomatal cavity and lateral vein. Gaz exchanges are shown in and out the stomata. **C** Enlarged view of lateral vein composed of xylem vessels (x, red) coated by bundle sheath cells (bsc, brown); c, cuticle; p, phloem; u, upper epidermis, pp, palisade parenchyma; sp, spongy parenchyma; g, guard cell; l, lower epidermis. Radial pathway: water flows through three sub-pathways: **apoplastic (grey)**, where water remains exclusively in extracellular medium; **symplastic (yellow)** where water flows through plasmodesma and transmembrane **(orange)**, where water crosses plasmalemma *via* aquaporins (▭).

Leaf Hydraulics: Methodologies, Characterization, Regulation and Relevance in Physiology of Tree and Woody Species

1. Introduction

Leaf hydraulic conductance is a relevant trait for the study of plants water use efficiency for well-watered and water-stressed plants. Water flows through plants from roots to leaves where molecules evaporate driven by transpiration and water potential gradients (Figure 1A). Organs oppose a variable resistance to water flow in order to prevent detrimental effects of excessive water loss *i.e.* xylem embolism, and leaf abscission. Plants hence operate a tight control over the resistance of roots, stem and leaves to maintain the organism integrity (Passioura 1984). The difficulty of studying plant-water relations relies in the fact that the components operating regulation are interdependent but also responsive to virtually all environmental conditions (*e.g.* temperature, light, air relative humidity, soil water content) and endogenous signals (*e.g.* hormones, growth, senescence, root-shoot signalling, circadian rhythm), all interacting together and some in opposite ways (Sack and Holbrook 2006). With the root system, leaves are widely considered as the two main bottlenecks in water flows. Moreover, leaf hydraulic conductance could be a determinant for gas exchange capacity by playing a role in its regulation. This review paper addresses the contribution of leaves to the overall water resistance in woody and tree species. Current knowledge, recent advances in the field and state of the art of molecular level regulation actors are summarized. Technical aspects of the different methodologies to measure leaf hydraulic conductance and water potential are herein detailed. Xylem embolism characterisation methods are mentioned since it was shown to negatively impact leaf hydraulic conductance.

1.1 Plant-level regulation

The electrical analogue of water flow in plants proposed by Cowan (1972), describes how the plant hydraulic architecture responding to atmospheric parameters can be modelled as roots, stem and leaves acting as resistors in series (Figure 1). This model received substantial support from physiological studies over the decades and the concept is now widely accepted. The resistance opposed by an organ to water flow (R) and its inverse, the conductance (K=1/R) are interchangeable terms, both being commonly used to describe water transport efficiency. Plant hydraulic conductivity (K_{plant}) can be easily calculated as the ratio of water loss by transpiration (E, mmol.m^{-2}.s^{-1}) by the water potential difference between the

soil and the leaves ($\Delta\psi = \psi_{soil} - \psi_{leaf}$, Mpa). E is a function of stomatal conductance to water vapour (g_s mmol. $m^{-2}.s^{-1}$) and vapour pressure deficit between leaves and air (VPD)

$$E = g_s \times \text{VPD}$$

$$K_{plant} = E/\Delta\psi$$

Plant resistance to water flow, as an analogue of Ohm's law, is the sum of resistance developed by roots, stem and leaves. Corresponding conductance in roots (K_{root}, also K_r, Lp or Lp$_r$ in some studies) stem (K_{stem}, K_s) and leaves (K_{leaf}, K_l, L or H are aliases) can be measured. Characterization of the aerial parts contribution to overall conductance led to different scenarii where the ratio of shoot-root resistances depends on the species (Tyree *et al.* 1993a, Nardini and Tyree 1999, Matzner and Comstock 2001). For species having a dominant contribution of shoot to overall resistance, leaves are a key component of water flux regulation. Shoot resistance has been subject to further dissection showing a gradient of increasing resistances from stem to leaves, with petioles having intermediate values (Tyree *et al.* 1993b, Yang and Tyree 1993). This distribution of resistances correlated with the compartment's xylem vulnerability to cavitation (Tyree *et al.* 1994, Tsuda and Tyree 1997), was thought to be a plant safety mechanism leading to the hydraulic segmentation theory. Like roots, leaves constitute a bottleneck for water fluxes and should be considered as important regulators of K_{plant} regardless of the root/shoot resistance contribution ratio. In hybrid poplar shoots, the stem contribution to the whole hydraulic resistance was shown to be negligible, hence operated by leaves mainly (Fichot *et al.* 2011). Equivalent observation was made on conifer species *Pinus pinaster* (Charra-Vaskou *et al.* 2012). Leaves contribution to whole plant resistance is highly variable between species and can represent up to 98% of the latter (Sack and Holbrook 2006).

1.2 Leaf-level regulation

Axial (vascular) and radial (extra-vascular) pathways ensure water transport between and within plant's organs (Figure 1C and Figure 2). The vascular pathway is ensured by xylem vessels and tracheids and is often associated with low resistance and long distance transport. Whereas the extra-vascular pathway, constricted by tissues downstream of the xylem vasculature is considered as more resistant to water flow (Tyree *et al.* 1999). Water is transported through axial pathway from root tips to leaves *via* stem vessels. In the extra-vascular pathway, water has to flow through living tissues (*i.e.* from roots tips to root vessels and from leaf xylem veins of decreasing order to reach stomatal cavities). Like the root/shoot contribution to plant overall resistance, the contributions of vascular/extra-vascular pathways

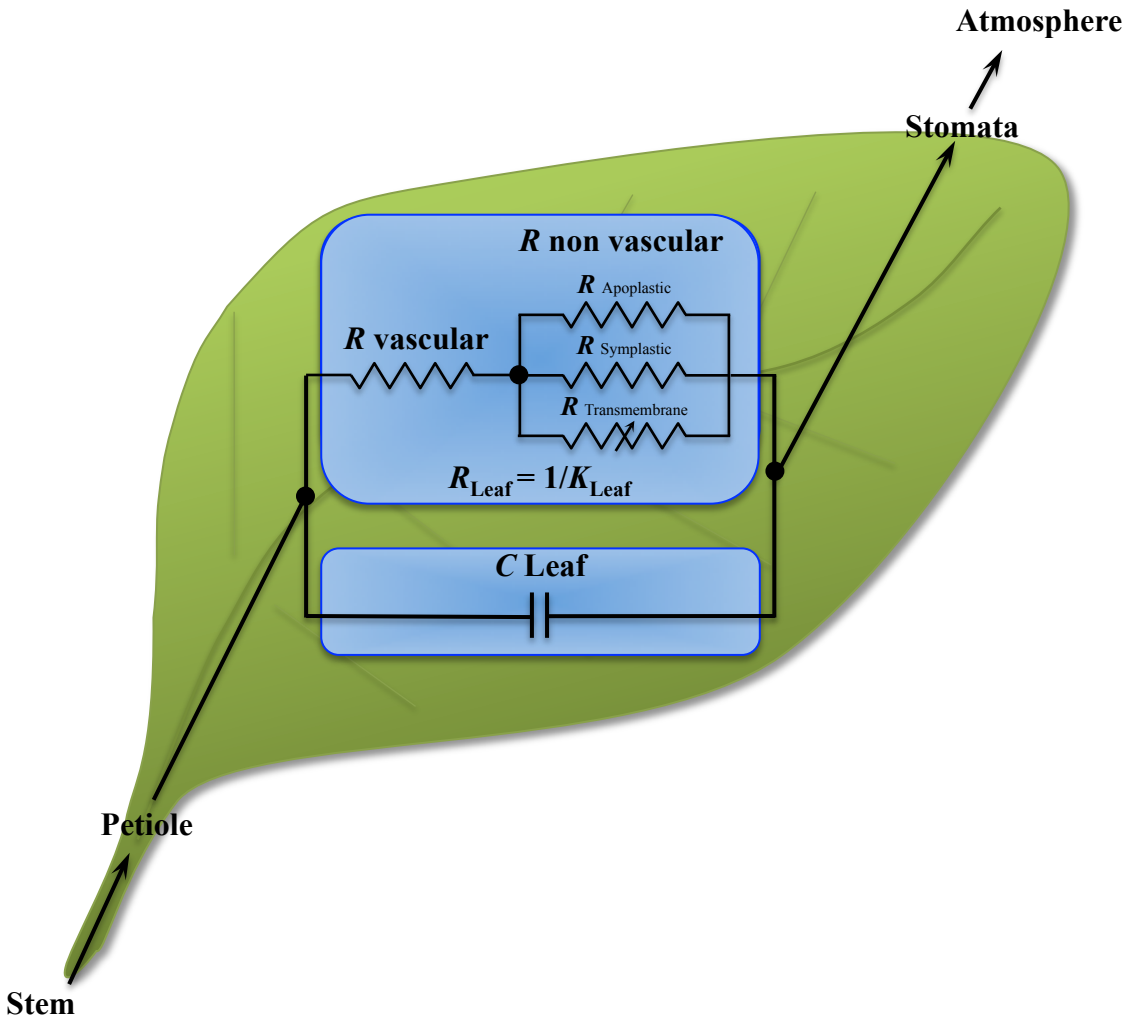

Figure 2 Leaf hydraulic resistance (R_{leaf}=1/K_{leaf}) symbolized with the electrical analogue with vascular and non vascular resistances acting in series. Leaf hydraulic capacitance is represented (C_{leaf}). The non-vascular resistance is further divided into apoplastic ($R_{apoplastic}$), symplasmic ($R_{symplasmic}$) and transmembrane ($R_{transmembrane}$) resistances acting in parallel. $R_{transmembrane}$ is modulated by aquaporins and is represented as a variable resistor.

seem to be dependant of the studied species. Early reports of Tyree and Cheung (1977) pointed the non-vascular pathway as dominant factor of leaf hydraulic resistance in *Fagus grandifolia*. Recent studies addressed the fine characterization of these two components contribution in K_{leaf} of broad leaves and needles. In their *Prunus laurocerasus* study, Nardini and colleagues (2001) showed that even if leaf midrib experienced significant xylem loss of conductivity (70%), whole leaf conductance was affected by only up to 10%. This finding, confirmed by computational simulation evidenced that leaf resistances was not the sum of midrib and leaf blade resistances, in other words, that the resistances did not act in series. The above study also hypothesized on vascular redundancy mechanism to bypass the altered vessels. A dynamic regulation of vascular pathway was shown by extensive severing of bean leaf veins (90%) also showed that the remaining functioning smaller veins had a several fold increase in their transport velocity (Hüve *et al.* 2002). Vein severing experiments further proved that the minor veins had the largest contribution to leaf resistance followed by the downstream tissues (*i.e.* mesophyll) in *Acer saccharum* and *Quercus rubra* (Sack *et al.* 2004).

In *Coffea arabica* leaves, the main resistance resides in the non-vascular pathway (Gasco *et al.* 2004). Nardini *et al.* (2005b) showed that the contribution of vascular and extra-vascular compartments could be an adaptation to the light regime of sun-establishing plants having higher conductance and lower contribution of the vasculature resistance. At the light of their results on *Juglans regia* where most of the resistance was found to be outside of the xylem, Cochard *et al.* (2004a) proposed the K_leaf model where R_{xylem} (vascular resistance) could be considered as negligible. However, Sack *et al.* (2004 and 2005) hypothesize for an approximately equal contribution of vascular and extravascular pathways. It was argued by the authors that chemical and mechanical treatments carried out to remove the extra-vascular resistance (Salleo *et al.* 2003, Trifilo *et al.* 2003, Cochard *et al.* 2004a) lead to an underestimated contribution, because treatments induced new pathways and also because the minor veins contribution was not taken into account. The study of the venation structure could provide an important framework for the dynamics of K_{leaf} (Sack *et al.* 2008, Scoffoni *et al.* 2011). The K_leaf model validity has been expanded by McKown *et al.* (2010) who simulated the behaviour of diverse vasculature structures, their effects on K_{leaf} and the associated cost of construction for the plant. In their comparative study, Zwieniecki *et al.* (2007) proposed three models for the quality of hydraulic connection between the vessels and leaf tissues based on rehydration kinetic profiles and leaf anatomical properties (See. § 2.4). In the studied Gymnosperms (*Gnetum gnemon, Gingko biloba, Metasequoia glyptostroboides, Larix laricina*), the dominance of the low rate phase is hypothesized to be associated with a

discontinuity between xylem vasculature and the rest of the leaf. In the opposite scenario, as observed for *Eucalyptus globulus,* all leaves tissues are thought to be well hydraulically connected to vasculature, with a quasi non-existing slow rate phase. An intermediate situation was observed for *Quercus rubra, Acer rubrum, Populus nigra* and *Lyriodendron tulipifera*. For these species, epidermis and stomata are hydraulically linked to xylem, in favour of hydraulic separation of photosynthetic mesophyll from transpiration stream, which in turn would prevent negative side effects of short scale dehydration on assimilation. The same hypothesis was proposed for sunflower leaves which had a large contribution of the extra-vascular component in R_{leaf} (Trifilo *et al.* 2003). At the light of these results, leaves should be considered as multiple interacting pools of water. This observation was experimentally supported by the existence of the short- and medium-term leaf capacitances, shown to buffer transpiration induced in diverse woody angiosperms (Blackman *et al.* 2011).

While the on-going debate on the contribution of each compartment has lots in common with the previous one for shoot/root contribution to K_{plant}, it is to note that Nardini *et al.* (2010) showed that the partitioning of resistances between vascular and extravascular components in lamina was dynamic across the season in *Aesculus hippocastanum*. Moreover, like K_{root}, K_{leaf} was shown to vary diurnally (see § 3) and the dynamic contributions of the two components can reasonably be expected to vary through the day. A resistive model consistent with the composite model for leaves submitted to dark and light conditions was proposed by Cochard *et al.* (2007). In this model, the vascular pathway supplying water to mesophyll is supposed constant for well-watered plants (Cochard *et al.* 2004a) and the existing water flows through apoplast or enters cell-to-cell pathway through aquaporins. As proposed in the composite transport model, radial pathway is the sum of three sub-pathways occurring in parallel (i) the apoplastic pathway, where water exclusively flows through extracellular compartment (i.e. the apoplast) (ii) the symplasmic pathway where plasmodesma are required to allow water moving from one cell to another and (iii) the transmembrane pathway where transporters are needed for membrane water permeability (*i.e.* aquaporins) (Figure 2). However, the contribution of the radial sub-pathways has still to be completely deciphered, despite substantial efforts to answer that question as initiated by Weatherley (1963) who hypothesized on a dominancy of the extracellular pathway (apoplast) in the leaf water flow. The current view of the regulation of extravascular or radial pathway involves the activity of aquaporins, membrane intrinsic proteins (Gasco *et al.* 2004, Nardini *et al.* 2005a and 2010, Cochard *et al.* 2007, Kim and Steudle 2007, Lovisolo *et al.* 2007, Sellin *et al.* 2008, Voicu *et al.* 2008 and 2009, Ye *et al.* 2008). Zwieniecki *et al.* (2007) also hypothesized that the

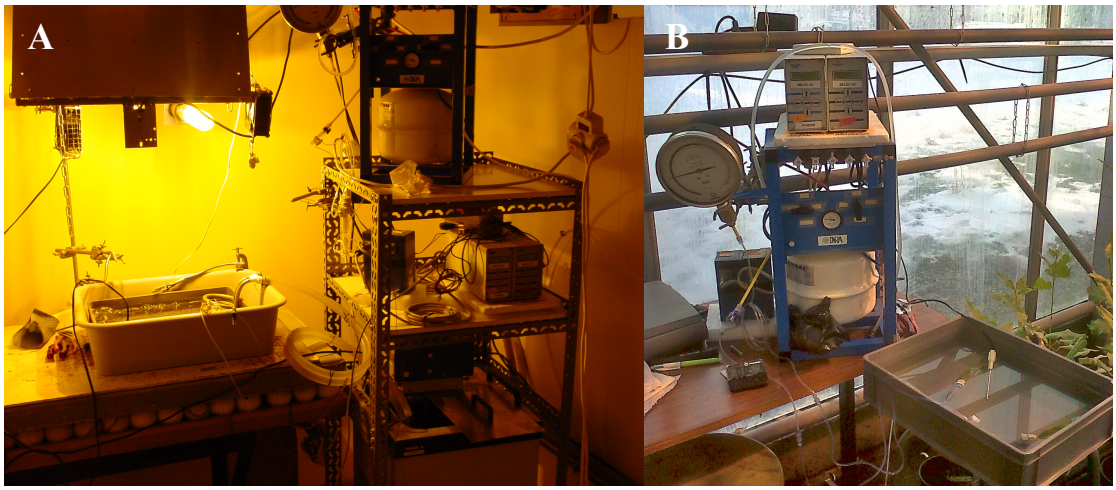

High Pressure Flow Meter (HPFM) en conditions expérimentales contrôlées (A) et en serre (B) Photographies présentées comme support à ce manuscrit mais non présentées dans la revue

involvement of aquaporins and/or plasmodesma could play a role in functional compartmentalisation of extravascular tissues.

2. Leaf hydraulic conductance methodologies

As an introductory remark, it should be noted that the term conductance and conductivities are commonly used interchangeably in the literature. However, conductance refers to a measure of flow rate, divided by the pressure applied while conductivity is equal to the conductance further normalized by the area, length or weight of the conductive sample. In some articles, conductivity can be termed leaf-specific conductivity, implying area normalisation. Leaf hydraulic conductance assessment constitutes itself a challenge since a measurement implies physical alteration of the plant and destruction of the sample. Furthermore, leaf samplings expose xylem vessels to atmospheric pressure likely to induce embolism expansion (Tyree and Sperry 1988), and triggers modification on gas exchange of the remaining leaves as shown in defoliation experiments (Galvez and Tyree 2009, Quentin *et al.* 2012). Above limits in measurements of hydraulic conductivity experiments rose concerns among physiologists about quality, reproducibility and relevance of their measurements. Thus they consistently compared results obtained with different techniques to validate their findings. The different methods developed for hydraulic conductance measurement are herein described and discussed.

2.1 High Pressure Flow Metter (HPFM)

The HPFM developed by Tyree *et al.* (1993a) is to date, the most frequently used method for conductance determination. Briefly, this technique uses a water solution perfused under high pressure (up to 0.5MPa) in leaves or shoots through the petiole or the stem. The sample is immersed in a temperate water bath in order to maintain a constant temperature and to prevent leaf transpiration. Conductance is computed by dividing water flow entering in the sample (F, typically in $mmol.s^{-1}$ but $Kg.h^{-1}$ are also used) by the pressure applied to the water solution (P, Mpa) normalised by leaf area (m^{-2}). The HPFM can be used in quasi-steady state (constant pressure) or in dynamic (transient) mode were the applied pressure varies and conductance is obtained with linear regression of flow rate *versus* pressure. However, conductance measured by the HPFM can be overestimated since it measures resistance to the liquid phase without taking into account water vapour diffusion in intercellular spaces, occurring at limiting rate in the transpiration driven conductance (Tyree *et al.* 1999). Sack *et*

al. (2002) argued against the use of HPFM on branches to determine K_{leaf} instead of using single leaves because of the complexity of shoot hydraulic architecture. In their comparison article, they showed two to five-time greater K_{leaf} values for *Acer rubrum*, *Acer saccharum* and *Quercus rubra* than the ones estimated using whole branches. Ease of use is another aspect for HPFM being widely adopted. A measurement, depending on the required stabilisation time for the studied species, can take only a couple of minutes. In these conditions, it is not unreasonable making numerous measurements through the day, in order to evaluate diurnal variations of conductance for instance. Another possibility offered by the method is the possibility to replace water by other solutions in order to manipulate conductance through its regulators. However, by forcing flows in the sample, native embolism can be displaced making this method unsuitable for such studies in stems, petioles and whole leaves (Cochard *et al.* 2002). Finally, HPFM was successfully used for gene expression investigation after conductance measurement (Cochard *et al.* 2007, Voicu *et al.* 2009, Ben Bâaziz *et al.* 2012b). In Ben Bâaziz *et al.* (2012b), authors showed that up to one hour measurement did not introduce bias in aquaporin gene expression patterns for leaves of four temperate tree species. Despite several studies showing HPFM yielded good K_{leaf} estimates, some concerns were raised on the physiological impact of flooding of the apoplast. Felle (2006) showed apoplast alkalinisation and cytoplasmic acidification induced by anoxia. However, Voicu *et al.* (2009) reported upon leaf irradiance, apoplastic acidification and K_{leaf} increasing. These pH changes are likely to have an effect on aquaporin regulation since their activity is pH sensitive (Luu and Maurel 2005) (See § 5). Modification of the HPFM method, using near atmospheric pressure made possible the determination of xylem embolism using flow meters (XYL'EM, Cochard *et al.* 2002). Notably, the method has been modified by Charra-Vaskou and Mayr (2011) to measure pine needles hydraulic conductance.

2.2 Evaporative Flux Method (EFM)

Unlike HPFM, this technique uses leaf or shoots transpiration as driving force for the water flow (Tsuda and Tyree 2000). The water potential is measured prior to experiment and the sample is connected to hydraulic circuit. Flow is measured with an analytical scale on which the water source is placed or alternatively, using a flow meter (Brodribb and Holbrook 2006). Unlike Vacuum Pump Method (See § 2.4) and HPFM, EFM allows direct readings of the water flow since no equilibration time is required. Additionally, EFM does not modify xylem cavitation, allowing its determination. EFM and HPFM measurements were compared and shown to give similar K_{leaf} for crops (Tsuda and Tyree 2000) and several woody species

(Sack *et al.* 2002, Scoffoni *et al.* 2008, Nardini *et al.* 2010, Ben Bâaziz *et al.* 2012a and b). However the 'light effect' evidenced by HPFM for some species is not measurable with EFM (Cochard *et al.* 2007) but Scoffoni *et al.* (2008) modified the method in order to evaluate maximum K_{leaf} in response to light.

2.3 Rehydration Kinetic Method (RKM)

Developed by Weatherley (1963) in order to investigate which of the apoplast or transmembrane water transport was dominant in leaves and roots, this method is now widely used for conductance determination. Initially, water flow was measured by following the meniscus in a potometer's tubing, which was then replaced by analytic scales. The method requires dehydration of a leaf that is let to rehydrate afterwards. The flow rate is given as the amount of volume of water uptake per time elapsed. Cruziat and colleagues (1980) modified the initially described protocol to become the standard for this type of experiments. The modifications were done to follow rehydration of a fully turgid leaf that experienced drastic dehydration (ψ ~1 MPa) prior to measurement. K_{leaf} is determined as a function of leaf capacitance (C_{leaf}) obtained with pressure-volume curve (Tyree and Hammel 1972), and expressed as a function of the time elapsed (t) between initial and final water potential (ψ_0 and ψ_f) where $K_{leaf}=C_{leaf} \times \ln(\psi_0 / \psi_f)/t$.

The method received substantial technical improvements by Zwieniecki *et al.* (2007) with the development of the 'reverse Polish guillotine' apparatus. Briefly, the method prevents the petiole xylem from free air exposure by having the leaf installed in the apparatus under water while still attached to the stem, in order to accurately measure initial rates of water flow. The kinetic typically gives a two phases plot where the initial phase is a fast uptake that corresponds to the transpiration stream pathway, followed by a low rate uptake representing a high resistance pathway, distinct of transpiration stream pathway (Weatherley 1963). This concept has been expanded by Zwieniecki *et al.* (2007) who proposed three water flow models based on anatomical properties and RKM profiles of a range of Gymnosperm and Angiosperm leaves (See § 1.2). Brodribb and Cochard (2009) further developed the technique by using a flowmeter which enabled measuring maximum water flow.

2.4 Vacuum Pump Method (VPM)

Developed by Kolb *et al.* (1996) for measuring root and shoot hydraulic conductance, VPM is also suitable for embolism determination when the pulling-tension does not exceed the organ water potential (Salleo *et al.* 2001, Trifilo *et al.* 2003). This method has been

successfully used to measure large samples and root systems (Nardini *et al.* 2001). The vacuum pump method gives a measure of the water flow through a sample using adjustable suction. The water flow is obtained similarly with a scale or flow meter. VPM has common characteristics with EFM and HPFM. Unlike HPFM and as EFM, water is pulled out of the leaf. The vacuum operates a quantifiable driving force and water flow is obtained by doing linear regression of flow *versus* pressure, like HPFM. The vacuum generating a greater driving force than transpiration, as HPFM it is likely that airspaces would also be flooded. However, airspace flooding was not observed in a methodological comparison (Sack *et al.* 2002). VPM has received modifications in order to evaluate xylem cavitation using fluorescein dye followed by microscopic imaging (Salleo *et al.* 2001, Trifilo *et al.* 2003).

2.5 Pressure probes

Cell pressure probes allow measuring ψ directly in the leaf xylem or mesophyll cell (Zimmermann *et al.* 1994, Tomos and Leigh, 1999, Kim and Steudle 2007 and 2009, for technical considerations, see Wei *et al.* 2001). Besides water potential, cell and xylem pressure probes can measure cell turgor, elastic volumetric modulus and half-times of pressure relaxations from which cell osmotic hydraulic conductivity can be deduced. Cell pressure-probe studies have permitted to show that *Zea mays* leaf cell hydraulic conductivity increased at low levels of light, and was inhibited with high irradiance levels, potentially related to an aquaporin-mediated water transport inhibition (Kim and Steudle 2007 and 2009). Quite recently, stomatal response of wild type and mutated *Arabidopsis thaliana* was dissected using a newly developed pressure probe method (Ache *et al.* 2010). Unlike cell and xylem pressure probes, this new non-invasive method based on patch-clamp allowed recordings for several days (Zimmerman *et al.* 2008). Unlike the previous pressure probe method, this one is claimed to be compatible with field measurements.

2.6 Leaf water status assessment methods

Water potential

Scholander-type pressure chambers are extensively used for water potential measurement and can be used in the field very efficiently (Scholander *et al.* 1965). Measurements give a good prediction of leaf water potential considering (i) the apoplastic osmotic pressure in xylem is negligible and (ii) the estimated hydrostatic pressure being the average ψ between symplast and apoplast at equilibrium (Lovisolo and Tramontini, 2010). However, some physiological concerns regarding the method have been raised (Tyree 1999).

Advances in water potential determination allow non-destructive and accurate measurements, but are not always compatible with field experiments and less time-efficient than pressure chambers.

The use of micropsychrometer in plant physiology is not recent (Boyer 1968) but currently regains attention for fine dissection of leaf hydraulics allowed by readings of *in situ* water potentials at different leaf locations (Matzner and Comstock 2001,Tyree *et al.* 2003).
Near Infrared Spectroscopy (NIRS) is a technique recently developed to evaluate water potential on grapevine (De Bei *et al.* 2011). NIRS requires proper calibration, but then rapidly predicts water potential values without the need of leaf sacrifice. NIRS is currently tested as an alternative method to estimate xylem cavitation. Another non-destructive method was recently proposed to estimate water status based on high resolution thermal imaging (Möller *et al.* 2007, Alchanatis *et al.* 2010) but these methods requires specific information technology skills to accurately use the model in order to yield good estimates of water status.

Xylem embolism determination

Xylem embolism was shown to produce ultrasound acoustic emissions (UAEs, Tyree and Dixon 1983). By measuring the number of UAEs estimated on a range of water potentials during dehydration, as for stems, one can evaluate the extent of cavitation occurring in leaf xylem and construct vulnerability curves (Kikuta *et al.* 1997, Salleo *et al.* 2001, Nardini *et al.* 2001, Charra-Vaskou *et al.* 2012). For a range of tree leaves from different habitats, the cumulative number of UAE (cUAE) is in good agreement with leaf cavitation: a linear relationship between cUAE and the loss of hydraulic conductance was found in the above studies. The setup for UAE measurement is still expensive, however this method proved to be very reliable and especially useful when pressure-based methods failed (Charra-Vaskou *et al.* 2012). Visual methods for estimating leaf water status have rapidly spread during the course of the last decade. Firstly, Cryo-scanning electron microscopy (Cryo-SEM) allows visualizing the embolized vessels, which appear empty in contrast with sap-filled ones (Cochard *et al.* 2000, Tyree and Cochard 2003, Cochard *et al.* 2004b, Mayr *et al.* 2007, Johnson *et al.* 2009b, Charra-Vaskou *et al.* 2012). Observations of embolized vessels of leaf tissues were supported by measures of the cavitation extent by methodologies classically used. The non-invasive method developed by Sapozhnikova *et al.* (2004) based on optical coherence tomography (OCM or OCT) allowed visualisation of leaf dehydration and rehydration dynamics with observable changes in size of individual cells. Authors showed that changes of parenchyma cells size accounted for the 80% of leaf water lost, which was reversed 40 minutes after re-

watering. Great improvements in our understanding of leaf radial water transport can be expected from the newly developed time of flight-secondary ion mass spectrometry (Tof-SIMS) cryo-system (Iijima *et al.* 2011). Using this high-resolution technique (1.8 µm), authors were able to track the movements of labelled water molecules between vessels, phloem, cambium and cortex.

First evidences of xylem embolism and recovery obtained on intact grapevine plants, were made possible by magnetic resonance imaging (MRI) on stem (Holbrook *et al.* 2001). In contrast with MRI method which makes 'slice' imaging of the sample, three dimensional X-Ray tomography enables to view a whole needle in three dimensions many times during dehydration with no cutting or treatment (Charra-Vaskou *et al.* 2012).

3. Diurnal regulation

Leaf hydraulic conductance was shown to vary seasonally (Aasamaa *et al.* 2005, Sellin and Kupper 2007, Domec *et al.* 2009, Nardini *et al.* 2010, Voicu and Zwiazek. 2011) and also in response to numerous endogenous and environmental signals. However, this review focuses on light induced and diurnal variations of K_{leaf}. Leaf hydraulic conductance and its impact on water use efficiency and plant physiology under water stress is further detailed in § 4.

3.1 Light effect

Early study conducted on sunflower leaves showed that they responded to light by dynamically adjusting their water conductivity (Boyer 1974). More recently, the number of experimental evidences of K_{leaf} increase in response to light substantially accumulated for various tree species with the help of HPFM (Sack *et al.* 2002, Tyree *et al.* 2005, Cochard *et al.* 2004a and 2007, Voicu *et al.* 2008, 2009, Sellin *et al.* 2008 and 2012, Ben Bâaziz *et al.* 2012a). The light intensity but also its quality (*i.e* wavelengths) were shown to induce specific K_{leaf} increasing (Voicu *et al.* 2008, Ben Bâaziz *et al.* 2012a). Voicu *et al.* (2008) also showed that the light effect relied on aquaporins to some extent, using $HgCl_2$, an aquaporin inhibitor. This light response was confirmed by EFM and RKM, described in § 2.2 and 2.3 (Scoffoni *et al.* 2008). After compiling all available data Scoffoni *et al.* (2008) also showed the light effect was greater for heterobaric species, the ones having bundle sheath extension (BSE) present in leaves. While BSE could play a role in the access of the mesophyll to light, Zwieniecki *et al.* (2007) hypothesized for a hydraulic link between BSEs and epidermis, stomata and

mesophyll. Among the potential actors of this increase, mesophyll was thought to play a greater role than vasculature in most studies. However, the hypothesis of a light effect on leaf conductance was recently challenged by Rockwell *et al.* (2011) who argued that *Q. rubra* leaf tissue was insensitive to light and that response was downstream of mesophyll, potentially through stomatal constriction. It was issued assuming that if aquaporins were involved in the irradiance response, a stronger effect would be expected for leaves having a dominant contribution of the extravascular pathway in K_{leaf} (Tyree *et al.* 2005, Lo Gullo *et al.* 2005). Using $HgCl_2$, the cell-to-cell pathway was shown to be responsible of the difference between light and dark values of K_{leaf} (Nardini *et al.* 2005a, Cochard *et al.* 2007, Sellin *et al.* 2008, Lopez *et al.* unpublished). Inhibitory experiments further pointed out a predominant role for transcription and translation of aquaporin genes in the light effect (Cochard *et al.* 2007). An increase in irradiance is associated with an increase in temperature at the leaf level. Temperature is also a relevant parameter affecting leaf conductance regulation (Matzner and Comstock 2001). Viscosity of water being increased by low temperatures and decreased by high ones, the high temperatures can account for a part of leaf water permeability modulation (Cochard *et al.* 2007). A very recent study of Way *et al.* (2012) conducted on trembling aspen seedlings submitted to a 5°C increase in ambient temperature showed a 30% increase in K_{leaf} as compared to normal temperature. Horse chestnut leaves showed a greater K_{leaf} response to temperature than expected by only a change in water viscosity (Nardini *et al.* 2010). Similarly, Sellin and Kupper (2007) showed the temperature dependant increasing in K_{leaf} in response to light accounted for only a part of the response but at least some of the response was due to changes in protoplast permeability.

Finally, K_{leaf} is a physiological trait related to the ecology of the species, in relation with water and light availability (Tyree *et al.* 1999, Brodribb *et al.* 2005, Brodribb and Holbrook 2006, Nardini *et al.* 2005a and b, Sack *et al.* 2005). *Betula pendula* leaves exposed to the sun exhibited higher values than the shaded ones (Sellin *et al.* 2008 and 2012). Relatively high values of leaf specific conductance were found for eight *P. euramericana* hybrids (Fichot *et al.* 2011); this result was associated with the pioneer behaviour of the species (Tyree *et al.* 1998, Nardini *et al.* 2005b). The light regime influence on K_{leaf} was studied in rainforest tree species, showing a significantly greater K_{leaf} for sun-establishing species than for shade-establishing ones (Sack *et al.* 2005). However, the distribution of within-leaf resistances was assessed in the same study and showed sun-establishing species had a greater contribution of xylem resistance, potentially to cope with higher fluxes and prevent xylem embolism.

3.2 Circadian regulation

Diurnal behaviours of K_{leaf} dynamics have been increasingly reported during the last decade with two trends observed, a diurnal increase or decrease. This valuable observation raises some concerns against studies comparing K_{leaf} values between species or the values obtained in response to various treatments without taking into account endogenous variability of K_{leaf}.

Diurnal increase

K_{leaf} has been shown to increase during the day concomitantly to a higher transpiration demand (Tusda and Tyree 2000, Tyree *et al.* 2005, Lo Gullo *et al.* 2005, Nardini *et al.* 2005a, Voicu and Zwiazeck 2011, Lopez *et al.* unpublished). Lo Gullo *et al.* (2005) showed for only two out the four studied species: *Aleuites moluccana* and *Platanus orientalis*, an increase of K_{leaf} with a maximum reached near midday followed by an afternoon decline. As hypothesized by Tsuda and Tyree (2000), this response could be observed under high evaporative demand if the water availability is not limiting. It was observed in the case of *A. moluccana* and *P. orientalis* where ψ_{leaf} did not show a marked drop, by contrast with the species that showed diurnal K_{leaf} decrease. Diurnal K_{leaf} increase is in agreement with the 'light effect' on leaf hydraulic conductance observed for detached leaves. The hypothesis of the involvement of aquaporins in the light response was shown in *Populus trichocarpa* and *Populus nigra* clones, both showing patterns of aquaporin transcripts and proteins concomitantly with diurnal increase of K_{leaf} (Lopez *et al.* unpublished).

Diurnal decrease

Diurnal K_{leaf} decrease can be easily understood as a typical response of the leaf to dehydration experienced with midday pressure drop as observed for stomatal conductance (Aasamaa *et al.* 2005, Silim *et al.* 2009, Johnson *et al*. 2009a and b, Almeida-Rodriguez *et al.* 2010).

Diurnal cycles of midday depression of K_{leaf}, g_s and CO_2 assimilation rate were reported in the tropical tree species *Simarouba glauca* (Brodribb and Holbrook, 2004). Nevertheless, the decline of leaf hydraulic conductance was hypothesized to find its origins in xylem embolism or in conduits deformation consistent with rapid recovery upon rehydration as observed in pine needles (Cochard *et al.* 2004b). The phenomenon of diurnal depression could be underestimated since this potential cause of decline could be masked in some studies

where measurements are carried out on fully hydrated leaves, or because of the use of techniques that refills embolized vessels (Brodribb and Holbrook 2006). Lo Gullo *et al.* (2005) showed diurnal decrease of K_{leaf} for *Persea americana* and *Quercus rubra* associated with ψ_{leaf} drops. Johnson *et al.* (2009a) showed two types of responses: (i) *Quercus garryana* and *Arbustus menziesii* K_{leaf} remained steady through the day and (ii) *Pseudotsuga menziesii* and *Pinus ponderosa* K_{leaf} decreased following ψ_{leaf} with a minimum reached at midday. The authors hypothesized the two responses are underlying two different strategies: maintaining constant K_{leaf} or loss of conductivity followed by its active recovery. Very recently, Yang *et al.* (2012) observed a similar diurnal decrease in K_{leaf} for *Sinarundinaria nitida*, a bamboo species. The authors interpreted the high leaf xylem vulnerability to embolism and the diurnal inhibition of leaf conductance as a part of the plant's strategy to prevent stem xylem embolism due to excessive tensions. Authors further hypothesized that the positive night root pressure would be responsible of leaf vessels refilling.

4. Physiological implications

4.1 Water stress

Water deficit impact on plant physiology has been the subject of a tremendous amount of scientific studies. Water deficit negatively impacts the biomass production and can ultimately compromise the tree survival, with greater effects expected for seedlings (Vilagrosa *et al.* 2003, Brodribb and Cochard 2009, Blackman *et al.* 2009, Allen *et al.* 2010). The K_{leaf} response to dehydration, soil water stress and high evaporative demand has been assessed in a wide range of plant species. To maintain stomata open and in turn allow gas exchange under high transpiration rates, a plant should maintain its hydraulic conductance high enough to prevent leaves from desiccation (Aasamaa *et al.* 2002, Nardini and Salleo 2000, Tyree *et al.* 2005). Stomatal conductance and K_{leaf} were reported to be inhibited with decreasing leaf water potentials in tree and woody species (Bond and Kavanagh 1999, Nardini *et al.* 2001, Salleo *et al.* 2001, Cochard *et al.* 2002, Brodribb and Holbrook 2006, Blackman *et al.* 2009). As for stem vulnerability curves, leaves are characterized by a threshold ψ below which K_{leaf} begins to decrease. ψ_{leaf} at $K_{leaf} = 0$ is either superior or equal to ψ at cell turgor loss point (Brodribb and Holbrook 2003 and 2006, Blackman *et al.* 2009). With contrast to linear ones, sigmoid responses to decreasing water potential show the existence of mechanisms which function was to maintain maximum K_{leaf} until a threshold potential ψ (Trifilo *et al.* 2003, Salleo *et al.* 2003, Brodribb and Holbrook 2003 and 2006, Bucci *et al.*

2012). After this threshold is reached, K_{leaf} decreases rapidly, potentially because of leaf xylem cavitation. *P50* defines the ψ value of a 50% maximal conductance decrease. $P50_{leaf}$ is an indicator of plants ability to maintain K_{leaf} in a range of water potential and thus indicate leaf resistance to water stress (Brodribb and Holbrook 2003, Blackman *et al.* 2010). Examining commercial soybean genotypes, Sinclair *et al.* (2008) showed that K_{leaf} was limited under high evaporative demand to prevent excessive dehydration, which could be a part of the plants drought tolerance strategy. Recently, *Pinus pinaster* needles were shown to have a more vulnerable extravascular than vascular pathway having an overall $P50_{needle}$ value less negative to the one estimated for xylem only (Charra-Vaskou *et al.* 2012). Low needle conductance and extravascular tissue vulnerability suggested to behave as an hydraulic fuse and were suggested to be a part of the plants strategy to prevent stem xylem embolism; which is consistent with the greater hydraulic safety margins attributed to conifers (Johnson *et al.* 2009a and 2012).

Maximum hydraulic safety, correlated to high xylem resistance to cavitation, has however a negative counterpart being the maximum permissible water extraction, which will in turn impact the amount of water lost by transpiration (Sperry *et al.* 2002). The cost and trade-offs associated with increasing xylem and mesophyll safety (lignin content) to prevent their collapse have been modelled (Hacke *et al.* 2001, McKown *et al.* 2010, Simonin *et al.* 2012, Nardini *et al.* 2012). However, it seems not to be the case of finest veins which were shown to loose conductivity at water potentials diurnally experienced by well-watered plants (Salleo *et al.* 2001, Trifilo *et al.* 2003) and would probably only play a role under low evaporation condition (Brodribb and Holbrook 2006). Loss of xylem conductivities could decrease ψ_{leaf} and K_{leaf} locally within the leaf tissue without significant change in bulk ψ_{leaf}, promoting a signal to stomata (Trifilo *et al.* 2003, Nardini and Salleo 2000, Lo Gullo *et al.* 2005, Tyree *et al.* 2005). This hypothesis is consistent with the hydraulic compartmentalisation of parenchyma with transpiration stream by having a preferential link between vessels, epidermis and stomata as proposed by Zwieniecki *et al.* (2007), received experimental support showing the involvement of aquaporins in this hydraulic continuum (Ye *et al.* 2008).

If xylem loss of conductivity in response to water stress has been the subject of a substantial amount of studies, effects on the extra-vascular compartment are less documented, but can also be expected. The linear relation between ψ_{leaf} and K_{leaf}, or the lack of sensitivity of K_{leaf} to vessel embolism suggest a dominance of the extravascular pathway in leaf resistance (Trifilo *et al.* 2003, Brodribb and Holbrook 2004 and 2006). Interestingly, water

stress effects on the leaf symplast showed that membrane stability was better at lower water potentials for *Quercus coccifera* than for *Pistacia lentiscus* suggesting that leaf symplast participates in drought tolerance and survival strategy (Vilagrosa *et al.* 2010). However, if the authors showed good relations between xylem resistance to cavitation and leaf symplast resistance, they did not measure K_{leaf} in their trees in relation with this trait.

Several studies have addressed the role of leaf aquaporins in the leaf response to water stress (Martre *et al.* 2002, Tsuchihira *et al.* 2010, Almeida-Rodriguez *et al.* 2010, Perrone *et al.* 2012, Pou *et al.* 2012). The transcription patterns of *PIP* aquaporins in leaves of two poplar clones submitted to drought stress were hypothesized to relate the different drought resistance strategies (Almeida-Rodriguez *et al.* 2010). However, the authors evaluated stomatal conductance to water vapour (g_s) but not K_{leaf}. Tsuchihira *et al.* (2010), showed a positive correlation between leaf PIP protein amount and the drought resistance for 19 wild provenances of *Eucalyptus camaldulensis*. In their poplar study, Larchevêque *et al.* (2011) showed that upon water stress, the crossing parent *Populus balsamifera* had higher rates of gas exchange and K_{leaf} than two hybrids (*P. balsamifera* x *P trichocarpa* and *P. balsamifera* x *P. maximowiczii*). While the crossing parent however experienced leaf shedding in response to water stress and slower recovery after re-watering. Very recently, Pou *et al.* (2012) showed a 30% reduction of K_{leaf} in response to drought for grapevine. The authors observed correlation with aquaporin expression patterns and K_{leaf} and g_s in their water stress treatment and concluded for a greater role of apoplastic pathway during water stress.

If the study of water stress effects plants greatly is valuable, it appears also extremely relevant to assess recovery effects during and after re-watering which can involve K_{leaf} (Blackman *et al.* 2009).

4.2 Water Use Efficiency

Leaf conductance to water has received substantial support, in part because of the link between hydraulics, gas exchange and CO_2 assimilation. Water Use Efficiency, is a widely accepted index of plant performance. Instantaneous water use efficiency (WUE_i, $mmol.mol^{-1}$) is obtained by the ratio of net CO_2 assimilation (A) by stomatal conductance g_s:

$$WUE_i = A / g_s$$

A time integrated WUE (Δ) can be estimated from carbon isotopic discrimination with mass spectrometry. The performance of a plant hence depends on its capacity to maximize its photosynthetic activity while regulating tightly water transport (Wong *et al.* 1979). Using chlorophyll fluorescence, Brodribb and Field (2010) showed strong relations between

photosynthetic capacity and shoot hydraulic conductance in 22 woody species. Photosynthetic capacity has been further linked to leaf hydraulic capacity in a wide range of land plants (ferns, conifers, and Angiosperms) (Sober 1997, Tyree 2003, Brodribb *et al.* 2005, Brodribb and Holbrook 2006). Across a range of species, maximum K_{leaf} correlates strongly with maximum CO_2 assimilation rate (Brodribb *et al.* 2005). The authors showed a relation between K_{leaf} and A, which was not linear but exponential with a plateau reached for K_{leaf} values above 10 $mmol.m^{-2}.s^{-1}.MPa^{-1}$; but high K_{leaf} is not synonym of correspondingly high assimilation. But high K_{leaf} usually associated with high g_s values, will likely benefit higher internal CO_2 concentrations and carboxylation efficiencies (Brodribb *et al.* 2005). As suggested by Zwieniecki *et al.* (2007), the hydraulic design is a determinant of photosynthetic performance, in part because species with high photosynthetic rates typically operate with small hydraulic margins. This hypothesis has received recent support by Brodribb *et al.* (2007) who showed venation and other leaf traits (thickness, shape) were correlated with K_{leaf} and maximum photosynthetic rate between 43 species. Holloway-Phillips and Brodribb (2010) further correlated maximal WUE with minimal hydraulic safety in ray-grass. Moreover, Sinclair *et al.* (2008) identified that reduced K_{leaf} at midday evaporative demand was preventing excessive water loss and hence driving upward the WUE. Contrastingly, at the interspecific level, no significant correlation was found between K_{leaf} and A or WUE in eight *P. euramericana* hybrids (Fichot *et al.* 2011). However, even non-significant, a better relationship existed between K_{leaf} and instantaneous WUE than with Δ.

PIP aquaporins could also play a role in water use efficiency at two levels by modulating K_{leaf} but also mesophyll conductance to CO_2 (Uehlein *et al.* 2003, Flexas *et al.* 2006, Terashima *et al.* 2006, Sade *et al.* 2010, Sadok and Sinclair 2010).

5. ABA and aquaporins, molecular actors of K_{leaf} regulation

Abscisic acid (ABA), a phytohormone induced in response to low soil water potentials is well known to trigger stomatal closure and was also shown to play a role in K_{leaf} modulation in some species. Aasamaa *et al.* (2002) showed the foliar concentration of ABA negatively correlated with g_s, K_{leaf}, and assimilation values in *Acer platanoides*, *Padus avium*, *Populus tremula*, *Quercus robur*, *Salix caprea* and *Tilia cordata.* The authors further showed the ABA concentration increased with the species drought tolerance. Blackman *et al.* (2009) demonstrated for 5 woody species that during drought stress recovery, g_s did not immediately reached pre-stress values whereas ψ_{leaf} did, suggesting leaves gradually desensitized to ABA.

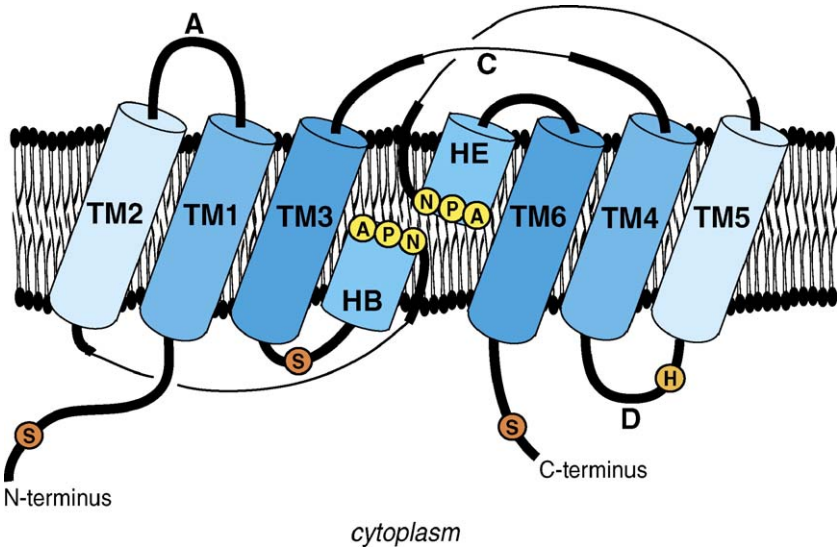

Structure schématique d'une aquaporine insérée dans le plasmalemme (Hachez *et al.* 2006, Schéma présenté comme support à ce manuscrit mais non présenté dans la revue) TM1 à 6 : domaines transmembranaires, HB et HE : hélices portant les domaines conservés NPA (Asparagine, Proline et Alanine) formant le pore. Au voisinage du domaine NPA se trouve la constriction aromatique/arginine (ar/R), qui joue le rôle de filtre sélectif pour les substrats passant dans le pore. Les résidus serine (S) cibles des phosphorylations et le résidu histidine (H), sensible au pH sont représentés. Les extrémités amine et carboxy-terminales sont du côté cytoplasmique et ont été identifiées comme importantes pour la régulation de l'ouverture du pore, des interactions protéines-protéines et de la perception osmotique (Chaumont *et al.,* 2005).

While ABA delivered by xylem had no effect on K_{leaf} in walnut (Tyree *et al.* 2005), it induced a reduction in Arabidopsis leaves (Shatil-Cohen *et al.* 2011, Pantin *et al.* 2012) and protoplast osmotic permeability (Morillon and Chrispeels 2001). With mutants lacking ABA sensitivity, or deficient in its synthesis, Morillon and Chrispeels (2001) showed that the cell-to-cell pathway, involving aquaporins, occurred preferentially in the case of low leaf conductance (*i.e.* low transpiration, closed stomata). Pantin *et al.* (2012) proposed that a first ABA signalling limiting water permeability in bundle sheath cells triggers a downstream ψ drop which would mediate stomatal closure, again *via* ABA.

Aquaporins are thought to play a major role in leaf hydraulic conductivity since they mediate most of the cell-to-cell pathway water flow through the lipid bilayer membranes. Aquaporins (AQPs) represent a family of channel proteins that transport water and/or small solutes across cell membranes in the three domains of life (Bacteria, Eukarya and Archaea). They belong to the major intrinsic protein superfamily (MIP), a highly conserved family with members in size ranging from 23 to 31 kDa (Gomes *et al.* 2009). More than 30 major intrinsic proteins (MIPs) have been isolated from *Arabidopsis thaliana* (Johansson *et al.* 2001), 65 in *Populus trichocarpa* (Gupta and Sankararamakrishnan 2009, Lopez *et al.* 2012) and 23 in *Vitis vinifera* (Fouquet *et al.* 2008). Among these proteins, at least five subfamilies can be identified in plants based on their sequence similarities (Johansson *et al.* 2001), plasma membrane intrinsic proteins (PIPs), tonoplast intrinsic proteins (TIPs), NOD26-like intrinsic proteins (NIPs), small intrinsic protein (SIPs) and the lastly identified X Intrinsic Proteins (XIPs) (Danielson and Johanson 2008, Gupta and Sankararamakrishnan 2009, Bienert *et al.* 2011). Among these isoforms, PIPs and TIPs were both experimentally shown to modulate membrane water permeability in *Xenopus* oocytes heterologous expression, also observed but to a lesser extent for poplar XIP (Lopez *et al.* 2012).

The PIP proteins are the most studied because of their plasma membrane location and their demonstrated high water transport capacity. The PIP subfamily can be further divided into PIP1s and PIP2s: PIP1s differing from the PIP2s in having a longer N-terminal extension and a shorter C-terminal end. They form hetero-tetramers in which each monomer acts as a functional channel (Fetter *et al.* 2004, Chaumont *et al.* 2005, Mahdieh *et al.* 2008). Although residues constituting their selectivity filters are similar (Ludewig and Dynowski 2009), allowing high water conductance, PIP1s and PIP2s have different functions (Wudick *et al.* 2009). PIP2s, are the most efficient water transporters (Chaumont *et al.* 2001, Katsuhara *et al.* 2002, Kaldenhoff *et al.* 2008), involved in many physiological processes such as cell

elongation, seed germination, leaf and stomatal movements (Maurel *et al.* 2008). They have been localized in walnut in vessel-associated cells, which play a major role in controlling solute flux between parenchyma cells and xylem vessels (Sakr *et al.* 2003). They are suspected to play notable roles in K_{leaf} modulation (Nardini *et al.* 2005, Cochard *et al.* 2007, Kim and Steudle 2007, Lovisolo *et al.* 2007, Hachez *et al.* 2008, Sellin *et al.* 2008, Voicu *et al.* 2008 and 2009, Sade *et al.* 2010, Postaire *et al.* 2010, Ben Baaziz *et al.* 2012a and b, Lopez *et al.* unpublished) since they have also been shown to influence root hydraulic conductance (Javot and Maurel 2002, Vandeleur *et al.* 2009, Postaire *et al.* 2010). While evidences attribute to PIP1s a role in mesophyll conductance to CO_2 (Uehlein *et al.* 2003, 2008 and 2012), they were also shown to contribute to leaf hydraulic conductance regulation (Kaldenhoff *et al.* 1998, Siefritz *et al.* 2002, Sade *et al.* 2010). Nevertheless, transgenic plants over- or under-expressing PIPs often failed to have a phenotype (Siefritz *et al.* 2002, Ma *et al.* 2004, Postaire *et al.* 2010). Similarly, transgenic *Arabidopsis thaliana* with silenced expression of both PIP1 and PIP2 had K_{leaf} similar to controls (Martre *et al.* 2002). Nevertheless, leaf and root protoplasts exhibited reduced osmotic hydraulic conductivities in the transgenic lines. More recently, Tsuchihira *et al.* (2010) showed a good correlation between water stress tolerance and PIP protein amount in leaves of wild type Eucalyptus. The authors also generated transgenic lines over-expressing a radish PIP2 which showed high photosynthetic activity and better growth under normal conditions. Their attempt to over-express a PIP1 turned to inhibit endogenous PIP1 and PIP2 levels and lower photosynthesis values.

In *Populus trichocarpa*, Secchi *et al.* (2010) reported aquaporins over-expression in a transcriptome analysis of xylem parenchyma cells after embolism formation. A recent study based on petiole transcriptome, showed over-expression of three *PIP1s* and two *PIP2s* after a water stress in grapewine that caused petiole embolism (Perrone *et al.* 2012). These data suggesting an involvement of aquaporins in embolism recovery, albeit, Nardini *et al.* (2008) showed that the embolism recovery was unaffected by an $HgCl_2$ treatment in sunflower.

PIP expression can be modulated through transcription upon various environmental changes such as water deficit, light or freeze-thaw events (Sakr *et al.* 2003, Alexandersson *et al.* 2005, Cochard *et al.* 2007), but also to translational and post-translational modifications and via membrane vesicle trafficking (Maurel *et al.* 2009, Luu *et al.* 2012) leading to increase or decrease in cell water permeability.

The roles of aquaporins in light-dependent modulation of hydraulic conductance remain partial. To date, Cochard *et al.* (2007) showed that leaf water permeability increase in

Juglans regia was independent of stomatal aperture, hence constricted by vascular and mesophyll resistances. Shatil-cohen *et al.* (2011) also showed that ABA and $HgCl_2$ induced osmotic water permeability decrease on leaf BSC protoplasts. Since it was shown for walnut that the vascular resistance was orders of magnitude lesser than the extra-vascular one (Cochard *et al.* 2004, McKown *et al.* 2010), it is likely that the light dependant K_{leaf} increase also occurs in the extra-vascular compartments. Cochard *et al.* (2007) also provided evidences supporting both transcription and translation of PIP aquaporins are needed for leaf water permeability modulation in this species, consitent with an hypothetic role of aquaporins in leaves having large sensitivity to light (Tyree *et al.* 2005, Salleo *et al.* 2003). More recently, Ben-Bâaziz *et al.* (2012b) showed that *Quercus robur*, *Fagus sylvatica*, *Populus tremula* and *Salix alba* leaf conductance increased in response to light and that the raise was associated with differential *PIP1s* and *PIP2s* transcriptional patterns. Besides, authors raised the concern that due to lack of consequent genomic databases on these species, generic primers were used in this study giving only partial information owing to isoform-specific pattern merged in an overall variation. Similar concern was raised by Voicu *et al.* (2009) in their leaf conductance study on *Q. macrocarpa*. While the authors clearly showed that specific wavelengths account each for a part of the K_{leaf} increase, no correlation was found with four followed PIP aquaporins in their transcriptional assays. This led the authors to hypothesize that other PIP isoforms could be involved evidenced by their previous demonstration of an $HgCl_2$ inhibition of the light effect (Voicu *et al.* 2008).

The involvement of aquaporins in the leaf cell-to-cell radial pathway can take place at several levels: (i) in the mesophyll with plasmalemma and tonoplast both being involved in water fluxes but also (ii) at the xylem - mesophyll interface (Figure 1). The first possibility is the functional compartmentalization of different tissues hydraulically linked where PIP aquaporins or plasmodesma could underlie the differences in the hydraulic linkages between tissues (Zwieniecki *et al.* 2007, Sadock and Sinclair 2010). Alternatively, as suggested by Zwieniecki *et al.* (2007), Cochard *et al*. (2007) and Nardini *et al.* (2010), bundle sheath cells could play a critical role in the hydraulic link between vasculature and downstream tissues. Ache *et al.* (2010) proposed that bundle sheath cells could be considered as a key checkpoint for water fluxes between xylem and stomata. Soon after, Shatil-Cohen *et al.* (2011) evidenced that aquaporins mediate regulation of osmotic water permeability in bundle sheath cells, which in turn would potentially cause the decrease of K_{leaf}.

New insights were recently provided by cDNA-amplified fragment length polymorphism (AFLP) analysis of walnut leaves submitted to high irradiance (Ben Bâaziz *et*

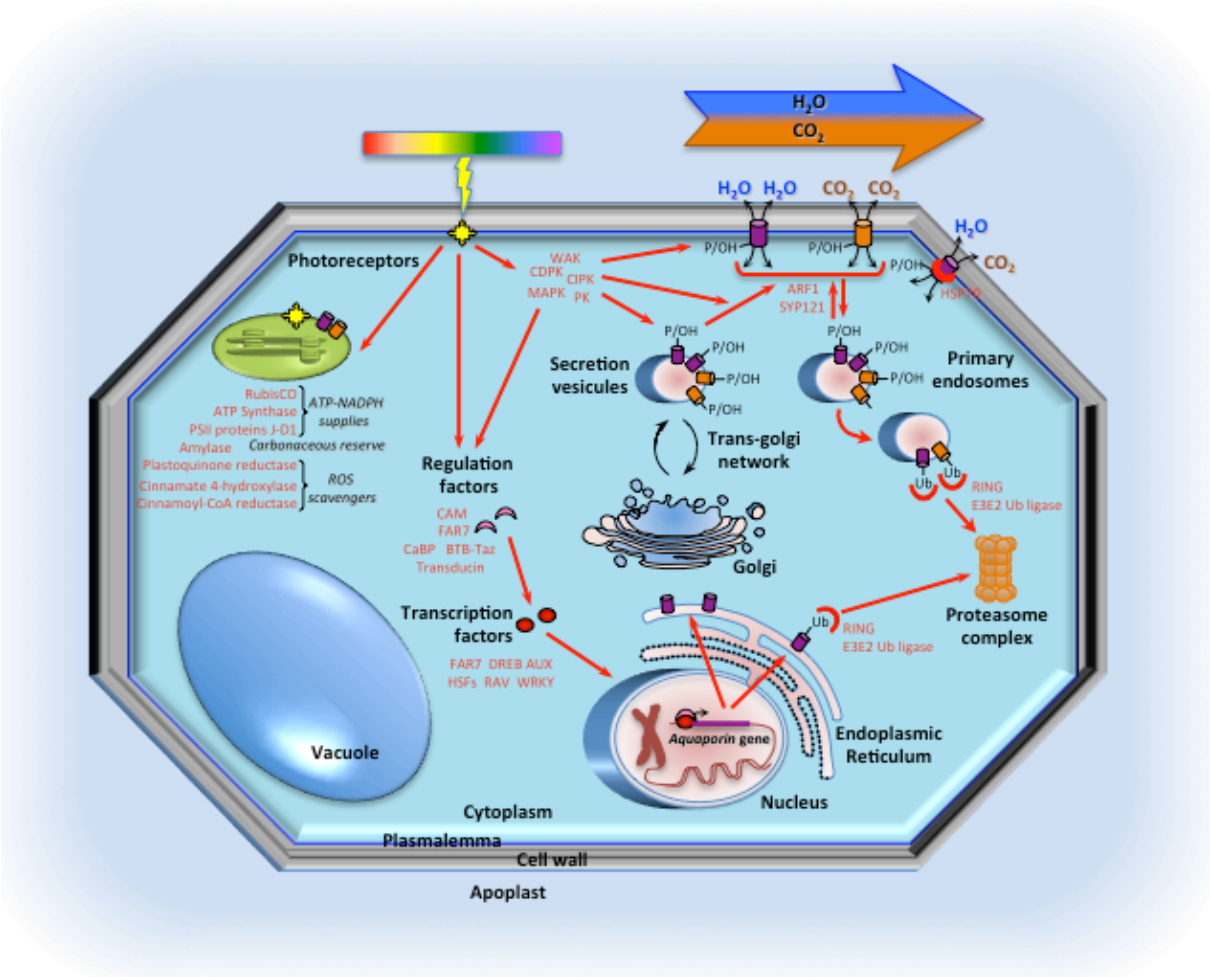

Figure 3 Molecular actors of the light response at cellular level identified by cDNA-AFLP (Ben Bâaziz *et al.* 2012a). The different wavelengths are perceived by photoreceptors in cytoplasm or chloroplast. Several proteins involved in photosynthetic activity identified are listed next to chloroplast. Upon irradiance, calcium signalling cascade members were differentially expressed (calcineurin interacting protein kinase CIPK, calmodulin CAM, calmodulin-like CaBP) which could trigger aquaporin expression *via* multiple transcription factors also transcribed (Far1-related sequence 7 FAR7, BTB-Taz, AUX, DREB, WRKY, RAV, heat shock transcription factor HSF). After translation, the aquaporin can experience retention in the endoplamic reticulum (ER) following ubiquitination. Poly-ubiquitination is also a signal for Proteasome 26S proteolysis. The aquaporin reach plasmalemma using the trans-golgi network, whose proteins involved in vesicle carrier are induced by light (ADP-rybosylation factor 1 ARF1 and synthaxin 121 SYP121). Several kinases were also identified (Ca^{2+} dependant protein kinase CDPK, mitogen activated protein kinase MAPK, serine/threonine kinase PK, Wall associated kinase WAK) activating aquaporins after phosphorylation (P/OH).

al. 2012a). The results, confirmed by RT-qPCR, identified 30 putative molecular actors among which several were already shown to play a role in assimilation, light perception and vesicle trafficking (Lee *et al.* 2008, Maurel *et al.* 2009, Luu *et al.* 2012), and proteasome-mediated proteolysis (Lee *et al.* 2009) are summarized in the Figure 3.

6. Conclusions and future prospects

Substantial progresses were made on the understanding of leaf hydraulics during the last decade. Because leaf hydraulic relations are complex to apprehend, modelling of the contribution of vascular and non-vascular pathways was of great interest and supported experimental evidences. Trade-offs between leaf hydraulic efficiency, xylem safety, costs and carbon gain (Sperry *et al.* 2008, Johnson *et al.* 2012, McKown *et al.* 2010, Simonin *et al.* 2012, Nardini *et al.* 2012) are now well understood.

Populus genus has received considerable attention being one of the most preferred tree species among the ecophysiological community (Aasamaa *et al*. 2002 and 2005a and b, Monclus *et al.* 2006, Zwieniecki *et al.* 2007, Bonhomme *et al.* 2008, Silim *et al.* 2009, Secchi *et al.* 2009, 2010 and 2011, Awad *et al.* 2010, Almeida-Rodriguez *et al.* 2010 and 2011, Fichot *et al.* 2011, Chamaillard *et al.* 2011, Ben Bâaziz *et al.* 2012b, Way *et al.* 2012). Besides the economic importance of this genus, the wide genetic background allowing contrasted responses for virtually any studied traits. Since Black cottonwood genome release (Tuskan *et al.* 2006), the genus has become even more impossible to circumvent in studies addressing the molecular dissections of physiological responses, and provide a reference genome for high throughput molecular profiling (Street *et al.* 2006, Cohen *et al.* 2010, Yan *et al.* 2012).

Non-invasive methods such as the newly developed cell pressure probe method and MRI allow following plant water dynamics for longer periods, which proved to be very useful by yielding pioneering insights. The growing interest for tomography and Cryo-SEM methods and the newly developed Tof -SIMS now permit fine visual observation of water status and movement while traditional methods only estimated them. However, if the access of such equipment is limited, their use offers exciting perspectives.

To conclude, a general consensus has emerged on the importance of the xylem/extra-vascular interphase in limiting K_{leaf}. Further attention should be addressed on this compartment and especially on the fine mechanisms of its regulation, which could partly explain the lack of consensus between species in K_{leaf} regulation or its partition.

Objectifs de la thèse

L'objectif général de cette thèse vise à caractériser la conductance hydraulique foliaire en réponse à la lumière chez le peuplier et à apprécier l'implication éventuelle des aquaporines dans sa régulation. Afin de répondre à cet objectif, les tâches suivantes ont été effectuées :

(i) La validation de la méthode du HPFM dans le cadre de caractérisations moléculaires.

(ii) L'identification des aquaporines codées par le génome du peuplier et le dessin d'amorces permettant de suivre spécifiquement chacune des isoformes, et ce de manière à ce qu'elles soient capables d'amplifier efficacement les gènes cibles sur le plus grand nombre d'espèces de peupliers possible.

(iii) L'évaluation du rôle des aquaporines dans la réponse à la lumière par l'utilisation d'inhibiteurs.

(iv) La caractérisation de la gamme de variabilité de la conductance hydraulique foliaire et de l'expression des aquaporines en réponse à la lumière chez plusieurs clones.

Différents clones de peupliers ont été sélectionnés au préalable de cette étude :

(i) *Populus trichocarpa*, le clone séquencé qui assure une étude exhaustive des gènes d'aquaporines (65, **Annexe 2**).

(ii) *Populus nigra*, qui revêt une importance particulière au niveau écologique : naturellement spontanée en France, elle fait l'objet de programmes de conservation dans le bassin de la Loire. L'espèce a été récemment séquencée, et ses informations génomiques sont actuellement en cours d'assemblage et d'annotation, ce qui en fera prochainement une nouvelle espèce modèle.

(iii) L'hybride *Populus tremula x Populus alba* clone INRA 717-1B4 qui est transformable génétiquement.

(iv) *P. euramericana* pour lequel nous avons généré des données préliminaires d'hydraulique et de biologie moléculaire qui ne sont pas présentées dans ce document.

Les mesures de conductances hydrauliques et les profils moléculaires ont été effectués sur des feuilles détachées de plantes poussant en milieu naturel (**Chapitre 1**) ou issues d'arbres en pots, placés en serre, et ayant poussé dans des conditions d'irrigation, d'humidité relative et d'éclairement contrôlées automatiquement (**Chapitre 2**, et **Annexes**).

Les résultats acquis sont présentés sous forme de deux chapitres. Le premier, qui aborde la modulation de la conductance hydraulique foliare et des transcrits PIP en réponse à la lumière chez cinq espèces d'arbres, a fait l'objet d'un article publié. Le second chapitre traite cette question de manière exhaustive chez deux clones de peupliers et a fait l'objet d'une publication soumise.

Les trois annexes sont trois articles. La première annexe, un article publié, présente les transcrits dont l'expression est modulée lors de la réponse à la lumière chez le noyer et identifiés par l'approche sans *a priori* cDNA-AFLP. La deuxième annexe, également publiée, découle directement de la deuxième tâche de la thèse, à savoir, l'identification de la totalité des 65 séquences d'aquaporines présentes dans le génome du peuplier. Nous avons pu identifier 9 membres appartenant à une sous-famille d'aquaporines nommée XIPs. De part les nombreuses singularités de cette sous-famille présente uniquement dans un panel restreint d'espèces végétales, et au vu des connaissances embryonnaires à leur propos, nous avons volontairement entrepris leur étude et leur valorisation. La dernière annexe est un article accepté où nous avons eu l'opportunité de valoriser les outils moléculaires développés dans cette thèse en les utilisant pour l'étude de réponses physiologiques au stress hydrique de la tige et des bourgeons.

Résultats

Chapitre 1

Modulation par la lumière de K_{leaf} et contribution des PIP1 et des PIP2 chez cinq espèces d'arbres

Modulation par la lumière de K_{leaf} et contribution des PIP1 et des PIP2 chez cinq espèces d'arbres : Etude de cas du noyer (*Juglans regia*)

Khaoula BEN BAÂZIZ*, **David LOPEZ***, Amélie RABOT, Didier COMBES, Aurélie GOUSSET, Sadock BOUZID, Hervé COCHARD, Soulaiman SAKR, Jean-Stéphane VENISSE

* ces auteurs ont contribués à proportions égales à ce travail

Tree Physiology (2012) **32**:423-434

Contexte

Aucun consensus de l'impact de la lumière sur la conductance hydraulique foliaire (K_{leaf}) en relation avec les aquaporines n'existe chez les espèces décrites dans la littérature. Dans cette étude, nous avons mesuré les variations de K_{leaf} et de transcrits d'aquaporines de type PIP1 et PIP2 en réponse à la lumière chez 5 espèces d'arbres (*Populus tremula* L., *Fagus sylvatica* L., *Quercus robur* L., *Salix alba* L. et *Juglans regia* L.). La réponse physiologique et moléculaire de la feuille de noyer a été plus finement étudiée en suivant individuellement 10 isoformes *PIP* en réponse à des lumières blanches ou dépourvues de bleu.

Résultats

Hormis pour *Salix alba*, une augmentation de K_{leaf} en réponse à la lumière est observée avec le HPFM. Cette méthode, bien que largement validée par des méthodes indépendantes, est critiquée car elle nécessite une mise sous pression des feuilles. Les valeurs de conductance hydraulique foliaire obtenues en réponse à la lumière pour l'espèce présentant la plus petite variation (*Salix alba*) et pour celle présentant les plus importantes variations (*Juglans regia*) ont été validées par une méthode basée sur les flux transpiratoires : l'EFM. Cette étude montre de plus, que la mise sous pression des feuilles soumises à l'éclairement ne modifie pas l'expression des transcrits aquaporines de type *PIP1* et *PIP2*. L'utilisation d'amorces génériques *PIP1* et *PIP2* a permis d'évaluer l'accumulation des transcrits de ces deux familles de gènes sur des feuilles d'obscurité et de lumière chez cinq espèces d'arbres. Pour *Fagus sylvatica*, *Quercus robur*, et *Juglans regia,* une induction des *PIP1* et une inhibition des *PIP2*

sont observées. *Populus tremula*, *Salix alba* ne montrent pas de variations significatives des transcrits de type *PIP*.

Huit nouvelles isoformes d'aquaporines *PIP* ont été identifiées chez le noyer et leur expression a été caractérisée en réponse à la lumière blanche et blanche dépourvue de sa composante bleue. L'utilisation de cette lumière filtrée chez le noyer induit une augmentation de K_{leaf} très inférieure à celle obtenue en réponse au spectre blanc complet, proche de la valeur mesurée à l'obscurité. L'expression des dix isoformes de PIP du noyer (4 PIP1 et 6 PIP2) est stimulée en réponse à la lumière blanche, cependant, certaines isoformes sont inhibées en absence de lumière bleue.

Conclusions

Ces travaux confirment que toutes les espèces ne présentent pas une augmentation de K_{leaf} en réponse à la lumière. Simultanement à l'augmentation de K_{leaf}, des modulations des transcrits de *PIP1* et *PIP2 sont* observées mais ne permettent pas de dégager une tendance générale. Le saule blanc et le tremble ne présentent pas de modulation significative des *PIP1* et des *PIP2*, cependant ces deux espèces ne montrent pas ou peu de variation de K_{leaf} dans les conditions étudiées. Cela dit, l'utilisation d'amorces génériques dans ce travail ne permet pas d'évaluer les contributions individuelles des isoformes *PIP1 et PIP2*. Enfin, la lumière bleue participe largement à l'effet inducteur sur K_{leaf} mais également à la transcription des *PIP1* et *PIP2* chez le noyer.

D'un point de vue méthodologique, il était primordial de vérifier que les réponses moléculaires enregistrées sur des échantillons pour lesquels des mesures de conductance ont été réalisées ne soient pas artéfactuelles. Ainsi nous affirmons dans cet article qu'il est possible de généraliser son utilisation dans le cadre de caractérisations moléculaires et écophysiologiques simultanées, notamment pour caractériser l'effet d'inhibiteurs.

Tree Physiology 32, 423–434
doi:10.1093/treephys/tps022

Research paper

Light-mediated K_{leaf} induction and contribution of both the PIP1s and PIP2s aquaporins in five tree species: walnut (*Juglans regia*) case study

Khaoula Ben Baaziz[1,2,3†], David Lopez[1,2†], Amelie Rabot[3], Didier Combes[4], Aurelie Gousset[1,2], Sadok Bouzid[3], Herve Cochard[2,1], Soulaiman Sakr[1,2,5,6] and Jean-Stephane Venisse[1,2,6]

[1]Clermont Université, Université Blaise Pascal, UMR547 PIAF, BP 10448, F-63000 Clermont-Ferrand, France; [2]INRA, UMR547 PIAF, F-63100 Clermont-Ferrand, France; [3]Laboratoire de Biologie végétale, Faculté des Sciences de Tunis, Campus universitaire, 1060 Tunis, Tunisia; [4]INRA, UR4 P3F, Equipe d'Ecophysiologie des plantes fourragères, Lusignan, France; [5]Agrocampus Ouest, Centre d'Angers, UMR SAGAH, IFR QUASAV 149, 2 rue le Nôtre, 49045 Angers Cedex, France; [6]Corresponding authors (soulaiman.sakr@agrocampus-ouest.fr, j-stephane.venisse@univ-bpclermont.fr)

†These authors contributed equally to this work.

Received December 9, 2011; accepted February 24, 2012; handling Editor Menachem Moshelion

Understanding the response of leaf hydraulic conductance (K_{leaf}) to light is a challenge in elucidating plant–water relationships. Recent data have shown that the effect of light on K_{leaf} is not systematically related to aquaporin regulation, leading to conflicting conclusions. Here we investigated the relationship between light, K_{leaf}, and aquaporin transcript levels in five tree species (*Juglans regia* L., *Fagus sylvatica* L., *Quercus robur* L., *Salix alba* L. and *Populus tremula* L.) grown in the same environmental conditions, but differing in their K_{leaf} responses to light. Moreover, the K_{leaf} was measured by two independent methods (high-pressure flow metre (HPFM) and evaporative flux method (EFM)) in the most (*J. regia*) and least (*S. alba*) responsive species and the transcript levels of aquaporins were analyzed in perfused and unperfused leaves. Here, we found that the light-induced K_{leaf} value was closely related to stronger expression of both the *PIP1* and *PIP2* aquaporin genes in walnut (*J. regia*), but to stimulation of *PIP1* aquaporins alone in *F. sylvatica* and *Q. robur*. In walnut, all newly identified aquaporins were found to be upregulated in the light and downregulated in the dark, further supporting the relationship between the light-mediated induction of K_{leaf} and aquaporin expression in walnut. We also demonstrated that the K_{leaf} response to light was quality-dependent, K_{leaf} being 60% lower in the absence of blue light. This decrease in K_{leaf} was correlated with strong downregulation of three *PIP2* aquaporins and of all the *PIP1* aquaporins tested. These data support a relationship between light-mediated K_{leaf} regulation and the abundance of aquaporin transcripts in the walnut tree.

Keywords: aquaporin gene expression, leaf hydraulic conductance, light, trees.

Introduction

Water homeostasis is crucial to the growth and survival of terrestrial plants. The sessile nature of plants requires dynamic adjustments of hydraulic efficiency in response to changing environmental factors. Plants have evolved a series of resistances to water flow in various organs along the soil–plant–atmosphere continuum (Tyree and Zimmerman 2002). Leaves constitute 30% of this total resistance to water flow through the plant (Sack and Holbrook 2006). Early studies focused principally on the measurement (Sack and Tyree 2005, Tyree et al. 2005) and partitioning of leaf hydraulic resistance (R_{leaf}; Sack et al. 2004). R_{leaf} is the sum of two key components: the vascular component, which includes the resistances of the petiole and major and minor veins, and the extravascular compartment, external to the

xylem (Trifilò et al. 2003, Cochard et al. 2004, Gascò et al. 2004). The respective contributions of these two components to R_{leaf} have been assessed in many species. For example, 64–80% of leaf hydraulic resistance in laurel (*Laurus nobilis* L.), sugar maple (*Acer saccharum* L.) and red oak (*Quercus rubra* L.) leaves is due to the vascular system (Zwieniecki et al. 2002, Sack et al. 2004). In this case, leaf water transport follows the apoplastic pathway. In contrast, the extravascular hydraulic resistance of leaves may account for 50–90% of whole-leaf resistance (Trifilò et al. 2003, Cochard et al. 2004), consistent with a major role of cell-to-cell water in leaves. These physiological targets indicate that water may flow across leaves by two different pathways, raising questions about the precise contribution of aquaporins to leaf hydraulic conductance.

Several studies have investigated the role of aquaporins in leaf hydraulic conductance and have yielded conflicting results. In *Arabidopsis* leaves, a negative correlation has been found between the intensity of transpiratory flux and plasma membrane intrinsic protein (PIP) abundance under conditions of strong transpiration (Morillon and Chrispeels 2001). Recently, another putative implication of aquaporins in K_{leaf} regulation was demonstrated on *Arabidospis* bundle-sheath cells (Shatil-Cohen et al. 2011). Bundle-sheath cells are suggested to be a key checkpoint of fluxes from the xylem to stomata as proposed by Ache et al. (2010). However, *Arabidopsis* plants lacking PIP1 and PIP2 have been found to have a hydraulic conductance similar to that of wild-type plants (Martre et al. 2002). Similarly, no difference in leaf hydraulic conductance (K_{leaf}) has been seen between wild-type and transgenic tobacco plants constitutively overproducing two aquaporin isoforms (PIP2,5 and PIP1,4), under conditions of both high (350 μmol m^{-2} s^{-1}) and low (10 μmol m^{-2} s^{-1}) irradiance (Lee et al. 2009). However, NtAQP1, a tobacco PIP1 which has a notable water channel activity in protoplasts, was shown to increase water use efficiency, stomatal conductance and transpiration rate when expressed in tomato and *Arabidopsis* (Sade et al. 2010). In other species, for which there is considerable circumstantial evidence pointing to aquaporin-dependent pathways, based on the pattern of aquaporin distribution in leaf cells (Kaldenhoff et al. 1995, Robinson et al. 1996, Sarda et al. 1997, Frangne et al. 2001, Hachez et al. 2008), the dynamic nature of K_{leaf} responses to environmental factors (Sack et al. 2004, Cochard et al. 2007) and sensitivity to certain chemical components (Nardini et al. 2005, Voicu et al. 2008). A close correlation between K_{leaf} and the abundance of aquaporin transcripts has also been reported in detached walnut leaves (Cochard et al. 2007). Experiments carried out with the high-pressure flow meter (HPFM) technique have shown that K_{leaf} increases strongly and rapidly in 15 min immediately following exposure to high levels of irradiance (Sack et al. 2002, Tyree et al. 2005, Cochard et al. 2007). This light-induced increase in K_{leaf} is independent of abscisic acid (an inhibitor of stomatal opening) and related to the upregulation of two aquaporin isoforms (*JrPIP2s*; Cochard et al. 2007). In the dark, both K_{leaf} and aquaporin abundance are low, adding support to a link between these two factors (Cochard et al. 2007). As in walnut, light increases K_{leaf} in bur oak (Voicu et al. 2008, 2009). However, no correlation has been found between light-induced K_{leaf} and the accumulation of transcripts for the four putative aquaporins isolated from leaves (Voicu et al. 2009). This suggests that light-induced K_{leaf} cannot be systemically linked to high levels of aquaporins, and additional studies are therefore required to clarify the role of aquaporins in leaf water transport.

Since the identification of the first aquaporins (*AtTIP*) in *Arabidopsis*, many studies have investigated their role in many fundamental plant processes (Maurel et al. 2008, Heinen et al. 2009). More than 30 major intrinsic proteins (MIPs) have been isolated from *Arabidopsis* (Johanson et al. 2001), maize (Chaumont et al. 2001) and rice (Sakurai et al. 2005). Plant aquaporins are classified into five main subfamilies on the basis of their location within the cell and sequence similarities: tonoplast intrinsic proteins (TIPs), PIPs, nodulin 26-like intrinsic membrane proteins (NIPs), small basic intrinsic proteins (SIPs) and X-intrinsic proteins (XIPs) (Danielson and Johanson 2008, Lopez et al. 2012). The PIP family has two main subgroups: PIP1s and PIP2s. The PIP1s differ from the PIP2s in having a longer N-terminal extension and a shorter C-terminal end. The PIP2s have a stronger effect on water conductance than PIP1s in *Xenopus laevis* oocytes (Chaumont et al. 2001, Katsuhara et al. 2002), whereas some PIP1s could be involved in CO_2 diffusion (Maurel 2007, Maurel et al. 2008). Aquaporins play a key role in plant water status. Their activity is therefore finely regulated at the post-translational level, by phosphorylation, intracellular pH and cations (Chaumont et al. 2005, Maurel 2007). Aquaporins are also amenable to transcriptional regulation, particularly in response to environmental factors, such as water deficit (Quist et al. 2004, Alexandersson et al. 2005, Liu et al. 2006, Porcel et al. 2006), freeze–thaw events (Sakr et al. 2003) and light (Cochard et al. 2007).

Light is one of the most important environmental factors governing many aspects of plant growth and development (Kendrick and Kronenberg 1994) and the K_{leaf} of many plants (Sack et al. 2003, 2005, Lo Gullo et al. 2005, Nardini et al. 2005, Tyree et al. 2005, Sack and Holbrook 2006, Cochard et al. 2007, Sellin et al. 2008, Scoffoni et al. 2008, Voicu et al. 2008, 2009, Lee et al. 2009, Savvides et al. 2012). The aim of this study was to investigate the contribution of aquaporins to light-induced K_{leaf}, by analyzing the accumulation of aquaporin transcripts. We explored the effects of light on K_{leaf} (HPFM approach) and aquaporin expression in the same experimental condition, for five species (*Fagus sylvatica*, *Juglans regia*, *Qercus robur*, *Salix alba* and *Populus tremula*) from the same location (Clermont-Ferrand, France), some of which had been studied before (Cochard et al. 2007, Voicu et al. 2008, 2009). With the

exception of *S. alba*, the species studied displayed increases of various magnitudes in hydraulic conductance in light-exposed leaves. A significant correlation between light-induced K_{leaf} and the levels of transcripts for both *PIP1* and *PIP2* aquaporins was found only in walnut. We further investigated the role of walnut aquaporins in light-induced K_{leaf}, identifying eight new plasma membrane aquaporin isoforms (4PIP2 and 4PIP1) and studying their transcript expression in conditions of high irradiance and darkness. Generally, *JrPIP2*s seemed to contribute more than *JrPIP1*s to light-induced K_{leaf}, and changes in light quality decreased K_{leaf}, by decreasing aquaporin expression. Lastly, conflicting results were recently obtained on *Q. rubra* K_{leaf} suggesting that HPFM experiments could lead to misinterpretation of the phenomenon and the contribution of each leaf compartment to bulk conductance (Rockwell et al. 2011). Here we also used evaporative flux method (EFM) technology to evaluate leaf conductance, which endorsed our HPFM dataset. In the same line, aquaporin gene expression primarily obtained on HPFM-perfused leaves was compared with unperfused leaves in the same irradiance conditions to eliminate uncertainty about any possible artifactual HPFM-induced aquaporin expression modulation, giving analogous results on five tree species. All these findings indicate that (i) HPFM is a robust technology to assess K_{leaf} on tree and (ii) aquaporins are a major target in the upregulation of K_{leaf} in response to light in walnut, and that this tree may be an appropriate model for dissection of the regulatory gene network involved in this process.

Material and methods

Plant material

The experiments were performed during the summers of 2008 and 2009, on leafy branches sampled from 15-year-old *Juglans regia* (L.) cv. Franquette (walnut), *Salix alba* (L.) (white willow), *Populus tremula* (L.) (aspen), *Fagus sylvatica* (L.) (beech) and *Quercus robur* (L.) (oak) trees growing in the INRA (Institut National de la Recherche Agronomique) arboretum near Clermont-Ferrand (France). Leafy branches were sampled at random from the part of the tree exposed to sunlight, and immediately re-cut under water. They were then enclosed in black plastic bags and kept in total darkness, at a high relative humidity, for 24 h before use. Only the mature, developed leaves from the branches were used for experiments.

Leaf hydraulic conductance measurements

Leaf hydraulic conductance was measured by the HPFM method, as previously described by Cochard et al. (2007). Briefly, degassed pressurized water was forced into the petiole of an excised leaf under positive pressure (P, MPa), and the flow of water into the petiole was measured. Light was provided by two 400 W high-pressure sodium lamps (SON-T pia, Philips France, Suresne) delivering ~600 μmol m^{-2} s^{-1} at leaf level. Water flow values (F, mmol s^{-1}) were recorded at room temperature (25 °C), every 30 s, with a computer connected to an HPFM, and leaf hydraulic conductance (K_{leaf}, mmol s^{-1} m^{-2} MPa^{-1}) was calculated as $K_{leaf} = F/(P \times LA)$, where LA is the total leaf area (m^2). Leaf hydraulic conductance was measured on leaves exposed to light for 120 min, and left in the dark for 120 min.

To ensure our HPFM results, another technique was used to determine K_{leaf} experimentally under the same light conditions using the EFM (Sack et al. 2002, Cochard et al. 2007). Unlike HPFM, this method allows free leaf transpiration under high irradiance. Walnut and willow shoots were harvested before dawn and enclosed in moist plastic bags to ensure high humidity around leaves. The bags were sealed at shoot base and kept dipping in distilled water until experimentation. To ensure the overnight rehydration, leaves were measured for initial water potential (>0.2 MPa, $n = 5$) using a pressure chamber (Model 600, Plant Moisture Stress). For the measurements, leaves were sampled from stems kept in the plastic bags. Petioles were rapidly re-cut with razor blades under water in order to prevent air bubbles in the xylem and triggering of embolism. They were maintained in water until they were connected to plastic tubing using compression fittings. The hydraulic circuit was filled with ultrapure degassed water. Instead of using a scale, the flow rate (F) was recorded using liquid mass flow meters (5–20 g h^{-1} LIQUI-FLOW, Bronkhorst, The Netherlands). After being connected with the hydraulic circuit and under low irradiance (<20 μmol m^{-2} s^{-1}), flow stabilization was reached after 10–15 min. A batch of five leaves was retrieved at this moment to obtain night conductance after water potential and area measurement. For another batch of five leaves, conductance after 120 min under high irradiance was measured. The light source, placed above the samples was then turned on, supplying 600 μmol m^{-2} s^{-1} at leaf level. A fan was also used in order to limit heating and also to favor a high transpiration rate. The water flow was measured for 120 min and final leaf water potential was measured at the end of the experiment to evaluate the driving force (Ψ_{leaf}) and calculate K_{leaf} from $K_{leaf} = F/(\Psi_{leaf} \times LA)$.

Light treatments

The effect of light quality on K_{leaf} was investigated in leaves exposed to light from which the blue light component had been removed with a blue light filter (Geste Scénique®, La Creche, France). We tested the effect of blue light on K_{leaf}, by illuminating leaves with blue-free light immediately after the dark phase. The leaves were then illuminated with white light, after removal of the blue light filter. White light was provided by two 400 W high-pressure sodium lamps (Philips SON-T pia) delivering 600 μmol m^{-2} s^{-1} at leaf level, and the leaves were placed at a distance of 28 cm from the lamp in the absence of the blue light filter, and 24 cm from the lamp in the presence of the blue light filter (distances determined with a neutral filter).

Comparison of PIP1 and PIP2 aquaporin abundance in the five species studied

We investigated the relationship between the effects of light on K_{leaf} and aquaporin abundance in these five species, by first identifying the PIP aquaporins in the light-exposed leaves of the various species, most likely to be involved in this physiological process. For this purpose, we explored the PIP subfamilies in each species using a panel of PIP1- and PIP2-related sequences as queries against the non-redundant and the expressed sequence tag (EST) databases available in the Molecular GenBank databases at the National Center for Biological Information, NCBI (http://www.ncbi.nlm.nih.gov/). As genomic databases were limited for the target species, very few PIP sequences had been obtained. To enrich this information, we set out to design degenerate oligonucleotide primers for PIP1s (PIP1DF and PIP1DR) and PIP2s (PIP2DF/PIP2DR) (Supplementary Table S1 available as Supplementary Data at *Tree Physiology* Online). Amplicons were cloned, and several clones were sequenced. We then designed generic oligonucleotide primer sets for PIP1s (PIP1GF/PIP1GR) and PIP2s (PIP2GF/PIP2GR), each binding to the most conserved coding regions of the aquaporin isoforms previously isolated from the five species (Supplementary Table S1 available as Supplementary Data at *Tree Physiology* Online).

Reverse transcriptase-quantitative polymerase chain reaction (RT-qPCR) amplification was performed in a 30-µl reaction mixture containing 0.5 U of platinum *Taq* polymerase (Clontech, Saint-Germain-en-Laye, France), 1× reaction buffer, 1.5 mM $MgCl_2$, 0.2 mM of each deoxyribonucleotide triphosphate, 0.2 µM of each primer, 0.3 µl of SYBR green I (1/10,000, Sigma, Saint Quentin Fallavier, France) and 3 µl of RT product diluted 1:20. The PCR conditions were: 94 °C for 3 min, then 40 cycles of 94 °C for 20 s, 52–60 °C for 20 s (depending on the optimal annealing temperature of the primer used) and 72 °C for 20 s. The *J. regia 18S ribosomal RNA* gene (accession No. AF399876) was used as internal standard. The relative changes in aquaporin transcript expression (Q_r) were calculated by comparison with the expression of the *18SrRNA* gene using the delta–delta method mathematical model (Livak and Schmittgen 2001). The biological dark control corresponded to HPFM-perfused leaves sampled just before illumination. Values are shown as $\log_2 Q_r$. As sampled leaves were under flooded physiological conditions, a simultaneous molecular analysis was carried out on unperfused leaves harvested from leafy branches in similar light- and time-course conditions.

Isolation of PIP1 and PIP2 sequences from walnut tree

*Jr*PIP1- and *Jr*PIP2-related ESTs from walnut were identified in the Molecular GenBank databases at NCBI, with *Arabidopsis thaliana* (L.) *At*PIP1 and *At*PIP2 protein sequences and *J. regia Jr*PIP2;1 (AY189973) and *Jr*PIP2;2 (AY189974) used as direct queries with the tBLASTn algorithm (Altschul et al. 1997). A multiple alignment of amino acid sequences was generated with ClustalW2 (http://www.ebi.ac.uk/Tools/clustalw2/index.html). If a set of ESTs could be identified, manual contigs were generated in conserved regions for further analysis using complete sequences. Redundant entries, including sequences with random point mutations or polymorphisms (similarities >98%), and single incomplete sequences with hypothetical lengths of less than 75% of their complete homologs were excluded from the analysis. For each putative isoform retrieved, full-length *J. regia* aquaporin clones were first generated with primer sets binding to the 5′/3′ untranslated regions. The amplicons were sequenced and specific new primer sets were designed for each isoform and used for RT-qPCR analyses.

The cDNAs generated by the reverse transcription of mRNA were amplified in an iCycler iQ (Bio-Rad Laboratories, Hercules, CA, USA), in 50 µl of reaction mixture containing 2 µl of a 1:40 dilution of cDNA, 0.5 U of platinum *Taq* DNA polymerase (Invitrogen, Carlsbad, CA, USA), and 10 µM primers (Supplementary Table S1 available as Supplementary Data at *Tree Physiology* Online). The PCR cycling program consisted of heating at 94 °C for 4 min, followed by 35 cycles of 94 °C for 30 s, 52–60 °C (Supplementary Table S1 available as Supplementary Data at *Tree Physiology* Online) for 30 s, 72 °C for 90 s and a final elongation step at 72 °C for 15 min. The PCR products were checked by electrophoresis in a 1.5% agarose gel. Bands of the expected size were excised from the gel and purified with the QIAquick PCR purification kit (Qiagen, Valencia, CA, USA). Purified PCR products were ligated into the pGEM®-T Easy plasmid (Promega, Madison, USA), and the resulting plasmid was introduced into *Escherichia coli* (thermo-competent JM109 cells), according to the standard protocols supplied by the manufacturer. The presence of inserts was checked by PCR with the SP6-T7 universal primers, essentially as described earlier. For each insert, we carried out restriction analysis on 10 µl of the resulting recombinant plasmids, selected at random and the DNA inserts from clones with different restriction patterns were sequenced on both strands (MWG Biotech, Courtaboeuf, France). Sequence data were analyzed with the NCBI BLAST server.

Bioinformatic analysis

The open reading frames (ORFs) of each cloned DNA sequence were translated into deduced amino acid sequences with the ExPASy proteomics server (http://www.expasy.org/tools/dna.html). These sequences were aligned with each other and with the complete sequences of the PIP1 and PIP2 aquaporin proteins from *A. thaliana*, *Populus trichocarpa* (Torr and Gray ex Hook) (PIP1 and PIP2 nomenclature according to Almeida-Rodriguez et al. 2010), *P. tremula*, *Q. robur*, *S. alba* and *Vitis vinifera* (L.). Partial sequences from *Quercus macrocarpa* Michx. were also included in this analysis, as they had been studied in different light conditions (Voicu et al. 2009). All multiple

alignments of the amino acid sequences were generated with ClustalW (Thompson et al. 1994, http://www.ebi.ac.uk/Tools/clustalw2/index.html). The unrooted phylogenetic trees were constructed using the maximum likelihood (ML) method implemented in the PhyML program v3.0 (Guindon and Gascuel 2003). Specifically, PhyML analyses were conducted with the Jones–Taylor–Thornton (JTT) substitution matrix and the stability for degree of support for each internal branch in the resulting trees was confirmed by 500 bootstrap trials. The Tree View program (Page 1996) was used to display the phylogenetic tree and bootstrap values >50% were reported. Percentages of amino acid similarity and identity were calculated using the NCBI bl2seq algorithm.

Transcript accumulation

The patterns of expression of the genes encoding the PIP1 and PIP2 aquaporins were analyzed in leaves subjected to various periods of white light (dark, 15 min, 1 h, 2 h and then 2 h after return to darkness) or after 1 h of exposure to blue-free light (corresponding to the maximum value of K_{leaf}). Samples were disconnected from the HPFM, immediately immersed in liquid nitrogen and stored at −80 °C until analysis. Total RNA was extracted from 200 mg of leaves in cetyl trimethylammonium bromide extraction buffer, as described by Chang et al. (1993). First-strand cDNA was synthesized from 1 µg of $_{tx}$RNA with SuperScript III (Invitrogen), according to the manufacturer's instructions. Quantitative PCR amplification was then carried out in an iCycler iQ (Bio-Rad) machine, in 30 µl of reaction mixture containing 3 µl of cDNA (1:20 dilution), 0.5 U of platinum *Taq* DNA polymerase (Invitrogen), 10 µM specific primers and a 1:1000 dilution of SYBR green I (Sigma). The PCR conditions were as follows: initial denaturing by heating at 94 °C for 3 min, followed by 35 cycles of denaturing at 94 °C for 20 s, annealing at 54/58 °C for 20 s and polymerization at 72 °C for 20 s. The relative quantity (Q_r) of aquaporin (AQP) transcripts using the *18S ribosomal* RNA gene as internal standard was calculated with the delta–delta method mathematical model (Livak and Schmittgen 2001); the biological dark controls were HPFM-perfused leaves sampled just before illumination. Values are shown as $\log_2 Q_r$. For each of the genes studied, we analyzed three independent biological replicates, and every run was carried out in triplicate. The values shown are means ± standard deviations. Primers were designed with the Primer3plus program (http://www.bioinformatics.nl/primer3plus; Rozen and Skaletsky 2000). The amplification efficiencies of all the primer sets were routinely checked (data not shown).

Statistical methods

The effect of the various treatments on leaf hydraulic conductance was assessed by one-way analysis of variance (ANOVA) followed by a Tukey's honestly significant difference (HSD) post hoc test. For qPCR, only statistically different results with $P < 0.05$ (Student's *t*-test) were considered.

Results

Light response of K_{leaf} and aquaporin transcipt levels in J. regia, F. sylvatica, Q. robur, S. alba and P. tremula

We investigated the link between light-increased K_{leaf} values and the accumulation of aquaporin transcripts, by analyzing these parameters together, in the same experimental conditions, in five species (*J. regia*, *F. sylvatica*, *Q. robur*, *S. alba* and *P. tremula*) growing at the same site. For all the species studied, K_{leaf} response was measured initially in the dark and then after 2 h of illumination using HPFM (Figure 1a).

In the dark, the K_{leaf} values of *J. regia*, *F. sylvatica* and *Q. robur* were very low (6, 3 and 2 mmol s^{-1} m^{-2} MPa^{-1}, respectively), well below those obtained after 2 h of illumination (K_{leaf} values of 26, 7 and 14 mmol s^{-1} m^{-2} MPa^{-1}, respectively; Figure 1a). Light-stimulated K_{leaf} increased only slightly for *P. tremula*, and no significant difference between light and dark conditions was found for *S. alba* using HPFM. To confirm the reliability of the HPFM approach, we used an independent method, EFM, to

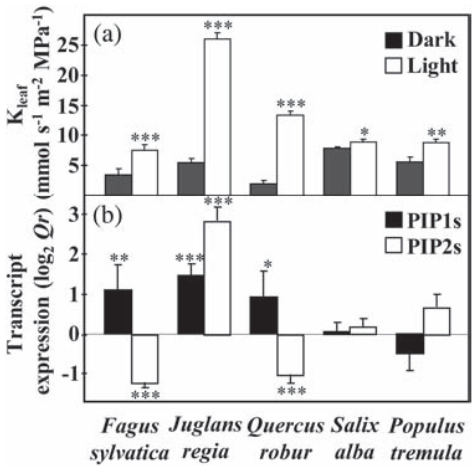

Figure 1. Leaf hydraulic conductivity (K_{leaf}, mmol s^{-1} m^{-2} MPa^{-1}), (a) and relative transcript expression of *PIP1*s and *PIP2*s aquaporin groups ($\log_2 Q_r$) (b) for five tree species in dark condition and after 2 h white light exposure. Leaf hydraulic conductance data were recorded using an HPFM method. Changes in transcript levels of the *PIP1*s (black) and *PIP2*s (clear) were monitored in leaves of the five tree species after 2 h exposure to white light. Dark leaves were used as controls for relative expression calculations. The *18SrRNA* gene expression was used as endogenous control. Expression levels ($\log_2$) are presented as expression ratio (treated to dark control). Relative transcript expressions were determined by real-time quantitative RT-PCR using generic *PIP1* or *PIP2* primer sets designed within conserved regions between selected species. Data correspond to means of three technical repeats from three independent biological experiments, and bars represent standard error ($n = 9$). Asterisks represent significant differences (Student's *t*) (*$0.01 < P < 0.05$; **$0.001 < P < 0.01$; ***$P < 0.001$.

evaluate K_{leaf}. Using concurrently HPFM and EFM, we measured *J. regia* and *S. alba* leaf conductance since these two species showed, respectively, the highest and lowest response under high irradiance in our initial HPFM assay. Flow measurements were recorded over the same duration. *Juglans regia* K_{leaf} increased upon illumination from 6.4 ± 0.5 to 26.7 ± 0.2 mmol s^{-1} m^{-2} MPa^{-1} after 120 min measured with EFM, which corresponds to a 313% increase and is the same range as found with HPFM (333%). Both measurements gave a fourfold increase for this species (Figure 2). For the same treatment, *S. alba* K_{leaf} measured using EFM increased from 6.4 ± 0.3 to 8.9 ± 0.3 mmol s^{-1} m^{-2} MPa^{-1} ($n = 5$), which is equivalent to a 39% increase, that is slightly greater than 11% obtained with HPFM.

This diversity of the K_{leaf} response to light provided a physiological framework for further investigations of the relationship between K_{leaf} profile and the relative abundance of aquaporin transcripts. To this end, we monitored the patterns of *PIP1* and *PIP2* transcripts simultaneously in the leaves of these five species, with generic oligonucleotide primers specific for *PIP1*s (PIP1GF/PIP1GR) and *PIP2*s (PIP2GF/PIP2GR).

In the dark, all these species had low K_{leaf} values associated with a low abundance of both *PIP1* and *PIP2* transcripts (data not shown). In the light, they displayed distinct profiles of aquaporin gene expression. In *J. regia*, light-induced K_{leaf} was associated with an increase in the abundance of *JrPIP1* and *JrPIP2* transcripts (three- and sevenfold) (Figure 1b). In *F. sylvatica* and *Q. robur*, light-stimulated K_{leaf} was associated with the accumulation of PIP1 transcripts only (doubling), the expression of PIP2 genes being repressed. No significant difference was found between light and dark conditions for *SaPIP1*, *SaPIP2* and *P. tremula PIP2* transcripts, and only a slight difference was found for *PoptrePIP1* transcripts (Figure 1b).

To ensure that the aquaporin expression trends were related to illumination but not to any flooding physiological state of the HPFM water-perfused leaves, a molecular analysis was subsequently carried out on unperfused leaves sampled from branches exposed to similar light conditions. Differences in relative changes emerged in terms of absolute values, but these differences were not statistically significant, and these data confirmed for each tree species the light-dependent transcript expression trends of PIP1 and PIP2 aquaporins (Figure 3).

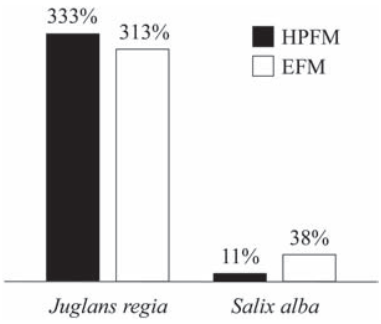

Figure 2. Methodological comparison of HPFM and EFM for measuring K_{leaf} after 2 h under high irradiance (%) relative to dark control in *J. regia* and *S. alba* ($n = 5$).

Identification and analysis of the sequence of J. regia PIP proteins

We investigated the expression of aquaporin genes in the light and its effects on K_{leaf} in greater detail by identifying eight new full-length aquaporins from the NCBI database, using the *Jr*PIP2;1 (AY189973) and *Jr*PIP2;2 (AY189974) and aquaporin protein sequences of *A. thaliana* as queries (see the Materials and methods section). The deduced amino acid sequences of these newly identified aquaporins displayed the characteristic features of MIPs. Phylogenetic analysis of the deduced protein sequences clearly demonstrated that four of these sequences were more closely related to the PIP1 group of aquaporins, while the other four were more closely related to the PIP2 group (Figure 4). The four *Jr*PIP1 sequences contained 287, 290, 285 and 292 amino acids and had, on average, 87% amino acid similarity (Supplementary Figure S1 available as Supplementary Data at *Tree Physiology* Online). Regarding the four new *Jr*PIP2 sequences, they contained 284, 280, 281 and 239 amino acids, and displayed a mean 80% similarity to the amino acid sequences of *Jr*PIP2;1 and *Jr*PIP2;2 (Sakr et al. 2003). The level of amino acid sequence similarity between the *Jr*PIP1 and *Jr*PIP2 groups was less than 70%, consistent

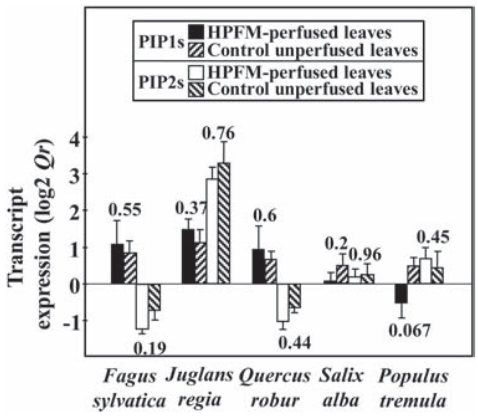

Figure 3. Comparison of transcript expression changes of *PIP1* and *PIP2* aquaporin groups for five tree species in dark condition and after 2 h white light exposure in HPFM water-perfused and control-unperfused leaves. Dark leaves were used as controls for relative expression calculations. The *18SrRNA* gene expression was used as endogenous control. Expression levels (log_2) are presented as expression ratio (treated to dark control). Relative transcript expressions were determined by real-time quantitative RT-PCR using generic PIP1 or PIP2 primer sets designed within conserved regions between selected species. Numbers represent Student's *t*-test *P* values for average HPFM-perfused expression versus control-unperfused levels (no difference in expression if $P < 0.05$).

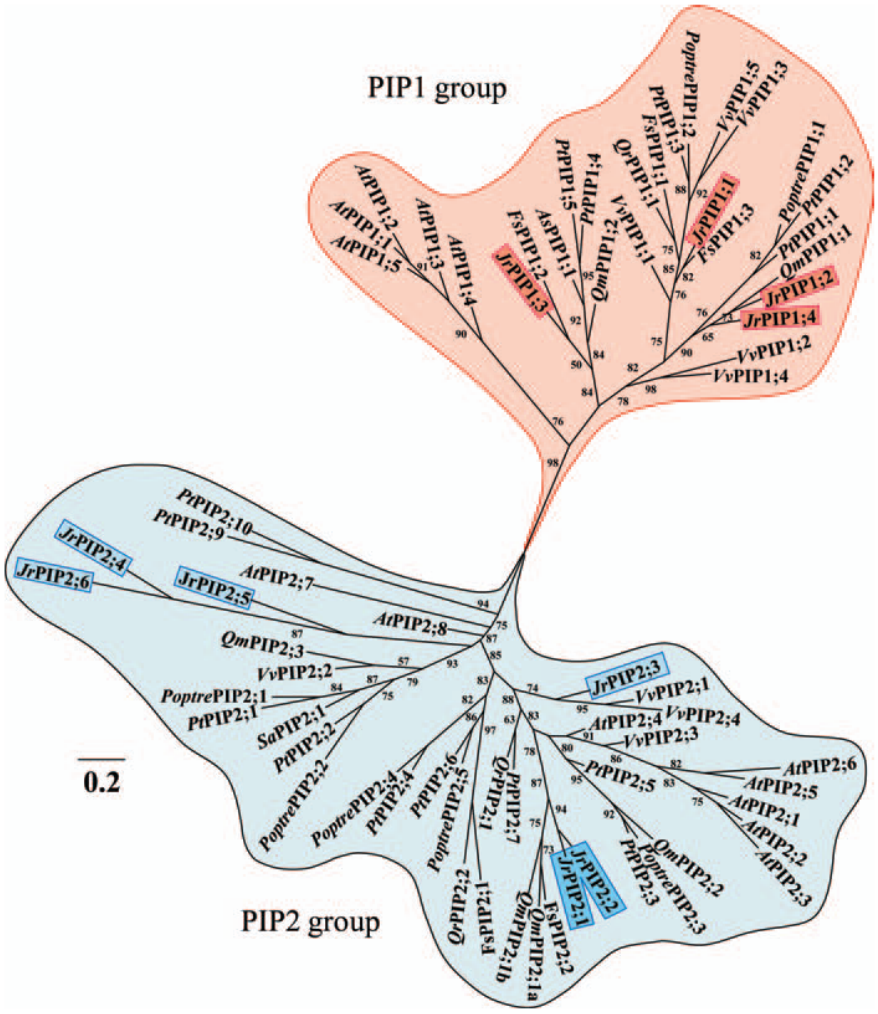

Figure 4. Phylogenetic tree analysis of *J. regia* (*Jr*) PIP1 and PIP2 aquaporin proteins with *A. thaliana* (*At*), *P. tremula* (*Poptre*), *P. trichocarpa* (*Pt*), *Q. macrocarpa* (*Qm*), *Q. robur* (*Qr*), *S. alba* (*Sa*) and *V. vinifera* (*Vv*), and PIP1 and PIP2 aquaporin proteins. The unrooted phylogeny of the PIP protein sequences was inferred using maximum likelihood. The tree was produced using PhyML with a genetic distance calculated by the JTT model of amino acid change. The numbers at the nodes represent percent of bootstrap values (above 50%) based on 500 replicates. The bar length is proportional to the number of amino acid substitutions per site. Species and accession numbers of each sequence are listed in Supplementary Table S2 available as Supplementary Data at *Tree Physiology* Online.

with the current PIP nomenclature (Johanson et al. 2001). Finally, as observed in classical plant PIP families, all *Jr*PIP1 sequences had a longer N-terminal sequence and a shorter C-terminal sequence than *Jr*PIP2 protein sequences. These sequences were thus named *Jr*PIP1;1 (FJ971053), *Jr*PIP1;2 (FJ971054), *Jr*PIP1;3 (FJ971055), *Jr*PIP1;4 (FJ970489) and *Jr*PIP2;3 (FJ971056), *Jr*PIP2;4 (FJ971057), *Jr*PIP2;5 (FJ971058), *Jr*PIP2;6 (FJ971059).

Expression patterns of the various JrPIP1 and JrPIP2 genes during irradiance

The expression patterns of the 10 *JrPIP* genes were monitored at five time points (0 dark; 15 min light; 1 h light; 2 h light and 2 h after return to the dark). When leaves were exposed to light, their K_{leaf} immediately began to increase, reaching a maximum after 2 h of irradiance (Figure 5a). In addition, for all the *JrPIP1* and *JrPIP2* genes investigated, transcript abundance was transiently upregulated by light and peaked after 1 h (*JrPIP1;1*, *JrPIP1;2*, *JrPIP1;3*, *JrPIP2;1* and *JrPIP2;4*) or 2 h (*JrPIP1;4*, *JrPIP2;2* and *JrPIP2;6*) of irradiance (Figure 5b and c). Only *JrPIP2;3* peaked earlier, with transcript levels peaking within the first 15 min of irradiance. Finally, K_{leaf} gradually declined toward the initial value when leaves were returned to the dark, as did the abundance of most of the *JrPIP1* and *JrPIP2* transcripts. The strongest upregulation (eightfold) was observed for *JrPIP2;1*, after 1 h of illumination.

Effect of blue light on J. regia K_{leaf} and JrPIP transcripts

Light may exert its effects through its intensity or its quality. We therefore investigated whether the K_{leaf} response to light

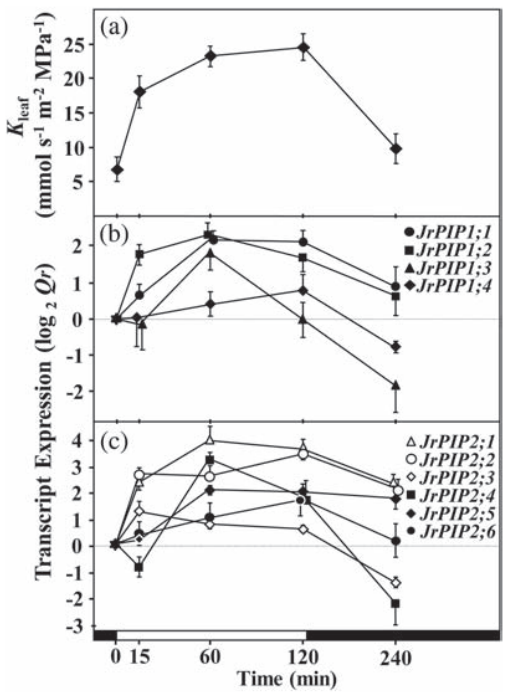

Figure 5. Time courses of leaf hydraulic conductance response (K_{leaf}) (a) and kinetic changes in transcript expression ($\log_2 Q_r$) of *JrPIP1*s (b) and *JrPIP2*s (c) in leaves of *J. regia* under conditions of light (white bar) and darkness (black bar). Leaf hydraulic conductance data were recorded using an HPFM method. Relative transcript expressions were determined by real-time quantitative RT-PCR using *PIP1* or *PIP2* specific primer sets for each isoform. Dark leaves were used as controls for relative expression calculations, and *18SrRNA* gene expression was used as endogenous control. Expression levels ($\log_2$) are presented as expression ratio (treated to dark control). Black and white bars on the *x*-axis correspond to the dark and light periods, respectively. Data correspond to means of three technical repeats from three independent biological experiments, and bars represent standard error ($n = 9$).

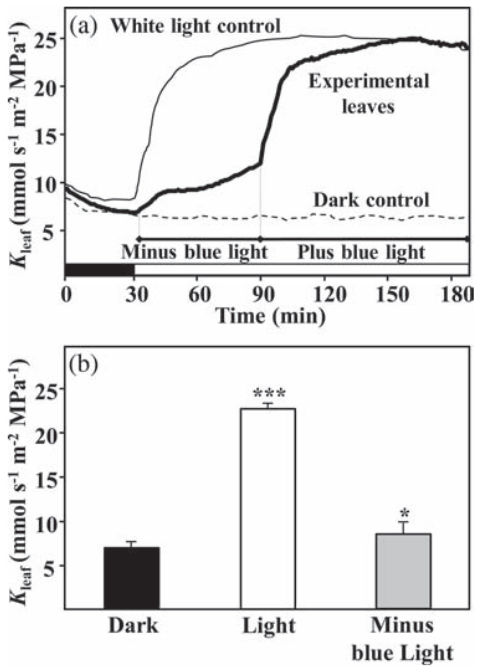

Figure 6. (a) Typical time courses of leaf hydraulic conductance (K_{leaf}) response of *J. regia* under white light and dark conditions (control mean), and under filtering for blue light wavelengths (minus blue light) followed by a return to ambient full spectrum white light condition (plus blue light) (experimental leaves). Leaf hydraulic conductance data were recorded using an HPFM method. Black bar on the *x*-axis corresponds to the dark periods. (b) Mean K_{leaf} values (±SE) in control dark, control light, and minus blue light leaves. Asterisks represent significant differences (Student's *t*) (*$0.01 < P < 0.05$; ***$P < 0.001$).

was dependent on light quality. The use of a blue light filter (excluding blue light) resulted in a K_{leaf} value 65% lower than that obtained in control conditions (8 and 23 mmol s^{-1} m^{-2} MPa^{-1} for minus blue light and white light, respectively; Figure 6a). K_{leaf} increased reversibly when the same leaf was returned to white light after removal of the blue light filter, with the maximum value reached at 160 min. A summary of the light quality-dependent K_{leaf} statistical values is shown in Figure 6b. The *JrPIP* transcript levels were modified by blue light deprivation (Figure 7). Transcript levels were much lower for *JrPIP2;3*, *JrPIP2;4* and *JrPIP2;5* and slightly but significantly lower for *JrPIP2;2* in the absence of blue light. All the *JrPIP1* aquaporins tested displayed a downregulation of transcript abundance in the absence of blue light, suggesting that *JrPIP1*s are more sensitive to a lack of blue light than *JrPIP2*s.

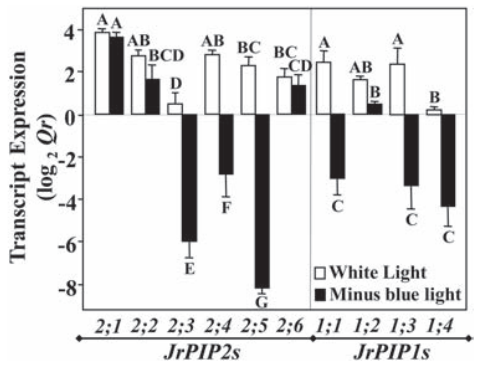

Figure 7. Changes in transcript levels of the *JrPIP1*s and *JrPIP2*s in leaves of *J. regia* after 2 h exposure to white light or with blue light wavelengths filtered out (minus blue light). Dark leaves were used as controls for relative expression calculations. The *18SrRNA* gene expression was used as endogenous control. Expression levels ($\log_2$) are presented as expression ratio (treated to dark control). Relative transcript expression of indicated genes was determined by real-time quantitative RT-PCR using specific primer sets for each isoform. Data correspond to means of three technical repeats from three independent biological experiments, and bars represent standard error ($n = 9$). Levels not connected by same letters are significantly different (Tukey HSD).

Discussion

The K_{leaf} stimulation by light has been reported to differ between species (Sack and Tyree 2005, Sack and Holbrook 2006).

It may be weak (<1.5-fold increase) or stronger (two- to seven-fold), depending on the species studied (Sack et al. 2003, Tyree et al. 2005, Cochard et al. 2007, Voicu et al. 2008). Using HPFM, we found that light strongly increased K_{leaf} in *Q. robur*, *F. sylvatica* and *J. regia* (seven-, three- and fourfold), with a smaller increase observed in *P. tremula* (about 1.5-fold) (Figure 1). Although significant, a smaller difference was observed in *S. alba* K_{leaf} with HPFM (11%) than with EFM (38%). The maximum values attained by K_{leaf} differed between these species, ranging from 7 mmol s^{-1} m^{-2} MPa^{-1} in *F. sylvatica* to 26 mmol s^{-1} m^{-2} MPa^{-1} in *J. regia*. Previous data for 107 species showed that the maximal value of light-induced K_{leaf} ranged between 0.76 and 49 mmol s^{-1} m^{-2} MPa^{-1} (Sack and Tyree 2005). The reasons for these differences remain unclear. Some studies have suggested that K_{leaf} intensity depends on the distribution of the xylem and extra-xylem pathways within the leaf (Sack and Holbrook 2006). The resistance of the leaf xylem (R_{xylem}) is a major component of R_{leaf} in *Q. rubra* and *A. saccharum* leaves (Zwieniecki et al. 2002, Sack et al. 2004), and differences in vein architecture between species may be reflected in differences in R_{leaf}. However, if R_{xylem} is negligible with respect to extra-xylem resistance ($R_{outside\ xylem}$), the difference in R_{xylem} between species will have little impact on overall R_{leaf} (Sack and Holbrook 2006). Other studies have reported that the hydraulic resistance of the leaf xylem is of about the same magnitude as that in the extra-xylem pathways (Cochard et al. 2004, Gascò et al. 2004, Sack et al. 2004, 2005, Nardini et al. 2005), and that species tend to vary in terms of partitioning. Water conductance may be higher in leaves with a higher minor vein density, due to the existence of a greater surface area for the exchange of xylem water with the surrounding mesophyll (Cochard et al. 2004) and the transport of water over smaller distances outside the xylem (Roth-Nebelsick et al. 2001, Sack and Frole. 2006).

There is also evidence to suggest that aquaporins contribute to leaf water transport in detached *J. regia* leaves (Cochard et al. 2007). In this species, the irradiance-dependent increase in leaf hydraulic conductance during HPFM measurements has been shown to be correlated with higher levels of *JrPIP2;1* and *JrPIP2;2* aquaporin gene expression (Cochard et al. 2007). These findings are entirely consistent with the data shown in Figure 5, clearly indicating that the light-induced K_{leaf} may be related to increases in the expression of many newly identified *J. regia* aquaporin genes from both the PIP1 (*JrPIP1;1*, *JrPIP1;2* and *JrPIP1;3*) and PIP2 (*JrPIP2;1*, *JrPIP2;2*, *JrPIP2;3*, *JrPIP2;4*, *JrPIP2;5* and *JrPIP2;6*) subfamilies. The accumulation of transcripts for these genes was observed between 1 and 2 h after exposure to light, except for *JrPIP2;3*. Thus, the effect of light on *J. regia* K_{leaf} involves both PIP2 and PIP1 aquaporins. However, based on the patterns of transcript accumulation observed, light had a much stronger effect on PIP2 than on PIP1 isoforms (Figure 5). The PIP1 aquaporins therefore appear to make less contribution to light-induced K_{leaf} than PIP2 aquaporins. Similar observations have been reported for other processes. Both PIP1 and PIP2 subfamilies are presented together for all species and organisms, e.g., in leaves of *A. thaliana* (Jang et al. 2004, Postaire et al. 2010), rice (Sakurai et al. 2005, 2008), maize (Hachez et al. 2008), *Q. macrocarpa* (Voicu et al. 2009) and *P. trichocarpa* (Secchi et al. 2009). These aquaporins may have different complementary functions within the leaf. For example, *NtAQP1* is involved not only in glycerol transport (Biela et al. 1999) and CO_2 diffusion (Uehlein et al. 2003) but also WUE and potentially water permeation (Sade et al. 2010). As for PIP2s, they are reportedly shown to play a key role in the flux of water across the plasma membrane. Lastly, aquaporins may increase water transport through the heterotetramerization of PIP1 and PIP2 aquaporin isoforms in the leaf (Fetter et al. 2004, Zelazny et al. 2007).

The relationship between light-induced K_{leaf} and aquaporin transcript levels does not extend to all herbaceous and woody species tested to date. In *A. thaliana*, leaf hydraulic conductance was similar in wild-type and double-antisense plants with only low levels of PIP1 and PIP2 aquaporins (Martre et al. 2002). In the same species, protoplasts isolated from leaves with high rates of transpiration had low osmotic water permeability whereas protoplasts from leaves with low levels of transpiration had high osmotic water permeability (Morillon and Chrispeels 2001). In tobacco plants, leaf hydraulic conductance is similar in wild-type and transgenic plants constitutively overexpressing the *PIP2;5* and *PIP1;4* aquaporin genes in conditions of both high- and low irradiance (Lee et al. 2009). In addition, cell pressure-probe studies have shown that cell hydraulic conductivity in leaves decreases in response to high levels of irradiance, probably due to the inhibition of aquaporin-mediated water transport (Kim and Steudle 2007, 2009, Lee et al. 2008, 2009). A recent study in *A. thaliana* leaves showed that darkness increased the transcript abundance of several *PIP* genes, including *AtPIP1;2* [initially referred to as *AthH2* or *PIP1b* (Kaldenhoff et al. 1995)], which accounts for a significant proportion of the aquaporin-mediated leaf water transport in plants grown in the dark for extended periods (Postaire et al. 2010). In woody species, aquaporins do not seem to contribute to leaf hydraulic conductance in some of the plants tested. Light increased K_{leaf} in *Q. robur*, *F. sylvatica*, *P. tremula* and *J. regia*, consistent with previous findings (Cochard et al. 2007, Voicu et al. 2008, Voicu and Zwiazek 2010). The strongest effects were observed for *Q. robur* and *J. regia*, at 14 and 24 mmol s^{-1} m^{-2} MPa^{-1}, respectively. Under the same experimental conditions, no correlation was found between K_{leaf} magnitude and PIP gene expression in any of the species other than *J. regia* (Figure 1a and b). In *Q. robur*, light strongly stimulated K_{leaf}, but *PIP2* transcript levels were downregulated and those of *PIP1*s remained similar to those in the control (T_0) (Figure 1b). Similar patterns of *PIP* gene expression were observed for *F.*

sylvatica. The absence of a link between the response of K_{leaf} to light and *PIP* expression was recently reported for *Q. macrocarpa* (Voicu et al. 2009). The authors suggested that aquaporins might function by regulating water homeostasis in leaves adapted to different light conditions. However, to date, in contrast to in vitro assays or root systems (Martinez-Ballesta et al. 2003, Coskun et al. 2012), knowledge about modulation of the cell homeostasis in relationship with aquaporins in leaves related with irradiance is deficient (Luu and Maurel 2005, Sack and Holbrook 2006). Similarly, the moderate light-induced increase in K_{leaf} in *P. tremula* is independent of *PIP* gene expression (Figure 1a and b), and seems instead to be linked to leaf metabolism (Voicu and Zwiazek 2010).

Lastly, it could be reasonably suspected from our molecular assays that the aquaporin transcript levels would be connected with the flooding physiological state of the HPFM water-perfused leaves (revealing any flooding tolerance phenotype of these tree species), and not to light exposure as such. To this end, for each tree species we also monitored the transcript expression patterns of *PIP1* and *PIP2* in unperfused leaves, harvested in leafy branches before dawn and then placed in similar light conditions. When relative changes are viewed strictly in value terms, minor differences in *PIP1* and *PIP2* transcript changes were apparent between analyses, but the expression trends of these analyses all significantly pointed in the same direction (Figure 3). These findings confirm that changes in aquaporin expression were rather due to light exposure than to folding physiological state of the HPFM experimentation. For leaf hydraulic conductance, HPFM measurements were supported by an independent method (EFM), which is not reported to induce flooding (Sack and Tyree 2005). Both gave similar values on *J. regia* and *S. alba*, respectively, the most and least light-responsive tested species according to HPFM. As reported, these methods were shown to give similar results on several woody species (Sack et al. 2002, Scoffoni et al. 2008) and on crop plants (Tsuda and Tyree 1999). Under high irradiance, increase in conductance was in the same range for *J. regia* (+333% for HPFM versus +313% for EFM), but HPFM might underestimate change in conductance for *S. alba* (+11%) relative to the 38.6% measured by EFM (Figure 2). In our experimental conditions, we assume HPFM to be a suitable assay method for accurately obtaining K_{leaf}.

Light is known to affect gene expression through changes in its intensity or quality (Girault et al. 2008, Voicu et al. 2008). When *J. regia* leaves were exposed to light rendered blue free light by a blue light filter, K_{leaf} was about 65% lower than that in the presence of white light (8 mmol s^{-1} m^{-2} MPa^{-1} versus 23 mmol s^{-1} m^{-2} MPa^{-1}) (Figure 6b). The only other comprehensive study investigating the effect of light quality on K_{leaf} reported similar results for *Q. macrocarpa* (Voicu et al. 2008). In this earlier study, the increase in leaf hydraulic conductance was greater in response to blue and green light than to visible light of longer wavelengths. Interestingly, the response of K_{leaf} to white light was also greater than to light of any single wavelength, suggesting that each wavelength acts individually (Voicu et al. 2008).

Under white light, all *J. regia* aquaporin transcripts were upregulated within 1 h of irradiance (except for *JrPIP1;4*). By contrast, in the absence of blue light, only *JrPIP2;1* and *JrPIP2;6* transcript levels were similar to those obtained under white light (Figure 7). The expression of these aquaporin genes is blue light independent, potentially accounting for the 35% higher K_{leaf} values obtained in these conditions than in the dark. Further studies with filters blocking other wavelengths of light (e.g., red) would be needed to investigate the contribution of different wavelengths to light-induced K_{leaf} and aquaporin levels. In contrast, aquaporin transcript accumulation was moderately lower for *JrPIP2;2* and much lower for the other aquaporins (*JrPIP2;3*, *JrPIP2;4*, *JrPIP2;5*, *JrPIP1;1*, *JrPIP1;3* and *JrPIP1;4*) in the absence of blue light. These findings suggest that blue light makes a major contribution to light-induced K_{leaf}, possibly related to the downregulation of *PIP1*s and *PIP2*s. *A. thaliana* AthH2, a blue light-responsive aquaporin, is upregulated in expanding and differentiated cells when plants are exposed to blue light (Kaldenhoff et al. 1995). In tobacco plants, Lorenz et al. (2003) have identified abundant flavin-binding sites in NtAQP1, an aquaporin of the PIP1 subfamily. The binding of flavin to the protein can be induced photochemically by blue light, providing evidence for a possible role of the riboflavin-binding protein PIP1 as a photoreceptor.

In conclusion, our data provide a cornerstone for the role of aquaporins (PIP1s and PIP2s) in the light-modulated K_{leaf} in the walnut tree. This species could be a useful model for gaining a better understanding of the molecular basis of such regulation.

Supplementary data

Supplementary data for this article are available at *Tree Physiology* Online.

Acknowledgments

We thank Labernia Sylvaine, Conchon Pierre and Bodet Christian for their contribution to RNA extractions and hydraulic measurements. We are grateful to the anonymous reviewers for their constructive suggestions.

Funding

This work was supported by the Ministère de l'Enseignement Supérieur et de la Recherche.

Conflict of interest

None declared.

References

Ache, P., H. Bauer, H. Kollist, K.A. Al-Rasheid, S. Lautner, W. Hartung and R. Hedrich. 2010. Stomatal action directly feeds back on leaf turgor: new insights into the regulation of the plant water status from non-invasive pressure probe measurements. Plant J. 62:1072–1082.

Alexandersson, E., L. Fraysse, S. Sjövall-Larsen, S. Gustavsson, M. Fellert, M. Karlsson, U. Johanson and P. Kjellbom. 2005. Whole gene family expression and drought stress regulation of aquaporins. Plant Mol. Biol. 59:469–484.

Almeida-Rodriguez, A., J.E.K. Cooke, F. Yeh and J.J. Zwiazek. 2010. Functional characterization of drought-responsive aquaporins in *Populus balsamifera* and *Populus simonii × balsamifera* clones with different drought resistance strategies. Physiol. Plant. 140:321–333.

Altschul, S.F., T.L. Madden, A.A. Schaffer, J. Zhang, Z. Zhang, W. Miller and D.J. Lipman. 1997. Gapped BLAST and PSI-BLAST: a new generation of protein database search programs. Nucleic Acids Res. 25:3389–3402.

Biela, A., K. Grote, B. Otto, S. Hoth, R. Hedrich and R. Kaldenhoff. 1999. The *Nicotina tabacum* plasma membrane aquaporin NTAQP1 is mercury-insensitive and permeable for glycerol. Plant J. 18:565–570.

Chang, S., J. Puryear and J. Cairney. 1993. A simple and efficient method for isolating RNA from pine trees. Plant Mol. Biol. Rep. 11:113–116.

Chaumont, F., F. Barrieu, E. Wojcik, M.J. Chrispeels and R. Jung. 2001. Aquaporins constitute a large and highly divergent protein family in maize. Plant Physiol. 125:1206–1215.

Chaumont, F., M. Moshelion and M.J. Daniels. 2005. Regulation of plant aquaporin activity. Biol. Cell 97:749–764.

Cochard, H., A. Nardini and L. Coll. 2004. Hydraulic architecture of leaf blades: where is the main resistance? Plant Cell Environ. 27:1257–1267.

Cochard, H., J.S. Venisse, T.S. Barigah, N. Brunel, S. Herbette, A. Guilliot, M.T. Tyree and S. Sakr. 2007. Putative role of aquaporins in variable hydraulic conductance of leaves in response to light. Plant Physiol. 143:122–133.

Coskun, D., D.T. Britto, Y.K. Jean, L.M. Schulze, A. Becker and H.J. Kronzucker. 2012. Silver ions disrupt K+ homeostasis and cellular integrity in intact barley (*Hordeum vulgare* L.) roots. J. Exp. Bot. 63:151–162.

Danielson, J.A.H. and U. Johanson. 2008. Unexpected complexity of the aquaporin gene family in the moss *Physcomitrella patens*. BMC Plant Biol. 8:45.

Fetter, K., V.V. Wider, M. Moshelion and F. Chaumont. 2004. Interactions between plasma membrane aquaporins modulate their water channel activity. Plant Cell 16:215–228.

Frangne, N., M. Maeshima, A.R. Schäffner, T. Mandel, E. Martinola and J.L. Bonnemain. 2001. Expression and distribution of a vacuolar aquaporin in young and mature leaf tissues of *Brassica napus* in relation to water fluxes. Planta 212:270–278.

Gascò, A., A. Nardini and S. Salleo. 2004. Resistance to water flow through leaves of *Coffea arabica* is dominated by extravascular tissues. Funct. Plant Biol. 31:1161–1168.

Girault, T., V. Bergougnoux, D. Combes, J.D. Viemont and N. Leduc. 2008. Light controls shoot meristem organogenic activity and leaf primordia growth during bud burst in *Rosa* sp. Plant Cell Environ. 31:1534–1544.

Guindon, S. and O. Gascuel. 2003. A simple, fast, and accurate algorithm to estimate large phylogenies by maximum likelihood. Syst. Biol. 52:696–704.

Hachez, C., R.B. Heinen, X. Draye and F. Chaumont. 2008. The expression pattern of plasma membrane aquaporins in maize leaf highlights their role in hydraulic regulation. Plant Mol. Biol. 68:337–353.

Heinen, R.B., Q. Ye and F. Chaumont. 2009. Role of aquaporins in leaf physiology. J. Exp. Bot. 60:2971–2985.

Jang, J.Y., D.G. Kim, Y.O. Kim, J.S. Kim and H. Kang. 2004. An expression analysis of a gene family encoding plasma membrane aquaporins in response to abiotic stresses in *Arabidopsis thaliana*. Plant Mol. Biol. 54:713–725.

Johanson, U., M. Karlsson, I. Johansson, S. Gustavsson, S. Sjövall, L. Fraysse, A.R. Weig and P. Kjellbom. 2001. The complete set of genes encoding major intrinsic proteins in *Arabidopsis* provides a framework for a new nomenclature for major intrinsic proteins in plants. Plant Physiol. 126:1358–1369.

Kaldenhoff, R., A. Kölling, J. Meyers, U. Karmann, G. Ruppel and G. Richter. 1995. The blue light-responsive AthH2 gene of *Arabidopsis thaliana* is primarily expressed in expanding as well as in differentiating cells and encodes a putative channel protein of the plasmalemma. Plant J. 7:87–95.

Katsuhara, M., Y. Akiyama, K. Koshio, M. Shibasaka and K. Kasamo. 2002. Functional analysis of water channels in barley roots. Plant Cell Physiol. 43:885–893.

Kendrick, R.E. and G.H.M. Kronenberg. 1994. Photomorphogenesis in plants. 2nd edn. Kluwer Academic Publishers, Dordrecht, The Netherlands.

Kim, Y.X. and E. Steudle. 2007. Light and turgor affect the water permeability (aquaporins) of parenchyma cells in the midrib of leaves of *Zea mays*. J Exp. Bot. 58:4119–4129.

Kim, Y.X. and E. Steudle. 2009. Gating of aquaporins by light and reactive oxygen species in leaf parenchyma cells of the midrib of *Zea mays*. J. Exp. Bot. 60:547–556.

Lee, S.H., J.J. Zwiazek and G.C. Chung. 2008. Light-induced transpiration alters cell water relations in leaf gourd (*Cucurbita ficifolia*) seedlings exposed to low root temperatures. Physiol. Plant. 133:354–362.

Lee, S.H., G.C. Chung and J.J. Zwiazek. 2009. Effects of irradiance on cell water relations in leaf bundle sheath cells of wild-type and transgenic tobacco (*Nicotiana tabacum*) plants over-expressing aquaporins. Plant Sci. 176:248–255.

Liu, H.Y., W.N. Sun, W.A. Su and Z.C. Tang. 2006. Co-regulation of water channels and potassium channels in rice. Physiol. Plant. 128:58–69.

Livak, K.J. and T.D. Schmittgen. 2001. Analysis of relative gene expression data using real-time quantitative PCR and the 2-ΔΔCT method. Methods 25:402–408.

Lo Gullo, M.A., A. Nardini, P. Trifolio and S. Salleo. 2005. Diurnal and seasonal variations in leaf hydraulic conductance in evergreen and deciduous trees. Tree Physiol. 25:505–512.

Lopez, D., G. Bronner, N. Brunel, et al. 2012. Insights into *Populus* XIP aquaporins: evolutionary expansion, protein functionality, and environmental regulation. J. Exp. Bot. 63:2217–2230.

Lorenz, A., R. Kaldenhoff and R. Hertel. 2003. A major integral protein of the plant plasma membrane binds flavin. Protoplasma 221:19–30.

Luu, D.T. and C. Maurel. 2005. Aquaporins in a challenging environment: molecular gears for adjusting plant water status. Plant Cell Environ. 28:85–96.

Martinez-Ballesta, M.C., R. Diaz, V. Martinez and M. Carvajal. 2003. Different blocking effects of HgCl2 and NaCl on aquaporins of pepper plants. J. Plant Physiol. 160:1487–1492.

Martre, P., R. Morillon, F. Barrieu, G.B. North, P.S. Nobel and M.J. Chrispeels. 2002. Plasma membrane aquaporins play a significant role during recovery from water deficit. Plant Physiol. 130:2101–2110.

Maurel, C. 2007. Plant aquaporins: Novel functions and regulation properties. FEBS Lett. 581:2227–2236.

Maurel, C., L. Verdoucq, D.T. Luu and V. Santoni. 2008. Plant aquaporins: membrane channels with multiple integrated functions. Annu. Rev. Plant. Biol. 59:595–624.

Morillon, R. and J.C. Chrispeels. 2001. The role of ABA and the transpiration stream in the regulation of the osmotic water permeability of leaf cells. Proc. Natl Acad. Sci. USA 20:14138–14143.

Nardini, A., S. Salleo and S. Andri. 2005. Circadian regulation of leaf hydraulic conductance in sunflower (*Helianthus annuus* L. cv Margot) Plant, Cell Environ. 6:750–759.

Page, R.D. 1996. Tree view: an application to display phylogenetic trees on personal computers. Comput. Appl. Biosci. 12:357–358.

Porcel, R., R. Aroca, R. Azcón and J.M. Ruiz-Lozano. 2006. PIP aquaporin gene expression in arbuscular mycorrhizal *Glycine max* and *Lactuca sativa* plants in relation to drought stress tolerance. Plant Mol. Biol. 60:389–404.

Postaire, O., C. Tournaire-Roux, A. Grondin, Y. Boursiac, R. Morillon, A.R. Schäffner and C. Maurel. 2010. A PIP1 aquaporin contributes to hydrostatic pressure-induced water transport in both the root and rosette of *Arabidopsis*. Plant Physiol. 152:1418–1430.

Quist, T.M., S. Yokoi, R.A. Bressan, P.M. Hasegawa and R.J. Joly. 2004. Differential regulation of plasma membrane aquaporin transcripts in *Arabidopsis* in response to environmental stress: proposed roles for aquaporins in regulating plant water balance. Recent Res. Dev. Biochem. 5:19–29.

Robinson, D.G., H. Sieber, W. Kammerloher and A.R. Schäffner. 1996. PIP1 aquaporins are concentrated in plasmalemmasomes of *Arabidopsis thaliana* mesophyll. Plant Physiol. 111:645–649.

Rockwell, F.E., N.M. Holbrook and M.A. Zwieniecki. 2011. Hydraulic conductivity of red oak (*Quercus rubra* L.) leaf tissue does not respond to light. Plant Cell Environ. 34:565–579.

Roth-Nebelsick, A., D. Uhl, V. Mosbrugger and H. Kerp. 2001. Evolution and function of leaf venation architecture: a review. Ann. Bot. 87:553–566.

Rozen, S. and H. Skaletsky. 2000. Primer3 on the WWW for general users and for biologist programmers. Methods Mol. Biol. 132:365–386.

Sack, L. and M.T. Tyree. 2005. Leaf hydraulics and its implications in plant structure and function. *In* Vascular Transport in Plants. Eds. N.M. Holbrook and M.A. Zweiniecki. Elsevier/Academic Press, Oxford, pp 93–114.

Sack, L. and N.M. Holbrook. 2006. Leaf hydraulics. Annu. Rev. Plant Biol. 57:361–381.

Sack, L. and K. Frole. 2006. Leaf structural diversity is related to hydraulic capacity in tropical rain forest trees. Ecology 87:483–491.

Sack, L., P.J. Melcher, M.A. Zwieniecki and N.M. Holbrook. 2002. The hydraulic conductance of the angiosperm leaf lamina: a comparison of three measurement methods. J. Exp. Bot. 53:2177–2184.

Sack, L., P.D. Cowan, N. Jaikumar and N.M. Holbrook. 2003. The 'hydrology' of leaves: coordination of structure and function in temperate woody species. Plant Cell Environ. 26:1343–1356.

Sack, L., C.M. Streeter and N.M. Holbrook. 2004. Hydraulic analysis of water flow through leaves of sugar maple and red oak. Plant Physiol. 134:1824–1833.

Sack, L., M.T. Tyree and N.M. Holbrook. 2005. Leaf hydraulic architecture correlates with regeneration irradiance in tropical rainforest trees. New Phytol. 167:403–413.

Sade, N., M. Gebretsadik, R. Seligmann, A. Schwartz, R. Wallach and M. Moshelion. 2010. The role of tobacco Aquaporin1 in improving water use efficiency, hydraulic conductivity, and yield production under salt stress. Plant Physiol. 152:245–254.

Sakr, S., G. Alves, R. Morillon, K. Maurel, M. Decourteix, A. Guilliot, P. Fleurat-Lessard, J.L. Julien and M.J. Chrispeels. 2003. Plasma membrane aquaporins are involved in winter embolism recovery in walnut tree. Plant Physiol. 133:630–641.

Sakurai, J., F. Ishikawa, T. Yamaguchi, M. Uemura and M. Maeshima. 2005. Identification of 33 rice aquaporin genes and analysis of their expression and function. Plant Cell Physiol. 46:1568–1577.

Sakurai, J., A. Ahamed, M. Murai, M. Maeshima and M. Uemura. 2008. Tissue and cell-specific localization of rice aquaporins and their water transport activities. Plant Cell Physiol. 49:30–39.

Sarda, X., D. Tousch, K. Ferrare, E. Legrand, J.M. Dupuis, F. Casse-Delbart and T. Lamaze. 1997. Two TIP-like genes encoding aquaporins are expressed in sunflower guard cells. Plant J. 12:1103–1111.

Savvides A., D. Fanourakis and W. Ieperen. 2012. Co-ordination of hydraulic and stomatal conductances across light qualities in cucumber leaves. J. Exp. Bot. 63:1135–1143.

Scoffoni, C., A. Pou, K. Aasamaa and L. Sack. 2008. The rapid light response of leaf hydraulic conductance: new evidence from two experimental methods. Plant Cell Environ. 31:1803–1812.

Secchi, F., B. Maciver, M.L. Zeidel and M.A. Zwieniecki. 2009. Functional analysis of putative genes encoding the PIP2 water channel subfamily in *Populus trichocarpa*. Tree Physiol. 29:1467–1477.

Sellin, A., E. Ounapuu and P. Kupper. 2008. Effects of light intensity and duration on leaf hydraulic conductance and distribution of resistance in shoots of silver birch (*Betula pendula*). Physiol. Plant. 134:412–420.

Shatil-Cohen, A., Z. Attia and M. Moshelion. 2011. Bundle-sheath cell regulation of xylem-mesophyll water transport via aquaporins under drought stress: a target of xylem-borne ABA? Plant J. 67:72–80.

Thompson, J.D., D.G. Higgins and T.J. Gibson. 1994. CLUSTAL W: improving the sensitivity of progressive multiple sequence alignment through sequence weighting, position-specific gap penalties and weight matrix choice. Nucleic Acids Res. 11:4673–4680.

Trifilò, P., A. Nardini, M.A. Lo Gullo and S. Salleo. 2003. Vein cavitation and stomatal behaviour of sunflower (*Helianthus annuus*) leaves under water limitation. Physiol. Plant. 119:409–417.

Tsuda, M. and M.T. Tyree. 1999. Plant hydraulic conductance measured by the high pressure flow meter in crop plants. J. Exp. Bot. 51:823–828.

Tyree, M.T. and M. Zimmerman. 2002. Xylem structure and the ascent of sap. 2nd edn. Springer, Berlin, 284 p.

Tyree, M.T., A. Nardini, S. Salleo, L. Sack and B. El Omari. 2005. The dependence of leaf hydraulic conductance on irradiance during HPFM measurements: any role for stomatal response? J. Exp. Bot. 56:737–744.

Uehlein, N., C. Lovisolo, F. Siefritz and R. Kaldenhoff. 2003. The tobacco aquaporin NtAQP1 is a membrane CO_2 pore with physiological functions. Nature 425:734–737.

Voicu, M.C. and J.J. Zwiazek. 2010. Inhibitor studies of leaf lamina hydraulic conductance in trembling aspen (*Populus tremuloides* Michx.) leaves. Tree Physiol. 30:193–204.

Voicu, M.C., J.J. Zwiazek and M.T. Tyree. 2008. Light response of hydraulic conductance in bur oak (*Quercus macrocarpa*) leaves. Tree Physiol. 28:1007–1015.

Voicu, M.C., J.E. Cooke and J.J. Zwiazek. 2009. Aquaporin gene expression and apoplastic water flow in bur oak (*Quercus macrocarpa*) leaves in relation to the light response of leaf hydraulic conductance. J. Exp. Bot. 60:4063–4075.

Zelazny, E., J.W. Borst, M. Muylaert, H. Batoko, M.A. Hemminga and F. Chaumont. 2007. FRET imaging in living maize cells reveals that plasma membrane aquaporins interact to regulate their subcellular localisation. Proc. Natl Acad. Sci. USA 104:12359–12364.

Zwieniecki, M.A., P.J. Melcher, C.K. Boyce, L. Sack and N.M. Holbrook. 2002. The hydraulic architecture of leaf venation in *Laurus nobilis* L. Plant Cell Environ. 25:1445–1450.

	*Jr*PIP1;1	*Jr*PIP1;2	*Jr*PIP1;3	*Jr*PIP1;4	*Jr*PIP2;1	*Jr*PIP2;2	*Jr*PIP2;3	*Jr*PIP2;4	*Jr*PIP2;5	*Jr*PIP2;6
***Jr*PIP1;1**	100	85	87	87	64	65	67	67	66	59
***Jr*PIP1;2**	-	100	85	91	67	67	70	68	67	60
JrPIP1;3	-		100	85	67	66	65	64	64	64
***Jr*PIP1;4**	-	-	-	100	66	67	70	67	67	59
***Jr*PIP2;1**	-	-	-	-	100	98	84	78	78	71
***Jr*PIP2;2**	-	-	-	-	-	100	84	78	79	70
***Jr*PIP2;3**	-	-	-	-	-	-	100	80	80	75
***Jr*PIP2;4**	-	-	-	-	-	-	-	100	94	83
***Jr*PIP2;5**	-	-	-	-	-	-	-	-	100	78
***Jr*PIP2;6**	-	-	-	-	-	-	-	-	-	100

Supplementary Figure 1. Amino acid similarity percentages between *Jr*PIP1s and *Jr*PIP2s protein sequences. Percentages were calculated using NCBI bl2seq algorithm.

Supplementary Table 1 List of primers used for PCR experiments

	Forward primer	Reverse primer	Tm (°C)
PIP1DF/PIP1DR	CTCMGGWGGRCACATCAACCC	GMAGDGCAGCDCCAATGAA	52
PIP2DF/PIP2DR	CCTCMGGWGGRCATAAACCC	GMAGDGCAGCDCCGATCAA	52
PIP1GF/PIP1GR	TCAACYAARGGTGATGGCCTTGG	GTTATGGGGATGGTAGCCA	54
PIP2GF/ PIP2GR	GGGTTTGCTGTGTTYATGGT	AATGGNCCAACCCAGAAYATCCA	54
JrPIP1.1	GGCACAGCTGCTCAGACAG	CCCACACTTTTACACTTACTG	60
JrPIP1.2	GGGAGCCGCCAGTACGGA	CCCAACCGAGGTCCTTGTC	52
JrPIP1.3	GGCGCCAATACTATAAGCAAG	ATCATTTAGACTTGAATGGACG	52
JrPIP1.4	TCGACCCAGGTAAAAATAAGTG	CTTACGTACTCGCCCTTCAA	52
JrPIP2.1	GCACTTTGATGTGGTTTGGG	CATGCACGAATGGACTGAGG	58,5
JrPIP2.2	CCCCTCTGCTCACCGATTT A	TAGGCAAATGGACATCCTCG	58,5
JrPIP2.3	GTCCAGAGTTCTGCCCCC	ACTTCTGAAGGAACCTAGAGCCTTA	60
JrPIP2.4	GGTACAAGAAGTCCGGACC	CAGAGTTGGTTCCACCACCAAGTGT	56
JrPIP2.5	CTACAAGAAGTCCGCGGATCC	CTGAGTTGGCTCCGCCACCCTGCGC	52
JrPIP2.6	CATACCAAGACTTCCAACCCC	AAGGACTACCTGCACCCACC	52
18S RNA	GGTGGGGGTGTAATGCCCCC	CGCGGGATTCTGCAATTCAC	52/60

Supplementary Table 2. Species and genebank accession numbers (http://www.ncbi.nlm.gov/) of the PIP1 and PIP2 aquaporin protein sequences used for the phylogenetic analysis.

Arabidopsis thaliana	***At* PIP1;1**	At3g61430	***At* PIP2;1**	At3g53420
	***At* PIP1;2**	At2g45960	***At* PIP2;2**	At2g37170
	***At* PIP1;3**	At1g01620	***At* PIP2;3**	At2g37180
	***At* PIP1;4**	At4g00430	***At* PIP2;4**	At5g60660
	***At* PIP1;5**	At4g23400	***At* PIP2;5**	At3g54820
			***At* PIP2;6**	At2g39010
			***At* PIP2;7**	At4g35100
			***At* PIP2;8**	At2g16850
Fagus sylvatica	***Fs* PIP1;1**	FR605789/FR597323	***Fs* PIP2;1**	FR611152/FR600205
	***Fs* PIP1;2**	FR617635/FR608348	***Fs* PIP2;2**	FR605419/FR604436
	***Fs* PIP1;3**	FR623762/FR604565		
Juglans regia	***Jr* PIP1;1**	FJ971053	***Jr* PIP2;1**	AY189973
	***Jr* PIP1;2**	FJ971054	***Jr* PIP2;2**	AY189974
	***Jr* PIP1;3**	FJ971055	***Jr* PIP2;3**	FJ971056
	***Jr* PIP1;4**	FJ970489	***Jr* PIP2;4**	FJ971057
			***Jr* PIP2;5**	FJ971058
			***Jr* PIP2;6**	FJ971059
Quercus macrocarpa	***Qm* PIP1;1**	ACV70039	***Qm* PIP2;1a**	ACV70052
	***Qm* PIP1;2**	ACV70046	***Qm* PIP2;1b**	ACV70047
			***Qm* PIP2;2**	ACV70053
			***Qm* PIP2;3**	ACV70056
Quercus robur	***Qr* PIP1**	FN752145	***Qr* PIP2;1**	FP053923/FP029419
Populus tremula	***Poptre* PIP1;1**	BU888712/BU892328	***Poptre* PIP2;1**	DN493870/DN487222
	***Poptre* PIP1;2**	BU817536/DN493366	***Poptre* PIP2;2**	BU862423/CK095903
			***Poptre* PIP2;3**	BU891915/BU891176
			***Poptre* PIP2;4**	BU862565/ CK095903
			***Poptre* PIP2;5**	DN496889/CK111120
Populus trichocarpa	***Pt* PIP1;1**	EF147065	***Pt* PIP2;1**	XM_002312916
	***Pt* PIP1;2**	XM_002312111	***Pt* PIP2;2**	EF147341
	***Pt* PIP1;3**	XM_002303560	***Pt* PIP2;3**	XM_002316331
	***Pt* PIP1;4**	XM_002309090	***Pt* PIP2;4**	XM_002311056
	***Pt* PIP1;5**	XM_002323529	***Pt* PIP2;5**	EF148546
			***Pt* PIP2;7**	XM_002322841
			***Pt* PIP2;8**	XM_002313474
			***Pt* PIP2;9**	XM_002327698
			***Pt* PIP2;10**	XM_002327697
Salix alba	***Sa* PIP1;1**	CB185367/CB185332	***Sa* PIP2;1**	CB185374/CB185412
Vitis vinifera	***Vv* PIP1;1**	ABN14347	***Vv* PIP2;1**	AAV69744
	***Vv* PIP1;2**	ABN14348	***Vv* PIP2;2**	ABN14351
	***Vv* PIP1;3**	ABN14349	***Vv* PIP2;3**	ABN14352
	***Vv* PIP1;4**	ABN14350	***Vv* PIP2;4**	ABN14353
	***Vv* PIP1;5**	ABN14355		

Chapitre 2

Implication des aquaporines dans la conductance hydraulique foliaire chez le Peuplier

Implication des aquaporines dans la conductance hydraulique foliaire chez le Peuplier

David LOPEZ, Jean-Stéphane VENISSE, Boris FUMANAL, François CHAUMONT, Esther GUILLOT, Mark DANIELS, Hervé COCHARD, Jean-Louis JULIEN, Aurélie GOUSSET-DUPONT

Cet article fait l'objet d'une soumission au journal *Plant cell physiology*

Contexte

Si de nombreuses espèces ont été identifiées comme présentant une augmentation de leur conductance hydraulique foliaire (K_{leaf}) en réponse à la lumière, peu de choses sont connues sur les variations de ce phénomène à l'échelle de la journée. Dans cette étude, la variation diurne de K_{leaf} a été mesurée *in situ* sur deux clones de peuplier, de façon concommitante à une quantification des transcrits et des protéines d'aquaporines. La contribution de la lumière dans les profils observés est mise en évidence grâce à un lot de plantes placées à l'obscurité forcée.

Résultats

Populus nigra et *Populus trichocarpa* montrent (i) une augmentation de la conductance hydraulique foliaire en réponse à l'éclairement et (ii) un maximum atteint en milieu de journée. En parallèle, parmi les 15 gènes d'aquaporines PIP suivis, 10 sont fortement induits en début de photopériode et présentent une diminution en milieu ou fin de journée pour retrouver leurs niveaux nocturnes. De façon surprenante, certains gènes ne suivent pas cette tendance majoritaire, en particulier *PIP1;4* dont l'expression est fortement inhibée en réponse à l'éclairement et *PIP2;9* qui semble induit à l'obscurité.

Afin d'identifier la contribution de la lumière dans le phénomène, des plantes ont été placées à l'obscurité forcée. Pour la plupart des gènes, la lumière induit un niveau d'expression différent chez les plantes placées à l'obscurité forcée (sauf pour *PIP2;5* et *PIP2;8*). L'expression des transcrits d'aquaporines *PIP* est donc à la fois sous l'influence de la lumière mais également sous un contrôle endogène circadien.

Les profils protéiques confirment le rôle de la lumière dans l'augmentation de la quantité des protèines PIP1 et PIP2 chez ces deux clones. Finalement, K_{leaf} décroit en présence du $HgCl_2$, un inhibiteur métabolique largement utilisé pour inhiber les aquaporines.

Conclusions

Les résultats de cette étude confortent les précédentes données obtenues chez le noyer montrant une forte implication des aquaporines de type PIP dans la perméabilité foliaire vis-à-vis de l'eau. Nous démontrons ici que le peuplier est un modèle adapté à la dissection de l'effet de la lumière sur K_{leaf}. Le problème posé par l'absence de données génomiques fiables est levé. L'utilisation d'inhibiteurs du trafic vésiculaire ou de la voie de signalisation calcique et de la voie Ubiquitine-Proteasome peut donc être réalisée sur cette espèce tel que le suggérent les travaux précédents. La localisation tissulaire des transcrits et des protéines PIP constituera le prochain objectif de cette caractérisation.

Title: Aquaporins And Leaf Hydraulics, New Lights From Poplar

David Lopez [1,2], Jean-Stéphane Venisse [1,2], Boris Fumanal [1,2], Francois Chaumont [3], Esther Guillot [1], Mark J Daniels [4], Hervé Cochard [2,1], Jean-Louis Julien [1,2], Aurélie Gousset-Dupont [1,2]

Authors' addresses :

[1] Clermont Université, Université Blaise Pascal, UMR547 PIAF, BP 10448, F-63000 Clermont-Ferrand, FRANCE.

[2] INRA, UMR547 PIAF, F-63100 Clermont-Ferrand, France

[3] Institut des Sciences de la Vie, Université catholique de Louvain, B-1348 Louvain-la-Neuve, BELGIUM.

[4] Department of Molecular Physiology and Biological Physics, University of Virginia, Charlottesville, VA 22908, USA.

Abstract:

To help understand leaf hydraulic conductance (K_{leaf}) modulation under high irradiance, well-watered poplars (*Populus Trichocarpa* Torr. & Gray ex Hook and *Populus nigra* L.) were diurnally studied at molecular and ecophysiological scales. Transcriptional and translational modulations of PIP aquaporins were evaluated on leaf samples during diurnal time courses. Among the 15 poplar PIPs, a subset of two PIP1s and seven PIP2s are precociously induced within the first hour of the photoperiod concomitantly with a K_{leaf} increase. Since expression patterns were cyclic and reproducible over days, we hypothesized that endogenous signals could be involved in PIP transcriptional regulation. To address that question, plants were submitted to forced darkness during their subjective photoperiod and compared to their control counterparts, which showed that some PIP1s and PIP2s have circadian regulation while others had not. Promoter analysis revealed that a large number of hormone, light, stress response and circadian elements were present. Finally, involvement of aquaporins is supported by the reduction of K_{leaf} by $HgCl_2$ treatment.

Introduction :

Understanding plant-water relations is a challenging research topic, but very worthwhile in the context of global climate change. Water uptake by the root system is driven by transpiration (*E*), which pulls water from the roots to the leaves where it is evaporated. Transpiration is the main driving force for water uptake, leading to the establishment of a water potential (Ψ) gradient through the plant. The process is regulated by stomatal aperture opening or conductance (g_s) and driven by the air water vapour pressure deficit (*VPD*). With a non-limiting water supply, poplar *E* and g_s are highly and positively linked to light availability and intensity (Hinckley *et al.* 1994). Under a limiting water supply, poplar leaf water potential (ψ_{leaf}) and g_s decrease with soil water potential (ψ_{soil}) (Silim *et al.* 2009, Almeida-Rodriguez *et al.* 2010). Leaf hydraulic conductance (K_{leaf}), representing the inverse of leaf resistance to water flux, is also modulated by light quality and intensity (Sellin *et al.* 2008, Scoffoni *et al.* 2008) in various plant models. The Plasma membrane Intrinsic Proteins (PIPs), a plant aquaporin subfamily, is suspected to play notable roles in K_{leaf} modulation (Cochard *et al.* 2007, Voicu *et al.* 2008) since its members have also been shown to influence root hydraulic conductance (Javot and Maurel 2002, Vandeleur *et al.* 2009, Postaire *et al.* 2009).

Aquaporins belong to the ubiquitous Major Intrinsic Protein (MIP) superfamily, a highly conserved family with members in size ranging from 23 to 31kDa (Gomes *et al.* 2009). Higher plants aquaporins are divided into five main subfamilies based on their sequence similarities (Johanson *et al.* 2001), among which PIPs and Tonoplast membrane Intrinsic Proteins (TIPs) are both experimentally shown to increase membrane water permeability (Daniels *et al.* 1994) The Nodulin 26-like Intrinsic membrane Proteins (NIPs) and the Small basic Intrinsic Proteins (SIPs) constitute the two other MIP subfamilies. Recently, X Intrinsic Proteins (XIPs) were identified in some plant and moss species (Danielson and Johanson 2008, Bienert *et al.* 2011). Poplar XIPs appear to be plasma-membrane specific aquaporins with lower water permeability than TIPs and PIPs (Lopez *et al.* 2012).

Among the MIP subfamilies, members of the PIP subfamily are historically the most studied because of their location in plasma membrane and mechanisms of regulation. PIPs form tetramers in which each monomer acts as a functional channel (Chaumont *et al.* 2005). The PIP subfamily is further divided into two groups PIP1 and PIP2. Although residues constituting their selectivity filters are similar, allowing high water conductance, PIP1s and PIP2s have different functions (Wallace and Roberts 2004). Nevertheless, all PIP2s expressed in *Xenopus* oocytes have higher water channel activity than PIP1s. NtAQP1, a tobacco PIP1 is

also associated with mesophyll conductance to CO_2 (Uehlein *et al.* 2003). Aquaporin-mediated water permeability can be modulated through transcription, translation and post-translational modifications and *via* membrane vesicle trafficking (Maurel *et al.* 2008). Gene expression can be influenced by environmental conditions and endogenous plant signals and PIP aquaporins have been shown to be regulated by both. For instance AtPIP1;2, shown to increase cell to cell water transport, is regulated by an endogenous circadian rhythm in roots, by blue light in leaves, temperature, gibberellic acid, abscissic acid, and cytosolic pH (Takase *et al.* 2011, Kaldenhoff *et al.* 1996, Kuwagata *et al.* 2012, Aharon et al. 2003, Tournaire-Roux *et al.* 2003). Previous work carried out on *Samanea saman* (rain tree) showed circadian regulation of leaf PIPs associated with diurnal patterns of water permeability (Moshelion *et al.* 2002). Tetrameric arrangements of PIP1s and PIP2s PIP2s could be an even higher level of aquaporin activity modulation by regulation of vesicular trafficking (Fetter et al. 2004, Zelazny et al. 2007, Mahdieh *et al.* 2008) and increased water transport activity (Secchi *et al.* 2010). Finally, inhibitor studies originally showed decreased water permeability in single cells and also in roots and leaves (Moshellion *et al.* 2002, Wan and Zwiazek 1999, Secchi *et al.* 2009)

Correlations between leaf-water relationships at ecophysiological and molecular levels in the poplar tree model are poorly understood. To investigate potential links, leaf PIP1 and PIP2 transcripts and proteins in well-watered plants were quantified on day and night courses while K_{leaf}, g_s and ψ_{leaf} were measured. PIP expression has already been characterized in roots and stems of the *Populus* genus (Marjanović *et al.* 2005, Secchi *et al.* 2010, 2011, Hacke *et al.* 2010, Almeida-Rodriguez *et al.* 2011, Leng *et al.* 2012). In addition, recent studies investigated leaf aquaporin expression (Almeida-Rodriguez *et al.* 2010) in water-stressed plants. Significantly, little is known of light-dependent PIP modulation in *Populus* leaf tissue. Our paper comprehensively describes light-mediated regulation of PIP transcripts and proteins in leaves of two poplar clones. Furthermore, in light of the conflicting results and conclusions that are given on the hydraulic functions within various species of plants and the involvement of aquaporins, we provide new results for poplar and compile them with available data for the genus. Finally, this work provides a resource for the systematic and detailed investigation of PIP transcripts in poplar, demonstrating success in monitoring 15 PIPs in various hybrids and cultivars including *Populus deltoides* x *P. nigra* (*P. euramericana*), *P. tremula* x *P. alba* and *P. deltoides* (Lopez *et al.* unpublished data).

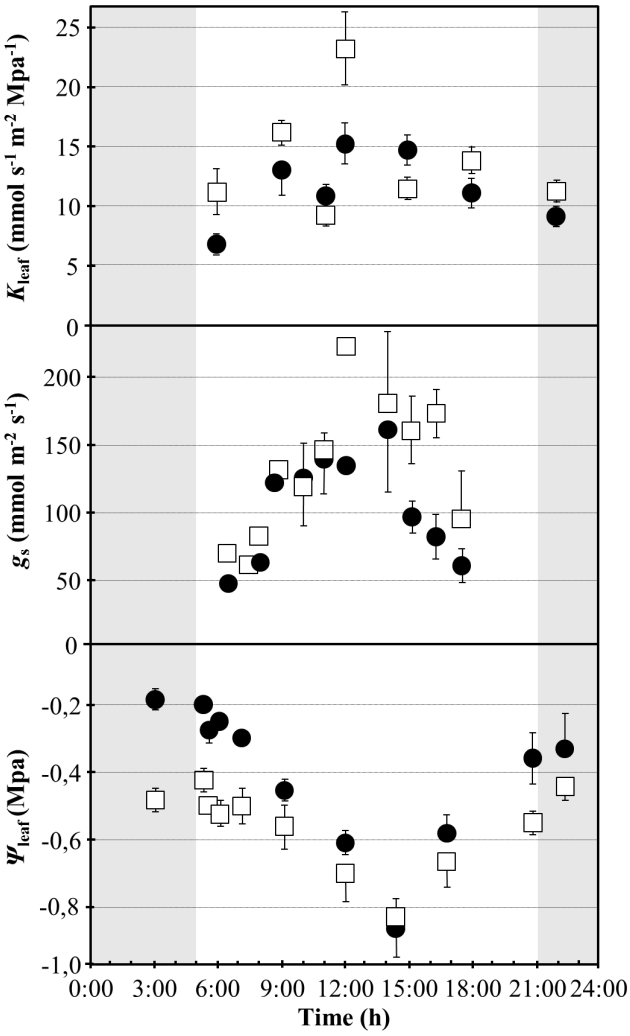

Fig. 1 Diurnal variation of leaf water conductance (K_{leaf}), stomatal conductance (g_s) and leaf water potential (ψ_{leaf}) for P. nigra (closed circles) and P. trichocarpa (open squares). Time of the day in 24 hour (hrs) format is indicated on the x axis. White area represents the 16-hour photoperiod beginning at 5:00h and shaded area the dark period. Results are given as mean ±SE (n ≥ 6 for each measure).

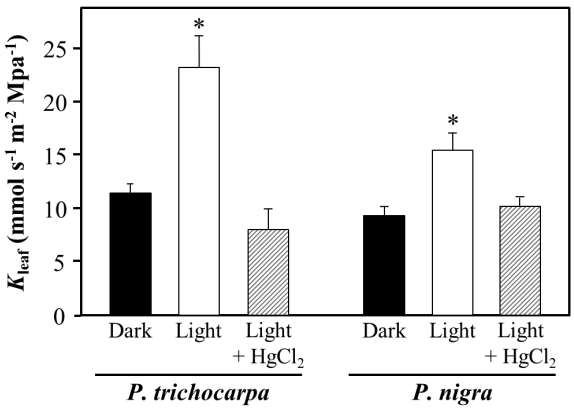

Fig. 2 K_{leaf} of P. nigra and P. trichocapra grown in normal conditions (white bars), in normal light with 1 h perfusion of 1mM $HgCl_2$ (hatched bars), and under darkness until midday (filled bars). Inhibitor treatments were carried out at 12:00h since both clones showed maximum Kleaf at this time of the day. Values at 23:00h are given to compare light dependent Kleaf increase and its relative reduction using $HgCl_2$. Results are given as means ±SE (n=14 per clone) asterisks indicate statistically significant differences ($p<0.05$, Tukey post hoc test after one-way Anova).

Results

Leaf hydraulics of *Populus* clones

Leaf hydraulic conductance (K_{leaf}), leaf water potential (ψ_{leaf}) and stomatal conductance (g_s) were measured daily on greenhouse potted clones of *P. trichocarpa* and *P. nigra* (Figure 1). We observed that two species had qualitatively and quantitatively similar ecophysiological behaviours. Under non-limiting water supply and irradiance, both showed relatively conserved hydraulic patterns over time. Both reached their lowest ψ_{leaf} (-0.83 ±0.06 MPa for *P. trichocarpa* and -0.81 ±0.1 MPa for *P. nigra*) between 12:00h and 14:00h, which corresponded to midday solar time. Even in non-limiting water supply conditions, *P. trichocarpa* reached a relatively low predawn ψ_{leaf} at -0.48 ±0.03 MPa while *P. nigra* predawn ψ_{leaf} was higher at -0.18 ±0.01 MPa. Both species also had very similar g_s during the day with a maximum at midday. *P. trichocarpa* clones have greater gs than *P. nigra* ones in the afternoon. Using High Pressure Flow Meter (HPFM) in the greenhouse to measure K_{leaf}, we observed that both clones showed an initial K_{leaf} increase during the morning followed by a depression at 11:00h. *P. nigra* clones then showed a limited K_{leaf} increase while *P. trichocarpa* clones showed a sharp increase up to midday. From 6:00h to 12:00h, *P. trichocarpa* and *P. nigra* leaves had an average K_{leaf} increase of 107.9%. and 120.9% respectively. From 12:00h to 23:00h, *P. trichocarpa* and *P. nigra* leaves experienced a 51.5% and 40.3% K_{leaf} decrease, respectively, reaching values similar to those measured at 6:00h.
$HgCl_2$, an aquaporin inhibitor was used in order to determine the part of K_{leaf} that could be attributed to aquaporin activity. Leaves were perfused with 1mM HgCl2 at midday (12:00h), during the period of maximum water flux. After one hour of treatment, *P. trichocarpa* and *P. nigra* K_{leaf} was reduced by 66.6% and 27.7%, respectively (Figure 2).

PIP1 and PIP2 gene expression is regulated diurnally in poplar

Predawn leaves (3:00h) were used as a reference point to study by RT-QPCR *PIP* gene expression modulation diurnally. The short-term responses of PIP expression to light was investigated by sampling leaves at 15, 30, 60 and 120 minutes after the beginning of photoperiod (5:00h). Mid and long-term responses were evaluated by sampling at midday, in the afternoon (18:00) and during the following night (21:30 and 23:00, Figure 3). The poplar genome encodes 15 PIPs including 5 PIP1s and 10 PIP2s, which were all included in this experiment. Interestingly, for most isoforms RNA expression patterns were well conserved between *P. trichocarpa* and *P. nigra* clones. Among PIP1s, *PIP1;1* expression was rapidly and highly upregulated reaching a maximum at midday, and then dramatically downregulated

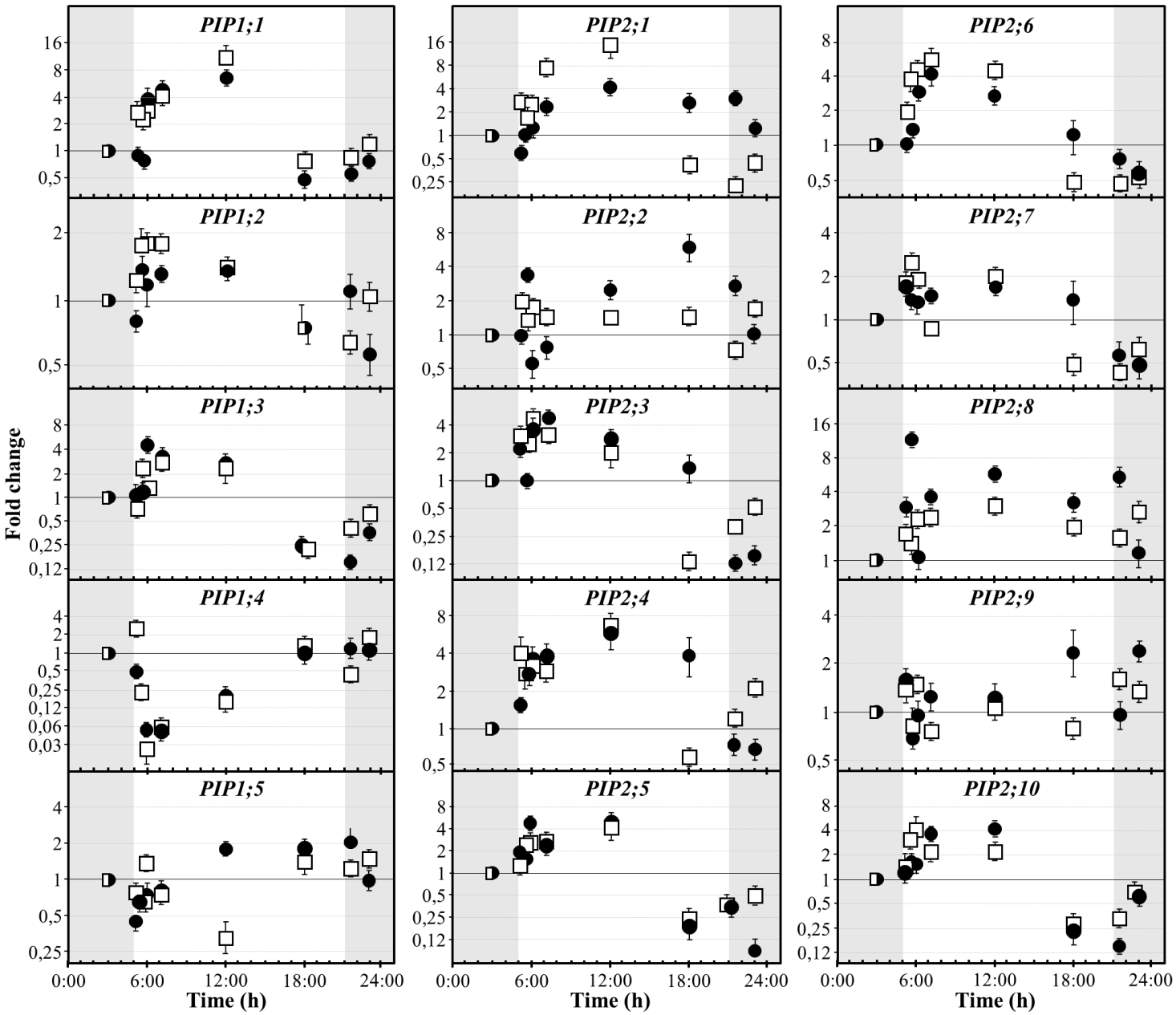

Fig. 3 Poplar *PIP1* and *PIP2* diurnal RNA expression patterns in leaves of *P. nigra* (closed circles) and *P. trichocarpa* (open squares). The 16 hour photoperiod, represented by the white area, starts at 5:00h and ends at 21:00h. Dark period shown as the shaded area. Expression levels are given as the relative fold change of each *PIP* transcript compared to t=0 (3:00h) value using the $2^{-\Delta\Delta Ct}$ method. Data are represented as mean ± SE (n=3 to 6).

to reach the predawn expression level in the afternoon. *PIP1;3* mRNA level also increased in the morning but to a lesser extent, and then also decreased in the afternoon. *PIP1;4* expression was strongly repressed starting 30 minutes after photoperiod onset. Its expression then steadily increased during the afternoon to reach predawn level. *PIP1;2* and *PIP1;5* levels remained stable in this experiment. Similarly, most PIP2s showed diurnal patterns of transcriptional regulation. Seven (*PIP2;1*, *PIP2;3* to *PIP2;6*, *PIP2.8* and *PIP2;10*) were rapidly induced in the morning for both *P. nigra* and *P. trichocarpa. PIP2;7* and *PIP2;9* diurnal modulation was significantly less important reaching a maximum twofold increase by midday. *PIP2;2* expression was slightly modulated in *P. trichocarpa* while in *P. nigra* this isoform is initially induced, followed by a decline with a second peak in the afternoon.
Some minor discrepancies in the overall conservation of diurnal transcription patterns between the two clones could be observed at different time points; and more specifically at 18:00h for *PIP1;5* and for most PIP2s. However, physiological patterns were similar for the two clones at this time of the day.

Light effect on leaf hydraulics and PIP expression

To identify whether *PIP* expression patterns were induced by light or by endogenous factors, "dark plants" were artificially maintained under full darkness until midday. Leaf water potential of dark plants remained steady during the course of the experiment. Midday ψ_{leaf} for dark plants was similar to the predawn value (*P. trichocarpa*: -0.34 ±0.1 MPa; *P.nigra* -0.15 ±0.06 MPa; both $p<0.001$), likely due to the absence of substantial transpiration. PIP expression of dark plants was then compared to plants grown under normal light conditions (Figure 4). *PIP1;1* and *PIP1;3*, expression was strongly induced in control plants while dark plants showed a slight variation in relative transcript abundance. *PIP1;4,* strongly downregulated during the morning in control plants showed little variation in dark plants. *PIP2;1*, *PIP2;3*, *PIP2;4* and *PIP2;6* were more strongly induced in control plants, although *P. nigra PIP2;4* mRNA was more abundant in the late morning. *PIP2;5*, *PIP2;8* and *PIP2;10* were upregulated in dark plants as in control plants. *PIP1;5, PIP2;2* and *PIP2;7* transcript levels do not vary diurnally with either treatment. Interestingly, *PIP2;9* appears to be a dark-induced isoform, which is also indicated by the relatively high expression levels found in the evening (Figure 3).

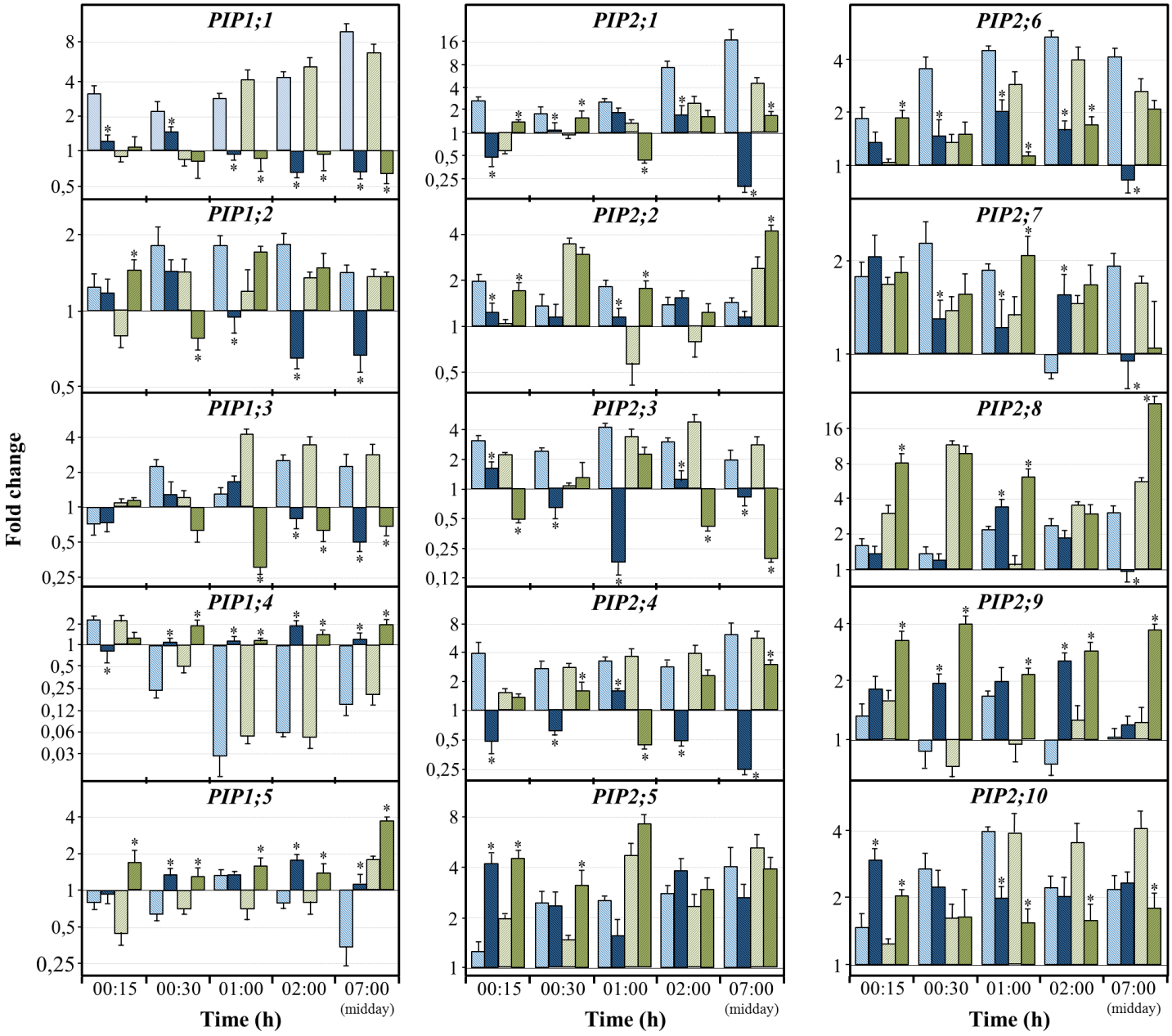

Fig. 4 Leaf poplar *PIP1* and *PIP2* RNA expression patterns in *P. nigra* (green bars) and *P. trichocarpa* (blue bars) submitted to forced darkness (dark couloured bars) compaired to their normal light counterparts (light coloured bars). Relative transcript accumulation is given at 15, 30, 60 and 120 minutes after photoperiod onset (5:00h) and at 12:00h. Levels are given as the relative fold change of each *PIP* compared to t=0 (3:00h, predawn) value using the $2^{-\Delta\Delta Ct}$ method. Data is represented as mean ± SE, (n=4) asterisks indicate statistically significant differences ($p<0.05$, Student t-test).

PIP proteins accumulates during the day

Ultimately, *PIP* transcripts will be translated into proteins, which will act as functional channels once trafficked to plasma membrane. Since the levels of PIP transcripts and proteins are not always correlated (Hachez *et al.* 2012), it is of great interest to evaluate the amount of the related proteins. Leaf samples from the two clones growing in normal light condition and forced darkness were harvested at predawn (3:00h, PD) and at midday (12:00h, MD and CDMD). Figure 5 shows that *P. trichocarpa*, and to a lesser extent *P. nigra*, an accumulation between PD and MD of a single PIP1 product at ~30 kDa, which corresponds to the predicted size of poplar PIP1s. For both species, the amount of protein recognized by the PIP1 antibody was lower at PD or CDMD than at MD. PIP2 antibody labelling revealed proteins corresponding to the size of PIP2 monomers and dimers (~30 kDa and ~58 kDa respectively, Bienert *et al.* 2012). Compared to PD and CDMD, MD levels of PIP2s did not change in *P. trichocarpa* but showed a MD peak in *P. nigra*. Observed levels of apparent PIP dimers followed the abundance of the monomer during these experiments.

Sequence analysis

The average amino–acid similarity between *PIP1;1* and *PIP1;3* is very high (95.5% pairwise identity) suggesting they are duplicates or paralogs. *PIP2;5* and *PIP2;10* have highly conserved sequences (98.3% pairwise identity) and also show similar transcriptional modulation in our experiments (Figure 3 and 4). The proximity of the two genetic loci (Potri.006G128000 and Potri.006G128200) further supports the hypothesis of a gene duplication event. Such gene clustering is not unique in the PIP family and other highly homologous PIP2s are located in proximity to another (Supplemental Table 1), although *PIP2;8* and *PIP2;9*, are largely divergent (65.9% pairwise id., resp. Potri.005G109300 and Potri.005G109200). *PIP1;4* (Potri.06G098100) is located close to a PIP1 pseudogene (Potri.06G097900) coding a premature stop codon. Duplication events usually lead to either loss of function for one of the duplicates, neo functionalization, or function overlapping (Conant and Wolfe 2008), and such events have been documented for poplar XIPs (Lopez *et al.* 2012).

Studying a fully sequenced model plant allows the study of non-expressed sequences, particularly those forming promoter domains. We analysed ~1.5 kb upstream of the initiation codons of the 15 poplar PIPs, two *Arabidopsis thaliana* PIPs (*AtPIP1;2* and *AtPIP2;1*) and four *Zea mays* PIPs (*ZmPIP1;1*, *ZmPIP1;5*, *ZmPIP2;1* and *ZmPIP2;5*), all of which are well characterized and known to have circadian regulation patterns (Takase *et al.* 2011; Lopez *et*

Table 1 Putative CIS-acting sequences detected by PLACE signal scan on 1.5kb proximal promoter region of 15 *P. trichocarpa* , 2 *A. thaliana* and 4 *Z. mays* PIPs.

		PIP1.1	*PIP1.2*	*PIP1.3*	*PIP1.4*	*PIP1.5*	*PIP2.1*	*PIP2.2*	*PIP2.3*	*PIP2.4*	*PIP2.5*	*PIP2.6*	*PIP2.7*	*PIP2.8*	*PIP2.9*	*PIP2.10*	*AtPIP1;2*	*AtPIP2;1*	*ZmPIP1;2*	*ZmPIP1;5*	*ZmPIP2;1*	*ZmPIP2;5*
Light	EBOXBNNAPA (S000144)	8	2	8	10	12	8	6	6	10	2	12	4	10	10	4	10	2	10		12	
	GATABOX (S000039)	12	13	11	7	12	10	5	12	3	10	8	8	7	18	8	12	15	4	10	12	5
	GTTCONSENSUS (S000198) / GT1CORE (s000125)	11	9	18	20	13	6	12	23	10	8	14	6	11	20	6	13	14	3	7	16	9
	IBOX (s000124) / IBOXCORE (S000199) / IBOXCORENT (S000199)	3	10	3	3	5		3	9	1	7	3	3	3	10	3	9	4	2	5	6	4
	INRNTPSADB (s000395)	5		2	3	4	3	1	12	2		1		2		1	1	2	1		6	1
	TBOXATGAPB (s000383)	1					1				2	1	2			1		1				1
Light / PhyA	SORLIP1AT (s000482) / SORLIP2AT (s000483) / SORLREP3AT (s000488) / SORLIP5AT (s000486)	3	2	3	5	1	2	3		3	1	5	2		1	2	2	3	2	10	2	6
Phytochrom	REALPHALGLHCB2I(s000362) / REBETALGLHCB21 (s000363)		1	1				3	1	1	1	2		2	5	4		2			1	
	count	43	36	45	48	47	30	30	62	29	30	44	25	33	59	25	47	41	12	42	42	38
Light / Circadian	-10PEHVPSB (s000392)	1	3			1	2			1	1	1	1	2								2
	CLACADIANLELHC (S000252)	2		1	2	1	1		5		1		1	1	2				1	2		
	count	3	3	1	2	2	3		5	1	2	1	2	3	2				1	2	2	2
ABA	ABRELATERD1 (s000414) / ACGTABREMOTIFA2OSEM (S000394) / DPBFCOREDCDC3 (s000292)	2	3	1	3	3	4	1	1	1	2	7	3	3	1	2		1	1	4	1	6
ABA / CA2+	ABRERATCAL (s000507)						1	1	1			2	1	1	1							3
ABA / WS	DRE2COREZMRAB17 (s000402)	1		1	1	1		1			1	1						1	1	1		1
MYB / ABA / Water stress	MYB1AT (S00408) / MYB2AT (S000177) / MYBATRD22 (S000175) / MYBCORE (s000176) / MYB2CONSENSUSAT (S000409)	10	2	9	3	11	10	14	4	5	12	4	5	5	10	2	3	5	3	9	3	14
MYC / ABA / Water stress	MYCATERD1 (S000413) / MYCATRD22 (S000174) / MYCCONSENSUSAT (s000407)	10	2	10	12	18	12	8	10	10	2	12	4	12	16	6	14	4		10	11	18
Water stress	CBFVII s(000497)	3		1	1	1					1	1	1					2	2	1		1
	count	26	7	22	20	34	27	25	16	16	17	27	14	21	28	10	17	13	7	25	15	43

Fig. 5 Western blot of microsomal proteins from leaves of P. trichocapra and P. nigra separated by SDS-PAGE and immunolabeled using PIP1 or PIP2 antisera. Protein was extracted from plants at predawn (PD, 3:00h), midday (MD, 12:00h), and midday on plants submitted to continuous darkness (CDMD, 12:00h). Unlike the PIP1 antisera, the PIP2 antibodies labelled probable dimers of ~60 kDa.

al. 2003). *In silico* analysis showed the regions upstream of poplar PIPs had putative response elements for virtually all plant hormones, including abscissic acid, salicylic acid, auxin, cytokinins, gibberelins, jasmonate, ethylene, and sugars, as well as to abiotic stress responses such as wounding, dehydration and cold. Since our interest is in diurnal leaf water relations, we focused on promoter elements putatively associated with drought and light responses (Table 1). Poplar PIPs have a substantial number of ABRE abscissic acid responsive elements as well as Myb and Myc response elements associated with water stress and drought. Numerous putative light response units (LRUs) were found, especially in PIP2;3, which correlates with our results showing that all poplar PIPs respond to light.

Discussion

The aim of this work was to characterize the diurnal modulations of leaf water permeability in poplar and the involvement of aquaporins in this process. Before commencing an analysis of poplar PIP1 and PIP2 gene and protein expression, it was necessary to correctly identify these using the current PIP nomenclature. In previous studies of poplar aquaporins, various overlapping AQP nomenclatures were created as occurred in *Arabidopsis* and other plants. In our work we use the original poplar PIP nomenclature presented by Secchi *et al.* (2009), which is consistent with the seven sequences originally released by Marjanović *et al.* (2005). Supplemental Table 1 lists the various aliases for the 15 poplar *PIP* genes along with their corresponding genomic loci in the newly released *P. trichocarpa* v3.0 annotation.

Diurnal regulation of poplar leaf hydraulics

To ensure that our results were informative, we generated control plants grown with non-limiting water and light availability. Control samples provide physiologists with the appropriate context for any investigation of a biological process. Regardless of any treatment, organisms used as experimental controls adjust themselves physiologically to their environmental conditions, particularly in response to their circadian rhythm(s). Therefore, instead of using our untreated plants as simple negative controls, their physiological responses were carefully analyzed. Leaf water potential was measured to ensure plants had a sufficient water supply, to avoid stomatal closure and concomittantly reduced leaf water flow and transpiration. In our experiments, when the water supply was non-limiting, the result was a relatively high midday ψ_{leaf} and an increase in diurnal K_{leaf}. Water-stressed plants tend to decrease the former and inhibit the latter (Aasamaa *et al.* 2005). Predawn ψ_{leaf} values

obtained in our experiments are in agreement with what is typically observed in non-stressed greenhouse poplars grown in pots (Cocozza *et al.* 2010; Awad *et al.* 2010; Larchevêque *et al.* 2011). These values were also close to those reported for plants grown in low to high irradiance (Almeida-Rodriguez *et al.* 2011). The relatively high predawn ψ_{leaf} observed with *P. trichocarpa* could be explained by relatively high night transpiration, which has been reported for this species in the field (Snyder *et al.* 2003). Supporting this is the observation of substantial night sap flow in *P. trichocarpa* X *P. deltoides* trees (Meiresonne *et al.* 1999).

Despite relatively similar hydraulic characteristics while not under stress, our two poplar clones differ remarkably in their susceptibility to xylem cavitation. *P. nigra* and *P. trichocarpa* are one of the least and one of the most susceptible species in the genus, respectively. Xylem embolism susceptibility is generally associated with decreased xylem conductivity. Given a sufficient water supply, having K_{leaf} positively linked with g_s diminishes the tension imposed on the water column and allows ψ_{leaf} to be maintained above the threshold value below which cavitation risks increase (Tyree *et al.* 2005).

Experimental evidence of diurnal variations in K_{leaf} of various plant species have led to conflicting conclusions. Measured *in situ*, our two poplar clones diurnally increased K_{leaf} as do bur oak (Voicu and Zwiazeck 2011) and sunflower (Tsuda and Tyree 2000) *Platanus orientalis* and *Aleurites moluccana* leaves (Lo Gullo *et al.* 2005). These results contrast with either steady or declining values in other species (*Pinus ponderosa*, *Pinus nigra*, *Castanopsis chrysophylla*, *Pieris japonic*a) as reviewed in Johnson *et al.* (2009, 2012). This scenario suggests that poplar can increase bulk leaf water permeability in response to evaporative demand when water availability is not limiting, as hypothesized by Tsuda and Tyree (2000). It is also consistent with previous studies that have shown increased $K_{leaf,}$ with high irradiance in various tree species (Sack *et al.* 2002, Cochard *et al.* 2007*,* Scoffoni *et al.* 2008, Voicu *et al.* 2008, Ben Bâaziz *et al.* 2012).

Unlike the apoplastic component of K_{leaf}, regulation of the cell-to-cell pathway involves membrane permeability, potentially via aquaporins. However, it is difficult to link K_{leaf} to specific aquaporin isoforms and expression patterns. While no parallel was found between the expression of four PIPs and the K_{leaf} response in bur oak (Voicu *et al.* 2009), we recently demonstrated an increase in K_{leaf} upon leaf illumination in *Juglans regia*, *Fagus sylvatica*, *Quercus robur* and *Populus tremula* that correlated with the differential regulation of *PIP1* and *PIP2* expression, depending on the species (Ben Bâaziz *et al.* 2012).

Roles of PIPs in plant-water relations

PIP aquaporin expression appears to follow species-specific patterns that are dependent on environmental conditions. During water stress, aquaporin transcription is either upregulated (*Nicotiana glauca* leaves, stem and roots, Smart *et al.* 2001, Hachez *et al*. 2012) or downregulated (*Arabidopsis thaliana* rosette, Alexandersson *et al.* 2005). While double antisense transgenic *A. thaliana* with reduced PIP1 and PIP2 levels show no difference in g_s, transpiration, ψ_{leaf}, K_{leaf} and K_{root} under non-limiting water supply or water deficit, drought recovery after rewatering was faster for wild-type plants than for transgenic ones (Martre *et al.* 2003). This strongly suggested that PIPs play a role in embolism refilling (Sakr *et al.* 2003, Secchi and Zwieniecki 2010, Perrone *et al.* 2012). Subsequent water stress experiments conducted on different poplar clones have clarified the involvement of aquaporins. Overall, a relative increase in PIP content was found in roots, stems and leaves of stressed plants (Almeida-Rodriguez *et al.* 2010 and 2011, Secchi and Zwieniecki 2010, Leng *et al.* 2012). It was hypothesized from stem expression patterns that *PIP1;1* and *PIP1;3* could play a role in embolism repair in *P. trichocarpa* (Secchi and Zwieniecki 2010). In *P. alba x P. glandulosa* stems and *P. balsamifera* x *P. simonii* leaves, the orthologs of these two genes are also induced in plants submitted to water-stress and recovery, further supporting the importance of the two genes in water-stress responses (Leng *et al.* 2012, Almeida-Rodriguez *et al.* 2010). We also observed a substantial increase in the transcription of these genes at midday. Since the leaves were de-petiolated after water potential measurements and prior to gene expression assays, the observed modulations only involve lamina parenchyma and vessels and hence do not relate to possible responses to diurnal petiole embolism recovery (Zufferey *et al.* 2011, Perronne *et al.* 2012). *PIP2;5* and *PIP2;10* orthologs, previously identified in *P. tremula* x *P. tremuloides*, *Q. macrocarpa* and *J. regia* are also thought to play a central role in leaf water relations (Marjanović *et al.* 2005, Voicu *et al.* 2009, Cochard *et al.* 2007, Ben Bâaziz *et al.* 2012). The daily variation in K_{leaf} experienced by the two poplar clones is associated with a substantial water flux capacity that must be supported by an accordingly high fluid reservoir in order to prevent hydraulic failure (Muries *et al.* 2011, Blackman and Brodribb 2011). These reservoirs yet remain to be spatially and temporally characterized.

Light and circadian regulation of poplar PIPs

Only few studies reports plant aquaporin promoter structure (Kaldenhoff *et al.* 1996, Yamada *et al.* 2000, Li *et al.* 2009, Tungngoen *et al.* 2009). Our analysis of poplar *PIP* promoters revealed a large number of hormone, stress and light response elements (Table 1).

Comparative analysis of *Arabidopsis* and maize *PIP* promoters showed that they also contain a large number of light, ABA and water stress response elements. Cis elements putatively involved in circadian regulation, present in virtually all poplar *PIP*s, did not corroborate all results arising from forced obscurity. Since these cis elements are missing in *Arabidopsis PIPs* and *ZmPIP1;1,* we hypothesize that other elements of these promoters are involved in *PIP* circadian regulation.

Our experiments with dark-morning plants showed that most of the variations in *PIP* expression are different than those in plants growing in normal light conditions, suggesting that they are independent of circadian regulation and associated with events occurring in full sunlight (*i.e.* high water flow, embolism recovery, CO_2 mesophyll conductance). *PIP1;1* and *PIP1;3* expression was induced in roots in response to increased evaporative demand in *P. trichocarpa* x *P. deltoides. PIP1;1* was also found to be induced in response to hormones and various abiotic stresses in leaves and cell cultures (Bae *et al.* 2011). Our experiments suggest a greater role for *PIP1;1* and *PIP1;3* in the leaf light response.

Several PIP2 isoforms merit special attention. *PIP2;5* was expressed independently of the presence or absence of light and could be under circadian regulation in leaves (Figure 4). Similarly, the expression of *PIP2;8* is to some extent also under endogenous regulation. In *P. deltoides* leaves, circadian expression of *PIP1;1* and *PIP2;6* was reported (Matsubara *et al.* 2005). In our clones, only *PIP2;6* was notably induced when plants were submitted to forced darkness, but not *PIP1;1*. However, we cannot rule out whether the differences in *PIP* expression between normal and dark-morning plants are induced by light as a signal *per se*, or are a consequence of the transpiration triggered by the photoperiod. Having said that, the most early time points of the kinetics (i.e. 15, 30 min) are not subject to controversy since the greenhouse VPD is not statistically different between predawn and up to one hour after the beginning of the photoperiod (0.59 kPa, $p>0.001$). Circadian variations in the expression of aquaporin genes and proteins have already been demonstrated in various plant models in both roots (*Zea maïs*, Lopez *et al.* 2003; Hachez et al., 2012; *A. thaliana,* Takase *et al.* 2011) and leaves (*Zea maïs*, Hachez *et al.* 2008), and were consistently associated with increased water permeability.

The water channel activities of poplar PIPs have been functionally characterized by heterologous expression in *Xenopus* oocytes (Secchi *et al.* 2009, Secchi and Zwieniecki 2010, Almeida-Rodriguez *et al.* 2010). When expressed alone, *PIP1;1* does not increase the water permeability of the oocyte membrane whereas all PIP2s do. However, the co-expression of *PIP1;1* and *PIP2;4* leads to a greater water permeability than *PIP2;4* expressed alone (Secchi

and Zwieniecki 2010). This synergistic interaction between PIP1s and PIP2s has been reported in various species (Fetter *et al.* 2004, Vandeleur et al. 2009, Bellati *et al.* 2010). However, the functional relevance of these hetero-oligomers remains to be established *in planta*.

Role of PIP proteins in K_{leaf}

In *A. thaliana*, both rosette water conductance (K_{ros}) and aquaporin mRNA expression are under circadian regulation; furthermore, K_{ros} is sensitive to aquaporin inhibitors (Postaire *et al.* 2010). The aquaporin inhibitor $HgCl_2$ has been reported as a K_{leaf} inhibitor in a wide range of plants (*Helianthus annuus*, Nardini *et al.* 2005; *Glycine max*, Sadock and Sinclair 2010; *P. tremuloides*, Voicu *et al.* 2010; *A. thaliana*, Shatil-Cohen *et al.* 2011). Furthermore, this inhibitor was found to reduce the water permeability (P_f) of oocytes expressing poplar PIP2 aquaporins (Secchi *et al.* 2007, 2009). In our work described here, $HgCl_2$ induced a decrease in K_{leaf} for leaves of both *P. nigra* and *P. trichocarpa* to levels comparable of dark ones, showing the involvement of mercury-sensitive components such as aquaporins in high diurnal K_{leaf} variations.

Immunoblots using promiscuous PIP1 and PIP2 antibodies showed differences in PIP protein levels in microsomal fractions from plant leaves taken at predawn, at midday and at midday in dark-morning plants. Since these antibodies recognize either multiple PIP1 or PIP2 isoforms, our experiments only allow for the observation of trends in levels of PIP1 and PIP2. However, both anti-PIP1 and anti-PIP2 targets were less abundant in *P. nigra* dark-morning plants than in midday or predawn control plants. Levels of *P. trichocarpa* PIP1 and PIP2 proteins appeared to be less subject to modulation, which could be associated with a less tightly regulated water exchange in the leaves of this species. Nevertheless, PIP2 proteins accumulated in response to light, for *P. nigra* and to a lesser extent for *P. trichocarpa.* Taken as a whole, our immunolabeling results suggest that PIP1 and PIP2 proteins are subject to diurnal turnover in poplar leaves, and these results correlate with our observations of *PIP* transcript levels. Interestingly, previous work showed a lack of correlation between RNA and protein levels (Muries *et al.* 2011, Hachez *et al*. 2012). Given the metabolic cost of *de novo* protein synthesis, it remains intriguing why poplars promote such high transcription and translation levels of PIP aquaporins diurnally instead of regulating them at the protein level (*e.g.* protein activity, vesicle trafficking); more information needs to be obtained about the stability and localisation of these proteins.

Conclusion

PIP aquaporin expression in *P. trichocarpa* and *P. nigra* follows complex patterns, not only in response to light but also to other endogenous factors (Figure 4 and 5). Increased expression levels during the day could therefore result in an increase in water permeability to supply high K_{leaf} while the specifically induced expression of *PIP2;9* in forced darkness could occur as a compensatory mechanism. Based on our observations, we hypothesize that PIPs are regulated via fine adjustments in the levels of transcripts and proteins in response to varying environmental conditions.

Water flux in leaves of *P. nigra* and *P. trichocarpa* are very similar, both at the ecophysiological level and also qualitatively and quantitatively at the molecular level when looking at diurnal and forced darkness expression patterns. The two species diurnally increase leaf water permeability in similar fashion when grown with a non-limiting water supply. Our results also show that non-stressed plants experience concomitant variations in their aquaporin levels. Under control conditions, it is striking how well conserved the expression patterns of the PIP1 and PIP2 orthologs are between the two species. This remarkable conservation can reasonably be associated to the conservation of underlying regulatory mechanisms that are fundamental to the *Populus* genus.

Our results indicate that in poplar the high levels of K_{leaf} under light involves both PIP1 and PIP2 aquaporins. Given that water and CO_2 fluxes are linked to the photosynthetic process and that aquaporins serve to facilitate the movement of these molecules, the tissue-specific location (e.g. parenchyma, stomata, vascular-associated cells) and contribution of each PIP1 and PIP2 isoform remains to be determined.

Material and Methods

Plant material and experimental design

Populus trichocarpa (Torr. & ray ex Hook) clone INRA 101-74 *and Populus nigra* L. clone INRA 71072-501 seedlings were provided by Dr. Catherine Bastien (INRA, Orléans, France). Homogenous 25 cm long cuttings were planted in 20 l pots filled with commercial substrate (40% Black, 30% brown and 30% blond peat moss, pH 6.1, DUMONA-RN 75-3851, Arandon, the Netherlands) and grown in a controlled-environment greenhouse (Blaise Pascal University, Clermont-Ferrand, France) under a 16-h light /8-h dark photoperiod, at 18/22 °C (night /day), with the relative humidity set at 70±10% and a daytime photosynthetic photon flux kept at ≥ 350 µmol m^{-2} s^{-1} using 400W Master son-T Pia Hg-Free lamps (Phillips, Suresnes, France). Pots were automatically watered by drip irrigation, maintaining daily field

capacity. To achieve forced darkness, an enclosure was placed over four plants of each clone in the greenhouse and leaves were sampled behind a curtain to shield plants from illumination. Statistical analyses were conducted using the R software package (http://www.R-project.org/, R Development Core Team).

Leaf water potential, stomatal conductance, leaf water conductance

Leaf water potential (ψ_{leaf}) was determined using a Scholander pressure chamber (PMS, Corvallis, OR, USA) at pre-dawn as a proxy of soil water potential, and during diurnal time courses. For each biological replicate, ψ_{leaf} values were obtained averaging three successive measurements on leaves of different plants. Leaves were depetiolated and immediately frozen in liquid nitrogen for subsequent expression assays. Stomatal conductance (g_s) was recorded using a LI-1600 leaf porometer (Li-Cor, Lincoln, NE, USA). Leaf hydraulic conductance was measured in the greenhouse by the High Pressure Flow Meter method (HPFM, Cochard *et al.* 2007). Briefly, deionized degassed water was pushed into the petiole of an excised leaf under positive pressure (P, MPa), and the water flow (F, mmol s^{-1}) was recorded with a computer connected to the HPFM apparatus. Leaf hydraulic conductance (K_{leaf}, mmol s^{-1} m^{-2} MPa^{-1}) was calculated as $K_{leaf} = F / (P \times LA)$, where LA is the leaf area (m^2), measured using an ImageJ macro written by Eric Badel (INRA, Clermont-Ferrand, France) after scanning (n=49 for each clone). Inhibitor experiments were carried out at midday when K_{leaf} values were the highest. For inhibitory experiments, deionized water with 1mM $HgCl_2$ was pushed for 1 h at 0.2 MPa into petioles of illuminated leaves and the relative reduction in K_{leaf} was calculated at the end of each measurement (n=14, per clone).

RNA isolation, PIP gene expression kinetics

Total RNA from leaf depetiolated was extracted according to Chang *et al.* (1993). First-strand cDNA was then synthesized from 1µg of total RNA using SuperScript III (Invitrogen, Carlsbad, CA, USA) following manufacturer instructions. Real-time PCR was performed using a MyiQ instrument (Bio-Rad, Hercules, CA, USA) with MESA GREEN qPCR MasterMix Plus (Eurogentec, Seraing, Belgium) containing 2µl of 20-fold diluted cDNA. PCR was started with an initial denaturation at 94°C for 3 min, followed by 40 cycles of amplification (94°C for 20s, then 54°C (*PIP1s*) or 58°C (*PIP2s*) for 20s, then 72°C for 20s). PCR efficiency was 100±2% for all primer pairs and specificity was checked using melting curves. The threshold cycle for each reaction (Ct) was determined using the Bio-Rad iCycler iQ v2.0 software. Gene expression was measured according to Livak and Schmittgen (2001)

and determined as the fold change of an isoform at a given time point relative to its expression at the initial predawn time point (t_0=3:00h). The normalisation of target gene expression was achieved using the software application BestKeeper v1 (http://www.gene-quantification.info; Pfaffl *et al.* 2004), first to determine the most suitable reference genes from nine widely used housekeeping genes (Czechowski *et al.,* 2005; Xu *et al.,* 2011), and then to estimate a BestKeeper Index, which is the geometric mean of most stable housekeeping genes and used as calibrator. The reference genes selected (*Actin1* Potri.001G309500, *SAND* Potri.009G014400, *TIP41-like* Potri.009G093200, *UP1* Potri.002G127700 and *EF1-α* Potri.010G309500) were chosen from different protein families in order to reduce the possibility of co-regulation. PIP primers were designed in order to be specific to a given isoform but usable on the most poplar species possible. To do so, all available PIP ESTs available for *Populus* (taxid 3684) were retrieved using BLASTn (Altschul *et al.* 1997) and aligned with ClustalW (Thompson *et al.* 1994) using the *P. trichocarpa* PIP sequences as references. Conserved regions between orthologs in the genus were targeted for primer design. All primers used for this study were designed with the Primer3plus application (http://www.bioinformatics.nl/primer3plus, Untergasser *et al.* 2007) and are listed in supplemental table 2.

Microsomal fractions isolation, protein separation and immunoblotting

Depetiolated leaves from predawn (PD), midday (MD) and continuous darkness until midday (CDMD) plants were flash frozen and pulverized under liquid nitrogen. Microsomal fractions were obtained by ultracentrifugation of the recovered laminas as described in Nilsson *et al.* (2010). Protein concentrations were determined using a Bradford assay (Sigma-Aldrich, Saint-Quentin Fallavier, France). Ten µg of each microsomal fraction was separated by 12% acrylamide SDS-PAGE and then transferred to a nitrocellulose membrane. To ensure homogenous loadings and efficient transfers, gels and membranes were stained using Coomassie blue and Ponceau S solutions (Bio-Rad, Hercules, CA, USA), respectively. Membranes were blocked using 5% skim milk and incubated for 1 h at room temperature with peptide antibodies with broad affinity for either PIP1 proteins (GKEEDVRVGANKFPERQPIGTSA, AS09487, Agrisera, Vännäs, Sweden) or for PIP2 proteins (AKDIEASGPEAGEFSAKD, provided by Dr François Chaumont) reported to cross-react with tamarack PIP2 (Calvo-Polanco *et al.* 2012). Putative epitopes on *Populus* PIP1 and PIP2 proteins are indicated in Supplemental table 1. Membranes were then incubated with an anti-rabbit IgG secondary antibody coupled to HRP (Southern Biotech, Birmingham, AL,

USA) for 2 h. Protein-antibody complexes were detected using the Immobilon Western HRP system (Millipore, Billerica, MA, USA).

Promoter analysis

Promoter sequences of poplar PIPs, *AtPIP1;2* (At2g45960), *AtPIP2;1* (At3g53420), *ZmPIP1;1* (X82633), *ZmPIP1;5* (AF326489), *ZmPIP2;1* (AF326491) and *ZmPIP2;5* (AF130975) were retrieved by searching JGI databases using Phytozome v8.0 (http://www.phytozome.net) and exporting ~1.5 kb genomic sequence upstream of the initiation codon. Retreived sequences were analyzed for putative *cis*-acting sequences using the Plant Cis-acting Regulatory DNA Elements (PLACE) signal scan software package (http://www.dna.affrc.go.jp/PLACE/signalscan.html, Higo *et al*. 1999).

Acknowledgement:

This work was supported by a “Ministère de la Recherche et de l’Enseignement Superieur” PhD grant. Authors would like to thank Mélanie Decourteix for help with Western Blot experiments, Christelle Boisselet for plant care, Sylvaine Blateyron for help with RNA sample preparation and Eric Badel for providing the ImageJ leaf area macro.

Supplemental Table 1 Poplar PIP proteins, aliases, *P. trichocarpa* JGI annotation identifiers, epitopes of anti-PIP1s and anti-PIP2s are underlined on the amino-acid sequences
* Gupta et al. 2009, Hacke et al. 2010, Almeida-rodriguez et al. 2010, Leng et al. 2012, Almeida-rodriguez and Hacke 2012
£ Secchi et al. 2010
Other alliases fetched on Phytozome pages

PIP subfamily	Nomenclature used for this paper	Aliases	ProteinID DbXref JGI	JGI v3.0 annotation name	JGI v2.0 annotation name	JGI v1.1 annotation name
PIP1	*PIP1;1*	*PoptrPIP1;2* *Pt-MDPIP1.3* *PoptrPIP1.1£* *PtPIP1;2**	656216	Potri.008G065600	POPTR_0008s06580	grail3.0049030302
	PIP1;2	*PoptrPIP1;3* *PoptrPIP1.2£* *PtPIP1;3**	711735	Potri.003G128600	POPTR_0003s12870	estExt_Genewise1_v1.C_LG_III0271
	PIP1;3	*PoptrPIP1;1* *PoptrPIP1;3£* *PtPIP1;1**	724520	Potri.010G191900	POPTR_0010s19930	estExt_Genewise1_v1.C_LG_X1818
	PIP1;4	*PoptrPIP1;4* *Pt-MDPIP1.4* *PtPIP1;4**	831918	Potri.006G098100	POPTR_0006s09920	estExt_fgenesh4_pm.C_LG_VI0336
	PIP1;5	*PoptrPIP1;5* *PoptrPIP1.5£* *PtPIP1;5**	835561	Potri.016G113300	POPTR_0016s12070	estExt_fgenesh4_pm.C_LG_XVI0408
		PoptrPIP1	417298	Potri.006G097900	POPTR_0006s09910	gw1.VI.1671.1
PIP2	*PIP2;1*	*PoptrPIP2;1* *PoptrPIP2.1£* *PtPIP2;1**	821084	Potri.009G136600	POPTR_0009s13890	estExt_fgenesh4_pg.C_LG_IX0306
	PIP2;2	*PoptrPIP2;2* *PoptrPIP2.2£* *Pt-PIP2.1* *PtPIP2;2**	648808	Potri.004G176300	POPTR_0004s18240	grail3.0045020302
	PIP2;3	*PoptrPIP2;7* *Pt-PIP2.2* *PoptrPIP2;3£* *PtPIP2;7**	735495	Potri.016G089500	POPTR_0016s09090	estExt_Genewise1_v1.C_LG_XVI2799
	PIP2;4	*PoptrPIP2;3* *PoptrPIP2;4£* *Pt-PIP2.3* *PtPIP2;3**	567607	Potri.010G222700	POPTR_0010s22950	eugene3.00102165
	PIP2;5	*PoptrPIP2;5* *PoptrPIP2.5£* *PtPIP2;5**	826419	Potri.006G128000	POPTR_0006s12980	estExt_fgenesh4_pg.C_280159
	PIP2;6	*PoptrPIP2;4* *PoptPP2.6£* *Pt-MDPIP1.2* *PtPIP2;4**	563742	Potri.008G039600	POPTR_0008s03950	eugene3.00080337
	PIP2;7	*PoptrPIP2;8* *PoptrPIP2;7£* *PtPIP2;8**	821627	Potri.009G013900	POPTR_0009s01940	estExt_fgenesh4_pg.C_LG_IX1411
	PIP2;8	*PoptrPIP2;9* *Pt-MDPIP1.1* *PoptrPIP2;8£*	836572	Potri.005G109300	POPTR_0005s11110	estExt_fgenesh4_pm.C_570016
	PIP2;9	*PoptrPIP2;10* *Pt-MDPIP1.5*	796664	Potri.005G109200	POPTR_0005s11100	fgenesh4_pg.C_scaffold_57000043
	PIP2;10	*PoptrPIP2;6* *PtPIP2;11£*	-	Potri.006G128200	POPTR_0006s13000	-

	JGI v3.0 annotation amino-acids sequences, putative epitopes for anti-PIP1 and Anti-PIP2 are underlined
PIP1:1	MEGKEIDVRLGANRENEIQGTLAQSLDDKDYKEPPPAPLEPEGELISWSFYRAGIAEFMATFLFLITVLTVMGVVKDQTKCTTVGIQGIAWAFGGMIFALVYCTAGESGHINPAVTFGLFLARKLSLTRAVFYMVMQCLGAICGAGVVKGFYGKCNYELHNGGANMVAHGYTKGDGLGAEIVGTFILVTTVFSATDAKRSAKRDSHVPILAPLPIGFAVFLVHLATIPITIGTGNPARSLGAAIFNKDSAWDDHWFWVGPFIGAALAALYHQVVIRALPFKK
PIP1:2	MEGKEIDVRLGANRENEIQGTLAQSLDDKDYKEPPPAPLEPEGELISWSFYRAGIAEFIATFLFLITVLTVMGVTKGTSSKSTVAQGLAWAFGGMIFALVYCTAGESGHINPAVTFGLFLARKLSLTRAVFYIMQCLGAICGAGVVKGLQSHINYELQGGANVVNHGYTKGDLGAIIVGTFVLVYTVFSATDAKRSAKRDSHVPILAPLPIGFAVFLVHLATIPITIGTGNPARSLGAAIFNKDSAWDDHWFWVGPFIGAALAAYYHQVIRAIPFKSSA
PIP1:3	MEGKEIDVRLGANRENEIQGTLAQSQDDKDYKEPPPAPLEPEGELISWSFYRAGIAEFMATFLFLITVLTVMGVVKDTTKCTTVGIQGIAWAFGGMIFALVYCTAGESGHINPAVTFGLFLARKLSLTRAVFYMLMQCLGAICGAGVVKGFYGKCNYELLSGGANMVSHGYTKGDLGAIIVGTFVLVYTVFSATDAKRSAKRDSHVPILAPLPIGFAVFLVHLATIPITGTGNPARSLGAAIFNKDSKWDDHWFWVGPFIGAALAYYHQVVIRAIPFKK
PIP1:4	MEEEFDVKVGANRVEGQDRGTLAQYTQHCKDYTEPPPAPLVQPEDFLSWSFYRAGFAEFVATFLFLITVLTVMGVMKSSTKCSTVGRQAWAFGGMIFVLVYCTAGESGHINPAVTFGLLTARKLTRAVFYMMQCLGAVCGAGVVKGFQKSPYTDLGGGANYVSYGKSSEGAVFITLIYTVFSATDAKRSAKRDSHVPVLAPLPIGFAVFLVHLATIPITGTGNPARSLGAALYNKDKAWDDHWFWVGPFYGAALASLYHQVIRAIPFKSK
PIP1:5	MEGREIDVRVGANYVEGRDRGTLAQAQDYKDYTDPPAPLEPEGELSSWSFYRAGIAFWATFLFLITVLTVMGVAKSFTKSTVGIQGIAWAYGGMIFALVYCTAGESGHINPAVTFGLLLARKLTRQGAVYMLMQCLGAICGAAWVKAFQKSQYTEMLGGGANYSTGYAKGSAILGAEIVGTFVLVYTVFSATDARKNARDSHVPILAPLPIGFAVFLVHLATIPITGTGNPARSLGAALYNKDQAWDDHWFWVGPFIGAALASLYHQVIRAIPFKSK
PIP2:1	MSKDVIEGQTITKDYVDPPAPLEPDVGELKLWSFYRALIAEFIALLFLLYVATVIGIRKANQDACGVGLLGIAWAFGGMIFLLVYCTAGESGHINPAVTFGLLLARKVSLIRAVGYMAVQCLGAVCGVGLVKALFAKPYYNSLGGGANNMAGYSTGTAYGALEIIGTFULVYTVFSATDPKRSARDSHIPVLAPLPIGFAVFDMVHLATIPITGTGNPAKSFGAAVIYNDKKAWDDHWFWVGPFIVGALLAAAAYHQYTLRAGLRKALGSFRSHPTN
PIP2:2	MSKEVSEVQGTIEKDYVDPPPAPLLDLGELKLWSFYRALIAEFIALLFLLYVTAVIGHRSNKDPCDGVGLLGIAWAFGGMIFLLVYCTAGISSGHINPAVTFGLFLARKVSLIRAVAWMQCLGAICGVGLVKAFMKKNYNSLGGGANYMAGYNTGTALGAEIIGTFVLVYTVFSATDPKRSARDSHVPVLAPLPIGFAVFDMVHLATIPITGTGNPARSFGAAVIFNSEKAWDDHWFWVGPFVGALAAAYYHQYTLRAAAWKALGSFRSSNPAN
PIP2:3	MGKDIVGGEISAKDYHDPPPAPLDAEIITQWSFYRAIAEFVATLLFLYTVLTVIGYYKSQTDYNKNGDDCGGVGLLGIAWAFGGMIFIIVYCTAGISSGHINPAVTFGLFLARKVSLVRALFYMVAQCLGAICGGTLVKAFQKSYYTNYGGEANGLANSYSKGTLGAEIIGTFVLVYTVFSATDPKRNARDSHPPVLAPLPIGFAVFMVHLATIPITGTGNPARSFGAAVYKSLGSFRSSPNI
PIP2:4	MAKDMIEVAGSSSAKDYHDPPPAPLDAEIITKWSFYRALIAEFIALLFLLYTVLTVIGYKSQDGSADSCGGVGLLGIAWAFGGMIFVLVYCTAGISSGHINPAVTFGLFLARKYSLIRAVMYMVAQCLGAICGVGLVKAFQKSYYKKYGGGANTLADGFSTGTGLGAEIIGTFVLVYTVFSATDPKRSARDSHVPVLAPLPIGFAVFMVHLATIPITGTGNPARSLGAAVYNQDKAWDGHWFWVGPFSGAALAFYHQFILRAGAVKALGSFRSAQRF
PIP2:5	MGKDIVGGEISSAKDYHDPPPAPLDAEIITQWSLYRAIAEFIATLLFLYTVLTVIGYYKSQTDTTKNSDACGGVGLLGIAWAFGGMIFVLVYCTAGISSGHINPAVTFGLFLARKVSLVRAVIYMAVQCLGAICGAGVLKAFQKSYYTKYGGGANVLADGYSTGTGLGAEIIGTFVLVYTVFSATDPKRSARDSHVPVLAPLPIGFAVFMVHLATIPITGTGNPARSFGAAVYNSKKAWHDQWIPWAGPFIGAALAAYYHQYILRAGAIKALGSFRSNPNV
PIP2:6	MAKDTVAEAGSSSAKDYQDPPPAPLIDAEIILTKWSFYRALIAEFIALTFLLYTVLTVIGYKSQDGNADPCGGVGLLGIAWAFGGMIFVLVYCTAGISSGHINPAVTFGLFLARKYSLIRAVMYMVAQCAGAICGVGLVKAFQKSYYTKYNGGANVLADGYSTGTGLGAEIIGTFVLVYTVFSATDPKRSARDSHVPVLAPLPIGFAVFMVHLATIPITGTGNPARSFGAAIAAYYHQYILRAGAIKALGSFRSNPNV
PIP2:7	MAKDIVAEHGETYKDYQDPPPDPLDAEIILGQWSFYRALIAEFIALLFLLYVTLTVVGYKSQTDDGNSLDACGGVGILGIAWAFGGMIFVLVYCTAGISSGHINPAVTFGLFLARKYSLIRAVLYMVAQCLGAICGCGALVKAFQKSYYNIYGGGANELQEGYNKGTGLGAEIIGTFVLVYTVFSATDPKRNARDSHVPVLAPLPIGFAVFMVHLATIPITGTGNPARSFGAAVIFNSSKAWDDHWLFWVGPFIGAALAAYYHQYILRAGAIKALGSFRSNA
PIP2:8	MELEQWSFYRALIAEFVATLFLFYGVTVVGYKGVHNNLCDGAGYLGVGAWAFGGMIFVLVYCTAGISGGHINPAVTFGLFLARKYSLIRAWAYMMAQCLGAMLGVWAYMIITGIPYTQAGGAWNVQPGYSKGTALGAEIIGTFVLVYTVLAATDPKRMARDSHVPVLAPLPIGFAVFVVHLALIPITGTGNPARSLGAAVYKQNAKEIWDHWIFWVGPFVGALAAAYYHQYILSSGAAKALASFRSNPTS
PIP2:9	MSSEERNDRQHGDYHDPPPAPLTDMEELKQWSFYRAVIAEFIALLFESISTYVNYKEPNYTDQCSKYGHLGFAWAMGGMIFVLVYCTAGISSGHINPAVTFGLMVARKSIRAAYMLAQCLGAFLIFLFLTIMGRDQQSSVGVNNVSRNNYSKGTAGAEIIGTFVLVYTVFSATDPKRNARDSHVPVLAPLPIGFAVFMVHLATIPITGTGNPARSLATALIHRSTAGMDLWHFWVGPFLGALAAAYYHKYVLRAGAVKTLKSFRLGSFQQPV
PIP2:10	MGKDIVREHLAKDYHDPPPAPLDAEIITQWSLYRAIAEFIATLFLFYTVLTVIGYYKSQTDTKNSDACGGVGLLGIAWAFGGMIFVLVYCTAGISSGHINPAVTFGLFLARKYSLIRAVLYMAVQCLGAICGGGLVKAFQKSYTKYGGGANILATGFSKGTGLGAEIIGTFVLVYTVFSATDPKRNARDSHVPVLAPLPIGFAVFMVHLATIPITGTGNPARSFGAAVYNKDKAWDDHWFWVGPFIGAALAYYHQYVLRAAWKALGSFRSSSNI

Supplemental Table 1 Poplar PIP proteinsepitopes of anti-PIP1s and anti-PIP2s are underlined on the amino-acid sequences

Supplementary Table 2 List of primers used for PCR experiments

	JGI v3.0 annotation name	Forward primer	Reverse primer
PIP1;1	Potri.008G065600	CAAGAAGTGATGAYTGTGATGC	ACGTCACTGTTATAGCACGC
PIP1;2	Potri.003G128600	TTCAAGAGCAGAGCTTAATTTC	TTCAAAAAGCTAGATAATTTACAC
PIP1;3	Potri.010G191900	AAGAAGTGATTATTATGATTATGG	GATTTGAAGAAACACGTATTGCTA
PIP1;4	Potri.006G098100	GACAGAAAACAAGGTTCTTTAGA	GAGTAATTTACATAAATGGAACC
PIP1;5	Potri.016G113300	TCGTTCCCAATCRATGGATGTT	AAGAATTCACTGAGAGGGAATA
PIP2;1	Potri.009G136600	TGCTAACATGGTGGCTCCC	GATCATCCCAGGCTTTCTTATC
PIP2;2	Potri.004G176300	TGGTACACTTGGCCACAATC	GCTAATGCTCCCACAAATGG
PIP2;3	Potri.016G089500	ATTCAGTTATGGAACGTACGC	AGCTCACAACCATGACATAAC
PIP2;4	Potri.010G222700	CCAACGGTTTTAAATCTCGGTTC	ACCGAAAGGGATAATAAAGGG
PIP2;5	Potri.006G128000	TGTGTACATTATGGTGTCGTG	CAAAGAAGCAGCACTACCTGAGAC
PIP2;6	Potri.008G039600	ATCCCAATCACAGGAACTGG	CTATGGCTGCACCAATGAAG
PIP2;7	Potri.009G013900	ATGACCATTGGCTCTTCTGG	GGCTTTAAGCATTGCTCCTG
PIP2;8	Potri.005G109300	GCAATCCTACTAGCTAAGGC	ACCCACATATCAAGTTGAGAC
PIP2;9	Potri.005G109200	ACTGGAACTGGCATCAATCC	CCAACCCAGAAAATCCACAG
PIP2;10	Potri.006G128200	CACAGTCGTGGTCAAGATGTC	ACTAGTTGATTATGAGATAGGGAG
Actin	Potri.001G309500	GAAGTGCTTCTAAGTTCTACAAG	CTCAATAAATTCTCCATATCAACC
EF1-α	Potri.010G218600	GTCTGTTGAGATGCACCACG	CAATGTGACAGGTGTGGCAG
Sand	Potri.009G014400	CATGATAAAGGCAACGGGGCG	CTGTGTTACAAGATATTTTTGGG
TIP41-like	Potri.009G093200	TAGTGATAGTGCAAATCCTGTCA	CTTACAAGTTACTGTGGACCAC
UP1	Potri.002G127700	TCGTCCTGTCACAGCTCCAAA	TCATCTGCGCCAGGACCATG

Discussion générale et perspectives

Les travaux réalisés dans le cadre de cette thèse poursuivent et étendent ceux engagés depuis une dizaine d'années au sein de l'équipe HYDRO de l'UMR 547 PIAF de Clermont-Ferrand sur la conductance hydraulique foliaire (K_{leaf}). Ce trait est identifié comme l'un des goulots d'étranglement majeur des flux hydriques dans la plante. Cette thèse s'inscrit dans l'étude exhaustive de la régulation par les aquaporines de K_{leaf} en réponse à la lumière chez les arbres avec pour modèle d'étude le peuplier. Les connaissances sur les mécanismes impliqués dans la modulation de K_{leaf} étant fragmentaires au début de ce travail, les champs d'investigation entrepris furent volontairement larges alliant les approches de cytologie (hybridation *in situ*), de biologie moléculaire (quantification de transcrits et de protéines) et d'écophysiologie. Ils se sont avérés très complémentaires et nous ont permis de receuillir de nombreuses informations nouvelles.

Un certain nombre d'études a mis en évidence un effet stimulateur de la lumière sur K_{leaf} chez de nombreuses espèces d'arbres. Dans le cadre des travaux de cette thèse, cet effet a également été montré chez de nouvelles espèces d'arbres tels *Fagus sylvatica*, *Quercus robur* et *Populus tremula* (**Chapitre 1**). Cette étude a permis d'apprécier des réponses de K_{leaf} contrastées à la lumière chez des espèces d'arbres aux exigences écologiques différentes. Cependant, les réponses observées nous permettent de nuancer l'hypothèse d'une plus grande conductance hydraulique foliaire qui devrait être observée chez les espèces pionnières ou qui bénéficient d'un plus fort éclairement (Sack *et al.* 2005, Barigah *et al.* 2006, Sellin *et al.* 2012). En effet, nous montrons que l'amplitude de variation de K_{leaf} en réponse à la lumière est plus faible pour les espèces pionnières (saule et tremble) que pour le chêne pédonculé et le noyer. Nos données avec celles issues de la littérature soulignent la difficulté de généraliser toutes interconnexions entre la conductance hydraulique foliaire, l'effet de la lumière et l'auto-écologie. En effet, elles ne sont pas systématiquement observées chez toutes les espèces telles *Laurus nobilis* (Cochard *et al.* 2004), *Salix alba* (Ben Bâaziz *et al.* 2012b), ni même au sein d'un genre : *Populus tremuloides* (Voicu et Zwiazek 2011), *Quercus rubra* (Rockwell *et al.* 2011).

Les raisons de cette distinction entre les espèces présentant des réponses différentielles à la lumière ne sont pas encore clairement identifiées, mais la structure foliaire jouerait un rôle déterminant. En 2007, Zwieniecki *et al.* ont émis l'hypothèse d'une dynamique de K_{leaf} médiée par la compartimentation au sein de la feuille entre le flux hydrique destiné à la transpiration et celui destiné au parenchyme photosynthétique ; suggérant l'implication des

aquaporines et/ou des plasmodesmes dans cette compartimentation. Cette hypothèse a été étayée depuis par les expériences de Ye *et al.* (2008) appuyant l'existence d'un lien hydraulique entre le xylème et l'épiderme chez *Tradescantia fluminensis* dépendant de l'activité d'aquaporines. De manière complémentaire, Scoffoni *et al.* (2008) ont montré que l'effet de la lumière sur K_{leaf} était plus important pour les espèces hétérobariques qui possèdent des extensions cellulaires à la gaine péri-vasculaire. Ces extensions amélioreraient l'évaporation et l'accès à la lumière des structures régulatrices de K_{leaf} ; ces structures n'ayant pas encore été identifiées. Le genre *Populus*, possède ces extensions particulières, et chez l'espèce *P. nigra* le trajet du flux transpiratoire n'impliquerait pas le parenchyme palissadique (Zwiniecki *et al.* 2007). Nos données écophysiologiques présentés dans le **chapitre 2** montrent que cette espèce augmente de façon importante sa conductance hydraulique en réponse à l'éclairement (environ 120%). Le lien des ces extensions avec les modulations de réponse de K_{leaf} à la lumière chez cette espèce, serait une piste très intéressante à explorer.

Cette stratégie de compartimentation hydraulique a cependant une contrepartie : si les cellules du mésophylle sont plutôt isolées du flux transpiratoire ce qui les protègent des variations de différence de potentiel hydrique à court terme, en revanche, ces mêmes cellules ne peuvent pas agir comme réserves afin de « tamponner » des variations plus importantes ou plus longues de chute de potentiel hydrique. Ce phénomène est connu sous le terme de capacitance hydraulique foliaire (C_{leaf}). *In fine*, si les stomates ne se ferment pas assez vite en réponse à la chute de potentiel hydrique, la colonne d'eau peut se rompre avec des risques d'embolie du xylème. Les récents travaux de Blackman et Brodribb (2011) supportent la théorie de la compartimentation hydrique où la K_{leaf} maximum est corrélé à la capacitance des tissus traversés par les flux transpiratoires et non pas à la capacitance de la feuille entière. L'étude de la dynamique des capacitances et de la coordination entre conductance stomatique et hydraulique en relation avec l'embolie du xylème foliaire constitue une perspective d'intérêt majeur afin de mieux comprendre les relations qui existeraient entre ces processus.

Parmi les déterminants potentiels de l'augmentation de K_{leaf} à la lumière, les aquaporines sont privilégiées. Une preuve indirecte de leur contribution est apportée par l'emploi d'inhibiteurs induisant des diminutions de perméabilité des cellules ou des organes étudiés. Lo Gullo *et al.* (2003) et Tyree *et al.* (2005) avancent l'implication des aquaporines dans l'augmentation de K_{leaf} à la lumière, avec un effet d'autant plus important chez des espèces présentant une dominance de la résistance extra-vasculaire. Le noyer dont la quasi-totalité de la contribution à la résistance foliaire totale est attribuée à la résistance extra-

vasculaire, montre une très forte augmentation de K_{leaf} suite à un éclairement (Cochard *et al.* 2004). Corrélée à cette réponse, une forte accumulation de transcrits d'aquaporines de type PIP est mesurée (**Chapitre 1 et Annexe 1**). Cette réponse est qualitativement modulable selon la qualité de la source d'éclairement. Une lumière dépourvue des longueurs d'ondes bleues (350-500nm) inhibe l'augmentation de K_{leaf} et par la même l'expression des aquaporines *PIP*. L'ensemble de ces données écophysiologiques et moléculaires soulignent la contribution de plusieurs voies de signalisations menant à la potentialisation de K_{leaf}. L'identification de la contribution des différentes longueurs d'ondes dans la modulation de K_{leaf} peut être explorée par le biais d'études de mutants « perte de fonction » pour les photorécepteurs et pour les cascades de signalisation qu'ils déclenchent.

La réponse moléculaire des mécanismes sous-jacents à l'augmentation de K_{leaf} a été entreprise par une analyse transcriptomique sans *a priori* cDNA-AFLP (**Annexe 1**). L'identification d'un panel de protéines nous a permis de révéler plusieurs voies métaboliques. Parmi elles, les voies de la stabilisation protéique et du transport vésiculaire semblent être des pistes à privilègier (HSP70, ARF1, SYP121, **Annexe 1).** Les cinétiques de réponse extrêmement rapide de K_{leaf} à la lumière ne peuvent être imputées uniquement aux seuls phénomènes de transcription-traduction des aquaporines. En effet, quand bien même la biosynthèse *de novo* de protéines soit nécessaire à l'établissement du processus (Cochard *et al.* 2007), des mécanismes d'action autres, plus rapides, entrent nécessairement en jeu. La régulation de l'activité des protéines est une possibilité, mais l'externalisation de vésicules enrichies en aquaporines pourrait également participer, en partie au moins à la précocité remarquable de ce phénomène par une augmentation de la perméabilité cellulaire. Cette hypothèse est soutenue par les données bibliographiques où la diminution de la conductance hydraulique racinaire en réponse au stress salin chez *Arabidopsis* était associée à l'internalisation de vésicules membranaires enrichies en aquaporines (Boursiac *et al.* 2005, Luu *et al.* 2012). De plus, le trafic vésiculaire est également responsable de la variation du volume des cellules de garde chez *Vicia faba* correlée à des modulations de permeabilité hydraulique membranaire (Shope et Mott 2006). Dans cette étude, aucune preuve directe de l'implication des aquaporines n'a été apportée. Sachant qu'il n'existe pas de continuité cellulaire entre les cellules de garde et les cellules épidermiques adjacentes, les flux hydriques requierent théoriquement la présence de cannaux dédiés.

Afin de vérifier notre hypothèse d'un impact du trafic vésiculaire sur la régulation de la conductance hydraulique foliaire à la lumière, des expériences de pharmacologie mettant en œuvre les inhibiteurs du trafic vésiculaire (Wortmannine et Cytochalasine D, Tyrphostine A23, Bréfeldine A) délivrés aux feuilles entières grâce au HPFM sont d'ores et déjà entreprises. Ces expériences seront également étendues à l'inhibition des cascades de transduction mises en lumière par l'approche cDNA-AFLP qui participeraient à la régulation de K_{leaf}.

L'effet de la lumière sur la K_{leaf} en conditions expérimentales est relativement bien documenté, mais paradoxalement, les données décrivant les variations de K_{leaf} *in natura* à l'échelle de la journée sont à ce jour limitées. La conductance hydraulique foliaire augmente significativement jusqu'au milieu de journée, au moment où le potentiel hydrique devient minimal chez *Populus trichocarpa* et *Populus nigra* (**Chapitre 2**). Ces résultats reflètent des réponses quasi-similaires de ces clones à des conditions de culture optimales sur le plan des apports hydriques et lumineux, suggérant une adaptation de la conductance en réponse à la plus forte demande évaporative, et ce, afin de limiter la tension exercée sur la colonne d'eau (Tyree *et al.* 2005).

L'implication des aquaporines, suggérée par diverses sources bibliographiques et les travaux précédemment décrits, a été validée par nos expériences. En effet, nous montrons que l'augmentation de K_{leaf} à la lumière est abolie par l'utilisation de chlorure de mercure, couramment employé pour inhiber les aquaporines. Les profils transcriptionnels en réponse à la lumière montrent une accumulation de certaines *PIP1* et *PIP2* ; il en est de même pour les protéines correspondantes (**Chapitre 2**). Ces résultats suggèrent une contribution substantielle des aquaporines dans l'augmentation du flux hydrique foliaire chez le peuplier. Cependant, le lieu d'action des aquaporines dans ce phénomène reste à définir. Des expériences de localisation par immuno-localisation et hybridation *in situ* des protéines et des transcrits PIP dont l'expression est stimulée par la lumière constituent une perspective majeure à ces travaux de thèse.

Les résultats issus de ces expériences pourraient mettre en exergue la compartimentation hydraulique foliaire. Cette hypothèse serait étayée par des profils différentiels de localisation des différentes isoformes. On peut également s'attendre à une forte localisation d'aquaporines au niveau de la gaine péri-vasculaire, celle- ci étant le lieu

privilégié du passage du compartiment apoplastique vers le symplaste. L'identification des populations de PIP dans ces cellules pourrait asseoir le rôle des isoformes identifiées en réponse à la lumière (**Chapitre 2**). Bien que la contribution de la voie vasculaire dans K_{leaf} n'ait pas été évaluée, les éléments montrant le rôle central des aquaporines dans la réponse à la lumière suggèrent que celle-ci est dominée par la voie transmembranaire. Les valeurs de conductance élevées à l'obscurité pourraient quant à elles traduire la contribution de la voie apoplastique.

Une des perspectives proposée à l'issue de l'expérience de cDNA-AFLP était l'analyse des régions promotrices des aquaporines afin d'identifier des boites *cis* de régulation. Le choix du peuplier comme espèce modèle a permis de réaliser cette étude. Celle-ci a permis de dégager de nombreux éléments de régulation putatifs impliqués dans les réponses aux phytohormones (ABA et Auxine pour les plus importantes), ainsi qu'à la lumière et au stress hydrique. L'utilisation de ce génome de référence a également permis d'identifier des événements de duplication de certains gènes d'aquaporines suggérant la redondance fonctionnelle chez les PIPs (cas de PIP1;1 / PIP1;3 et de PIP2;5 / PIP2;10, **Chapitre 2**), et à la perte de fonction d'un des gènes dupliqués ou à sa néo-fonctionnalisation chez les XIPs (respectivement XIP3;1b et XIP3;2, **Annexe 2**).
Enfin, un intérêt important de l'utilisation du peuplier réside dans sa relative facilité à le transformer génétiquement. En effet, la validation fonctionnelle est une condition *sine qua non* pour statuer sur le rôle d'un gène dans un processus. Cependant, la transformation stable du peuplier est une stratégie longue dont la réussite risque d'être aléatoire vis a vis de notre question, notamment parce que les phénotypes issus de transformation stables ne seront pas forcement contrastés. Une des causes possibles proviendrait de phénomènes de compensation dus au nombre important d'isoformes d'aquaporines, laissant supposer des redondances fonctionnelles. Une alternative consistera à faire exprimer des constructions de manière transitoire par des protoplastes de peuplier afin d'en estimer l'impact sur la conductivité hydraulique de cellules isolées (Moshelion *et al.* 2004). Cette méthode aura l'avantage certain d'apprécier directement sur la cellule différents stimuli lumineux (qualité et intensité), mais également celui des inhibiteurs précédemment cités.

Pour résumer, la grande majorité des travaux présentés dans cette thèse abordent le fonctionnement hydraulique foliaire de plantes en conditions hydriques non-limitantes. Nous souhaitons appuyer l'utilité de l'étude de plantes non-stressées poussant dans des conditions

optimales. Paradoxalement, le fonctionnement « normal » des plantes n'étant pas totalement élucidé, les observations de plantes en stress sont généralement mises en avant mais restent relatives au détriment des données des plantes témoin, couramment minorées. Notre étude s'est révélée être fondamentalement riche en informations. En effet, les mécanismes sous-jacents à celui-ci n'étaient pas clairement établis au début de cette thèse, nous avons cependant dégagé plusieurs éléments de réponse clé:

(i) Le peuplier est capable d'ajuster sa conductance hydraulique foliaire pendant la journée pour faire face au flux transpiratoire.

(ii) L'augmentation de la conductance se fait de façon simultanée avec la transcription et la traduction d'aquaporines en réponse à l'éclairement.

(iii) L'augmentation de K_{leaf} peut être atténuée par un inhibiteur des aquaporines.

Autre fait significatif, ces résultats ont été obtenus chez deux clones très différents ce qui nous fait émettre l'hypothèse que les mécanismes responsables de ces observations sont potentiellement conservés au sein du genre *Populus* et donc essentiels à son mode de vie.

Par ailleurs, nos travaux ont mis en évidence chez le peuplier la régulation de la transcription d'aquaporines en réponse à la lumière certes, mais également en situation de déficit hydrique dans la feuille et la tige (**Annexe 2)**, dans l'écorce, le bois et les bourgeons (**Annexe 3**). L'implication des aquaporines dans la réponse au stress hydrique a été étudiée chez de nombreuses espèces, y compris chez le peuplier (Almeida-Rodriguez *et al.* 2010) montrant des profils différents de transcrits de certaines aquaporines potentiellement impliquées dans la tolérance à ce stress chez deux clones. Bien que pertinents, ces profils de transcription doivent être généralisés aux autres aquaporines et ces études doivent être réalisées sur d'autres espèces de peupliers aux tolérances au stress hydrique contrastées afin de valider le rôle de ces gènes dans ce phénomène.

En conclusion, l'originalité de ces travaux de thèse réside dans la pluridisciplinarité des méthodes employées pour approcher la question biologique : l'écophysiologie moléculaire. L'exhaustivité de cette approche n'est rendue possible que par l'exploitation d'un génome de référence, le peuplier. Cette contrainte s'est traduite par des réponses de conductance moins spectaculaires que celles observées chez le noyer (100-120% contre 400% pour le noyer). En contrepartie, cette contrainte sur le trait physiologique est compensée par l'accès immédiat de toutes les séquences génétiques d'intérêt (séquences codantes et régions promotrices) mais aussi par les perspectives de validation fonctionnelle.

Bibliographie

Aasamaa, K., Sober, A., Rahi, M., (2001). Leaf anatomical characteristics associated with shoot hydraulic conductance, stomatal conductance and stomatal sensitivity to changes of leaf water status in temperate deciduous trees. Funct Plant Biol *28*, 765-774.

Aasamaa, K., Sober, A., Hartung, W., and Niinemets, U. (2002). Rate of stomatal opening, shoot hydraulic conductance and photosynthetic characteristics in relation to leaf abscisic acid concentration in six temperate deciduous trees. Tree Physiol *22*, 267-276.

Aasamaa, K., Niinemets, U., and Sober, A. (2005a). Leaf hydraulic conductance in relation to anatomical and functional traits during *Populus tremula* leaf ontogeny. Tree Physiol *25*, 1409-1418.

Aasamaa, K., and Sober, A. (2005b). Seasonal courses of maximum hydraulic conductance in shoots of six temperate deciduous tree species. Funct Plant Biol *32*, 1077-1087.

Ache, P., Bauer, H., Kollist, H., Al-Rasheid, K.A.S., Lautner, S., Hartung, W., and Hedrich, R. (2010). Stomatal action directly feeds back on leaf turgor: new insights into the regulation of the plant water status from non-invasive pressure probe measurements. Plant J *62*, 1072-1082.

Aharon, R., Shahak, Y., Wininger, S., Bendov, R., Kapulnik, Y. and Galili, G. (2003) Overexpression of a plasma membrane aquaporin in transgenic tobacco improves plant vigor under favorable growth conditions but not under drought or salt stress. Plant Cell *15*: 439-447.

Alchanatis, V., Cohen, Y., Cohen, S., Moller, M., Sprinstin, M., Meron, M., Tsipris, J., Saranga, Y., and Sela, E. (2010). Evaluation of different approaches for estimating and mapping crop water status in cotton with thermal imaging. Precision Agric *11*, 27-41.

Alexandersson, E., Fraysse, L., Sjovall-Larsen, S., Gustavsson, S., Fellert, M., Karlsson, M., Johanson, U., and Kjellbom, P. (2005). Whole gene family expression and drought stress regulation of aquaporins. Plant Mol Biol *59*, 469-484.

Allen, C.D., Macalady, A.K., Chenchouni, H., Bachelet, D., McDowell, N., Vennetier, M., Kitzberger, T., Rigling, A., Breshears, D.D., Hogg, E.H., *et al.* (2010). A global overview of drought and heat-induced tree mortality reveals emerging climate change risks for forests. Forest Ecol *259*, 660-684.

Almeida-Rodriguez, A.M., Cooke, J.E.K., Yeh, F., and Zwiazek, J.J. (2010). Functional characterization of drought-responsive aquaporins in *Populus balsamifera* and *Populus simonii×balsamifera* clones with different drought resistance strategies. Physiol Plant *140*, 321-333.

Almeida-Rodriguez, A.M., Hacke, U.G., and Laur, J. (2011). Influence of evaporative demand on aquaporin expression and root hydraulics of hybrid poplar. Plant, Cell Env, *34*: 1318-1331.

Altschul, S.F., Madden, T.L., Schaffer, A.A., Zhang, J., Zhang, Z., Miller, W. *et al.* (1997) Gapped BLAST and PSI-BLAST: a new generation of protein database search programs. Nucleic Ac Res *25*: 3389-3402

Awad, H., Barigah, T., Badel, E., Cochard, H., and Herbette, S. (2010). Poplar vulnerability to xylem cavitation acclimates to drier soil conditions. Physiol Plant *139*, 280-288.

B

Bae, E.K., Lee, H., Lee, J.S., Noh, E.W. (2011) Drought, salt and wounding stress induce the expression of the plasma membrane intrinsic protein 1 gene in poplar (*Populus alba* x *P. tremula* var. *glandulosa*). Gene *483*: 43-48.

Barigah, T.S., Ibrahim, T., Bogard, A., Faivre-Vuillin, B., Lagneau, L.A., Montpied, P., and Dreyer, E. (2006). Irradiance-induced plasticity in the hydraulic properties of saplings of different temperate broad-leaved forest tree species Tree Physiol. *26*, 1505-1516.

Ben Bâaziz, K., Lopez, D., Bouzid, S., Cochard, H., Venisse, J.S., and Sakr, S. (2012a). Early gene expression in the walnut tree occurring during stimulation of leaf hydraulic conductance by irradiance. Biol Plant *56*, 657-666.

Ben Baaziz, K., Lopez, D., Rabot, A., Combes, D., Gousset, A., Bouzid, S., Cochard, H., Sakr, S., and Venisse, J.-S. (2012b). Light-mediated Kleaf induction and contribution of both the PIP1s and PIP2s aquaporins in five tree species: walnut (*Juglans regia*) case study. Tree Physiol *32*, 423-434.

Bienert, G.P., Bienert, M.D., Jahn, T.P., Boutry, M., and Chaumont, F. (2011). Solanaceae XIPs are plasma membrane aquaporins that facilitate the transport of many uncharged substrates. Plant J *66*, 306-317.

Blackman, C.J., Brodribb, T.J., and Jordan, G.J. (2009). Leaf hydraulics and drought stress: response, recovery and survivorship in four woody temperate plant species. Plant Cell Env *32*, 1584-1595.

Blackman, C.J., Brodribb, T.J., and Jordan, G.J. (2010). Leaf hydraulic vulnerability is related to conduit dimensions and drought resistance across a diverse range of woody angiosperms. New Phytol *188*, 1113-1123.

Blackman ,C.J., Brodribb, T.J., (2011) Two measures of leaf capacitance: insights into the water transport pathway and hydraulic conductance in leaves. Func Plant Biol *38*,118–126.

Bond, B.J., and Kavanagh, K.L. (1999). Stomatal behavior of four woody species in relation to leaf-specific hydraulic conductance and threshold water potential. Tree Physiol *19*, 503-510.

Bonhomme, L., Barbaroux, C., Monclus, R., Morabito, D., Berthelot, A., Villar, M., Dreyer, E., and Brignolas, F. (2008). Genetic variation in productivity, leaf traits and carbon isotope discrimination in hybrid poplars cultivated on contrasting sites. Ann For Sci *65*.

Boursiac, Y., Chen, S., Luu, D.T., Sorieul, M, Van den Dries, N., and Maurel, C. (2005) Early effects of salinity on water transport in Arabidopsis roots. Molecular and cellular features of aquaporin expression. Plant Physiol. *139 (2)* 790-805.

Boyer, J.S. (1968). Relationship of water potential to growth of leaves. Plant Physiol *43*, 1056-1062.

Boyer, J.S. (1974). Water transport in plants: Mechanism of apparent changes in resistance during absorption. Planta *117*, 187-207.

Brodribb, T.J., and Holbrook, N.M. (2003). Stomatal closure during leaf dehydration, correlation with other leaf physiological traits. Plant Physiol *132*, 2166-2173.

Brodribb, T.J., and Holbrook, N.M. (2004). Diurnal depression of leaf hydraulic conductance in a tropical tree species. Plant Cell Env *27*, 820-827.

Brodribb, T.J., Holbrook, N.M., Zwieniecki, M.A., and Palma, B. (2005). Leaf hydraulic capacity in ferns, conifers and angiosperms: impacts on photosynthetic maxima. New Phytol *165*, 839-846.

Brodribb, T.J., and Holbrook, N.M. (2006). Declining hydraulic efficiency as transpiring leaves desiccate: two types of response. Plant Cell Env *29*, 2205-2215.

Brodribb, T.J., Feild, T.S., and Jordan, G.J. (2007). Leaf maximum photosynthetic rate and venation are linked by hydraulics. Plant Physiol *144*, 1890-1898.

Brodribb, T.J., and Cochard, H. (2009). Hydraulic failure defines the recovery and point of death in water-stressed conifers. Plant Physiol *149*, 575-584.

Brodribb, T.J., and Feild, T.S. (2010). Leaf hydraulic evolution led a surge in leaf photosynthetic capacity during early angiosperm diversification. Ecol Lett *13*, 175-183.

Bucci, S.J., Scholz, F.G., Campanello, P.I., Montti, L., Jimenez-Castillo, M., Rockwell, F.A., La Manna, L., Guerra, P., Lopez Bernal, P., Troncoso, O.*, et al.* (2012). Hydraulic differences along the water transport system of South American Nothofagus species: do leaves protect the stem functionality? Tree Physiol *32*, 880-893.

Chamaillard, S., Fichot, R., Vincent-Barbaroux, C., Bastien, C., Depierreux, C., Dreyer, E., Villar, M., and Brignolas, F. (2011). Variations in bulk leaf carbon isotope discrimination, growth and related leaf traits among three *Populus nigra* L. populations. Tree Physiol *31*, 1076-1087.

Chang, S.J., Puryear, J. and Cairney, J. (1993) A simple and efficient method for isolating RNA from pine trees. Plant Mol Biol Rep *11*: 113-116.

Charra-Vaskou, K., and Mayr, S. (2011). The hydraulic conductivity of the xylem in conifer needles (*Picea abies* and *Pinus mugo*). J Exp Bot *62*, 4383-4390.

Charra-Vaskou, K., Badel, E., Burlett, R., Cochard, H., Delzon, S., and Mayr, S. (2012). Hydraulic efficiency and safety of vascular and non-vascular components in Pinus pinaster leaves. Tree Physiol *32*, 1161-1170.

Chaumont, F., Barrieu, F., Wojcik, E., Chrispeels, M.J., and Jung, R. (2001). Aquaporins constitute a large and highly divergent protein family in maize. Plant Physiol *125*, 1206-1215.

Chaumont, F., Moshelion, M., and Daniels, M.J. (2005). Regulation of plant aquaporin activity. Biol Cell *97*, 749-764.

Cochard, H., Bodet, C., Ameglio, T., and Cruiziat, P. (2000). Cryo-scanning electron microscopy observations of vessel content during transpiration in walnut petioles. Facts or artifacts? Plant Physiol *124*, 1191-1202.

Cochard, H., Coll, L., Le Roux, X., and Ameglio, T. (2002). Unraveling the effects of plant hydraulics on stomatal closure during water stress in walnut. Plant Physiol *128*, 282-290.

Cochard, H., Froux, F., Mayr, S., and Coutand, C. (2004). Xylem wall collapse in water-stressed pine needles. Plant Physiol *134*, 401-408.

Cochard, H., Nardini, A., and Coll, L. (2004). Hydraulic architecture of leaf blades: where is the main resistance? Plant, Cell Env *27*, 1257-1267.

Cochard, H., Venisse, J.S., Barigah, T.S., Brunel, N., Herbette, S., Guilliot, A., Tyree, M.T., and Sakr, S. (2007). Putative role of aquaporins in variable hydraulic conductance of leaves in response to light. Plant Physiol *143*, 122-133.

Cohen, D., Bogeat-Triboulot, M.B., Tisserant, E., Balzergue, S., Martin-Magniette, M.L., Lelandais, G., Ningre, N., Renou, J.P., Tamby, J.P., Le Thiec, D.*, et al.* (2010). Comparative transcriptomics of drought responses in *Populus*: a meta-analysis of genome-wide expression profiling in mature leaves and root apices across two genotypes. BMC Genomics *11*.

Cocozza, C., Cherubini, P., Regier, N., Saurer, M., Frey, B. and Tognetti, R. (2010) Early effects of water deficit on two parental clones of *Populus nigra* grown under different environmental conditions. Functional Plant Biology *37*: 244-254.

Conant, G.C. and Wolfe, K.H. (2008) Turning a hobby into a job: how duplicated genes find new functions. Nature Review Genetic *9*: 938-950.

Cowan, I.R. (1972). An electrical analogue of evaporation from, and flow of water in plants. Planta *106*, 221-226.

Cruiziat, P., Tyree, M.T., Bodet, C., and Logullo, M.A. (1980). Kinetics of rehydration of detached sunflower leaves following substantial water-loss. New Phytol *84*, 293-306.

Czechowski, T., Stitt, M., Altmann, T., Udvardi, M.K., Scheible, W.R. (2005) Genome-wide identification and testing of superior reference genes for transcript normalization in *Arabidopsis*. Plant Physiol *139*: 5-17.

Danielson, J.A., and Johanson, U. (2008). Unexpected complexity of the aquaporin gene family in the moss *Physcomitrella patens*. BMC Plant Biol *8*, 45.

De Bei, R., Cozzolino, D., Sullivan, W., Cynkar, W., Fuentes, S., Dambergs, R., Pech, J., and Tyerman, S. (2011). Non-destructive measurement of grapevine water potential using near infrared spectroscopy. Aust J GR W *17*, 62-71.

Domec, J.C., Noormets, A., King, J.S., Sun, G., McNulty, S.G., Gavazzi, M.J., Boggs, J.L., and Treasure, E.A. (2009). Decoupling the influence of leaf and root hydraulic conductances on stomatal conductance and its sensitivity to vapour pressure deficit as soil dries in a drained loblolly pine plantation. Plant Cell Env *32*, 980-991.

Felle, H.H. (2006). Apoplastic pH during low-oxygen stress in Barley. Ann Bot *98*, 1085-1093.

Fetter, K., Van Wilder, V., Moshelion, M., and Chaumont, F. (2004). Interactions between plasma membrane aquaporins modulate their water channel activity. Plant Cell *16*, 215-228.

Fichot, R., Chamaillard, S., Depardieu, C., Le Thiec, D., Cochard, H., Barigah, T.S., and Brignolas, F. (2011). Hydraulic efficiency and coordination with xylem resistance to cavitation, leaf function, and growth performance among eight unrelated *Populus deltoidesxPopulus nigra* hybrids. J Exp Bot *62*, 2093-2106.

Flexas, J., Ribas-Carbo, M., Hanson, D.T., Bota, J., Otto, B., Cifre, J., McDowell, N., Medrano, H., and Kaldenhoff, R. (2006). Tobacco aquaporin NtAQP1 is involved in mesophyll conductance to CO_2 *in vivo*. Plant J *48*, 427-439.

Fouquet, R., Leon, C., Ollat, N., Barrieu, F. (2008) Identification of grapevine aquaporins and expression analysis in developing berries. Plant Cell Rep *27*:1541-1550.

G

Galvez, D.A., and Tyree, M.T. (2009). Impact of simulated herbivory on water relations of aspen (*Populus tremuloides*) seedlings: the role of new tissue in the hydraulic conductivity recovery cycle. Oecologia *161*, 665-671.

Gasco, A., Nardini, A., and Salleo, S. (2004). Resistance to water flow through leaves of *Coffea arabica* is dominated by extra-vascular tissues. Funct Plant Biol *31*, 1161-1168.

Gomes, D., Agasse A., Thiebaut P., Delrot S., Geros H., and Chaumont F. (2009) . Aquaporins are multifunctional water and solute transporte highly divergent in living organisms. BBA Biomembranes *1788* : 1213 – 1228 .

Gupta, A.B., and Sankararamakrishnan, R. (2009). Genome-wide analysis of major intrinsic proteins in the tree plant *Populus trichocarpa*: characterization of XIP subfamily of aquaporins from evolutionary perspective. BMC Plant Biol *9*, 134.

H

Hachez C., Moshelion M., Zelazny E., Cavez D., & Chaumont F. (2006). Localization and quantification of plasma membrane aquaporin expression in maize primary root: a clue to understanding their role as cellular plumbers. *Plant Mol Biol 62*, 305-323.

Hachez, C., Heinen, R.B., Draye, X., and Chaumont, F. (2008). The expression pattern of plasma membrane aquaporins in maize leaf highlights their role in hydraulic regulation. Plant Mol Biol *68*, 337-353.

Hacke, U.G., Sperry, J.S., Pockman, W.T., Davis, S.D., and McCulloch, K.A. (2001). Trends in wood density and structure are linked to prevention of xylem implosion by negative pressure. Oecologia *126*, 457-461.

Hacke, U.G., Plavcova, L., Almeida-Rodriguez, A., King-Jones, S., Zhou, W.C. and Cooke, J.E.K. (2010) Influence of nitrogen fertilization on xylem traits and aquaporin expression in stems of hybrid poplar. Tree Physiol *30*: 1016-1025.

Higo, K., Ugawa, Y., Iwamoto, M. and Korenaga, T. (1999) Plant cis-acting regulatory DNA elements (PLACE) database. Nucleic Acids Res *27*: 297-300.

Hinckley, T.M., Brooks, J.R., Cermak, J., Ceulemans, R., Kucera, J., Meinzer, F.C. *et al.* (1994) Water flux in a hybrid poplar stand. Tree Physiol *14*: 1005-1018.

Holbrook, N.M., Ahrens, E.T., Burns, M.J., and Zwieniecki, M.A. (2001). In vivo observation of cavitation and embolism repair using magnetic resonance imaging. Plant Physiol *126*, 27-31.

Holloway-Phillips, M.M., and Brodribb, T.J. (2011). Minimum hydraulic safety leads to maximum water-use efficiency in a forage grass. Plant Cell Env *34*, 302-313.

Hüve, K., Remus, R., Lüttschwager, D., and Merbach, W. (2002). Water Transport in Impaired Leaf Vein Systems. Plant Biol *4*, 603-611.

I

Iijima, M., Yoshida, T., Kato, T., Kawasaki, M., Watanabe, T., and Somasundaram, S. (2011). Visualization of lateral water transport pathways in soybean by a time of flight-secondary ion mass spectrometry cryo-system. J Exp Bot *62*, 2179-2188.

Javot, H., and Maurel, C. (2002). The role of aquaporins in root water uptake. Ann Bot *90*, 301-313.

Johanson, U., Karlsson, M., Johansson, I., Gustavsson, S., Sjovall, S., Fraysse, L., Weig, A.R., and Kjellbom, P. (2001). The complete set of genes encoding major intrinsic proteins in *Arabidopsis* provides a framework for a new nomenclature for major intrinsic proteins in plants. Plant Physiol *126*, 1358-1369.

Johnson, D.M., Meinzer, F.C., Woodruff, D.R., and McCulloh, K.A. (2009a). Leaf xylem embolism, detected acoustically and by cryo-SEM, corresponds to decreases in leaf hydraulic conductance in four evergreen species. Plant Cell Env *32*, 828-836.

Johnson, D.M., Woodruff, D.R., McCulloh, K.A., and Meinzer, F.C. (2009b). Leaf hydraulic conductance, measured in situ, declines and recovers daily: leaf hydraulics, water potential and stomatal conductance in four temperate and three tropical tree species. Tree Physiol *29*, 879-887.

Johnson, D.M., McCulloh, K.A., Woodruff, D.R., and Meinzer, F.C. (2012). Hydraulic safety margins and embolism reversal in stems and leaves: Why are conifers and angiosperms so different? Plant Sc *195*, 48-53.

Kaldenhoff, R., Kolling, A. and Richter, G. (1996) Regulation of the *Arabidopsis thaliana* aquaporin gene *AthH2* (PIP1b). J Photochem Photobiol B. *36*: 351-354.

Kaldenhoff, R., Grote, K., Zhu, J.J., and Zimmermann, U. (1998). Significance of plasmalemma aquaporins for water-transport in *Arabidopsis thaliana*. Plant J *14*, 121-128.

Kaldenhoff, R., Ribas-Carbo, M., Sans, J.F., Lovisolo, C., Heckwolf, M., and Uehlein, N. (2008). Aquaporins and plant water balance. Plant Cell Env *31*, 658-666.

Katsuhara, M., Akiyama, Y., Koshio, K., Shibasaka, M., and Kasamo, K. (2002). Functional analysis of water channels in barley roots. Plant Cell Physiol *43*, 885-893.

Kikuta, S.B., LoGullo, M.A., Nardini, A., Richter, H., and Salleo, S. (1997). Ultrasound acoustic emissions from dehydrating leaves of deciduous and evergreen trees. Plant Cell Env *20*, 1381-1390.

Kim, Y.X., and Steudle, E. (2007). Light and turgor affect the water permeability (aquaporins) of parenchyma cells in the midrib of leaves of *Zea mays*. J Exp Bot *58*, 4119-4129.

Kim, Y.X., and Steudle, E. (2009). Gating of aquaporins by light and reactive oxygen species in leaf parenchyma cells of the midrib of *Zea mays*. J Exp Bot *60*, 547-556.

Kolb, K.J., Sperry, J.S., and Lamont, B.B. (1996). A method for measuring xylem hydraulic conductance and embolism in entire root and shoot systems. J Exp Bot *47*, 1805-1810.

Kuwagata, T., Ishikawa-Sakurai, J., Hayashi, H., Nagasuga, K., Fukushi, K., Ahamed, A., *et al.* (2012) Influence of Low Air Humidity and Low Root Temperature on Water Uptake, Growth and Aquaporin Expression in Rice Plants. Plant Cell Physiol *53*: 1418-1431.

L

Larchevêque, M., Maurel, M., Desrochers, A., and Larocque, G.R. (2011). How does drought tolerance compare between two improved hybrids of balsam poplar and an unimproved native species? Tree Physiol *31*, 240-249.

Lee, H.K., Cho, S.K., Son, O., Xu, Z., Hwang, I., and Kim, W.T. (2009). Drought stress-induced Rma1H1, a RING membrane-anchor E3 ubiquitin ligase homolog, regulates aquaporin levels via ubiquitination in transgenic *Arabidopsis* plants. Plant Cell *21*, 622-641.

Lee, Y., Lee, H.S., Lee, J.S., Kim, S.K., and Kim, S.H. (2008). Hormone- and light-regulated nucleocytoplasmic transport in plants: current status. J Exp Bot *59*, 3229-3245.

Leng, H., Lu, M. and Wan, X. (2012) Variation in embolism occurrence and repair along the stem in drought-stressed and re-watered seedlings of a poplar clone. Physiol Plant doi: 10.1111/j.1399-3054.2012.01665.x.

Li, Y., Wu, Z., Ma, N. and Gao, J. (2009) Regulation of the rose Rh-PIP2;1 promoter by hormones and abiotic stresses in *Arabidopsis*. Plant Cell Rep *28*: 185-196.

Livak, K.J. and Schmittgen, T.D. (2001) Analysis of relative gene expression data using real-time quantitative PCR and the 2(-Delta Delta C(T)) Method. Methods *25*: 402-408.

Lo Gullo, M.A., Nardini, A., Trifilo, P., and Salleo, S. (2003). Changes in leaf hydraulics and stomatal conductance following drought stress and irrigation in *Ceratonia siliqua* (Carob tree). Physiol Plant *117*, 186-194.

Lo Gullo, M.A., Nardini, A., Trifilo, P., and Salleo, S. (2005). Diurnal and seasonal variations in leaf hydraulic conductance in evergreen and deciduous trees. Tree Physiol *25*, 505-512.

Lopez, D., Bronner, G., Brunel, N., Auguin, D., Bourgerie, S., Brignolas, F., Carpin, S., Tournaire-Roux, C., Maurel, C., Fumanal, B.*, et al.* (2012). Insights into *Populus* XIP aquaporins: evolutionary expansion, protein functionality, and environmental regulation. J Exp Bot *63*, 2217-2230.

Lopez, F., Bousser, A., Sissoeff, I., Gaspar, M., Lachaise, B., Hoarau, J., *et al.* (2003) Diurnal regulation of water transport and aquaporin gene expression in maize roots: contribution of PIP2 proteins. Plant Cell Physiol *44*: 1384-1395.

Lovisolo, C., Secchi, F., Nardini, A., Salleo, S., Buffa, R., and Schubert, A. (2007). Expression of PIP1 and PIP2 aquaporins is enhanced in olive dwarf genotypes and is related to root and leaf hydraulic conductance. Physiol Plant *130*, 543-551.

Lovisolo, C., and Tramontini, S. (2010). Methods for Assessment of Hydraulic Conductance and Embolism Extent in Grapevine Organs. In Methodologies and Results in Grapevine Research, S. Delrot, H.l. Medrano, E. Or, L. Bavaresco, and S. Grando, eds. (Springer Netherlands), pp. 71-85.

Ludewig, U., and Dynowski, M. (2009). Plant aquaporin selectivity: where transport assays, computer simulations and physiology meet. Cell Mol Life Sci *66*, 3161-3175.

Luu, D.-T., Martinière, A., Sorieul, M., Runions, J., and Maurel, C. (2012). Fluorescence recovery after photobleaching reveals high cycling dynamics of plasma membrane aquaporins in *Arabidopsis* roots under salt stress. Plant J *69*, 894-905.

Ma, S., Quist, T.M., Ulanov, A., Joly, R., and Bohnert, H.J. (2004). Loss of TIP1;1 aquaporin in *Arabidopsis* leads to cell and plant death. Plant J *40*, 845-859.

Mahdieh, M., Mostajeran, A., Horie, T., and Katsuhara, M. (2008). Drought stress alters water relations and expression of PIP-type aquaporin genes in *Nicotiana tabacum* plants. Plant Cell Physiol *49*, 801-813.

Marjanović, Z., Uehlein, N., Kaldenhoff, R., Zwiazek, J.J., Weiss, M., Hampp, R., *et al.* (2005) Aquaporins in poplar: what a difference a symbiont makes! Planta *222*: 258-268.

Martre, P., Morillon, R., Barrieu, F., North, G.B., Nobel, P.S., and Chrispeels, M.J. (2002). Plasma membrane aquaporins play a significant role during recovery from water deficit. Plant Physiol *130*, 2101-2110.

Matsubara, S., Hurry, V., Druart, N., Benedict, C., Janzik, I., Chavarria-Krauser, A., *et al.* (2006) Nocturnal changes in leaf growth of *Populus deltoides* are controlled by cytoplasmic growth. Planta *223*: 1315-1328.

Matzner, S., and Comstock, J. (2001). The temperature dependence of shoot hydraulic resistance: implications for stomatal behaviour and hydraulic limitation. Plant, Cell Env *24*, 1299-1307.

Maurel, C., Verdoucq, L., Luu, D.T., and Santoni, V. (2008). Plant aquaporins: membrane channels with multiple integrated functions. Annu Rev Plant Biol *59*, 595-624.

Maurel, C., Santoni, V., Luu, D.T., Wudick, M.M., and Verdoucq, L. (2009). The cellular dynamics of plant aquaporin expression and functions. Curr Opin Plant Biol *12*, 690-698.

Mayr, S., Cochard, H., Ameglio, T., and Kikuta, S.B. (2007). Embolism formation during freezing in the wood of *Picea abies*. Plant Physiol *143*, 60-67.

McKown, A.D., Cochard, H., and Sack, L. (2010). Decoding Leaf Hydraulics with a Spatially Explicit Model: Principles of Venation Architecture and Implications for its Evolution. Am Nat *175*: 447-460.

Meiresonne, L., Nadezhdin, N., Cermak, J., Van Slycken, J. and Ceulemans, R. (1999) Measured sap flow and simulated transpiration from a poplar stand in Flanders (Belgium). Agr For Met *96*: 165-179.

Moshelion, M., Becker, D., Biela, A., Uehlein, N., Hedrich, R., Otto, B., *et al.* (2002) Plasma membrane aquaporins in the motor cells of *Samanea saman*: diurnal and circadian regulation. Plant Cell *14*: 727-739.

Moshelion, M., Moran, N., and Chaumont, F., (2004) Dynamic changes in the osmotic water permeability of protoplast plasma membrane. Plant Physiol. *135(4)* 2301-2317.

Möller, M., Alchanatis, V., Cohen, Y., Meron, M., Tsipris, J., Naor, A., Ostrovsky, V., Sprintsin, M., and Cohen, S. (2007). Use of thermal and visible imagery for estimating crop water status of irrigated grapevine. J Exp Bot *58*, 827-838.

Monclus, R., Dreyer, E., Villar, M., Delmotte, F.M., Delay, D., Petit, J.M., Barbaroux, C., Thiec, D., Brechet, C., and Brignolas, F. (2006). Impact of drought on productivity and water use efficiency in 29 genotypes of *Populus deltoides x Populus nigra*. New Phytol *169*, 765-777.

Morillon, R., and Chrispeels, M.J. (2001). The role of ABA and the transpiration stream in the regulation of the osmotic water permeability of leaf cells. Proc Natl Acad Sci U S A *98*, 14138-14143.

Muries, B., Faize, M., Carvajal, M. and Martinez-Ballesta, M.C. (2011) Identification and differential induction of the expression of aquaporins by salinity in broccoli plants. Molecular BioSystems. DOI 10.1039/c0mb00285b.

N

Nardini, A., and Tyree, M., T. (1999). Root and shoot hydraulic conductance of seven Quercus species. Ann For Sci *56*, 371-377.

Nardini, A., and Salleo, S. (2000). Limitation of stomatal conductance by hydraulic traits: sensing or preventing xylem cavitation? Trees *15*, 14-24.

Nardini, A., Tyree, M.T., and Salleo, S. (2001). Xylem cavitation in the leaf of *Prunus laurocerasus* and its impact on leaf hydraulics. Plant Physiol *125*, 1700-1709.

Nardini, A., Gortan, E., and Salleo, S. (2005a). Hydraulic efficiency of the leaf venation system in sun- and shade-adapted species. Funct Plant Biol *32*, 953-961.

Nardini, A. and Salleo, S. (2005) Water stress-induced modifications of leaf hydraulic architecture in sunflower: co-ordination with gas exchange. J Exp Bot *56*: 3093-3101.

Nardini, A., Salleo, S., and Andri, S. (2005b). Circadian regulation of leaf hydraulic conductance in sunflower (*Helianthus annuus* L. cv Margot). Plant, Cell Env *28*, 750-759.

Nardini, A., Ramani, M., Gortan, E., and Salleo, S. (2008). Vein recovery from embolism occurs under negative pressure in leaves of sunflower (Helianthus annuus). Physiol Plant *133*, 755-764

Nardini, A., Raimondo, F., Lo Gullo, M.A., and Salleo, S. (2010). Leafminers help us understand leaf hydraulic design. Plant Cell Env *33*, 1091-1100.

Nardini, A., Peda, G., and Rocca, N.L. (2012). Trade-offs between leaf hydraulic capacity and drought vulnerability: morpho-anatomical bases, carbon costs and ecological consequences. New phytol *196*, 788-798.

Nilsson, R., Bernfur, K., Gustavsson, N., Bygdell, J., Wingsle, G. and Larsson, C. (2010) Proteomics of Plasma Membranes from Poplar Trees Reveals Tissue Distribution of Transporters, Receptors, and Proteins in Cell Wall Formation. Mol Cel Proteomics *9*: 368-387.

P

Pantin, F., Monnet, F., Jannaud, D., Costa, J.M., Renaud, J., Muller, B., Simonneau, T., and Genty, B. (2012). The dual effect of abscisic acid on stomata. New Phytol doi: 10.1111/nph.12013.

Passioura, J. (1984). Hydraulic Resistance of Plants. I. Constant or Variable? Funct Plant Biol *11*, 333-339.

Perrone, I., Pagliarani, C., Lovisolo, C., Chitarra, W., Roman, F., and Schubert, A. (2012). Recovery from water stress affects grape leaf petiole transcriptome. Planta *235*, 1383-1396.

Pfaffl, M.W., Tichopad, A., Prgomet, C. and Neuvians, T.P. (2004) Determination of stable housekeeping genes, differentially regulated target genes and sample integrity: BestKeeper--Excel-based tool using pair-wise correlations. Biotech Let *26*: 509-515.

Postaire, O., Tournaire-Roux, C., Grondin, A., Boursiac, Y., Morillon, R., Schaffner, A.R., and Maurel, C. (2010). A PIP1 Aquaporin Contributes to Hydrostatic Pressure-Induced Water Transport in Both the Root and Rosette of *Arabidopsis*. Plant Physiology *152*, 1418-1430.

Pou, A., Medrano, H., Flexas, J., and Tyerman, S.D. (2012). A putative role for TIP and PIP aquaporins in dynamics of leaf hydraulic and stomatal conductances in grapevine under water stress and re-watering. Plant, Cell Env, doi: 10.1111/pce.12019.

Q

Quentin, A.G., O'Grady, A.P., Beadle, C.L., Mohammed, C., and Pinkard, E.A. (2012). Interactive effects of water supply and defoliation on photosynthesis, plant water status and growth of *Eucalyptus globulus Labill*. Tree Physiol *32*, 958-967.

R

R Development Core Team (2011). R: A language and environment for statistical computing. R Foundation for Statistical Computing, Vienna, Austria. ISBN 3-900051-07-0, http://www.R-project.org/.

Rockwell, F.E., Holbrook, N.M., and Zwieniecki, M.A. (2011). Hydraulic conductivity of red oak (*Quercus rubra* L.) leaf tissue does not respond to light. Plant Cell Env *34*, 565-579.

S

Sack, L., Melcher, P.J., Zwieniecki, M.A., and Holbrook, N.M. (2002). The hydraulic conductance of the angiosperm leaf lamina: a comparison of three measurement methods. J Exp Bot *53*, 2177-2184.

Sack, L., Streeter, C.M., and Holbrook, N.M. (2004). Hydraulic analysis of water flow through leaves of sugar maple and red oak. Plant Physiol *134*, 1824-1833.

Sack, L., Tyree, M.T., and Holbrook, N.M. (2005). Leaf hydraulic architecture correlates with regeneration irradiance in tropical rainforest trees. New Phytol *167*, 403-413.

Sack, L., and Holbrook, N.M. (2006). Leaf hydraulics. Annu Rev Plant Biol *57*, 361-381.

Sack, L., Dietrich, E.M., Streeter, C.M., Sanchez-Gomez, D., and Holbrook, N.M. (2008). Leaf palmate venation and vascular redundancy confer tolerance of hydraulic disruption. Proc Natl Acad Sci USA *105*, 1567-1572.

Sade, N., Gebretsadik, M., Seligmann, R., Schwartz, A., Wallach, R., and Moshelion, M. (2010). The role of tobacco Aquaporin1 in improving water use efficiency, hydraulic conductivity, and yield production under salt stress. Plant Physiol *152*, 245-254.

Sadok, W., and Sinclair, T.R. (2010). Transpiration response of 'slow-wilting' and commercial soybean (*Glycine max* (L.) Merr.) genotypes to three aquaporin inhibitors. J Exp Bot *61*, 821-829.

Sakr, S., Alves, G., Morillon, R., Maurel, K., Decourteix, M., Guilliot, A., Fleurat-Lessard, P., Julien, J.L., and Chrispeels, M.J. (2003). Plasma membrane aquaporins are involved in winter embolism recovery in walnut tree. Plant Physiol *133*, 630-641.

Salleo, S., Lo Gullo, M.A., Raimondo, F., and Nardini, A. (2001). Vulnerability to cavitation of leaf minor veins: any impact on leaf gas exchange? Plant Cell Env *24*, 851-859.

Salleo, S., Raimondo, F., Trifilo, P., and Nardini, A. (2003). Axial-to-radial water permeability of leaf major veins: a possible determinant of the impact of vein embolism on leaf hydraulics? Plant Cell Env *26*, 1749-1758.

Sapozhnikova, V.V., Kamensky, V.A., Kuranov, R.V., Kutis, I., Snopova, L.B., and Myakov, A.V. (2004). In vivo visualization of *Tradescantia* leaf tissue and monitoring the physiological and morphological states under different water supply conditions using optical coherence tomography. Planta *219*, 601-609.

Scholander, P.F., Bradstreet, E.D., Hemmingsen, E.A., and Hammel, H.T. (1965). Sap Pressure in Vascular Plants: Negative hydrostatic pressure can be measured in plants. Science *148*, 339-346.

Scoffoni, C., Pou, A., Aasamaa, K., and Sack, L. (2008). The rapid light response of leaf hydraulic conductance: new evidence from two experimental methods. Plant Cell Env *31*, 1803-1812.

Scoffoni, C., Rawls, M., McKown, A., Cochard, H., and Sack, L. (2011). Decline of Leaf Hydraulic Conductance with Dehydration: Relationship to Leaf Size and Venation Architecture. Plant Physiol *156*, 832-843.

Secchi, F., Lovisolo, C., Uehlein, N., Kaldenhoff, R. and Schubert, A. (2007) Isolation and functional characterization of three aquaporins from olive (*Olea europaea* L.). Planta *225*: 381-392.

Secchi, F., MacIver, B., Zeidel, M.L., and Zwieniecki, M.A. (2009). Functional analysis of putative genes encoding the PIP2 water channel subfamily in *Populus trichocarpa*. Tree Physiol *29*, 1467-1477.

Secchi, F., and Zwieniecki, M.A. (2010). Patterns of PIP gene expression in *Populus trichocarpa* during recovery from xylem embolism suggest a major role for the PIP1 aquaporin subfamily as moderators of refilling process. Plant Cell Env *33*, 1285-1297.

Secchi, F., and Zwieniecki, M.A. (2011). Sensing embolism in xylem vessels: the role of sucrose as a trigger for refilling. Plant Cell Env *34*, 514-524.

Sellin, A., and Kupper, P. (2007). Temperature, light and leaf hydraulic conductance of little-leaf linden (*Tilia cordata*) in a mixed forest canopy. Tree Physiol *27*, 679-688.

Sellin, A., Ounapuu, E., and Kupper, P. (2008). Effects of light intensity and duration on leaf hydraulic conductance and distribution of resistance in shoots of silver birch (*Betula pendula*). Physiol Plant *134*, 412-420.

Sellin, A., Ounapuu, E., Kaurilind, E., and Alber, M. (2012). Size-dependent variability of leaf and shoot hydraulic conductance in silver birch. Trees *26*, 821-831.

Shatil-Cohen, A., Attia, Z., and Moshelion, M. (2011). Bundle-sheath cell regulation of xylem-mesophyll water transport via aquaporins under drought stress: a target of xylem-borne ABA? Plant J, *67*(1):72-80.

Shope, J.C., Mott, K.A. (2006) Membrane trafficking and osmotically induced volume changes in guard cells. J Exp Bot. *57(15):*4123-31.

Siefritz, F., Tyree, M.T., Lovisolo, C., Schubert, A., and Kaldenhoff, R. (2002). PIP1 plasma membrane aquaporins in tobacco: from cellular effects to function in plants. Plant Cell *14*, 869-876.

Silim, S., Nash, R., Reynard, D., White, B., and Schroeder, W. (2009). Leaf gas exchange and water potential responses to drought in nine poplar (*Populus* spp.) clones with contrasting drought tolerance. Trees *23*, 959-969.

Simonin, K.A., Limm, E.B., and Dawson, T.E. (2012). Hydraulic conductance of leaves correlates with leaf lifespan: implications for lifetime carbon gain. New Phytol *193*, 939-947.

Sinclair, T.R., Zwieniecki, M.A., and Holbrook, N.M. (2008). Low leaf hydraulic conductance associated with drought tolerance in soybean. Physiol Plant *132*, 446-451.

Smart, L.B., Moskal, W.A., Cameron, K.D. and Bennett, A.B. (2001) MIP genes are down-regulated under drought stress in *Nicotiana glauca*. Plant Cell Physiol *42*: 686-693.

Snyder, K.A., Richards, J.H. and Donovan, L.A. (2003) Nighttime conductance in C3 and C4 species: do plants lose water at night? J Exp Bot *54*: 861-865.

Sober, A. (1997). Hydraulic conductance, stomatal conductance, and maximal photosynthetic rate in bean leaves. Photosynthetica *34*, 599-603.

Sperry, J.S., Hacke, U.G., Oren, R., and Comstock, J.P. (2002). Water deficits and hydraulic limits to leaf water supply. Plant Cell Env *25*, 251-263.

Sperry, J.S., Meinzer, F.C., and McCulloh, K.A. (2008). Safety and efficiency conflicts in hydraulic architecture: scaling from tissues to trees. Plant Cell Env *31*, 632-645.

Street, N.R., Skogstrom, O., Sjodin, A., Tucker, J., Rodriguez-Acosta, M., Nilsson, P., Jansson, S., and Taylor, G. (2006). The genetics and genomics of the drought response in *Populus*. Plant J *48*, 321-341.

Takase, T., Ishikawa, H., Murakami, H., Kikuchi, J., Sato-Nara, K. and Suzuki, H. (2011) The circadian clock modulates water dynamics and aquaporin expression in *Arabidopsis* roots. Plant Cell Physiol *52*: 373-383.

Terashima, I., Hanba, Y.T., Tazoe, Y., Vyas, P., and Yano, S. (2006). Irradiance and phenotype: comparative eco-development of sun and shade leaves in relation to photosynthetic CO_2 diffusion. J Exp Bot *57*, 343-354.

Thompson, J.D., Higgins, D.G. and Gibson, T.J. (1994) CLUSTAL W: improving the sensitivity of progressive multiple sequence alignment through sequence weighting, position-specific gap penalties and weight matrix choice. Nucleic Acids Res *22:* 4673-4680.

Tomos, A.D., and Leigh, R.A. (1999). The pressure prob: A Versatile Tool in Plant Cell Physiology. Annu Rev Plant Physiol Plant Mol Biol *50*, 447-472.

Tournaire-Roux, C., Sutka, M., Javot, H., Gout, E., Gerbeau, P., Luu, D.T., *et al.* (2003) Cytosolic pH regulates root water transport during anoxic stress through gating of aquaporins. Nature *425*: 393-397.

Trifilo, P., Nardini, A., Lo Gullo, M.A., and Salleo, S. (2003). Vein cavitation and stomatal behaviour of sunflower (*Helianthus annuus)* leaves under water limitation. Physiol Plant *119*, 409-417.

Tsuchihira, A., Hanba, Y.T., Kato, N., Doi, T., Kawazu, T., and Maeshima, M. (2010). Effect of overexpression of radish plasma membrane aquaporins on water-use efficiency, photosynthesis and growth of Eucalyptus trees. Tree Physiol *30*, 417-430.

Tsuda, M., and Tyree, M.T. (1997). Whole-plant hydraulic resistance and vulnerability segmentation in *Acer saccharinum*. Tree Physiol *17*, 351-357.

Tsuda, M., and Tyree, M.T. (2000). Plant hydraulic conductance measured by the high pressure flow meter in crop plants. J Exp Bot *51*, 823-828.

Tungngoen, K., Kongsawadworakul, P., Viboonjun, U., Katsuhara, M., Brunel, N., Sakr, S., *et al.* (2009) Involvement of HbPIP2;1 and HbTIP1;1 aquaporins in ethylene stimulation of latex yield through regulation of water exchanges between inner liber and latex cells in *Hevea brasiliensis*. Plant Physiol *151:* 843-856.

Tuskan, G.A., DiFazio, S., Jansson, S., Bohlmann, J., Grigoriev, I., Hellsten, U., Putnam, N., Ralph, S., Rombauts, S., Salamov, A*., et al.* (2006). The genome of black cottonwood, *Populus trichocarpa* (Torr. & Gray). Science *313*, 1596-1604.

Tyree, M.T., and Hammel, H.T. (1972). The Measurement of the Turgor Pressure and the Water Relations of Plants by the Pressure-bomb Technique. J Exp Bot *23*, 267-282.

Tyree, M.T., and Cheung, Y.N.S. (1977). Resistance To Water-Flow In *Fagus-Grandifolia* Leaves. Canadian Journal of Botany *55*, 2591-2599.

Tyree, M.T., and Dixon, M.A. (1983). Cavitation Events In *Thuja-Occidentalis* L - Utrasonic Acoustic Emissions From The Sapwood Can Be Measured. Plant Physiol *72*, 1094-1099.

Tyree, M.T., and Sperry, J.S. (1988). Do Woody Plants Operate Near the Point of Catastrophic Xylem Dysfunction Caused by Dynamic Water Stress? : Answers from a Model. Plant Physiol *88*, 574-580.

Tyree, M.T., Sinclair, B., Lu, P., and Granier, A. (1993a). Whole Shoot Hydraulic Resistance In *Quercus* Species Measured With A New High-Pressure Flowmeter. Ann Sci For *50*, 417-423.

Tyree, M.T., Cochard, H., Cruiziat, P., Sinclair, B., and Ameglio, T. (1993b). Drought-induced leaf shedding in walnut: evidence for vulnerability segmentation. Plant Cell Env *16*, 879-882.

Tyree, M.T., Kolb, K.J., Rood, S.B., and Patino, S. (1994). Vulnerability To Drought-Induced Cavitation Of Riparian Cottonwoods In Alberta - A Possible Factor In The Decline Of The Ecosystem. Tree Physiol *14*, 455-466.

Tyree, M.T., Velez, V., and Dalling, J.W. (1998). Growth dynamics of root and shoot hydraulic conductance in seedlings of five neotropical tree species: scaling to show possible adaptation to differing light regimes. Oecologia *114*, 293-298.

Tyree, M.T., Sobrado, M.A., Stratton, L.J., and Becker, P. (1999). Diversity of hydraulic conductance in leaves of temperate and tropical species: possible causes and consequences. Journal of Tropical Forest Science *11*, 47-60.

Tyree, M.T. (2003). Hydraulic limits on tree performance: transpiration, carbon gain and growth of trees. Trees *17*, 95-100.

Tyree MT, Cochard H. (2003) Vessel contents of leaves after excision: a test of the Scholander assumption. J Exp Bot *54*(390):2133-9.

Tyree, M.T., Engelbrecht, B.M., Vargas, G., and Kursar, T.A. (2003). Desiccation tolerance of five tropical seedlings in panama. Relationship to a field assessment of drought performance. Plant Physiol *132*, 1439-1447.

Tyree, M.T., Nardini, A., Salleo, S., Sack, L., and El Omari, B. (2005). The dependence of leaf hydraulic conductance on irradiance during HPFM measurements: any role for stomatal response? J Exp Bot *56*, 737-744.

U

Uehlein, N., Lovisolo, C., Siefritz, F., and Kaldenhoff, R. (2003). The tobacco aquaporin NtAQP1 is a membrane CO_2 pore with physiological functions. Nature *425*, 734-737.

Uehlein, N., Otto, B., Hanson, D.T., Fischer, M., McDowell, N., and Kaldenhoff, R. (2008). Function of *Nicotiana tabacum* aquaporins as chloroplast gas pores challenges the concept of membrane CO2 permeability. Plant Cell *20*, 648-657.

Uehlein, N., Sperling, H., Heckwolf, M., and Kaldenhoff, R. (2012). The *Arabidopsis* aquaporin PIP1;2 rules cellular CO(2) uptake. Plant Cell Env *35*, 1077-1083.

Untergasser, A., Nijveen, H., Rao, X., Bisseling, T., Geurts, R. and Leunissen, J.A. (2007) Primer3Plus, an enhanced web interface to Primer3. Nucleic Acids Res *35*: W71-74.

V

Vandeleur, R.K., Mayo, G., Shelden, M.C., Gilliham, M., Kaiser, B.N., and Tyerman, S.D. (2009). The role of plasma membrane intrinsic protein aquaporins in water transport through roots: diurnal and drought stress responses reveal different strategies between isohydric and anisohydric cultivars of grapevine. Plant Physiol *149*, 445-460.

Vilagrosa, A., Bellot, J., Vallejo, V.R., and Gil-Pelegrin, E. (2003). Cavitation, stomatal conductance, and leaf dieback in seedlings of two co-occurring Mediterranean shrubs during an intense drought. J Exp Bot *54*, 2015-2024.

Vilagrosa, A., Morales, F., Abadia, A., Bellot, J., Cochard, H., and Gil-Pelegrin, E. (2010). Are symplast tolerance to intense drought conditions and xylem vulnerability to cavitation coordinated? An integrated analysis of photosynthetic, hydraulic and leaf level processes in two Mediterranean drought-resistant species. Env Exp Bot *69*, 233-242.

Voicu, M.C., Zwiazek, J.J., and Tyree, M.T. (2008). Light response of hydraulic conductance in bur oak (*Quercus macrocarpa*) leaves. Tree Physiol *28*, 1007-1015.

Voicu, M.C., Cooke, J.E., and Zwiazek, J.J. (2009). Aquaporin gene expression and apoplastic water flow in bur oak (*Quercus macrocarpa*) leaves in relation to the light response of leaf hydraulic conductance. J Exp Bot *60*, 4063-4075.

Voicu, M.C. and Zwiazek, J.J. (2010) Inhibitor studies of leaf lamina hydraulic conductance in trembling aspen (*Populus tremuloides* Michx.) leaves. Tree Physiol *30*: 193-204.

Voicu, M.C., and Zwiazek, J.J. (2011). Diurnal and seasonal changes of leaf lamina hydraulic conductance in bur oak (Quercus macrocarpa) and trembling aspen (*Populus tremuloides*). Trees *25*, 485-495.

W

Wallace, I.S. and Roberts, D.M. (2004) Homology modeling of representative subfamilies of *Arabidopsis* major intrinsic proteins. Classification based on the aromatic/arginine selectivity filter. Plant Physiol *135*: 1059-1068.

Way, D.A., Domec, J.-C., and Jackson, R.B. (2012). Elevated growth temperatures alter hydraulic characteristics in trembling aspen (*Populus tremuloides*) seedlings: implications for tree drought tolerance. Plant Cell Env, doi: 10.1111/j.1365-3040.2012.02557.x..

Weatherley, P.E. (1963). The pathway of water movements across the root cortex and leaf mesophyll in transpiring plants. The Water Relations of Plants *eds A. Rutter & F. Whitehead Blackwell, London, UK*, 85-100.

Wei, C., Steudle, E., Tyree, M.T., and Lintilhac, P.M. (2001). The essentials of direct xylem pressure measurement. Plant Cell Env *24*, 549-555.

Wong S.C., Cohan I.R. and Farquhar J.D. (1979) Stomatal conductance correlates with photosynthetic capacity. Nature *282*, 424-426.

Wudick, M.M., Luu, D.T., and Maurel, C. (2009). A look inside: localization patterns and functions of intracellular plant aquaporins. New Phytol *184*, 289-302.

Xu, M., Zhang, B., Su, X., Zhang, S. and Huang, M. (2011. Reference gene selection for quantitative real-time polymerase chain reaction in *Populus*. Anal Biochem *408*: 337-339.

Yamada, S. and Bohnert, H.J. (2000) Expression of the PIP aquaporin promoter-MipA from the common ice plant in tobacco. Plant Cell Physiol *41*: 719-725.

Yan, D.H., Fenning, T., Tang, S., Xia, X.L., and Yin, W.L. (2012). Genome-wide transcriptional response of *Populus euphratica* to long-term drought stress. Plant Sci *195*, 24-35.

Yang, S.D., and Tyree, M.T. (1993). Hydraulic Resistance In *Acer-Saccharum* Shoots And Its Influence On Leaf Water Potential And Transpiration. Tree Physiol *12*, 231-242.

Yang, S.-J., Zhang, Y.-J., Sun, M., Goldstein, G., and Cao, K.-F. (2012). Recovery of diurnal depression of leaf hydraulic conductance in a subtropical woody bamboo species: embolism refilling by nocturnal root pressure. Tree Physiol *32*, 414-422.

Ye, Q., Holbrook, N.M., and Zwieniecki, M.A. (2008). Cell-to-cell pathway dominates xylem-epidermis hydraulic connection in *Tradescantia fluminensis* (Vell. Conc.) leaves. Planta *227*, 1311-1319.

Z

Zimmermann, D., Reuss, R., Westhoff, M., Gessner, P., Bauer, W., Bamberg, E., Bentrup, F.W., and Zimmermann, U. (2008). A novel, non-invasive, online-monitoring, versatile and easy plant-based probe for measuring leaf water status. J Exp Bot *59*, 3157-3167.

Zimmermann, U., Meinzer, F.C., Benkert, R., Zhu, J.J., Schneider, H., Goldstein, G., Kuchenbrod, E., and Haase, A. (1994). Xylem water transport: is the available evidence consistent with the cohesion theory? Plant Cell Env *17*, 1169-1181.

Zufferey, V., Cochard, H., Ameglio, T., Spring, J.L. and Viret, O. (2011) Diurnal cycles of embolism formation and repair in petioles of grapevine (*Vitis vinifera* cv. Chasselas). J Exp Bot *62*: 3885-3894.

Zwieniecki, M.A., Brodribb, T.J., and Holbrook, N.M. (2007). Hydraulic design of leaves: insights from rehydration kinetics. Plant Cell Env *30*, 910-921.

Annexes

Annexe 1

Expression précoce de gènes lors de la stimulation lumineuse de la conductance hydraulique foliaire chez le noyer

DOI: 10.0007/s10535-012-0120-4 BIOLOGIA PLANTARUM 56 (4): 657-666, 2012

Early gene expression in the walnut tree occurring during stimulation of leaf hydraulic conductance by irradiance

K. BEN BÂAZIZ[1,2,3], D. LOPEZ[1,2], S. BOUZID[3], H. COCHARD[1,2], J.-S. VENISSE[1,2] and S. SAKR[1,2,4]*

Clermont-Université, UMR 547 PIAF, 24 avenue des Landais, F-63177 Aubière Cedex, France[1]
INRA, UMR 547 PIAF, F-63000 Clermont-Ferrand, France[2]
Laboratoire de Biologie végétale, Faculté des Sciences de Tunis, Campus Universitaire, 1060 Tunis, Tunisia[3]
Agrocampus Ouest, Centre d'Angers, UMR SAGAH, IFR QUASAV 149, F-49045 Angers Cedex, France[4]

Abstract

Leaf hydraulic conductance (K_{leaf}) plays a significant part in plant-water regulation. In walnut leaves, K_{leaf} is stimulated by irradiance and closely relates to the accumulation of *JrPIP2s* aquaporin transcripts, but it is independent of stomatal aperture. To provide an insight into the early molecular events occurred during light-induced K_{leaf}, a large-scale transcriptomic analysis consisting of the cDNA-amplified fragment length polymorphism (AFLP) was carried out on walnut leaves maintained under irradiance or in darkness. Of the total 12 000 transcript-derived fragments (TDFs) obtained using cDNA-AFLP with 128 primer pairs, 187 TDFs were selected after sequencing, and only 93 (49 %) that had been ascribed known functions through *BLAST* searching of the *GenBank* databases. Most of these TDFs correspond to genes whose protein products are involved in cellular regulation (57.9 %) and global metabolism (39.8 %). To validate cDNA-AFLP expression patterns, 30 TDFs were further analyzed using real-time quantitative polymerase chain reaction. Moreover, exposure of leaves to irradiance was accompanied by the modification of the Ca^{2+}-signaling pathway, ubiquitin-proteasome pathway, vesicle trafficking process and expression of multiple transcription factors.

Additional key words: aquaporin, cDNA-AFLP, *Juglans regia*, leaf water transport, plasma membrane intrinsic protein; qRT-PCR.

Introduction

Regulation of water transport is important for the adaptation and survival of terrestrial plants. It provides flexibility so the plant can respond to environmental factors by optimizing the use of water resources. Part of this regulation takes place in leaves, which are the major site of evaporation and photosynthesis. The hydraulic resistance of foliar tissues (R_{leaf}) contributes up to 60 - 80 % of shoot resistance (Yang and Tyree 1993, Nardini and Tyree 1999, Nardini and Salleo 2000) and up to 30 % of the whole plant hydraulic resistance (Sack and Holbrook 2006).

Leaf hydraulic conductance ($K_{leaf} = 1/R_{leaf}$) is defined as the ratio of water flow through the leaf to driving force of the flow, normalized by the leaf area (Sack and Holbrook 2006). K_{leaf} depends upon plant species (Tyree *et al.* 1998, Cosmstock 2000, Brodribb *et al.* 2002) and is modulated by environmental factors, such as water stress (Nardini *et al.* 2003, Nardini and Salleo 2005), temperature (Fredeen and Sage 1999, Cochard *et al.* 2000, 2007, Sack *et al.* 2004) and also by circadian rhythms (Brodribb and Holbrook 2004, Lo Gullo *et al.* 2005). K_{leaf} has long been thought to be mainly associated with the regulation of stomatal aperture, suggesting a minor contribution of aquaporins. This scenario seems to contradict much recent physiological and molecular data, advocating the key role of plasma membrane intrinsic proteins (PIPs) in the determination of K_{leaf}. In the walnut, the stimulation of K_{leaf} by irradiance was insensitive to high concentrations of abscisic acid (an inhibitor of stomatal opening), excluding a major role of stomatal limitation in this process (Tyree *et al.* 2005). On the other hand, in leaves of the *Helianthus annuus*, the presence of $HgCl_2$, an inhibitor of aquaporin activity, prompted a sharp reduction in K_{leaf} (Nardini and Salleo 2005). These findings underpin the idea that a substantial part of leaf water movement occur through the mercury-

Received 17 May 2010, *accepted* 30 April 2011.
Abbreviations: AFLP - amplified fragment length polymorphism; HPFM - high pressure flow meter; K_{leaf} - leaf hydraulic conductance; K_{root} - root hydraulic conductance; PIP - plasma membrane intrinsic protein; PCR - polymerase chain reaction; qRT-PCR - quantitative real-time PCR; R_{leaf} - leaf hydraulic resistance; TDF - transcript-derived fragment.
* Corresponding author; fax: (+33) 2 41 22 55 99, e-mail: soulaiman.sakr@agrocampus-ouest.fr

sensitive aquaporin pathway. In addition, aquaporins were reported to be localized in different leaf cells, including bundle sheath (Kaldenhoff *et al.* 1995, Frangne *et al.* 2001) and mesophyll cells (Otto and Kaldenhoff 2000, Hachez *et al.* 2008, Sakurai *et al.* 2008). Stimulation of K_{leaf} in walnut by irradiance was independent of stomatal aperture, but closely related to up-regulation of two isoforms of aquaporins (Cochard *et al.* 2007). Based on physiological investigations, two distinct water pathways have been proposed. The first one, characterized as an aquaporin-independent pathway (water movement occurs *via* the apoplastic and symplasmic routes), takes place both in dark and light conditions and is correlated with basal K_{leaf} values. The second one, identified as an aquaporin-dependent pathway, takes place in response to irradiance and corresponds to high, modulated K_{leaf} values (Voicu *et al.* 2009, Ben Baaziz *et al.* 2012). This high K_{leaf} requires a stimulation of PIP gene expression and de *novo* protein biosynthesis (Cochard *et al.* 2007), assuming that this early regulation of K_{leaf} by irradiance is very complex and may act at multiple levels. Such K_{leaf} regulation can prevent a substantial drop in leaf water potential under high transpiration, thereby providing a physiological advantage for plant growth and development.

Mechanisms responsible for perception and transduction of the signal of changing irradiance have been widely documented in relation to germination, flowering, phototropism and etiolation. However, little is known about the mechanism through which irradiance can regulate K_{leaf} and aquaporin expression. As a first step for elucidation of this task, amplified fragment length polymorphism-based mRNA fingerprinting (cDNA-AFLP) has been carried out on leaves exposed to irradiance for short time periods. 93 transcript-derived fragments (TDFs) were identified and grouped into ten functional categories. The efficiency of cDNA-AFLP was evaluated by monitoring the expression profile of 30 TDFs. This work provides the possibility to investigate the link(s) between these identified TDFs, aquaporins and stimulation of K_{leaf} by irradiance.

Materials and methods

The experiments were performed during the summer of 2006 and 2008, on leafy branches sampled from 15-year-old walnut trees (*Juglans regia* L. cv. Franquette) growing in the Institut National de la Recherche Agronomique (INRA) orchard near Clermont-Ferrand (South-central France). Leafy branches were randomly sampled from the sun-exposed part of the tree, and immediately recut under water. They were then enclosed in a black plastic bag and kept in full darkness at high value of humidity for 24 h before their use in this study. Only the mature developed leaves from the branches were used for experiments.

Measurement of leaf hydraulic conductance was carried out at room temperature (25 °C) as previously described Cochard *et al.* (2007). Briefly, the experiment consists of pushing degassed and pressurized water into the petiole of an excised leaf under a pressure P of 0.15 MPa. Irradiance of approximately 600 µmol m^{-2} s^{-1} at leaf level was provided by two 400 W iodine lamp. Water flow values (F, mmol s^{-1}) were recorded every 30 s using a high pressure flow meter (HPFM; *Bronkhorst*, Montigny Les Cormeilles, France) connected to computer. Leaf hydraulic conductance (K_{leaf}, mmol m^{-2} s^{-1} MPa^{-1}) was calculated as: $K_{leaf} = F/(P \times LA)$, where LA was the total leaf area [m^2]. F was measured on leaves exposed to irradiance for 120 min, and then during darkness for 120 min. Then leaves were immediately immersed in liquid nitrogen and stored at -80 °C.

Total RNA was extracted according to the method of Chang *et al.* (1993) and quantified in Clermont University using a spectrophoto-meter *ND-1000* (*Nanodrop*, France). First-strand cDNA was synthesized from 2 µg total RNA using *oligo(dT)*$_{30}$ AFLP primer and *AMV* reverse transcriptase (*Promega*, Madisson, WI, USA). Second-strand cDNA was made using 25 U of DNA polymerase I (*Promega*) and blunted with 6 U of T_4 DNA polymerase (*Promega*). cDNA double strand ($cDNA_{ds}$) were successively purified with 1 volume of isoamyl: phenol:chloroform (1:25:24) and 1 volume of isoamyl: chloroform (1:24), and precipitated using 3 volumes of 100 % ethanol added to 0.1 volume of ammonium acetate (3 M). Extracted $cDNA_{ds}$ were quantified using a *Nanodrop* spectrophoto-meter and checked by electrophoresis on a 2 % agarose gel. The AFLP reactions were performed according to Vos *et al.* (1995) and Bachem *et al.* (1996) with minor modifications. 500 ng of $cDNA_{ds}$ were digested by restriction enzyme pairs *Eco*RI/*Msp*I or *Eco*RI/*Mse*I (10 U each) (*BioLabs*, Ozyme, France). The restriction fragments were ligated to specific double strand adaptors with 400 U of T_4 DNA ligase (*Promega*) at 16 °C for 4 h. The PCR pre-amplification step was carried out on 0.004 cm^3 of ligated products diluted 10-fold in sterile water using the combinations *Eco*RI/*Msp*I or *Eco*RI/*Mse*I primers without selective nucleotides and 1 U of *Red GoldStar*™ Taq polymerase (*Eurogentec*, Seraing, Belgium). The PCR cycling conditions consisted in an initial step of 2 min at 94 °C followed by 25 cycles (94 °C for 30 s ; 55 °C for 1 min ; 72 °C for 1.30 min). The PCR products were diluted 20-fold in water and 0.004 cm^3 served as a matrix for selective amplification with 64 possible combinations of *Eco*RI adaptator (+N) and *Msp*I or *Mse*I adaptator (+NN) primers. PCR selective amplification consisted in 35 cycles including 11 touchdown cycles (65 - 56 °C in 0.7 °C step) subsequently maintained at 56 °C for the last 24 cycles. A final step of 72 °C for 10 min was adopted. About 0.003 cm^3 of heat denatured PCR product was resolved on a 5 % denaturing polyacrylamide (*Bio-Rad*, Marne la Coquette, France) sequencing gel containing

7 M urea. The amplicon bands were visualized by silver staining (0.1 %) according to Chalhoub *et al.* (1997). The reproducibility of the method was tested by comparing the pattern of two independent cDNA-AFLP procedures on three samples with 5 primer sets (data not shown).

Selection of differentially expressed transcript-derived fragments (TDFs) was visually made on AFLP-derived gels. These identified TDFs were excised from dried gels, eluted into 0.02 cm^3 of *Taq* polymerase buffer (1×) (*Qiagen*), heated at 94 °C for 4 min and then left to diffuse overnight at 4 °C. PCR re-amplification was performed with 0.01 cm^3 cDNA extracted using the same conditions and the non-selective *Eco*RI and *Msp*I or *Mse*I primers used for the non-selective amplification. PCR products were checked on a 2 % agarose gel and cloned into *pGEM®T-easy* vector (*Promega*) and then transfected into competent *Escherichia coli DH5α* (*Promega*) in accordance with the manufacturer's instructions. One clone pre-amplified fragment was sequenced (*Cogenics*, *Genome Express*, Rhône Alpes, France). Analysis of the nucleotide sequence as well as potential relative translated sequences was carried out using respectively *BLASTN* and *BLASTX* algorithmic tools (Altschul *et al.* 1997) from publicly available *GenBank* non-redundant genes/transcripts databases (http:// www.ncbi.nlm.gov/BLAST). In parallel, sequences were compared with the expressed sequence tag (EST) databases using the *BLASTN* algorithm by targeting *Juglans* organism (*NCBI* web server; *taxid 16718*) to gain potential further information. Sequences were manually assigned to putative functional categories based on the scientific literature analysis and the information reported for each sequence by *The Gene Ontology Consortium* (http://www.geneontology.org). Sequence data from this article can be found in the *GenBank/EMBL* data libraries under *GenBank* accession numbers GR410235 to GR410424.

Real-time quantitative RT-PCR (qPCR) was used to assess the expression pattern of 30 TDFs (third of 93 identified TDFs by cDNA-AFLP analysis), and of two *JrPIP2s* (*JrPIP2;1*, AY189973 and *JrPIP2;2*, AY189974) in leaves. Experiments were carried out after 0, 5, 10, 15, 30, 60 and 120 min under irradiance and 120 min after return to darkness). *Juglans regia* 18S rRNA gene (AF399876) was chosen as an internal reference for normalization of transcript abundance of the target genes. Three independent leaves were used for each time point.

All sets of primers and the related annealing temperature are described on http://www.sakretal2011.blogspot.com/). The amplification efficiency of all primer sets was checked routinely (data not shown).

Total RNA was extracted according to the method of Chang *et al.* (1993), and 2 µg was used for the single-stranded cDNA synthesis, using *SuperScript III* (*Invitrogen*, Carlsbad, CA, USA) following the manufacturer's instructions. qPCR amplification was performed using an *iCycler iQ* (*Bio-Rad*, Hercules, CA, USA) in 0.03cm^3 reaction mix using platinum *Taq* DNA polymerase (*Invitrogen*) according to the supplier's instructions, 10 µM specific primers (supplementary data 2, http://www.sakretal2011.blogspot.com/) and 0.5 mm^3 SYBR green I (1/1000, *Sigma,* Lyon, France). The PCR conditions were 94 °C for 3 min for denaturation, followed by 35 cycles of 94 °C for 20 s, 50/61 °C for 20 s and 72 °C for 20 s for amplification. Relative quantification (Qr) of the target genes was determined by comparison with the reference gene and calculated using the $2^{-\Delta\Delta CT}$ method (Livak and Schmittgen 2001) where $\Delta\Delta C_T$ is calculated as follows:

$\Delta\Delta C_T = (C_{Tt0} - C_{Ttx})_{Target}/(C_{Tt0} - C_{Ttx})_{18s}$, where C_T represents threshold cycle number of real-time PCR, tx represents time x for any point of the kinetic and t0 corresponds to the darkness control. Values were represented as $\log_2$ of Qr. For each investigated gene, three independent technical replicates were performed in addition to a second biological replicate. Values described represent means ± standard deviation.

For water flow parameters, each value is mean of 5 independent measurements. The effect of the different treatments on leaf hydraulic conductance was assessed by one-way *ANOVA* followed by a Tukey HSD post-hoc test. We considered the results statistically different at $P < 0.01$.

Results

Response of K_{leaf} and aquaporin transcripts to irradiance: In order to re-confirm the correlation between the pattern of K_{leaf} and the transcript level of two aquaporin isoforms (*JrPIP2;1* and *JrPIP2;2*) real-time quantitative RT-PCR was carried during a 120 min irradiance and 120 min after return to darkness (Fig. 1). Our data showed that the kinetics of K_{leaf} paralleled those of *JrPIP2s*. The abundance of both *JrPIP2s* transcripts increased significantly within the first 15 min of irradiance. Maximum values of K_{leaf} and transcript levels of *JrPIP2s* were achieved 1 h after the onset of irradiance. A concomitant drop in K_{leaf} and PIP2s transcripts occurred after return to darkness.

Isolation of radiation-responsive TDFs: Overall, the analysis of the 128 primers with 3 × 2 neighboring selective nucleotide combinations (*EcoR*I-N3 and *Mse*- or *Msp*I-N2) yielded a profiling of about 12 000 TDFs. Their sizes ranged between 50 to 1 300 bp, and all bands > 50 bp were analyzed. A comparison of cDNA-AFLP patterns revealed 592 TDFs with differentially up- and down-modulated expression between assayed samples. These regulations were defined herein as having clear differential band intensities under irradiance and in darkness for one or more of the early time points. From this pool, a subset of 225 quantitatively reliable TDFs was chosen due to their earlier responsiveness to

irradiance (15 and/or 30 min). Among them, 126 were up-regulated and 99 down-regulated genes. 38 TDFs were redundant sequences. Finally, 187 TDFs were used as queries for a bioinformatic characterization to search significant similarities and potential structural homologies with public nucleotide and amino acid sequence databases, using *BLASTN* and *BLASTX*, respectively. A minimal expectation value corresponding to the probability that a homology could be random was fixed at 10^{-4}, except for a short sequence TDF046 (78 bp) which had an *E*-value of 1.1 for 87 % of identities with the ethylene responsive element binding factor type 5 (*ATERF5*) of *Arabidopsis thaliana* (BAA97157). Nucleotide sequences of all TDFs identified through this study have been recorded and are available in the *GenBank/EMBL* sequence database.

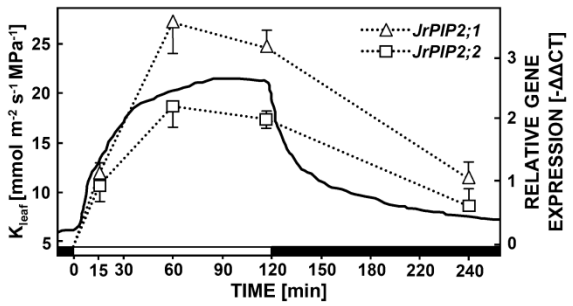

Fig. 1. Real-time quantitative RT-PCR analyses of the relative expression rate of genes encoding aquaporines *JrPIP2;1* and *JrPIP2;2* in walnut leaves at 15, 60 and 120 min under irradiance and 120 min after return to dark. Relative gene expression was normalized by comparing ΔΔCt of the *JrPIP2s* genes and *J. regia* 18S rRNA gene, where the starting state quantity was the dark control point 0 min. K_{leaf} values are mean of five independent leaves and PCR values are mean of three independent measurements.

Functional classification of radiation-responsive TDFs: A functional classification of the TDFs identified in this research was carried out according to *Gene Ontology* (http://www.geneontology.org). A total of 93 TDFs were identified, and divided into 10 categories containing their putative functions (suppl. data 4, http://www.sakretal2011.blogspot.com/). The largest number of TDFs was related to signal transduction (19 TDFs; 20.5 %). This category was followed by maintenance protein (14 TDFs; 15 %), DNA/RNA maintenance (12 TDFs; 12.9 %), binding regulatory proteins (9 TDFs; 9.7 %), fatty acid metabolism (9 TDFs; 9.7 %), cellular metabolism (9 TDFs; 9.7 %), and sugar metabolism (7 TDFs; 7.5 %). These first four categories, involved in regulator modules in management and transmission of cellular signal, comprise 54 TDFs (57.9 %). The lowest number of TDFs was found for three functional categories: stress and defense-related proteins (6 TDFs; 6.4 %), transport facilitation (5 TDFs; 5.4 %), and metabolism (3 TDFs; 3.2 %). 21 TDFs showed similarities with protein sequences found in others plant species but were devoid of any known function. 68 TDFs returned no similarity match with known sequences, including 31 up-regulated and 37 down-regulated genes after exposure to light (suppl. data 3; http://www.sakretal2011.blogspot.com/). These "anonymous ESTs" can not be identified because *1*) their sequences are too short to reveal significant homology, *2*) their amplified sequences were located in the highly variable gene sequence, or *3*) they have never been cloned before, because of the scarcity of molecular research that covers *Juglans* taxon. Finally, 5 TDFs showed no similarity with sequences from other green organisms, but significant similarities with prokaryote sequences revealing a natural contamination artifact. These fragments were not further investigated.

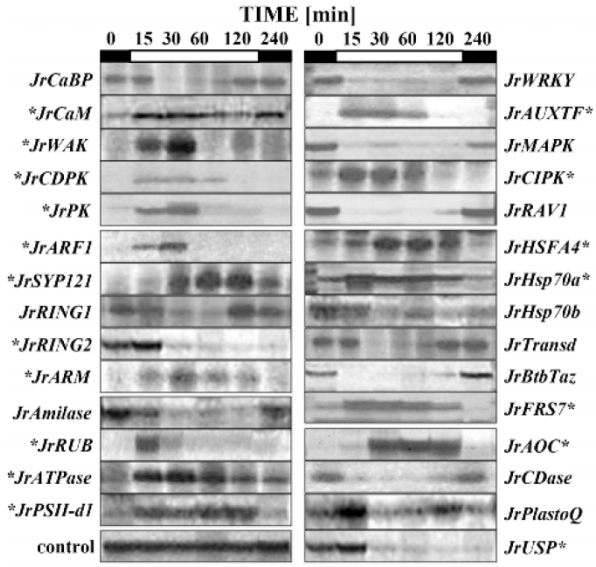

Fig. 2. Putative functional classification categories of the early differentially-expressed light-regulated transcript-derivated fragments (TDFs) identified by cDNA-AFLP in walnut leaves. Predictive functions were established on the basis of the best matches obtained from *BlastX* and *BlastN* searches to sequences in the *NCBI* database. Expected values greater than e^{-04} are considered not statistically significant (* corresponds to the up-regulated TDFs under light).

Pattern expression of 30 TDFs: The efficiency of cDNA-AFLP was evaluated by real-time quantitative RT-PCR (qPCR) analysis, conducted on 30 TDFs (Fig. 3). No significant difference was found between data of cDNA-AFLP and those of qPCR experiments, highlighting the robustness and reproducibility of this approach. Of these 30 selected radiation-responsive TDFs, 11 genes were related to signal transduction (Fig. 3*A*,*B*), 5 to binding regulatory proteins (Fig. 3*C*), 2 to fatty acid metabolism, 1 to cell wall strengthening, 2 to stress defense (Fig. 3*D*), 1 to sugar metabolism, 3 to photosynthesis (Fig. 3*E*), 2 to synthesis *de novo* and vesicles trafficking of protein and 3 to ubiquitination (Fig. 3*F*).

Among the TDFs of the signal transduction category,

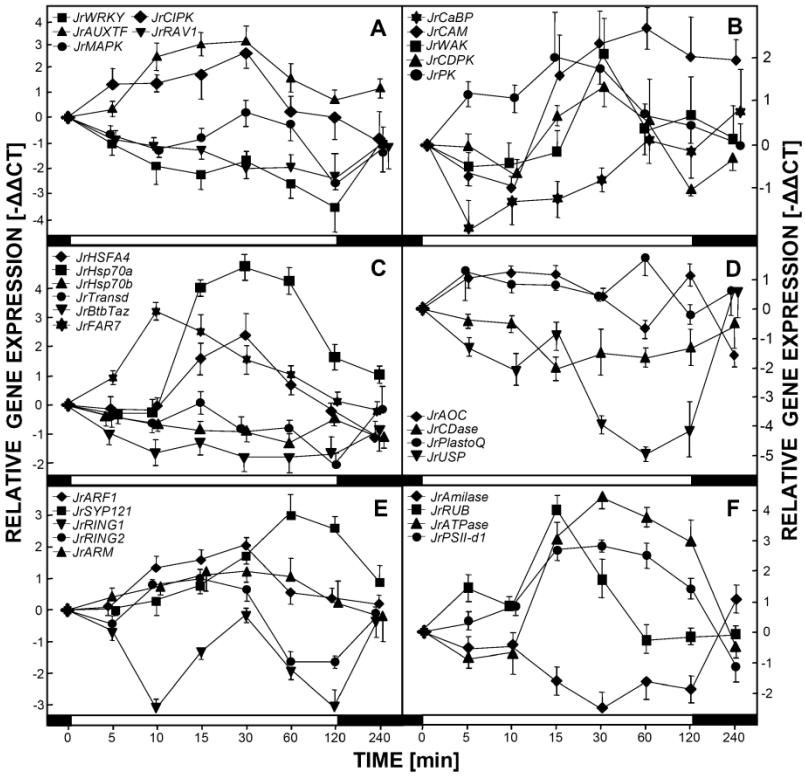

Fig. 3. Real-time quantitative RT-PCR analyses of the expression of selected TDFs in walnut leaves after 5, 10, 15, 30, 60 and 120 min under irradiance and 120 min after return to dark. TDFs were selected from the 7 following functional categories: transduction of signal (*A*, *B*), protein regulation (*C*), cell-wall integrity and stress defense (*D*), photosynthesis (*E*), ubiquitination and vesicle trafficking (*F*). Relative gene expression was normalized by comparing ΔΔCt of genes of interest and *J. regia* 18S rRNA gene, where the starting level was the dark control point 0 min. Relative transcript abundance were represented as log of Qr. Values are means of three independent measurements.

JrCIPK (calcineurin interacting protein kinase), *JrCAM* (calmodulin), *JrCDPK* (Ca^{2+}-dependent protein kinase) and *JrCaBP* (calmodulin-like) were identified. Transcript levels of *JrCIPK*, *JrCDPK and JrCAM* were transiently up-regulated by irradiance, and peaked after 15 min (6-fold), 30 min (3-fold) and 60 min (5-fold), respectively. Except for *JrCAM*, *JrCIPK* and *JrCDPK* returned to its basal expression after 120 min, and remained constant when leaves were back in darkness. Conversely, *JrCaBP* expression significantly and transiently decreased, to reach its lowest level after 60 min, before returning to basal levels when leaves were back in darkness (Fig. 3*B*).

In the same functional categories, transcript levels of *JrAUXTF* (auxin response transcription factor-like protein) and *JrPK* (receptor serine/threonine kinase) were found to be transiently up-regulated by irradiance and peaked after 15 min (Fig. 3*A*,*B*), whereas those of *JrWRKY* (WRKY-type transcription factor), *JrRAV* (AP2 domain transcription factor RAV1-type) and *JrMAPK* (mitogen activated protein kinase) were down-regulated in response to irradiance. Up-regulation of *JrWAK* (wall-associated kinase) peaked at 15 min, but was preceded by a diminution within the first 10 min of irradiance.

As concern binding regulatory proteins, two sets of TDFs could be distinguished (Fig. 3*C*) according to their response to irradiance, *JrHsp70a* (heat shock protein 70), *JrHSFA4* (heat shock transcription factor) and *JrFAR7* (FAR1-related sequence 7) underwent early up-regulation. Transcript levels of *JrHsp70a* peaked after 10 min, and those of *JrHSFA4* and *JrFAR7* did so after 30 min. Conversely, transcript accumulation of *JrTransd* (transducine-like), *JrHsp70b* (heat shock protein 70) and *JrBtbTaz* [protein with an N terminal BTB/POZ (broad-complex, tramtrack, and bric-a-brac/poxvirus and zinc finger) domain, a central TAZ (transcriptional adaptor zinc finger) domain and a C terminal calmodulin-binding domain (CaMBD)] were down-regulated.

For the category cell wall and stress defense-related (Fig. 3*D*), three TDFs [*JrXTR* (xyloglucan endotransglycosylase), *JrUSP* (universal stress protein) and *JrCDase* (ceramidase)] were down-regulated during irradiance. The highest inhibition was found for *JrXTR* and *JrUSP* after a 2-h exposure. In contrast, *JrPlastQ* and *JrAOC* were slightly up-regulated. Most of these TDFs returned to their basal level when leaves were back in darkness.

Most of TDFs concerning photosynthesis (Fig. 3*E*),

were early and transitory up-regulated by irradiance. These TDFs [*JrRUB* (ribulose biphosphate carboxylase), *JrATPase* (ATP synthase) and *JrPSII-d1* (protein D1 of photosystem 2)] peaked after 15 min. Under the same experimental condition, *JrAmylase* (amylase β-type) was down-regulated and the highest reduction was observed at 30 min after irradiance.

The majority of genes concerning ubiquitination and trafficking were up-regulated by irradiance [*JrARF1* (ADP-ribosylation factor 1), *JrARM* (armadillo/catenin repeat family protein) and *JrSYP121* (syntaxin 121)] (Fig. 3*F*). The highest stimulation was found for *JrSYP121* after 60 min. Expression pattern of *JrRING2* was marked by a slight stimulation during the first 30 min, followed by a down-regulation until 120 min of irradiance. *JrRING1* (RING-finger copine like protein) was early and strongly down-regulated by light. Expression of all these TDFs returned to its basal level when leaves were back in darkness.

Discussion

The cDNA-AFLP approach offered, for the first time, a large review of dynamic modulations in the transcriptome profiling of *Juglans* leaves under exposure to irradiance. 93 TDFs were selected due to the sensitivity and reliability of their expression pattern, and to their significant similarity with known proteins. In addition, the data of qPCR experiments carried out on 30 pre-selected TDFs were consistent with those of cDNA-AFLP (Fig. 3).

Ten functional categories were identified (suppl. data 4, http://www.sakretal2011.blogspot.com/). Cellular regulation including 3 major categories (signal transduction, protein and nucleotide matrices maintenance, and binding regulatory protein) was the largest with 54 TDFs. Here, the hypothetical link between one, or many, functional category and K_{leaf} is discussed.

Four TDFs encoding ribulose bisphophate carboxylase (*JrRUB*), protein J of photosystem II, protein D1 of photosystem II (*JrPSII-d1*) and a chloroplastic ATP synthase β-subunit (*JrATPase*) were found to undergo early and significant up-regulation by irradiance (Fig. 3*E*). These results might suggest a link between mechanisms regulating photosynthesis and K_{leaf} including *JrPIP2s*. This hypothesis may fit in with recent data showing direct evidence of a role for the PIP homologue of *Nicotiana tobacum* NtAQP1 in CO_2 transport in leaves and its localization in both the plasmalemma membrane and chloroplast envelope (Flexas *et al.* 2007, Uehlein *et al.* 2008). Within the latter, NtAQP1 could account for ~90 % of CO_2 permeability. An important future task will be to determine whether stimulation of K_{leaf} by irradiance could be related to stimulation of photosynthesis and mesophyll conductance (g_m) to CO_2 (Evans *et al.* 2009).

One of the TDFs exhibited a high homology with gene encoding the cell wall enzyme xyloglucan endotransglycosylase (*JrXTR*) (Fig. 3*D*). The XTR is able to cut and graft xyloglucan molecules to each other (Thompson *et al.* 1997, Ito and Nishitani 1999), and thereby contributes to the loosening of cell walls (Hayashi 1989, Fry 1989, McCann *et al.* 1990). The inhibition of the transcript level of *JrXTR* modified the extensibility of the cell wall, required for the regulation of cell pressure potential. Such an event coupled with a stimulation of *JrPIP2s* (Fig. 1) could promote a high leaf water content and pressure potential in our experimental conditions.

A significant outcome of this study was the identification of TDFs involved in the first signal transduction step, including kinases [wall associated kinase (*JrWAK*); serine/threonine kinase (*JrPK*), CBL-interacting protein kinase (*JrCIPK*), calcium-dependant protein kinase (*JrCDPK*), mitogen activated protein kinase (*JrMAPK*)], receptor kinase (Ferronia receptor-like) and two calcium-dependent proteins [camoduline (*JrCAM*), calcium binding protein (*JrCaBP*)]. These comprise one of the higher modulated categories. Many of these TDFs share the common property of being associated with calcium, one of the major chemical mediators for living organisms. Here, 4 TDFs related to Ca^{2+}-signaling and encoded for the four major groups of calcium-binding proteins in plants [CaM, CaBP, CIPKs and CDPKs (Snedden and Fromm 2001, Luan *et al.* 2002, Sanders *et al.* 2002)] were found to be regulated by irradiance (Figs. 3*A,B*). The response of aquaporins to calcium variation has been shown in plants. Indeed, the fluctuation of Ca^{2+} concentration can affect either expression of respective genes (Maathuis *et al.* 2003), or activities of aquaporins (Johnson and Chrispeels 1992, Johansson *et al.* 1996, Alleva *et al.* 2006, Van Wilder *et al.* 2008).

There were 9 early modulated putative transcription factors: an AP2domain RAV1-subfamily, an ethylene responsive binding factor 5-type, an auxin responsive factor, a homeotic transcription factor, 2 heat shock transcription factors (see below), and 3 WRKY transcription factors. Among these, WRKY TF are a large family of regulatory proteins (Eulgem *et al.* 1999, Wei *et al.* 2008), defined as master regulators of plant response to biotic and abiotic stimuli (Du and Chen. 2000, Pandey and Somossich 2009, Ren *et al.* 2010). However, few studies have described the involvement of these transcription factors in light signaling. The only available data indicated that an over-expression of WRKY89 enhances UV-B tolerance and disease resistance in rice plants (Wang *et al.* 2007). Here, we showed, for the first time, that 3*WRKY* TDFs were early down-regulated in response to irradiance. These new findings might emphasize the importance of WRKY factors in transcriptional reprogramming of plant in responses to irradiance, probably acting as negative regulators. The expression pattern of *JrWRKY* revealed a negative

correlation with K_{leaf} dynamics and the expression pattern of *JrPIP2s* (Fig. 3*A*,*C*). As K_{leaf} was closely related with transcript abundance of two walnut aquaporins, *JrPIP2,1* and *JrPIP2,2* (Fig. 1), the identification of a *JrWRKY*-responsive *cis*-element on the promoter of these aquaporins might support a possible role of WRKY TF in induction of K_{leaf} by irradiance.

Of particular interest is the identification of two genes that encode putative regulatory proteins. Two of them are discussed: FRS7 (for FAR1-related Sequence 7), and BTB and TAZ domain protein. They were found to be up- and down-regulated, respectively, in leaves under irradiance (Fig. 3*C*). FRS7 protein is a member of the nuclear FRS protein family that appears to be linked to the phytochrome signaling pathway (Lin and Wang 2004). These interact with diverse partners to control a broad range of signaling processes (Wang and Deng 2002), as being essential positive signal transducers for phyA-mediated FR-high irradiance responses (HIRs) in response to white light. With respect to *JrBtbTaz* TDF, this is one member of a BTB protein subfamily (Ren *et al.* 2007, Robert *et al.* 2008, Mandadi *et al.* 2009). The role of BTB proteins in mediating signaling pathways of diverse stimuli were recently documented (Mandadi *et al.* 2009). In this respect, the *Arabidopsis thaliana* gene BT2 is maximally expressed in the dark and it is under circadian control (Mandadi *et al.* 2009). Consistently with these data, *JrBtbTaz* was found to be down-regulated under irradiance, and almost returned to its high level when leaves were back in darkness. It will be useful to determine whether these two transduction modulators could bind directly to transcription factors targeting aquaporin genes.

The effect of irradiance can also be extended to components involved in regulation of proteins, including heat stress proteins (HSPs). These proteins play an essential role in maintenance and/or restoration of protein homeostasis (Baniwal *et al.* 2004) under normal and stress conditions (Lee and Vierling 2000). The modulation of their related genes is under the control of heat shock transcription factors (HSFs). Under our experimental conditions, a transient transcript accumulation encoding five HSP (18, 40, 70, 101 kD) and two HSFs (HsfA2 and HsfA4-types) was observed (Fig. 3*C*). This is rather unexpected because HSPs have been commonly studied in heat stress contexts. Here, we paid particular attention to three of them, the chaperone *JrHsp70* and the two heat stress transcription factors, *JrHsfA2* and *JrHsfA4*-types, which showed simultaneous early differential transcript abundance (Figs. 3*C* and 4). The protein product of *Hsp70* is implicated in trafficking and stabilization of newly synthesized proteins (Baniwal *et al.* 2004), including membrane channel proteins such as K^+-channel (Negulyaev *et al.* 1996). We have identified two *HSP70* isoforms which each harbored contrasted modulation: *JrHsp70a* was up-regulated whereas *JrHSP70b* was down-regulated. Such a regulation supports the idea of an auto-repression in this class of chaperones (Kim and Schöffl 2002). Under high irradiance, increasing the K_{leaf} may be essential not only to supply CO_2 and water for challenged cells, but also for leaf cooling. Thus, HSP70 may contribute to the aquaporin protein structure strengthening and so safeguard their transport function when the temperature of leaves increases with differential water movements. The similar role of *JrHSFA* in K_{leaf} induction may be possible, due to the significance of the *de novo* protein biosynthesis in this process (Cochard *et al.* 2007). Therefore, it is tempting to speculate that HSFA4 and HSFA2 differentially expressed in our light irradiance condition may be the potential transcription factors which control the modulation of the *JrHSP70* and *JrPIP2s* genes. A detailed analysis of *cis*-regulating motifs within their promoters would provide answers to such assumptions.

Modification of vesicle trafficking upon irradiance is consistent with the up-regulation of the vesicle-targeted genes *ADP-ribosylation-factor 1(ARF1)* and *SYP121* (syntaxin 121) (Fig. 3*F*). ARF1 proteins are considered central to orchestrating asymmetrical cell vesicle trafficking, and are primarily localized in Golgi apparatus and a subpopulation of post-Golgi vesicles (Matheson *et al.* 2008). Concomitant induction of *SYP121*, a *SNAP receptor/protein anchor* [SNAP for soluble NSF (N-ethylmaleimide-sensitive fusion protein) - attachment protein] located in *cis*-Golgi cisternae, reinforces the indication of enhanced protein trafficking between endoplasmic reticulum (ER) and Golgi. The modification of *trans*-Golgi vesicle trafficking as well as endocytosome (spherical bodies in Fig. 4) seems to be under the control of clathrin coat adaptators, themselves regulated by ARFs (Ooi *et al.* 1998). Interestingly, the steady state level of certain PIP subfamily aquaporins in *Arabidopsis* undergo a constitutive cycling mediated by clathrin-coated vesicles, and a possible in-cell internalization through the sorting *Nexin 1* (SNX1) endosomes (Paciorek *et al.* 2005, Dhonukshe *et al.* 2007, Jaillais *et al.* 2008). The use of *Brefeldin A* and/or *Tyrphostin A23*, an inhibitor of cargo protein trafficking from endosomes to the plasmalemma membrane and a structural analog of tyrosine which interferes with clathrin function, may highlight the involvement of such a trafficking pathway in the light stimulation of *JrPIP2s*.

In the same way, a TDF exhibited high homology with a gene encoding ceramidase (*JrCDase*) (Fig. 3*D*) that is a central enzyme in sphingolipid metabolism and signaling (Worrall *et al.* 2008). By cleaving fatty acids from ceramides (knows as sphingosine), this produces a sphingosine that in turn is phosphorylated by a sphingosine kinase to form sphingosine-1-phosphate (S1P). Sphingosine and S1P are two motile second messengers, found in the plant kingdom. In addition, S1P is an active Ca^{2+}-mobilizing messenger in guard cells during drought and abscissic signaling (Ng *et al.* 2001). Down-regulation of ceramidase by irradiance may mean that perception of a signal elicits a fluctuation of cytosolic Ca^{2+} content *via* production of S1P in leaves. Because these compounds can cross the entire lipid bilayer, they

seem to be particularly important in membrane domain formation and vesicle trafficking, vesicle endocytosis, and diverse cellular signaling pathways (Rohrbough *et al.* 2003, Helms and Zurzolo 2004). However, the means by which ceramide acts as a signaling molecule are not clear.

In this research, twelve genes putatively related to the proteolysis underwent early and significant up-regulation by irradiance (suppl. data 4, http://www.sakretal2011.blogspot.com/). Among the most significant, we found a gene encoding E2 ubiquitin protein ligase, and various isoforms of E3 ubiquitin ligases and RING-finger copine-like protein and two F-box proteins. Among the F-box protein family, a transducin was reported to be up-regulated under irradiance and plays an important role in the protein degradation by acting as components of SKP cullin F-BOX protein ligases that selectively act on a subset of proteins including β-catenin. A gene encoding an armadillo/catenin repeat family protein (*JrARM)* was among the radiation-responsive TDFs identified. These findings fit in with recent research highlighting the role of ubiquitin-/26S proteasome-mediated protein degradation in the light-signaling pathway (Hoecker 2005). In addition, the role of ubiquitination in the aquaporin function was directly shown by Lee *et al.* (2009). These authors established novel links in plants between ubiquitination and aquaporin trafficking and degradation, with an implication of physical interaction of a RING membrane anchor E3 ubiquitin ligase to aquaporin (*AtPIP2;1*). Such a regulation of aquaporin by ubiquitination is reminiscent of the hypertonicity-dependent degradation of mammalian AQP1 (Leitch *et al.* 2001). To uphold this hypothesis in our experimental conditions, pharmacological investigations based on the utilization of 26 proteasome inhibitor (MG132) will be carried out in the near future.

In conclusion, K_{leaf} increases within minutes after exposure to irradiance in parallel with the transcription of two members of *JrPIP2s*. However, such a short time underpins the idea that these physiological events cannot be only explained through a single transcription of aquaporin genes. By obtaining early temporal expression profiles, the diversity of up- and down-regulated TDFs suggest that regulation of K_{leaf} might be paralleled with very complex processes, and that further analyses are certainly required to identify which ones could directly be involved in light-induced K_{leaf}. These considerations may lay the foundations of the mechanistic aspects of light-mediated regulation of both hydraulic conductance and aquaporin expression, and their integration could be central for a deeper understanding of the leaf-water relations.

References

Alleva, K., Niemietz, C.M., Maurel, C., Parisi, M., Tyerman, S.D., Amodeo, G.: Plasma membrane of *Beta vulgaris* storage root shows high water channel activity regulated by cytoplasmic pH and a dual range of calcium concentrations. - J. exp. Bot. **57**: 609-621, 2006.

Altschul, S.F., Madden, T.L., Schaffer, A.A., Zhang, J., Zhang, Z., Miller, W.: Gapped BLAST and PSI-BLAST: a new generation of protein database search programs. - Nucl. Acids Res. **25**: 3389-3402, 1997.

Bachem, C.W., Van der Hoeven, R.S., De Bruijn, S.M., Vreugdenhil, D., Zabeau, A., Visser, R.G.: Visualization of differential gene expression using a novel method of RNA fingerprinting based on AFLP: analysis of gene expression during potato tuber development. - Plant J. **9**: 745-753, 1996.

Baniwal, S.K., Bharti, K., Chan, K.Y., Fauth, M., Ganguli, A., Kotak, S.: Heat stress response in plants: a complex game with chaperones and more than twenty heat stress transcription factors. - J. Biosci. **29**: 471-487, 2004.

Ben Baaziz K., Lopez, D., Combes, D., Gousset, A., Bouzid, S., Cochard, H., Sakr, S., Venisse J.S.: Light-mediated K_{leaf} induction and contribution of both the PIP1s and PIP2s aquaporins in five tree species; walnut (*Juglans regia*) case study. - Tree Physiol., in press, 2012.

Brodribb, T.J., Holbrook, N.M.: Diurnal depression of leaf hydraulic conductance in a tropical tree species. - Plant Cell Environ. **27**: 820-827, 2004.

Brodribb, T.J., Holbrook, N.M., Gutierrez, M.V.: Hydraulic and photosynthetic coordination in seasonally dry tropical forest trees. - Plant Cell Environ. **25**: 1435-1444, 2002.

Chalhoub, B.A., Thibault, S., Laucou, V., Rameau, C., Hofte, H., Cousin, R.: Silver staining and recovery of AFLP amplification products on large denaturing polyacrylamide gels. - BioTechnology **22**: 216-220, 1997.

Chang. S., Puryear, J., Cairney, J.: A simple and efficient method for isolating RNA from pine trees. - Plant mol. Biol. Rep. **11**: 113-116, 1993.

Cochard, H., Marton, R., Gross, P., Bogeat-Triboulot, M.B.: Temperature effects on hydraulic conductance and water relations of *Quercus robus* L. - J. exp. Bot. **51**: 1255-1259, 2000.

Cochard, H., Venisse, J.S., Barigah, T.S., Brunel, N., Herbette, S., Guilliot, A., Tyree, M.T., Sakr, S.: Putative role of aquaporins in variable hydraulic conductance of leaves in response to light. - Plant Physiol. **143**: 122-133, 2007.

Cosmstock, J.: Variation in hydraulic architecture and gas exchange in two desert sub-shrubs, *Hymenoclea salsola* and *Ambrosia dumosa*. - Oecologia **125**: 1-10, 2000.

Dhonukshe, P., Aniento, F., Hwang, I., Robinson, D.G., Mravec, J., Stierhof, Y.D., Friml, J.: Clathrin-mediated constitutive endocytosis of PIN auxin efflux carriers in *Arabidopsis*. - Curr. Biol. **17**: 520-527, 2007.

Du, L., Chen, Z.: Identification of genes encoding receptor-like protein kinases as possible targets of pathogen- and salicylic acid-induced WRKY DNA-binding proteins in *Arabidopsis*. - Plant J. **24**: 837-847, 2000.

Eulgem, T., Rushton, P.J., Schmelzer, E., Hahlbrock, K., Somssich, I.E.: Early nuclear events in plant defence signaling: rapid gene activation by WRKY transcription factors. - EMBO J. **18**: 4689-4699, 1999.

Evans, J.R., Kaldenhoff, R., Genty, B., Terashima, I.: Resistances along the CO_2 diffusion pathway inside leaves. - J. exp. Bot. **60**: 2235-2248, 2009.

Flexas, J., Diaz-Espejo, A., Galmés, J., Kaldenhoff, R.,

Medrano, H., Ribas-Carbo, M.: Rapid variations of mesophyll conductance in response to changes in CO_2 concentration around leaves. - Plant Cell Environ. **10**: 1284-1298, 2007.

Frangne, N., Maeshima, M., Schäffner, A.R., Mandel, T., Martinola, E., Bonnemain, J.L.: Expression and distribution of a vacuolar aquaporin in young and mature leaf tissues of *Brassica napus* in relation to water fluxes. - Planta **212**: 270-278, 2001.

Fredeen, A., Sage, R.F.: Temperature and humidity effects on branchlet gas-exchange in white spruce: an explanation for the increase in transpiration with branchlet temperature. - Trees **14**: 161-168, 1999.

Fry, S.C.: Cellulases, hemicelluloses and auxin-stimulated growth: a possible relationship. - Physiol. Plant. **75**: 532-536, 1989.

Hachez, C., Heinen, R.B., Draye, X., Chaumont, F.: The expression pattern of plasma membrane aquaporins in maize leaf highlights their role in hydraulic regulation. - Plant mol. Biol. **68**: 337-353, 2008.

Hayashi, T.: Xyloglucans in the primary cell wall. - Annu. Rev. Plant Physiol. Plant mol. Biol. **40**: 139-168, 1989.

Helms, J.B., Zurzolo, C.: Lipids as targeting signals: lipid rafts and intracellular trafficking. - Traffic **5**: 247-254, 2004.

Hoecker, U.: Regulated proteolysis in light signaling. - Curr. Opin. Plant Biol. **8**: 469-476, 2005.

Ito, H., Nishitani, K.: Visualization of EXGT-mediated molecular grafting activity by means of a fluorescent-labeled xyloglucan oligomer. - Plant Cell Physiol. **40**: 1172-1176, 1999.

Jaillais, Y., Fobis-Loisy, I., Miège, C., Gaude, T.: Evidence for a sorting endosome in *Arabidopsis* root cells. - Plant J. **53**: 237-247, 2008.

Johansson, I., Larsson, C., Ek, B., Kjellborm, P.: The major integral proteins of spinach leaf plasma membranes are putative aquaporins and are phosphorylated in response to Ca^{2+} and water potential. - Plant Cell **8**: 1181-1191, 1996.

Johnson, K.D., Chrispeels, M.J.: Tonoplast-bound protein kinase phosphorylates tonoplast intrinsic protein. - Plant Physiol. **100**: 1787-1795, 1992.

Kaldenhoff, R., Kölling, A., Meyers, J., Karmann, U., Ruppel, G., Richter, G.: The blue light-responsive *Ath*H2 gene of *Arabidopsis thaliana* is primarily expressed in expanding as well as in differentiating cells and encodes a putative channel protein of the plasmalemma. - Plant J. **7**: 87-95, 1995.

Kim, B.H., Schöffl, F.: Interaction between *Arabidopsis* heat shock transcription factor 1 and 70 kDa heat shock proteins. - J. exp. Bot. **53**: 371-375, 2002.

Lee, G.J., Vierling, E.: A small heat shock protein cooperates with heat shock protein 70 system to reactivate a heat-denatured protein. - Plant Physiol. **122**: 189-197, 2000.

Lee, H.K., Cho, S.K., Son, O., Xu, Z., Hwang, I., Kim, W.T.: Drought stress-induced Rma1H1, a RING membrane-anchor E3 ubiquitin ligase homolog, regulates aquaporin levels via ubiquitination in transgenic *Arabidopsis* plants. - Plant Cell. **21**: 622-641, 2009.

Leitch, V., Agre, P., King, L.S.: Altered ubiquitination and stability of aquaporin-1 in hypertonic stress. - Proc. nat. Acad. Sci. USA **98**: 2894-2898, 2001.

Lin, R., Wang, H.: *Arabidopsis* FHY3/FAR1 gene family and distinct roles of its members in light control of *Arabidopsis* development. - Plant Physiol. **136**: 4010-4022, 2004.

Livak, K.J., Schmittgen, T.D.: Analysis of relative gene expression data using real-time quantitative PCR and the $2^{-\Delta\Delta CT}$ method. - Methods **25**: 402-408, 2001.

Lo Gullo, M.A., Nardini, A., Trifolio, P., Salleo, S.: Diurnal and seasonal variations in leaf hydraulic conductance in evergreen and deciduous trees. - Tree Physiol. **25**: 505-512, 2005.

Lu, H.A., Sun, T.X., Matsuzaki, T., Yi, X.H., Eswara, J., Bouley, R.: Heat shock protein 70 interacts with aquaporin-2 and regulates its trafficking. - J. biol. Chem. **282**: 28721-28732, 2007.

Luan, S., Kudla, J., Rodriguez-Concepcion, M., Yalovsky, S., Gruissem, W.: Calmodulins and calcineurin B-like proteins: calcium sensors for specific signal response coupling in plants. - Plant Cell **14**: 389-400, 2002.

Maathuis, F.J., Filatov, V., Herzyk, P., Krijger, G.C., Axelsen, K.B., Chen, S.: Transcriptome analysis of root transporters reveals participation of multiple gene families in the response to cation stress. - Plant J. **35**: 675-692, 2003.

Mandadi, K.K., Misra, A., Ren, S., McKnight, T.D.: BT2, a BTB protein, mediates multiple responses to nutrients, stresses, and hormones in *Arabidopsis thaliana*. - Plant Physiol. **150**: 1930-1939, 2009.

Matheson, L.A., Suri, S.S., Hanton, S.L., Chatre, L., Brandizzi, F.: Correct targeting of plant ARF GTPases relies on distinct protein domains. - Traffic **9**: 103-120, 2008.

McCann, M.C., Wells, B., Roberts, K.: Direct visualization of cross-links in the primary plant cell wall. - J. cell. Sci. **96**: 323-334, 1990.

Nardini, A., Salleo, S.: Limitation of stomatal conductance by hydraulic traits: sensing or preventing xylem cavitation? Trees **15**: 14-24, 2000.

Nardini, A., Salleo, S.: Water stress-induced modifications of leaf hydraulic architecture in sunflower: co-ordination with gas exchange. - J. exp. Bot. **56**: 3093-3101, 2005.

Nardini, A., Salleo, S., Raimondo, F.: Changes in leaf hydraulic conductance correlate with leaf vein embolism in *Ceris siliquastrum* L. - Trees **17**: 529-534, 2003.

Nardini, A., Tyree, M.T.: Root and shoot hydraulic conductance of seven *Quercus* species. - Ann. Forest Sci. **56**: 371-377, 1999.

Negulyaev, Y.A., Vedernikova, E.A., Kinev, A.V., Voronin, A.P.: Exogenous heat shock protein hsp70 activates potassium channels in U937 cells. - Biochem. biophys. Acta **1282**: 156-162, 1996.

Ng, C.K., Carr, K., McAinsh, M.R., Powell, B., Hetherington, A.M.: Drought-induced guard cell signal transduction involves sphingosine-1-phosphate. - Nature **410**: 596-599, 2001.

Ooi, C.E., Dell'Angelica, E.C., Bonifacino, J.S.: ADP-ribosylation factor 1 (ARF1) regulates recruitment of the AP-3 adaptor complex to membranes. - J. cell. Biol. **142**: 391-402, 1998.

Otto, B., Kaldenhoff, R.: Cell-specific expression of the mercury-insensitive plasma-membrane aquaporin NtAQP1 from *Nicotiana tabacum*. - Planta **211**: 167-172, 2000.

Paciorek, T., Zazímalová, E., Ruthardt, N., Petrásek, J., Stierhof, Y.D., Kleine-Vehn, J., Morris, D.A., Emans, N., Jürgens, G., Geldner, N., Friml, J.: Auxin inhibits endocytosis and promotes its own efflux from cells. - Nature **435**: 1251-1256, 2005.

Pandey, S.P., Somssich, I.E.: The role of WRKY transcription factors in plant immunity. - Plant Physiol. **150**: 1648-1655, 2009.

Ren, S., Mandadi, K.K., Boedeker, A.L., Rathore, K.S., McKnight, T.D.: Regulation of telomerase in *Arabidopsis* by BT2, an apparent target of TELOMERASE

ACTIVATOR1. - Plant Cell **19**: 23-31, 2007.

Ren, X.-J., Huang, W.-D., Li, W.-Z., Yu, D.-Q.: Tobacco transcription factor WRKY4 is a modulator of leaf development and disease resistance. - Biol. Plant. **54**: 684-690, 2010.

Robert, H.S., Quint, A., Brand, D., Vivian-Smith, A., Offringa, R.: BTB and TAZ DOMAIN scaffold proteins perform a crucial function in *Arabidopsis* development. - Plant J. **58**: 109-121, 2008.

Rohrbough, J., Rushton, E., Palanker, L., Woodruff, E., Matthies, H., Acharya, U., Acharya, J., Broadie, K.: Ceramidase regulates synaptic vesicle exocytosis and trafficking. - J. Neurosci. **24**: 7789-7803, 2003.

Sack, L., Holbrook, N.M.: Leaf hydraulics. - Ann. Rev. Plant Biol. **57**: 361-381, 2006.

Sack, L., Streeter, C.M., Holbrook, N.M.: Hydraulic analysis of water flow through leaves of sugar maple and red oak. - Plant Physiol. **134**: 1824-1833, 2004.

Sakurai, J., Ahamed, A., Murai, M., Maeshima, M., Uemura, M.: Tissue and cell-specific localization of rice aquaporins and their water transport activities. - Plant Cell Physiol. **49**: 30-39, 2008.

Sanders, D., Brownlee, C., Harper, J.F.: Communicating with calcium. - Plant Cell **11**: 691-706, 1999.

Sanders, D., Pelloux, J., Brownlee, C., Harper, J.F.: Calcium at the crossroads of signaling. - Plant Cell **14**: 401-417, 2002.

Snedden, W.A., Fromm, H.: Calmodulin as a versatile calcium signal transducer in plants. - New Phytol. **151**: 35-66, 2002.

Thompson, J.E., Smith, R.C., Fry, S.C.: Xyloglucan undergoes interpolymeric transglycosylation during binding to the plant cell wall *in vivo*: evidence from $^{13}C/^{3}H$ dual labelling and isopycnic centrifugation in caesium trifluoroacetate. - Biochem. J. **327**: 699-708, 1997.

Tyree, M.T., Nardini, A., Salleo, S., Sack, L., Bouchra, O.: The dependence of leaf hydraulic conductance on irradiance during HPFM measurements: any role for stomatal response? - J. exp. Bot. **412**: 737-744, 2005.

Tyree, M.T., Velez, V., Dalling, K.: Growth dynamics of roots and shoots hydraulic conductance in seedlings of JW five neotropical tree species: scaling to show possible adaptation to differing light regimes. - Oecologia **114**: 293-298, 1998.

Uehlein, N., Otto, B., Hanson, D.T., Fischer, M., McDowell, N., Kaldenhoff, R.: Function of *Nicotiana tabacum* aquaporins as chloroplast gas pores challenges the concept of membrane CO_2 permeability. - Plant Cell **3**: 648-657, 2008.

Van Wilder, V., Miecielica, U., Degand, H., Derua, R., Waelkens, E., Chaumont, F.: Maize plasma membrane aquaporins belonging to the PIP1 and PIP2 subgroups are *in vivo* phosphorylated. - Plant Cell Physiol. **49**: 1364-1377, 2008.

Voicu, M.C., Cooke, J.E., Zwiazek, J.J.: Aquaporin gene expression and apoplastic water flow in bur oak (*Quercus macrocarpa*) leaves in relation to the light response of leaf hydraulic conductance. - J. exp. Bot. **60**: 4063-4075, 2009.

Vos, P., Hogers, R., Bleeker, M., Reijans, M., Van de Lee, T., Hornes, M.: AFLP: a new technique for DNA finger-printing. - Nucl. Acids Res. **23**: 4407-4414, 1995.

Wang, H., Deng, X.W.: *Arabidopsis* FHY3 defines a key phytochrome A signaling component directly interacting with its homologous partner FAR1. - EMBO J. **21**: 1339-1349, 2002.

Wang, H., Hao, J., Chen, X., Hao, Z., Wang, X., Lou, Y., Peng, Y., Guo, Z.: Overexpression of rice WRKY89 enhances ultraviolet B tolerance and disease resistance in rice plants. - Plant mol. Biol. **65**: 799-815, 2007.

Wei, W., Zhang, Y., Han, L., Guan, Z., Chai, T.: A novel WRKY transcriptional factor from *Thlaspi caerulescens* negatively regulates the osmotic stress tolerance of transgenic tobacco. - Plant Cell Rep. **27**: 795-803, 2008.

Worrall, D., Liang, Y.K., Alvarez, S., Holroyd, G.H., Spiegel, S., Panagopulos, M., Gray, J.E., Hetherington, A.M.: Involvement of sphingosine kinase in plant cell signalling. - Plant J. 56: 64-72, 2008.

Yang, S., Tyree, M.T.: Hydraulic resistance in *Acer saccharum* shoots and its influence on leaf water potential and transpiration. - Tree Physiol. **12**: 231-242, 1993.

Supplemental Table 1. cDNA-AFLP primer sets
List of primers used for amplified fragment length polymorphism-based mRNA fingerprinting (cDNA-AFLP) experiments in this study

Reverse transcription procedure	
Oligo-dT30-AFLP	5'-T_6TGCAAGCTTGAATTCGCT$_{30}$N-3'

AFLP procedure	
Adaptators	
AdaptEco-A	5'-AGGACTCGTAGACTGCGTACC-3'
AdaptEco-B	5'-GAGCATCTGACGCATGGTTAA-3'
AdaptMsp-A/Mse-A	5'-AGGAGACGATGAGTCCTGAA-3'
AdaptMsp-B	5'-GCAAGTCCTGAGTAGCAG-3'
AdaptMse-B	5'-ATAAGTCCTGAGTAGCAG-3'
PCR Amplification	
Pre-Amplif-Eco+0	5'-CTCGTAGACTGCGTACCAATTC-3'
Amplif-Eco+N	5'-CTCGTAGACTGCGTACCAATTCN-3'
Pre-Amplif-Msp+0	5'-GACGATGAGTCCTGAACGG-3'
Amplif-Msp+NN	5'-GACGATGAGTCCTGAACGGNN-3'
Pre-Amplif-Mse+0	5'-GACGATGAGTCCTGAATAA-3'
Amplif-Mse+NN	5'-GACGATGAGTCCTGAATAANN-3'

Supplemental Table 2. qRT-PCR primer sets
List of primer sets used for real-time quantitative-PCR experiments in this study.
Annealing temperature of PCR in °C

Transduction			
JrWRKY	AGTGCACTTATCCCAATTGCC	GAATCCACGTGTCCGTTACC	57°C
JrAUXFT	CGTTCACAACATGCAAACTCC	AGACTGCGTACCAATTCAGC	55.5°C
JrCIPK	GAATTCGCTAAAGCCAACGAG	TTAGCCTCCACCACTACCAG	53°C
JrRAV1	CCAAAGCTGAGATTGTGGAC	GAAGGAATTACCGAGAAATCC	54°C
JrMAPK	TTCACCGATGTTTACATTGCC	TCTTAAGGTCACAATTTGCATTC	55°C
JrCaBP	GAGAGTTGCTTTTCAATGACCG	CTTGCCGGATGTCATTGTTCC	53°C
JrCAM	CGGTTGCATCACTACCAAGG	CTCAGGGAAGTCAATGGTTCC	53°C
JrWAK	CAGTTTATAAAGGTGTTTTATCC	CTGAGAAAGTACAAGCACCTCG	52°C
JrCDPK	TAAGAGGCTCCATTGATCCG	TATCGGCCGGGGGGGCTACT	58°C
JrPK	CATTAACGACAATCCAAAATC	AAGATGAGGATCAAAGTCGCG	50°C
JrHSFA4	GGTTGATTCCTTTCTCCGGC	ACGAATGTAGTTCGTAAATGAA	54°C
Protein regulation			
Jr Hsp70a	CTGGAAAATTACGCGTACAAC	CGGCCTTCTCCATCTTCTG	53°C
Jr Hsp70b	GGCATGGAGCTGAAAAGGAG	GTTTGGTCGTCCTCGACGG	53°C
JrTansd	AGCAGAGATTCTGAGATGC	GCTGTGCTGTCAAATGATGC	58°C
JrBtbTaz	TCCGAGCGAGTCATTCCAATAC	AGAGGTCCGGTGCGTCGCAC	60°C
JrFAR7	CGGATTGGTCAATTGTTTCGTT	GCTCCACAACCTACTCTTGAAG	52°C
Cell wall strenghten - Stress defence related			
Jr AOC	AAAGCACAAACGCCAGTGCC	CTTCTACACGTTTTACCTCAAG	54°C
Jr CDase	TACACTGAGAATGGCGAGC	CAGATGGACCTGGAGCTTTTG	61°C
JrPlastoQ	CGAATATGATATTTTCTGGGCA	ATTCTAAATTGTAGCCAAGCAT	53°C
JrUSP	GTGATGGCAAGAGCTGAAGC	GAAACCATATCCATGGCTTCC	57.5°C
Photosynthesis - Carboneceous resource			
JrAmilase	CTGCTTCCATGGCTCCTGG	GGGGAGATCATCGGAATGC	54°C
Jr RUB	CTATTGGGATGTACTATTAAACC	CTCATCATCTTTGGTAAAATC	57°C
JrATPase	GGGTCGAGATACTACCGGTC	CAGGCGCAGATCTATGAATAG	52°C
JrPSII-d1	GTGCTTGGGAGTCCCTAATG	CAGAAGTTGCGGTCAATAAGG	53.5°C
Ubiquitination and vesicles trafficking			
JrARF1	CACTCACTCCGTCAACGCC	CTACAGGTAGTAACGATGATGTC	58°C
JRSYP121	GATGAGTCCTGAACGGCGG	GTATAGTGTCCATAACTCTTCC	57.5°C
JrRing1	CAGGGTTCCTCTTCCCCC	CACACTTCGAGATCTTCTCC	60°C
JrRing2	CAGGGTTCCTCTTCCCCC	CAGCACAGCTCCATCATCAAG	56°C
JrARM	CGGATTATCGACGACACCGA	CGAGCTGGGCGGACATTTTG	54°C
Aquaporins			
JrPIP2;1	GCACTTTGATGTGGTTTGGG	CATGCACGAATGGACTGAGG	58.5°C
JrPIP2;2	CCCCTCTGCTCACCGATTTA	TAGGCAAATGGACATCCTCG	58.5°C
Reference			
Jr18S	GGTGGGGGTGTAATGCCCCC	CGCGGGATTCTGCAATTCAC	60°C

Supplemental Table 3. Unknown sequences revealed by amplified fragment length polymorphism-based mRNA fingerprinting (cDNA-AFLP) analysis to be early modulated in leaves of walnut under light exposure. BlastX and BlastN searches were performed with the NCBI non-redondant databases (genomic and EST).

[a] A single representative clone is given for those cases in which multiple cDNA were identified.

[b] Induction (+) or repression (-) by light at early time point of the kinetic.

TDF[a]	Accession Number	AFLP[b] profil	Size (pb)
TDF009	GR410241	+	71
TDF001	GR410235	+	80
TDF004	GR410237	+	122
TDF013	GR410245	+	222
TDF014	GR410246	+	93
TDF016	GR410248	+	141
TDF020	GR410252	+	83
TDF026	GR410258	+	152
TDF028	GR410260	+	215
TDF069	GR410299	+	250
TDF072	GR410302	+	999
TDF076	GR410306	+	230
TDF088	GR410317	+	102
TDF092	GR410320	+	124
TDF099	GR410326	+	81
TDF100	GR410327	+	150
TDF102	GR410329	+	133
TDF103	GR410330	+	169
TDF105	GR410332	+	167
TDF106	GR410333	+	72
TDF112	GR410339	+	149
TDF115	GR410341	+	123
TDF126	GR410346	+	124
TDF127	GR410347	+	264
TDF133	GR410350	+	151
TDF136	GR410353	+	63
TDF140	GR410355	+	145
TDF141	GR410356	+	149
TDF145	GR410360	+	160
TDF151	GR410365	+	133
TDF153	GR410367	+	87
TDF035	GR410266	-	87
TDF037	GR410268	-	158
TDF040	GR410271	-	172
TDF042	GR410273	-	176
TDF043	GR410274	-	268

TDF048	GR410279	-	188
TDF049	GR410280	-	255
TDF052	GR410283	-	224
TDF054	GR410285	-	196
TDF055	GR410286	-	190
TDF056	GR410287	-	158
TDF057	GR410288	-	136
TDF058	GR410289	-	118
TDF059	GR410290	-	102
TDF063	GR410293	-	55
TDF065	GR410295	-	86
TDF066	GR410296	-	223
TDF067	GR410297	-	59
TDF174	GR410381	-	202
TDF175	GR410382	-	248
TDF177	GR410384	-	426
TDF179	GR410386	-	84
TDF180	GR410387	-	229
TDF183	GR410390	-	182
TDF184	GR410391	-	214
TDF187	GR410394	-	259
TDF189	GR410395	-	201
TDF193	GR410398	-	139
TDF198	GR410402	-	324
TDF199	GR410403	-	68
TDF208	GR410409	-	126
TDF212	GR410413	-	110
TDF218	GR410418	-	267
TDF220	GR410419	-	54
TDF221	GR410420	-	84
TDF223	GR410422	-	73

Supplemental Table 4. Functional classification of the 186 transcript-derivated fragments (TDFs) revealed by amplified fragment length polymorphism-based mRNA fingerprinting (cDNA-AFLP) analysis to be early modulated in leaves of walnut under light exposure. Predictive functions were established on the basis of the best matches obtained from BlastX and BlastN searches to sequences in the NCBI non-redondant databases. Percentages specified for each category were calculated on the basis of the 186 nonredundant sequences. TDFs mentioned in bold abbreviation were monitored by real-time quantitative RT-PCR.

[a] A single representative clone is given for those cases in which multiple cDNA were identified.
[b] Induction (+) or repression (-) by light at early time point of the kinetic.
[c] Putative identification and relative source of comparison generally indicate the best match to a sequence in the NCBI non-redundant protein and nucleotide database. Source of similarity and relative Genbank accession numbers of sequence homologous to AFLP fragments are in parentheses.
[d] Expected values greater than e^{-04} are considered not statistically significant. All *e* values were taken from BlastX search of NCBI, excepted for TDF107 and TDF073 which were taken from BlastN.

TDF[a]	Accession Number	AFLP[b] profil	Size pb	Putative identification[c]	*E* value[d] score
Signal transduction (10.2 %)					
TDF012	GR410244	+	107	Homeotic transcription factor protein [*Ricinus communis*-EEF38266]	1e-05
TDF017	GR410249	+	140	Wall-associated kinase [*Ricinus communis*-EEF52934] ***JrWAK***	4e-11
TDF031	GR410263	+	105	CBL-interacting protein kinase [*Populus trichocarpa*-ABJ91223] ***JrCIPK***	6e-10
TDF075	GR410305	+	254	Calmodulin [*Zea mays*-ACG25844]	1e-25
TDF108	GR410335	+	288	Calmodulin [*Quercus petraea*-CAH57708] ***JrCAM***	5e-38
TDF083	GR410313	+	223	FERONIA receptor-like[*Vitis vinifera*-CAO49183]	3e-07
TDF084	GR410314	+	080	Beta family G-protein [*Musa acuminate*-AY463016]	8e-10
TDF121	GR410344	+	083	Heat shock transcription factor A4 [*Ricinus communis*-EEF40128] ***JrHSFA4***	3e-40
TDF138	GR410354	+	166	Serine/threonine kinase [*Arabidopsis thaliana*-CAB87849] ***JrPK***	5e-23
TDF152	GR410366	+	617	Calcium-dependent protein kinase [*Populus trichocarpa*-EEE75232] ***JrCDPK***	3e-15
TDF159	GR410369	+	454	Auxin response factor-like protein [*Mangifera indica*-AAP06759] ***JrAUXTF***	6e-10
TDF224	GR410423	-	206	Mitogen-activated protein kinase 3 [Solanum lycopersicum-U086227] ***JrMAPK***	7e-48
TDF046	GR410277	-	078	Ethylene responsive binding factor 5 [*A. thaliana*-BAA97157]	2e-02
TDF051	GR410282	-	225	WRKY-type transcription factor [*Glycine max*-ABY84656]	6e-32
TDF222	GR410421	-	449	WRKY-type transcription factor [*Populus trichocarpa*-EEE95882] ***JrWRKY***	6e-25
TDF041	GR410272	-	181	WRKY-type transcription factor [*Vitis thunbergii*-CAP08303]	1e-06
TDF060	GR410291	-	073	Heat shock transcription factor A2-type [*Pisum sativum*-CAA09301]	6e-07
TDF061	GR410292	-	107	Calcium-binding EF-hand protein [*Ricinus communis*-EEF41088] ***JrCaBP***	8e-07
TDF171	GR410378	-	143	AP2 domain transcription factor (RAV1) [*Vitis vinifera*-CAN68564] ***JrRAV1***	3e-11
Protein maintenance (7.5%)					
TDF011	GR410243	+	142	E3 ubiquitin ligase [*Ricinus communis*-EEF35056]	6e-10
TDF147	GR410362	+	249	E3 ubiquitin ligase [*Ricinus communis*-EEF35056]	4e-20
TDF090	GR410319	+	238	E3 ubiquitin ligase [*Ricinus communis*-EEF35056]	7e-27
TDF070	GR410300	+	345	E2-ubiquitin-protein ligase [*Arabidopsis thaliana*-NP174228]	4e-23
TDF143	GR410358	+	325	Ubiquitin-protein ligase [*Ricinus communis*-EEF40124]	7e-27
TDF156	GR410368	+	352	RING-finger copine like protein [*Ricinus communis*-EEF47612]	4e-31
TDF071	GR410301	-	370	RING-finger copine like protein [*Ricinus communis*-EEF47612] ***JrRING1***	6e-31
TDF077	GR410307	-	247	RING-finger copine like protein [*Ricinus communis*-EEF47612] ***JrRING2***	7e-32
TDF079	GR410309	+	156	Syntaxin121 (SYP121) [*Arabidopsis thaliana*-NP974288] ***JrSYP121***	7e-11
TDF026	GR410258	+	152	Alpha-1,3-mannosyltransferase [*Mus musculus*-NP064382]	2e-10
TDF225	GR410424	+	206	ADP-ribosylation factor 1 [*Populus trichocarpa*-XM002320238] ***JrARF1***	2e-35
TDF030	GR410262	+	085	F-box family protein [*Arabidopsis thaliana*-NP568408]	1e-04
TDF191	GR410397	+	138	Armadillo/catenin repeat family protein [*A. thaliana*-NP201421] ***JrARM***	3e-08
TDF216	GR410416	-	300	Polyubiquitin [*Populus trichocarpa*-EEE72016]	3e-05
DNA/RNA maintenance (6.4%)					
TDF022	GR410254	+	093	RNA-binding protein, putative [*Ricinus communis*-XP002279792]	5e-09
TDF074	GR410304	+	109	CCR4 associated factor 1-related protein [*C. annuum*-ABG66307]	2e-05
TDF134	GR410351	+	089	CCR4 associated factor 1-related protein [*C. annuum*-ABG66307]	3e-05
TDF135	GR410352	+	089	CCR4 associated factor 1-related protein [*C. annuum*-ABG66307]	1e-07
TDF086	GR410315	+	276	DNA-directed RNA polymerase [*Vitis vinifera*-XP002285900]	4e-38
TDF073	GR410303	+	299	Plastid 16S rRNA gene [*Vitis vinifera*-AJ639615]	*5e-140*[d]
TDF078	GR410308	+	923	Retrotransposon gag protein [*Vitis vinifera*-XP002271436]	6e-33
TDF107	GR410334	+	315	Ribosomal 26S RNA gene [*Juglans nigra*-AF479105]	*4e-161*[d]

TDF039	GR410270	-	224	Retrotransposon Gag-Pol protein [*Solanum demissum*-AAT38724]	4e-22
TDF047	GR410278	-	226	Retrotransposon protein [*Oryza sativa*-ABF97084]	5e-18
TDF182	GR410389	-	218	Transposase family tnp2 [*Oryza sativa*-AAX95566]	1e-14
TDF196	GR410400	-	212	Reverse transcriptase [*Vitis vinifera*-CAN79321]	2e-24
Binding regulatory protein (4.8%)					
TDF008	GR410240	+	119	FRS7 (FAR1-Related Sequence 7) [*Arabidopsis thaliana*-NP566278] ***JrFAR7***	2e-14
TDF023	GR410255	+	288	ATP-dependent RNA helicase [*Oryza sativa Japonica*-BAD54014]	4e-36
TDF029	GR410261	+	098	Heat shock protein 70 [*Populus trichocarpa*-EEE70412] ***JrHSP70a***	7e-08
TDF087	GR410316	-	131	BTB and TAZ domain protein [*Ricinus communis*-EEF51878] ***JrBtbTAz***	5e-08
TDF064	GR410294	-	223	Heat shock protein 40 / DnaJ homolog [*Salix gilgiana*-BAA35121]	3e-32
TDF170	GR410377	-	334	Heat shock protein 70 [*Oryza sativa* cv.*j aponica*-AAT39165] ***JrHSP70b***	1e-16
TDF186	GR410393	-	160	Heat shock protein HSP101 [*Nicotiana tabacum*-AAC83688]	2e-20
TDF201	GR410404	-	067	Heat shock protein HSP17.8 [*Populus trichocarpa*-EEE76050]	2e-04
TDF197	GR410401	-	195	Transducin WD-40 repeat protein [*Vitis vinifera*-CAO64276] ***JrTrans***	6e-28
Cellular metabolism (4.8%)					
TDF015	GR410247	+	150	NADH dehydrogenase ND1 sub. [*Guizotia abyssinic*-ACB86576]	1e-07
TDF019	GR410251	+	158	Hexose-phosphate guanyltransferase [*Prunus persica*-BAH03300]	5e-20
TDF024	GR410256	+	239	Adenosine 5'-phosphosulfate reductase [*P. trichocarpa*-AAQ57202]	2e-34
TDF025	GR410257	+	139	Threonine dehydratase/deaminase [*Ricinus communis*-EEF33728]	1e-12
TDF093	GR410321	+	111	Cytochrome P450 monooxygenase [*Pyrus communis*-AAR25996]	4e-06
TDF116	GR410342	+	122	Reticuline oxidase precursor [*Ricinus communis*-EEF32495]	2e-04
TDF148	GR410363	+	158	Chloroplastic ATP synthase [*Juglans mandshu*-AAP88222] ***JrATPase***	2e-21
TDF178	GR410385	-	383	Alcohol dehydrogenase [*Alnus glutinosa*-CAJ21172]	3e-64
TDF204	GR410407	-	156	Alanine aminotransferase [*Hordeum vulgare*-CAA81231]	2e-10
Fatty acid metabolism (4.8%)					
TDF006	GR410239	+	182	Allene oxide cyclase *[Medicago truncatula*-CAC83767] ***JrAOC***	1e-12
TDF021	GR410253	+	082	Fatty acid hydroxylase/desaturase [*Ricinus communis*-EEF39915]	3e-05
TDF146	GR410361	+	171	Fatty acid hydroxylase/desaturase [*Ricinus communi*-EEF39915*s*]	4e-05
TDF129	GR410348	+	110	Fatty acid hydroxylase/desaturase [*Ricinus communis*-EEF39915]	3e-13
TDF114	GR410340	+	203	Sérine C-palmitoyltransferase [*Vitis vinifera*-CAO67084]	8e-26
TDF111	GR410338	+	263	Ceramidase [*Vitis vinifera*-CAO21530]	1e-29
TDF110	GR410337	-	238	Ceramidase [*Vitis vinifera*-CAO21530] ***JrCDase***	6e-36
TDF053	GR410284	-	213	Patatin-like phospholipase [*Vitis vinifera*-XP002282546]	1e-27
TDF215	GR410415	-	302	Triacylglycerol lipase [Arabidopsis thaliana-EEE84272]	1e-06
Carbohydrate metabolism (3.7%)					
TDF005	GR410238	+	093	Ribulose bisphosphate carboxylase [*Juglans nigra*-AF206785] ***JrRUB***	6e-10
TDF094	GR410322	+	217	Photosystem II protein J [*Nicotiana tabacum*-NP054513]	7e-08
TDF125	GR410345	+	257	Formate dehydrogenase [*Quercus robur*-CAE12168]	9e-35
TDF150	GR410364	+	220	Photosystem II protein D1 [*Phaseolus vulgaris*-ABH88068] ***JrPSII-d1***	1e-28
TDF168	GR410375	-	203	Amilase *β*-type [*Cicer arietinum*-CAA07229] ***JrAmilase***	2e-23
TDF169	GR410376	-	134	Xyloglucan endotransglycosylase [*Cucumis sativus*-CAD87536] ***JrXRT***	3e-11
TDF181	GR410388	-	194	Formate dehydrogenase [*Quercus robur*-CAE12168]	4e-24
Stress and defence related (3.2%)					
TDF010	GR410242	+	186	Cinnamate 4-hydroxylase [*Vitis vinifera*-CAO66538]	2e-30
TDF080	GR410310	+	150	Drought-responsive protein [*Arabidopsis thaliana*-NP849286]	9e-06
TDF097	GR410324	+	087	Cinnamoyl-CoA reductase [*Betula luminifera*-ACJ38670]	2e-04
TDF050	GR410281	-	161	Universal Stress Protein (USP) [*Populus trichocarpa*-EEE82033] ***JrUSP***	9e-13
TDF045	GR410276	-	160	Senescence-associated protein [*Pisum sativum*-BAB33421]	2e-23
TDF211	GR410412	-	319	Nonsymbiotic hemoglobin [*Alnus firma*-BAE75956]	2e-48
Transport falicitation (2.6%)					
TDF089	GR410318	+	162	Proton-dependent oligopeptide transport [*Vitis vinifera*-CAO63418]	3e-15
TDF119	GR410343	+	176	ABC transporter homolog [*Populus nigra*-EEF10682]	1e-24
TDF130	GR410349	+	259	ABC transporter homolog [*Vitis vinifera*-CAO39997]	7e-20
TDF081	GR410311	+	189	ACT domain-containing protein [*Arabidopsis thaliana*-AAK74028]	3e-24
TDF068	GR410298	-	261	Plasma membrane H^+-ATPase [*Prunus persica*-CAB69823]	1e-26
Derivated metabolism (1.6%)					
TDF104	GR410331	+	060	NADH-plastoquinone reductase[*Illicium oligandrum*-YP001294275] ***JrPlastoQ***	4e-05
TDF034	GR410265	-	058	Maturase chloroplast gene [*Juglans regia*-AF118038]	5e-08
TDF163	GR410372	-	060	NADH-plastoquinone reductase[*Illicium oligandrum*-YP001294275]	4e-05
Hypothetical protein (11.2%)					
TDF018	GR410250	+	159	Hypothetical chloroplastic protein *[Nandina domestica*-ABI49909]	2e-14
TDF109	GR410336	+	185	Chloroplast membrane protein [*Fagus sylvatica*-AF525759]	8e-23
TDF142	GR410357	+	199	Hypothetical protein [*Ricinus communis*-EEF30461]	1e-20
TDF101	GR410328	+	063	Hypothetical protein [*Vitis vinifera*-CAN82657]	8e-04

TDF202	GR410405	-	105	Hypothetical protein [*Arabidopsis thaliana*-AAL49847]	5e-09
TDF038	GR410269	-	191	Hypothetical protein [*Vitis vinifera*-XP002275129]	1e-09
TDF165	GR410374	-	138	Hypothetical protein [*Ricinus communis*-EEF51999]	2e-06
TDF176	GR410383	-	263	Hypothetical protein [*Vitis vinifera*-CAO64333]	9e-27
TDF172	GR410379	-	182	Hypothetical protein [*Populus trichocarpa*-EEE87280]	1e-11
TDF162	GR410371	-	243	Hypothetical protein [*Populus trichocarpa*-EEE87280]	4e-08
TDF044	GR410275	-	100	hypothetical protein [*Vitis vinifera*-CAN75225]	4e-09
TDF036	GR410267	-	197	Hypothetical Zing-finger protein [*Ricinus communis*-EEF31539]	4e-19
TDF207	GR410408	-	315	Hypothetical protein [*Arabidopsis thaliana*-BAF01964]	2e-53
TDF173	GR410380	-	315	Hypothetical protein [*Arabidopsis thaliana*-BAF01964]	2e-53
TDF185	GR410392	-	167	Hypothetical protein [*Populus trichocarpa*-EEF09401]	7e-16
TDF190	GR410396	-	192	Hypothetical protein [*Vitis vinifera*-CAO14912]	1e-16
TDF194	GR410399	-	352	Hypothetical protein [*Medicago truncatula*-ABO81861]	1e-16
TDF203	GR410406	-	302	Hypothetical chloroplast protein [*Morus indica*-YP762304]	1e-35
TDF209	GR410410	-	252	Hypothetical protein [*Populus trichocarpa*-EEE78734]	2e-24
TDF210	GR410411	-	309	Hypothetical protein [*Ricinus communis*-EEF41177]	1e-07
TDF214	GR410414	-	244	Hypothetical protein [*Populus trichocarpa*-EEE87280]	9e-21

Putative unicellular contamination (2.5%)

TDF002	GR410236	+	211	Phosphoenolpyruvate synthase [*P.syringae. Oryzae*-ZP04591238]	2e-32
TDF160	GR410370	+	176	N-acetylglucosaminyltransferase [*Bradyrhizobium* sp-CAD90583.]	2e-04
TDF082	GR410312	+	183	Transposase component [*Pseudomonas putida*-YP709289]	8e-12
TDF098	GR410325	+	178	Hypothetical protein [*Pseudomonas fluorescens*-YP350507]	3e-20
TDF217	GR410417	-	177	Cell wall-associated hydrolase [*Escherichia coli*-ABJ03470]	2e-05

Unknown sequences (36.3%)

Depicted in supplemental Table 3

Annexe 2

Les aquaporines XIP chez le Peuplier, expansion évolutive, fonctionnalité et régulation en réponse à des facteurs environnementaux

Journal of Experimental Botany, Vol. 63, No. 5, pp. 2217–2230, 2012
doi:10.1093/jxb/err404 Advance Access publication 5 January, 2012

Journal of Experimental Botany
www.jxb.oxfordjournals.org

RESEARCH PAPER

Insights into *Populus* XIP aquaporins: evolutionary expansion, protein functionality, and environmental regulation

D. Lopez[1,2], G. Bronner[3], N. Brunel[1,2], D. Auguin[4,5], S. Bourgerie[4,5], F. Brignolas[4,5], S. Carpin[4,5], C. Tournaire-Roux[6], C. Maurel[6], B. Fumanal[1,2], F. Martin[7], S. Sakr[8], P. Label[5], J.L. Julien[1,2], A. Gousset-Dupont[1,2] and J.S. Venisse[1,2,*]

[1] Université Blaise Pascal UMRA 547 PIAF, BP 10448, F-63000 Clermont-Ferrand, France
[2] INRA, UMRA 547 PIAF, F-63100 Clermont-Ferrand, France
[3] Université Blaise Pascal, UMR LMGE, BP 10448, F-63000 Clermont-Ferrand, France
[4] Université d'Orléans, Laboratoire de Biologie des Ligneux et des Grandes Cultures, UPRES EA 1207, F-45067 Orléans, France
[5] INRA, USC1328 Arbres et Réponses aux Contraintes Hydriques et Environnementales (ARCHE), BP 6759, F-45067, France
[6] Biochimie et Physiologie Moléculaire des Plantes, Institut de Biologie Intégrative des Plantes, UMR 5004 CNRS/UMR 0386 INRA/Montpellier SupAgro/Université Monptellier 2, F-34060 Montpellier Cedex2, France
[7] Unité Mixte de Recherche 1136, Institut National de la Recherche Agronomique/Nancy Université, Interactions Arbres/Micro-organismes, Centre de Nancy, 54280 Champenoux, France
[8] Agrocampus Ouest, Centre d'Angers, UMR SAGAH, IFR QUASAV 149, 2 rue le Nôtre, F-49045 Angers, France

* To whom correspondence should be addressed. E-mail: j-stephane.venisse@univ-bpclermont.fr

Received 1 September 2011; Revised 14 November 2011; Accepted 16 November 2011

Abstract

A novel category of major intrinsic proteins which share weak similarities with previously identified aquaporin subfamilies was recently identified in land plants, and named X (for unrecognized) intrinsic proteins (XIPs). Because XIPs are still ranked as uncharacterized proteins, their further molecular characterization is required. Herein, a systematic fine-scale analysis of XIP sequences found in flowering plant databases revealed that XIPs are found in at least five groups. The phylogenetic relationship of these five groups with the phylogenetic organization of angiosperms revealed an original pattern of evolution for the XIP subfamily through distinct angiosperm taxon-specific clades. Of all flowering plant having XIPs, the genus *Populus* encompasses the broadest panel and the highest polymorphism of XIP isoforms, with nine *Pt*XIP sequences distributed within three XIP groups. Comprehensive *PtXIP* gene expression patterns showed that only two isoforms (*PtXIP2;1* and *PtXIP3;2*) were transcribed in vegetative tissues. However, their patterns are contrasted, *PtXIP2;1* was ubiquitously accumulated whereas *PtXIP3;2* was predominantly detected in wood and to a lesser extent in roots. Furthermore, only *Pt*XIP2;1 exhibited a differential expression in leaves and stems of drought-, salicylic acid-, or wounding-challenged plants. Unexpectedly, the *Pt*XIPs displayed different abilities to alter water transport upon expression in *Xenopus laevis* oocytes. *Pt*XIP2;1 and *Pt*XIP3;3 transported water while other PtXIPs did not.

Key words: Aquaporin, evolution, *in situ* hybridization, molecular physiology, *Populus*, XIP.

Introduction

Water flux across biological membranes can occur directly through the lipid bilayer, but predominantly happens through water channel proteins named aquaporins (AQPs) (Agre *et al.*, 1993). AQPs are integral membrane proteins of the larger major intrinsic protein (MIP) superfamily. These channels are found in all living organisms, from archea and eubacteria to fungi, animals, and plants (Engel and Stahlberg, 2002). Looking at this global distribution, AQPs are

© The Author [2012]. Published by Oxford University Press [on behalf of the Society for Experimental Biology]. All rights reserved.
For Permissions, please e-mail: journals.permissions@oup.com

especially abundant in plants, with expression in virtually all cell types (Kjellbom *et al.*, 1999; Wallace and Roberts, 2004). AQPs constitute a large and divergent family with 35 members identified in *Arabidopsis thaliana* (Johanson *et al.*, 2001), 36 in *Zea mays* (Chaumont *et al.*, 2001), 33 in *Oryza sativa* (Sakurai *et al.*, 2005), 37 in *Solanum lycopersicon* (Sade *et al.*, 2009), and 65 members in *Populus trichocarpa* (Gupta and Sankararamakrishnan, 2009). Some AQPs form channels facilitating bidirectional water fluxes, whereas others can conduct a wide range of small neutral solutes including urea, lactic acid, glycerol, hydrogen peroxide, silicic acid, metalloids, and gases such as ammonia and carbon dioxide. AQPs play a central role in plant–soil water relations, seed germination, cell elongation, drought resistance, salt tolerance, and fruit ripening. Based on sequence similarities, AQPs of most plant species can typically be divided into four subfamilies: the plasma membrane intrinsic proteins (PIPs), the tonoplast intrinsic proteins (TIPs), the nodulin 26-like intrinsic proteins (NIPs), and the small basic intrinsic proteins (SIPs). Most of these subfamilies are being extensively investigated with respect to their structural signatures, expression patterns, subcellular localizations, and substrate specificities. Phosphorylation, pH, Ca^{2+}, and osmotic gradients were also reported to affect their water channel activities. Moreover, recent insights into their co- and post-translational modifications and cellular trafficking have led to promising models that explain the regulation of their transport activity in various physiological processes, including photosynthesis, osmotic regulation, tree embolism recovery, and water use efficiency. Recent reviews have summarized increasing knowledge about these processes (Chaumont *et al.*, 2005; Kaldenhoff and Fischer, 2006; Maurel, 2007; Maurel *et al.*, 2009).

Three additional AQP subfamilies were recently described in the non-vascular moss *Physcomitrella patens*: GlpF-like intrinsic proteins (GIPs) homologous to some glycerol channels of Gram-positive bacteria (Gustavson *et al.*, 2005), the hybrid intrinsic proteins (HIPs), and uncategorized members designated X intrinsic proteins (XIPs) (Danielson and Johanson, 2008). Members of the latter subfamily are found in protozoa, fungi, and land plant kingdoms. Since XIPs are not encoded by the sequenced genomes of certain plants such as *Arabidopsis, Oryza* or *Zea*, partial knowledge together with hypothetical functions of plant XIPs are starting to emerge (Danielson and Johanson, 2008; Sade *et al.*, 2009; Gupta and Sankararamakrishnan, 2009; Shelden *et al.*, 2009; Park *et al.*, 2010; Bienert *et al.*, 2011).

Plant XIP sequences have substantially diverged from those of fungi and protozoa. Strikingly, such sequence divergence is encountered even within the plant kingdom itself, as observed when comparing the Lycopodiophyta *Selaginella moellendorffii*, the Bryophyta *Physcomitrella patens*, and various Magnoliophyta (angiosperms) XIP sequences. Within this last plant division, the XIP subclass seems to be exclusive to *Magnoliopsida* (dicots) and its members have been phylogenetically clustered into two groups (XIP1 and XIP2). As these proteins harbour amino acid variations in regions corresponding to the primary selection filter and the major checkpoint for solute permeability [i.e. the first Asn-Pro-Ala (NPA) box and aromatic/arginine region (ar/R)] (Beitz *et al.*, 2006; Tornroth-Horsefield *et al.*, 2006; Mitani-Ueno *et al.*, 2011), it was first hypothesized that XIPs are non-functional as water channels but instead are dedicated to the transport of hydrophobic solutes (Danielson and Johanson, 2008; Gupta and Sankararamakrishnan, 2009). These predictions have been recently validated by Bienert and his collaborators (2011) on XIPs from three Solanales: *Nicotiana tabacum, Solanum lycopersicon,* and *Solanum tuberosum*.

Although substantial progress has been made regarding the XIP molecular structure, subcellular localization, transcriptional regulation, and functional gating, the reason for their availability in plants is not understood, and several questions remain to be answered. For instance, (i) to what extent did the evolutionary expansion of XIP occur in plants? The evolutionary history of the XIPs was partially explained in a broad phylogenetic survey including some sequences of flowering plants (angiosperms), protozoa, fungi, and mosses (Gupta and Sankararamakrishnan, 2009). This was paradoxically done without considering the angiosperm evolutionary story and this Viridiplantae division encompasses the largest number of XIP sequences. It follows that previous XIP phylogenetic data alone were not conclusive. (ii) Can some XIPs different from those studied in Solanales be considered as multifunctional channels, being able to transport water? Indeed, many members in each MIP subclass present differential selectivity for substrates, and this is particularly true in the case of plants which comprise the most remarkable MIP diversity.

In the study, XIP sequences from a wide variety of plants were first retrieved and compared, making full use of the available expressed sequence tag (EST) as well as plant genome sequences databases. This data set was used to analyse their phylogenetic relationship, together with an integrative amino acid-based evolutionary partitioning of this subfamily during angiosperm evolution. Among this set, poplar, with nine sequences, is to date the species with the largest number of XIPs with significant amino acid diversity, making it a suitable model to re-examine this AQPs subfamily molecularly. Expression analyses using quantitative real-time PCR revealed that only two *PtXIP* genes (*PtXIP2;1* and *PtXIP3;2*) were expressed in vegetative tissues, and only *PtXIP2;1* was differentially and strongly modulated in response to abiotic stresses. Supplementary *in situ* hybridization experiments showed that the *PtXIP2;1* and *PtXIP3;2* genes were highly expressed in well-defined cell types or poplar tissues. Finally, *Pt*XIP2;1 and *Pt*XIP3;3 were functionally characterized as being the poplar XIPs able to transport water in *Xenopus* oocyte expression assays.

Materials and methods

Plant material and experimental design

Populus trichocarpa (Torr. & Gray ex Hook), clone INRA 101-74 kindly provided by Dr Catherine Bastien (INRA, Orléans, France), was selected for the experiments as it is increasingly being

used as the male parent for genetic research programmes. Homogeneous 25 cm long woody stem cuttings were planted in 10.0 l pots filled with a commercial substrate (40% black, 30% brown, and 30% blond peat moss, pH 6.1, DUMONA-RN 75-3851 Arandon, The Netherlands) and placed in a controlled-environment greenhouse under a 16 h/8 h light/dark photoperiod, at 18/22 °C (day/night), with relative humidity set at 70±10% and a daytime photosynthetic photon flux ≥350 μmol m^{-2} s^{-1}. Three treatments were conducted on 3-month-old plants. Phytohormone treatment was carried out on fully expanded leaves with 1 mM salicylic acid (SA) dissolved in 100 μl of absolute ethanol before concentration adjustment in distilled water and then pulverization. Drought conditions were produced by withholding water until the first basal leaves showed signs of severe dehydration (soil water potential $\Psi_s \approx -1.2 \pm 0.15$ MPa). Rehydration conditions were obtained by re-watering the soil. For mechanical wounding treatments, 40% of the leaf area was lightly crushed using large clamps. At each sampling time, harvested tissues were immediately frozen in liquid nitrogen and stored at –80 °C until RNA extraction.

Bioinformatics analysis

The plant XIP gene subfamily was explored using XIP sequences previously described (Danielson and Johanson, 2008; Gupta and Sankararamakrishnan, 2009) as initial queries. Basic Local Alignment Search Tool (BLAST) search tools, tBLASTn and BLASTp (Altschul *et al.*, 1997), were used against Viridiplantae taxon non-redundant generalist databases National Center for Biotechnology information (NCBI, http://www.ncbi.nlm.nih.gov/) and Department of Energy's Joint Genome Institute (JGI, http://www.jgi.doe.gov/), and from plant-dedicated assembly genome projects: Coffee Genome Project (http://www.lge.ibi.unicamp.br/cafe), Genome Database for Rosacae (http://www.rosaceae.org), Genoscope (http://www.genoscope.cns.fr), Public *Eucalyptus* Genome resource (http://eucalyptusdb.bi.up.ac.za), and Sol Genomics Network (http://solgenomics.net). Incomplete sequences showing conserved regions were manually assembled for further analysis, whereas redundant entries, including sequences with putative point mutations or polymorphism (similarities >98%), and single incomplete sequences displaying a hypothetical length <80% compared with its putative poplar orthologue were discarded.

The poplar MIP gene family was uncovered via two bioinformatics explorations: *P. trichocarpa* whole genome shotgun (WGS) sequences expanded with GenBank *Populus* EST collections and full-length cDNAs, and the recent release of the *P. trichocarpa* genome from JGI database assembly version 2.2 [JGI v2.2 annotation of the v2.2 assembly (JGIv2.2) available via Phytozome version 7.0 (www.phytozome.net)] in comparison with the older JGI annotation of the v1.1 assembly (JGIv1.1). A complementary analysis was carried out on the Molecular Genbank non-redundant sequence databases using the tBLASTn search tool server in order to identify potential poplar ESTs related to each MIP sequence previously identified. This made it possible to redefine any sequence with false predictions. The nomenclature of Gupta and Sankararamakrishnan (2009) was used for naming *Populus* MIPs, except for the *Pt*XIP subfamily, for which an updated nomenclature was proposed based on the percentage of amino acid similarity between members and the phylogenetic studies presented herein.

Percentages of amino acid similarity and identity were calculated using the NCBI bl2seq algorithm. Multiple sequence alignment analysis was performed using PRALINE-PSI (Simossis and Heringa, 2005) with a five PSI-BLAST iteration search (with an *e*-value cut-off of 0.01) within the non-redundant database. Jalview (Clamp *et al.*, 2004) was used with the ClustalX colour code to illustrate the alignment results.

The unrooted phylogenetic trees were constructed using the maximum likelihood (ML) method implemented in the PhyML program v3.0 (Guindon and Gascuel, 2003). Specifically, PhyML analyses were conducted with the Jones–Taylor–Thornton (JTT) substitution matrix, 1000 bootstrap replicates to assess the reliability for degree of support for each internal branch on the phylogenetic trees, estimated proportion of invariable sites, four rate categories, and estimated gamma distribution parameter. Trees were viewed and edited with TreeDyn (Chevenet *et al.*, 1997), and bootstrap values >50% were reported. Except for *Pt*XIP3;1b (ProteinID 829126), all other related pseudogenes and truncated amino acid sequences were eliminated from further analysis.

Total RNA isolation, cDNA synthesis, and amplification

Total RNA was extracted from 150 mg of roots, the apical part of the stem, bark (including phloem) and wood from the intermediate part of the stem, buds, and leaves using cetyltrimethylammonium bromide (CTAB) extraction buffer according to Chang *et al.* (1993). First-strand cDNA was synthesized from 1 μg of total RNA using SuperScript III (Invitrogen, Carlsbad, CA, USA) following the manufacturer's instructions. Real-time PCR amplification was performed using a MyiQ thermocycler (Bio-Rad, Hercules, CA, USA) with MESA GREEN qPCR MasterMix Plus (Eurogentec, Belgium) containing 2 μl of 40-fold diluted cDNA according to the manufacturer's protocol. The thermal profile of the reaction was: 94 °C for 3 min and 40 cycles of 94 °C for 20 s, 54–58 °C for 20 s, and 72°C for 20 s. The specificity of amplicons was routinely verified by melting curve analysis, and checked by gel electrophoresis. PCR efficiencies were deduced for each gene according to Pfaffl's (2001) procedures. The crossing cycle number (C_t) was automatically determined for each reaction by the iCycler iQ v2.0 software with default parameters. For normalization of the target gene abundance, the software application *BestKeeper* v1 (http://www.gene-quantification.info; Pfaffl *et al.*, 2004) was used according to the developers' manual to determine the best suited reference genes from nine widely used housekeeping genes (Czechowski *et al.*, 2005; Xu *et al.*, 2011), and then to estimate a *BestKeeper Index*. The reference genes selected (gene locus; GM, geometric mean of C_t ±SD; CV, BestKeeper coefficient of Pearson correlation; and *r*, variance from all sample at all time points) were *Actin1* (POPTR_0001s31700; GM, 24.78±0.59; CV, 2.40; *r*, 0.864), *SAND* (POPTR_0009s01980; GM, 29.74±0.59; CV, 1.99; *r*, 0.870), and *TIP41a-like* (POPTR_0001s30580; GM, 27.12±0.77; CV, 2.66; *r*, 0.787), chosen from different protein families in order to reduce the possibility of co-regulation. Constitutive MIP transcript steady-state levels in each vegetative tissue were assessed by comparison of the mean of the C_t after normalization with the *BestKeeper Index*. The final results from each statistical output were graphically represented after distribution and assignation of a score value between 0 and 100, an arbitrary scoring range. A C_t of 20 was assigned an arbitrary value of 100 (corresponding to the highest MIP expression level in *Populus*), while a C_t of 40 was assigned an arbitrary value of 0 (no expressed gene). Then all other C_ts were assigned values between 0 and 100, scaled based on their relative distributions. As for differential accumulation of MIP transcripts in response to stresses, the relative changes were calculated with the equation $2^{-\Delta\Delta Ct}$ according to Pfaffl procedure's (2001). Circadian *PtXIP* expression under control conditions was first monitored allowing 't_0' untreated samples to be used as controls (corresponding to leaves sampled just before experiments). For legibility, and especially for down-regulated genes, values were graphically normalized to 0, this course representing no change in gene expression. Each unit on both sides of 0 corresponds to a 2-fold increase and a 2-fold decrease. The mean C_t value was determined from three independent biological replicates for each sample, and every PCR was carried out in triplicate. Values are given as means ±SD. Primers were designed using the Primer3plus application (http://www.bioinformatics.nl/primer3plus; Rozen and Skaletsky, 2000), and are listed in Supplementary Table S3 available at *JXB* online. A concomitant analysis of genomic DNA and cDNA was carried out in order to evaluate the robustness of each primer set (data not shown).

In situ hybridization

Fresh stems and leaves were harvested, cut, and immediately fixed in 4% (w/v) paraformaldehyde + 2.5% (v/v) glutaraldehyde overnight at 4 °C. Fixed samples were dehydrated and embedded in methacrylate resin (methyl methacrylate–butyl methacrylate resin, EMS, Mündelsheim, France) according to the manufacturer's instructions. Polymerization occurred in gelatin capsules overnight at 60 °C. Transverse sections of 3–4 μm thickness were cut with a rotary microtome, mounted on SuperFrost Plus slides (Fisher Scientific, Elancourt, France), and dried at 42 °C for 2 d. A 5 min incubation in pure acetone removed the methacrylate resin. *In situ* hybridization (ISH) was performed as described in Leblanc-Fournier *et al* (2008). Gene-specific RNA probes were designed to be located in the variable 3′-untranslated region (UTR) of *Pt*XIP2;1 and *Pt*XIP3;2 transcripts with an average size of 250 ribonucleotides (primers listed in Supplementary Table S3 at *JXB* online). DNAs encoding the probes were cloned in pGEM® T-Easy vector (Promega, Madison, WI, USA). Briefly, sense and antisense digoxigenin (DIG)-labelled RNA probes were synthesized as described in Leblanc-Fournier *et al* (2008) using an *in vitro* transcription kit [DIG RNA labeling kit (SP6/T7), Roche Diagnostics, Mannheim, Germany] according to the manufacturer's instructions. The antisense and sense probes were transcribed from SP6 or T7 polymerase promoters (after vector linearization with *Nco*I or *Spe*I, respectively). Stem and leaf sections were incubated overnight at 50 °C with 1.5 ng μl^{-1} or 3 ng μl^{-1}, respectively, of sense and antisense probes. They were then washed with 2× SSC/50% formamide. Detection was performed using anti-dioxigenin–alkaline phosphatase conjugate, followed by colorimetric detection of phosphatase activity (Bio-Rad). After suitable colour development, the reaction was stopped by rinsing in water, and sections were dried and mounted in Eukitt (Euromedex, Mündelsheim, France). Observations were performed under an Axioplan 2 microscope (Zeiss, Jena, Germany). Data were recorded on a digital camera (AxioCam HR, Zeiss) using Axiovision digital imaging software.

Expression in Xenopus laevis *oocytes and osmotic water transport assay*

The *PtXIP* cDNAs cloned in a pGEM®-T Easy vector were amplified by PCR (primers listed in Supplementary Table S3 at *JXB* online). Upstream of each *PtXIP* primer specific for the 5′-UTR and 3′-UTR, the *Bgl*II and *Spe*I restriction sites were introduced, respectively. The amplicons were digested by *Bgl*II and *Spe*I (Promega) and the resulting fragments were cloned in the corresponding sites of a T7Ts vector, fused with the 5′- and 3′-UTR sequences of a *Xenopus* γ-globin gene, to favour stability of the derived complementary RNA (cRNA). The integrity of the two constructs was checked by sequencing. Plasmids were linearized by *Eco*RI before *in vitro* transcription, and functional expression of aquaporins in *X. laevis* oocytes was as described by Maurel *et al.* (1993). The statistical analysis was performed on data pooled from all experiments using a one-way analysis of variance (ANOVA; $P < 0.001$), and post-hoc multiple comparisons were run using a Tukey test on the same set of data for which normality was checked. In the figures, the bars indicate the SEM and different letters denote statistically significant ($P < 0.001$) differences.

Results

Phylogenetic analysis of the angiosperm XIP group

An evolutionary lineage fine analysis of all available angiosperm XIP-like proteins was performed, based on the current angiosperm phylogeny. To accomplish this, all XIP sequences previously reported by Danielson and Johanson (2008) and by Gupta and Sankararamakrishnan (2009) were used as queries against various genomic and EST angiosperm collections. From slightly less than 200 XIP-related sequences retrieved, 55 non-redundant representative sequences were selected (Supplementary Table S1 at *JXB* online). As previously mentioned, except for *Liriodendron tulipefera* (Magnoliales), all XIP sequences came from the dicotyledonous phylum. In addition, an unrooted tree constructed from alignments of protein sequences confirmed that XIPs split into two independent clusters, identified as XIP-A and XIP-B in this study (Fig. 1; sequence alignments in Supplementary Fig. S3). These two subgroups correspond to XIP2 and XIP1, respectively, in the former nomenclature (Gupta and Sankararamakrishnan, 2009). A fine reading of the phylogenetic XIP distribution led to further refinement of the former nomenclature. The XIP-A cluster encompassed 15 orthologous sequences from mesangiosperms (Magnolianae superorder with *L. tulipefera*), and various core eudicots within the Rosanae taxon exclusively. These XIP-A sequences shared an average amino acid similarity of 77%, which fell to ~60% with XIP-B members. The second cluster, XIP-B, reflected the emergence of four major clades: XIP2, XIP3, XIP4, and XIP5 with well-supported to strong bootstrap support (82, 95, 99, and 95%, respectively). Interestingly, XIP-Bs were exclusive to eudicots and, unlike XIP-As, distinctly clustered into plant taxon-specific clades. Thus, XIP2 and XIP3 were spread into the Rosideae superorder: XIP2 encompassed sequences from Malpighiales (*Euphorbia*, *Gossypium*, *Manihot*, *Populus*, and *Ricinus*), Brassicales (*Carica*), and Rosales (*Malus* and *Prunus*), while XIP3 members were encountered in Malpighiales (*Manihot* and *Populus*) and Sapindales (*Citrus*). The XIP4 and XIP5 clades were, in contrast, exclusively linked to the Asteranae superorder: XIP4 members were linked to Lamiids (*Ipomea*, *Mimulus*, *Nicotiana*, *Solanum*, and *Triphysaria*), while XIP5 members were linked to Campanulids (*Centaurea*, *Cichorium*, *Helianthus*, *Guizotia*, and *Lactuca*). Members within each XIP-B clade shared a minimum of 85% amino acid sequence similarity, and an average between-clade similarity of 79%. Finally, as reported for the monophyletic *Liliopsida* taxon (Danielson and Johanson 2008), if the absence of XIP sequences is true and not an artefact due to limited data sets, plants belonging to ferns, ANITA (the basal angiosperms, Amborella, Nymphaeales, Illiciales, Trimeniaceae, and Austrobaileya), and coniferophyte monophyletic taxa lack the XIP subfamily.

A more integrative view of this phylogenetic XIP clade distribution (Fig. 2) was also revealed when considering the current angiosperm phylogeny (Angiosperm Phylogeny Website, V.9 http://www.mobot.org/MOBOT/research/APweb/, complemented with the Angiosperm Phylogeny Group III system, Chase and Reveal 2009). This analysis showed a XIP-A branch in which members diverged parallel to the plant species divergence, whereas the XIP-B branch would reflect clade divergences in a plant taxon-specific manner, both with their own evolutionary rate.

Features of the XIP *gene subfamily in* Populus

The molecular characterization of the *Populus XIP*-like genes was updated using the XIP protein sequences retrieved from

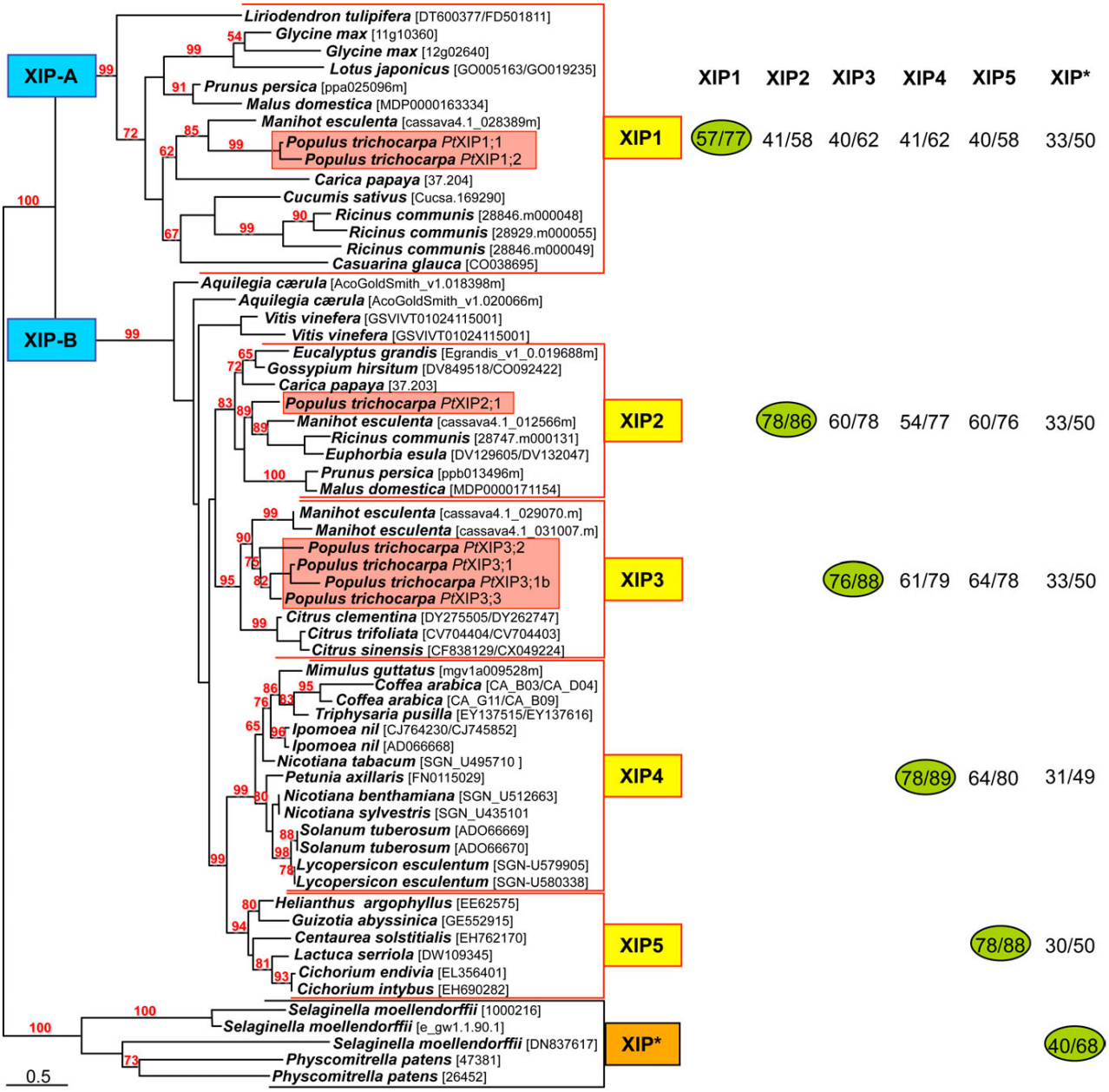

Fig. 1. Evolutionary relationship between Viridiplantae plant XIPs. The unrooted phylogeny of the XIP protein sequence was inferred using maximum likelihood. The tree was produced using PhyML with a genetic distance calculated by the JTT model of amino acid change. The numbers at the nodes represent the percentage bootstrap values (>50%) based on 1000 reassembling. The distance scale denotes the number of amino acid substitutions per site. Green circled numbers represent the percentage amino acid sequence identity and similarity intragroup; other numbers are amino acid sequence identity and similarity intergroups. *Populus* XIP sequences are highlighted in red. Species and accession numbers are listed in Supplementary Table S1 at *JXB* online. *Selaginella moellendorffii* and *Physcomitrella patens* XIP sequences (XIP*) were edited for information purposes, and were used as angiosperm taxon outgroups.

a reiterative search against the Phytozome Version 7.0. This upgraded version includes the last JGI v2.2 annotation of the *P. trichocarpa* assembly (JGIv2.2). The opportunity to retrieve the whole poplar *MIP* gene complement and to re-examine their sequences was also taken. Sixty-five sequences are by default annotated as putative '*Aquaporin (major intrinsic protein family)*', leading to 54 full-length open reading frames (ORFs) as initially reported (Gupta and Sankararamakrishnan, 2009, Almeida-Rodriguez *et al*, 2010). This research has led to the retrieval of two other sequences belonging to the XIP subfamily: *Pt*XIP1;2 (POPTR_0009s13105) and a pseudogene at the nucleotide position 10 525 867–10 526 066 located on the scaffold IX and not annotated. Sequences and final Phytozome v7.0 labelling are given in Supplementary Table S2 at *JXB* online. In agreement with previous works, the 56 ORFs

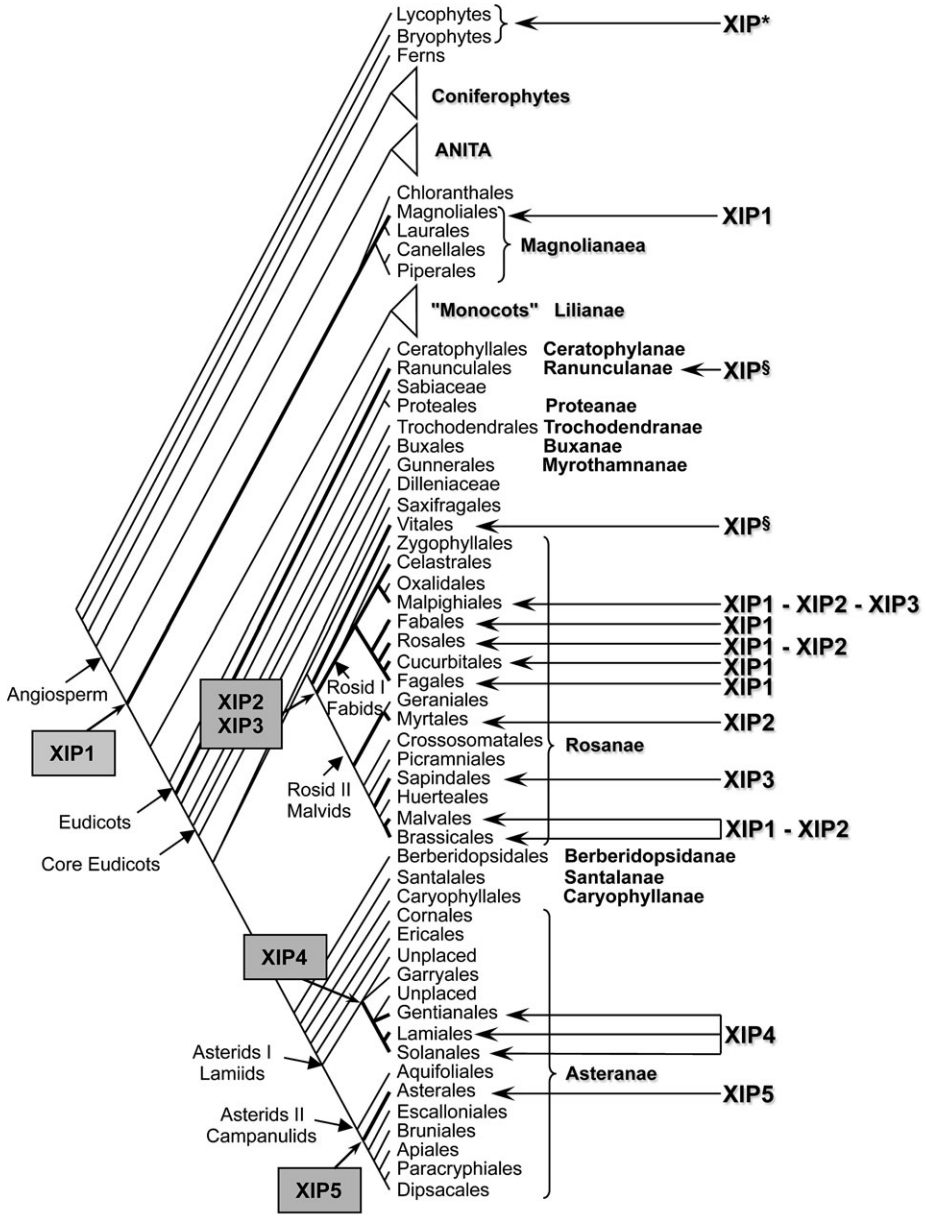

Fig. 2. Evolutionary relationship of XIP sequence divergence and consensus angiosperm phylogeny. The rooted tree proposed here was a compilation of APGIII (2009) and Missouri Botanical Garden (MBG; www.mobot.org) trees. Arrows indicate the presence of XIP groups in taxa. *Selaginella moellendorffii* (Lycopodiophyta) and *Physcomitrella patens* (Bryophyta) XIP sequences (XIP*), and *Aquilegia* (Ranunculanae) and *Vitis* (Vitales) XIP sequences (XIP§) were placed for information purposes, but are not discussed further.

were phylogenetically assigned to five distinct subfamilies (phylogenetic distribution and sequence alignments detailed in Supplementary Figs S1 and S2): PIPs (with 15 members subdivided into five PIP1s and 10 PIP2s), TIPs (17 members), NIPs (11 members), and SIPs (six members). For consistency, gene names specified by Gupta and Sankararamakrishnan (2009) were used for this work. These groups will not be discussed further. The fifth subfamily defines the as yet uncharacterized XIPs, and constitutes the main issue of the present discussion.

The poplar *XIP* subfamily appears to comprise nine putative members with seven full-length protein sequences (DbXrefJGI 557138, 821124, 557139, 759781, 829126, 767334, and POPTR_0009s13105) and two pseudogene sequences (DbXrefJGI 579650 and *PtXIP*-nd). The 829126 sequence (*PtXIP3;1b*) was a truncated sequence due to an ATA triplet insertion within the coding sequence, generating a stop codon nine bases downstream of the initiation codon in relation to its paralogue 557139 (*PtXIP3;1*). This insertion was validated by sequencing multiple clones.

Finally, the full-length *Pt*XIP-related proteins were classified into three groups: *Pt*XIP1 (with two members: *Pt*XIP1;1-557138 and PtXIP1;2-POPTR_0009s13105), *Pt*XIP2 (with one member: *Pt*XIP2;1-821124), and *Pt*XIP3 (with three members: *Pt*XIP3;1-557139, *Pt*XIP3;2-767334, and *Pt*XIP3;3-759781). This new nomenclature is supported by the following three arguments.

(i) Conventionally, plant aquaporins are divided into subfamilies (i.e. NIPs, PIPs, SIPs, and TIPs) that are further divided into groups of related proteins. To maintain consistency with the AQP nomenclature principles of Johanson *et al.* (2001), the *Pt*XIP subfamily should be divided into three groups. Additionally, this repartition was confirmed by the phylogenetic distribution of *Pt*XIPs alone (Fig. 3A). Proposed names for *Pt*XIPs consisted of the subfamily name followed by a number indicating the XIP master group and a second number characterizing the individual XIP member within the group. Intergroup amino acid sequence similarities between *Pt*XIP1 and *Pt*XIP2 or *Pt*XIP3 were ~59%, and ~81% between *Pt*XIP2 and *Pt*XIP3 (Fig. 3B). *Pt*XIP1 members were highly conserved, with a similarity of 94%, as well as *Pt*XIP3s with an average of 90% similarity. The pseudogene sequences and the truncated protein 829126-related sequence (*Pt*XIP3;1b in Fig. 3) were not classified, although they seem to be paralogues of *Pt*XIP2;1 and *Pt*XIP3;1, respectively.

(ii) *Pt*XIP1;2 was distinguished by a gene structure with a unique intron, whereas *Pt*XIP1;1 was an intronless gene. Both exhibited a longer N-terminus as compared with other MIP homologues, a hydrophilic C-loop region deleted of eight amino acid residues specific to the dicot XIP subfamily, and the substitution of the first NPA motif by an SPV motif (Supplementary Fig. S3 at *JXB* online). This substitution was also encountered in *Lotus* and *Glycine max* sequences, while the other XIP1 clustered sequences showed a substitution of the alanine residue of the NPA motif by a valine, isoleucine, or cysteine residue. Remarkably, *Pt*XIP2;1 had both NPA motifs strictly conserved. *Pt*XIP3 members shared in their first NPA motif a substitution of the alanine by an isoleucine or leucine residue.

(iii) Lastly, the evolutionary relationships of the poplar *Pt*XIPs in a compilation of all the angiosperm XIP-like proteins characterized so far backed up overall the choice of nomenclature (Fig. 1).

The new JGIv2.2 nomenclature showed that *Populus MIP* genes were evenly spread over 18 of the 19 haploid 'chromosomes' constituting the poplar genome (Supplementary Table S2 at *JXB* online). Yet, seven out of the nine *Pt*XIP sequences were arranged head-to-tail on linkage group IX (in order, and taking the new nomenclature into account: *PtXIP2;1–PtXIP1;2–PtXIP3;1b–PtXIP*-nd–*PtXIP1;1–PtXIP3;1–PtXIP3;2*); one was located on linkage group IV (*Pt*XIP3;3), and the final one (*PtXIP*-579750) was located on a scaffold that had not yet been assigned to a specific linkage group (Fig. 3C). Such scaffolds were reported to be heterochromatic or derived from substantially divergent haplotypes in the sequenced clone (Tuskan *et al.*, 2007; Kelleher *et al.*, 2008).

Expression pattern of PtXIP *transcripts*

The transcriptional expression of the *PtXIP* gene subfamily and two *PtPIP* genes as references, *PtPIP1;2* (mentioned as

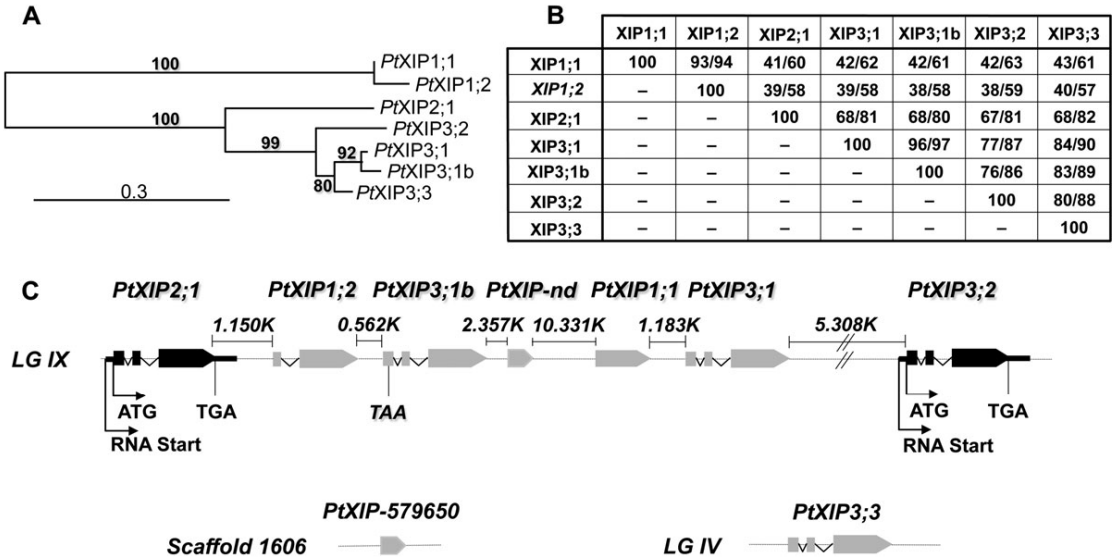

	XIP1;1	XIP1;2	XIP2;1	XIP3;1	XIP3;1b	XIP3;2	XIP3;3
XIP1;1	100	93/94	41/60	42/62	42/61	42/63	43/61
XIP1;2	–	100	39/58	39/58	38/58	38/59	40/57
XIP2;1	–	–	100	68/81	68/80	67/81	68/82
XIP3;1	–	–	–	100	96/97	77/87	84/90
XIP3;1b	–	–	–	–	100	76/86	83/89
XIP3;2	–	–	–	–	–	100	80/88
XIP3;3	–	–	–	–	–	–	100

Fig. 3. Valuer's *Pt*XIP subfamilly. (A) Phylogenetic trees of the *Pt*XIP subfamily. The truncated sequence *PtXIP3;1b* (829126) was included in the analysis, whereas the pseudogenes Scaffold 1606 (*PtXIP-579650*) and XIP-nd related sequences were discarded. Full-length amino acid sequences were analysed by the maximum likelihood method with genetic distance calculated by the JTT model of amino acid change. The numbers at the nodes represent the percentage bootstrap values based on 1000 replicates. The distance scale denotes the number of amino acid substitutions per site. (B) Amino acid identity and similarity percentages between *Populus trichocarpa* cv. Nisqually XIP protein sequences. Percentages were calculated using the NCBI bl2seq algorithm. (C) Schematic representation of the genomic distribution of the nine *PtXIP* genes according to Phytozome v6.0 information (*Populus trichocarpa* cv. Nisqually). Black box regions refer to untranslated mRNA sequences and coding exon sequences transcribed from *P. trichocarpa* cultivar INRA no.101-74, and cloned for this work. Introns are represented by dotted lines, and the numbers above indicate the number of base pairs. The TAA codon stop in *PtXIP3;1b* was corollary generated to the ATA insertion event. LG, linkage group.

PtPIP1;1 in Secchi *et al.*, 2009) and *PtPIP2;2*, was traced in various vegetative organs and in plants exposed to different stresses. The steady-state level of constitutive transcript accumulation relative to the XIP subfamily was monitored in different vegetative tissues including dormant buds (apical and axillary buds mixed), leaves at different maturation stages, apical growing stems, wood and bark (including phloem) of 2-year-old mature stems, and roots (Fig. 4). Of the nine members, only *PtXIP2;1* and *PtXIP3;2* showed detectable expression in *P. trichocarpa* 101-74. No transcripts of *PtXIP1* genes *PtXIP3;1*, or *PtXIP3;3* were detected. *PtXIP2;1* was ubiquitously expressed in vegetative tissues, with high accumulation in buds and immature organs (stems and leaves). It decreased significantly in mature leaves and dropped drastically in senescent leaves. A moderate transcript accumulation was monitored in roots. As regards *PtXIP3;2*, its expression was high in wood, and to a lesser extent, in buds and roots. In all other organs, *PtXIP3;2* expression was very low (mature leaves and bark) or not detectable. *PtXIP1* genes, *PtXIP3;1*, and *PtXIP3;3* did not show significant transcript accumulation under the observed conditions. *PtPIP1;2* and *PtPIP2;2* were highly expressed in all the vegetative tissues of *P. trichocarpa* studied.

PtXIP2;1 and *PtXIP3;2* gene expression was assessed in leaves and branches of plants subjected to severe drought followed by soil re-watering when the most basal leaves showed signs of physiological dehydration. Expression of *PtXIP* genes was also monitored in leaves exposed to SA or mechanical wounding (Fig. 5). Regardless of treatments, *PtXIP2;1* showed a marked transcriptional modulation, whereas *PtXIP3;2* showed limited transcriptional modulation including in stems where its constitutive accumulation appears substantial. No circadian variations in *Pt*XIP mRNA expression patterns were observed (data not shown). During water stress and re-watering (Fig. 5A), *PtXIP2;1* gene expression was greater in leaves than in stems. *PtXIP2;1* was quickly and drastically down-regulated in response to drought. Interestingly, *PtXIP2;1* expression increased 30 min after induction by re-watering and then dropped to its lowest level at 6 h. Gene expression recovered to the basal level 12 h after re-watering. Under SA and wounding treatments, transcripts of *PtXIP2;1* were transiently up-regulated (Fig. 5B, C). Although modulation occurred earlier under SA than wounding, transcripts peaked at 12 h and returned to a steady-state expression level at 24 h in both cases.

Similar to *PtXIP2;1*, *PtPIP* modulations in response to drought were more marked in leaves than in stems. *PtPIP1;2* transcript abundance showed an early and marked up-regulation, whereas *PtPIP2;2* transcript abundance was down-regulated. Both returned to basal levels only 6 h after re-watering. Lastly, transcript levels of *PtPIP1;2* were down-regulated by SA and transiently up-regulated by wounding, whereas transcript levels of *PtPIP2;2* were up-regulated by both SA and wounding.

In situ hybridization

ISH experiments performed on cross-sections of non-stressed *Populus* stems and leaves showed that *PtXIP2;1* transcripts were highly abundant in most vegetative tissues (Fig. 6A–D, I–N), while *PtXIP3;2* expression seemed to be restricted to stems (Fig. 6E–H; Supplementary Fig. S4 at *JXB* online). In stems, *PtXIP2;1* expression was detected in bark, phloem, and wood with a relatively high intensity (Fig. 6A, C). *PtXIP3;2* transcripts co-located well with those of *PtXIP2;1* (Fig. 6E, G). In leaves, due to the cell turgor level and a predominantly vacuolar cell volume, coloration is located in the cell periphery. *PtXIP2;1* expression was detected in almost all parts of the midrib except the cambium (Fig. 6I). In the lamina (Fig. 6K, M) *PtXIP2;1* was present in the epidermis, spongy parenchyma, and vascular tissues of lateral veins (Fig. 6M, arrow lv).

Water transport properties of PtXIPs

To gain further insights into the function of *Pt*XIPs, cRNAs encoding the related proteins were transcribed *in vitro* and injected into *Xenopus* oocytes. After 2–3 d, oocytes were

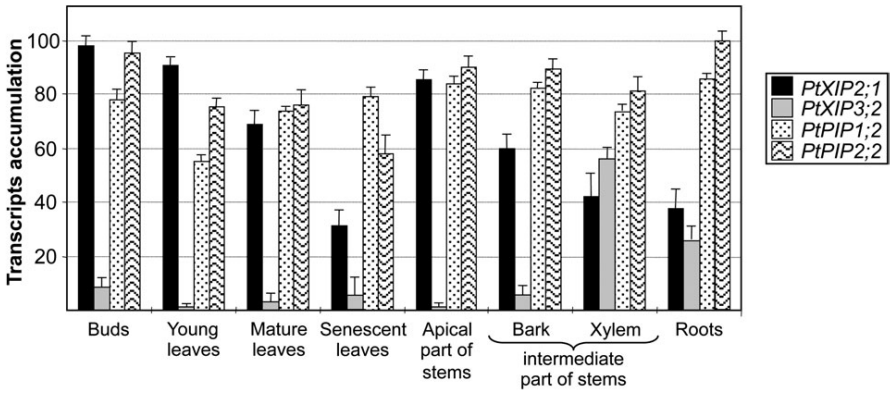

Fig. 4. Real-time quantitative RT-PCR analyses of the constitutive *PtXIP2;1* and *PtXIP3;2* transcript accumulation in vegetative tissues. The expression level of *PtActin 1*, *PtSAND*, and *PtTIP41-like* gene was used as the normalization internal control. *PtPIP1;2* and *PtPIP2;2* expression was followed for comparison purposes. Bars represent standard deviations of at least three technical repetitions from three independent biological experiments. Four plants were pooled for this biological analysis.

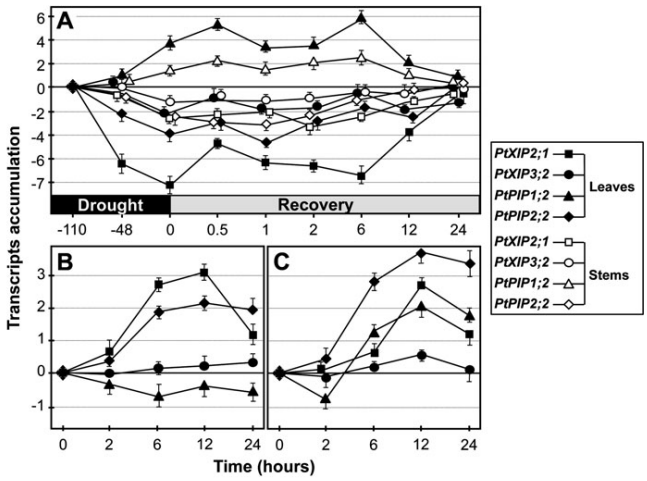

Fig. 5. Real-time quantitative RT-PCR analyses of *PtXIP2;1* and *PtXIP3;2* transcript accumulation kinetics in stress-challenged plants: (A) in leaves and intermediate parts of the stems during the drought stress time-course followed by recovery (re-watering noted at time 0), (B) in 1 mM SA-treated leaves, and (C) in wounded leaves. The expression level of *PtActin 1*, *PtSAND*, and *PtTIP41-like* genes was used as the normalization internal control. *PtPIP1;2* and *PtPIP2;2* genes were followed for comparison purposes. Bars represent the standard deviations of at least three technical repetitions from three independent biological experiments. Three plants were pooled per biological assay.

transferred into an hypo-osmotic solution and their osmotic water permeability (P_f) was deduced from the swelling kinetics of individual oocytes. Oocytes that did not receive any cRNA or that expressed the highly active aquaporin *Pt*PIP2;2 were taken as negative and positive controls, respectively. Figure 7 shows that whereas injection of *Pt*XIP1s, *Pt*XIP3;1, and *Pt*XIP3;2 cRNA did not induce any change in oocyte P_f, expression of *Pt*XIP2;1 and *Pt*XIP3;3 increased P_f by ~2.5-fold. In parallel experiments, oocytes expressing *Pt*PIP2;2 showed an even more pronounced (~8-fold) increase in P_f. The standard errors are very small because of the high number of cell replicates, which is much higher than in other similar studies. Checks were carried out to verify that similar results (i.e. enhanced P_f in *Pt*XIP2;1 oocytes) were obtained in several independent oocyte batches and cRNA preparations. The present data establish a significant water channel activity for *Pt*XIP2;1 and *Pt*XIP3;3 but not for *Pt*XIP1s, *Pt*XIP3;1, and *Pt*XIP3;2.

Discussion

XIP diversification in the light of angiosperm evolutionary expansion

To date, the comparison of XIP sequences from fungi and plant phyla has been limited to residues that constitute loops and ar/R selectivity filters, and to exon–intron organization (Gupta and Sankararamakrishnan, 2009). In this previous work, it was asserted that during evolution amino acids of the ar/R filter became more hydrophobic in dicot XIPs than in their homologues of fungi and moss. This could reflect a distinct spectrum of solutes transported by these XIPs, which would entail a notable evolutionary divergence between various living kingdoms. Although this previous study sketched interesting evolutionary features, it did not provide insights into the angiosperm taxon by itself which, however, encompasses the great majority of XIP members. By pointing to a notable sequence diversity in angiosperms, the present work highlights evolutionary dynamics of XIPs within this taxon. Without an *a priori* use of previously described XIP sequences, a new query against plant EST collections resulted in the retrieval of 55 putative XIP sequences. All came from a very wide range of flowering plants which, except for *Liriodendron*, were land dicotyledonous plants. Yet, the most striking observation lies in the relationship between the phylogenetic XIP distribution and the currently established phylogeny of angiosperms (Figs 1, 2). The present data emphasizes a prospective evolutionary scheme where XIP members clustered into at least five significantly distinct groups, including four which paralleled the divergence of angiosperm taxa. Although it is likely that the XIPs from angiosperms have originated from a common ancestral gene and have duplicated early after the emergence of this plant clade, it appears clearly that they have then substantially diverged into two clusters (XIP-A and XIP-B). The XIP-A (or XIP1) cluster might include the oldest angiosperm XIP sequences. Indeed, it encompasses the only sequences found in the early-diverging Magnoliales taxa. In core eudicots, except for a clade belonging to Rosanae (Fabibs) in which XIP1s are expressed, the XIP1 evolutionary pathway marks genes for silencing in all other clades. Furthermore, no XIP1 homologues appear in the Asteranae sister clade. As for the second XIP-B cluster, it represents the most interesting expanded subset, with at least four groups. As these groups are only found after core eudicot emergence, they may result from a more recent expansion compared with XIP-A. Thus, XIP2s and XIP3s are exclusively linked to the Rosanae superorder. XIP4s and XIP5s are represented exclusively in Asteranae plants. Finally, this discriminative organization contrasts with the homogenous PIP subfamily and the more heterogeneous NIP, TIP, and SIP subfamilies in which members do not spilt in such a plant taxa-classified manner.

Following gene duplication events, paralogous genes can take on different fates: this includes loss of some of paralogues, divergence and functional differentiation, or maintenance of partially overlapping functions (Conant and Wolfe, 2008). The various diversification scenarios displayed by the XIP subfamily offer a great opportunity to tackle four fundamental questions. (i) As XIP-A members showed a significant divergence and loss of expression in several core eudicots clades, would this branch be subject to loss of function over time? (ii) Would the XIP-B members be newly evolved sequences, suggesting specialized functions? (iii) Would natural selection pressure under *XIP* gene divergence ultimately be involved in speciation processes? (iv) Taken as a whole, despite the actual impossibility of

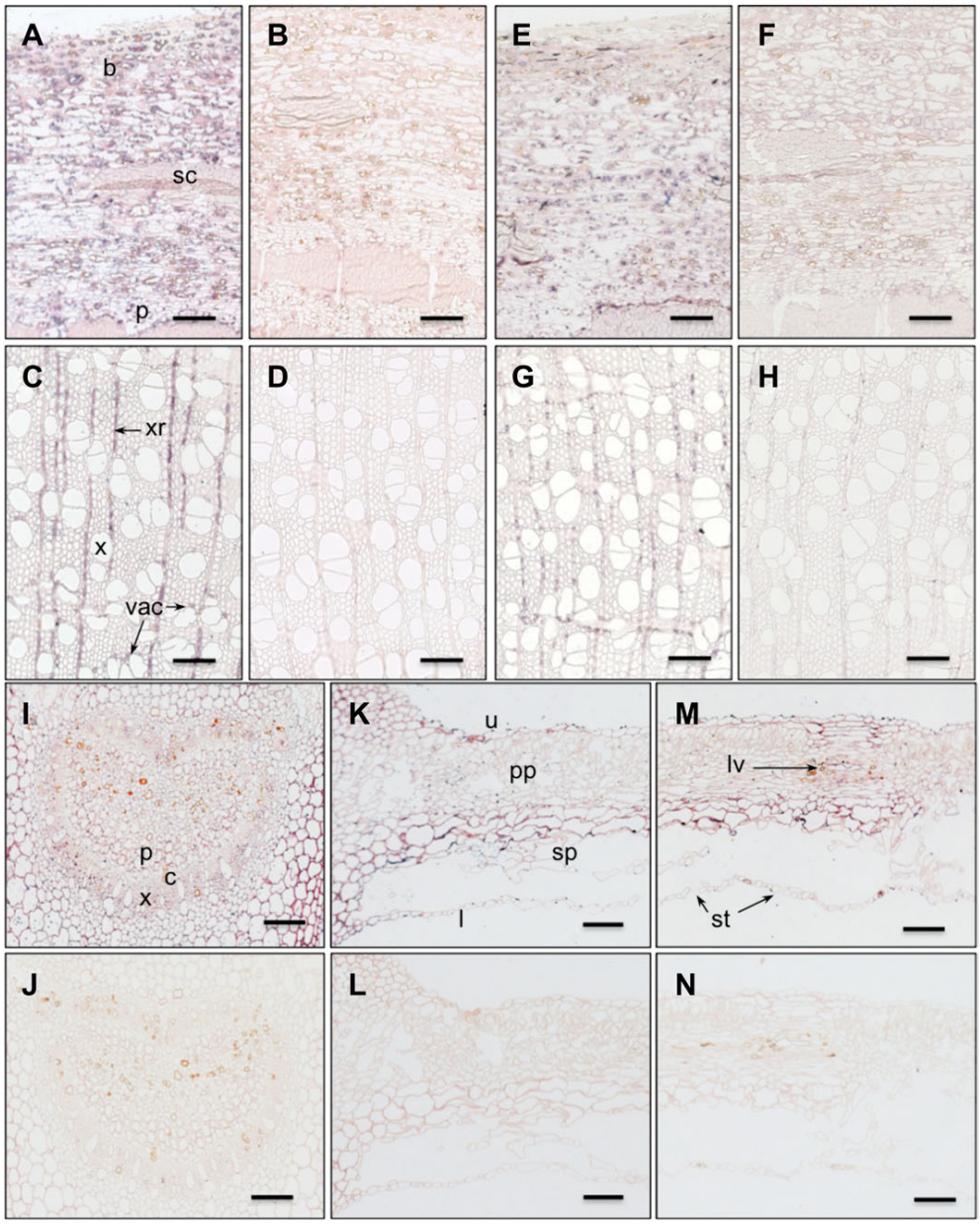

Fig. 6. *In situ* localization of *PtXIP2;1* mRNA in stems (A–D) and in leaves (I–N), and *PtXIP3;2* mRNA in stems (E–H). Methacrylate-embedded *Populus trichocarpa* transversal sections of leaf and stem sample hybridized with specific antisense probes (positive) A, C, E, G, I, K, M; or with sense probes as negative controls (B, D, F, H, J, L, N). b, bark; sc, sclerenchyma; p, phloem; c, cambium; x, xylem vessels; xr, xylem rays; vac, vessel-associated cells; u, upper epidermis; pp, palisade parenchyma; lv, lateral vein; sp, spongy parenchyma; st, stomata; l, lower epidermis. Positive hybridization signals are visualized by violet staining using a DIG-labelled RNA immunodetection system as described in the Material and methods. Arrows indicates alkaline phosphatase staining. Bar indicates 100 μm.

interpreting the presence of XIPs in numerous plant taxa which differ fundamentally (Judd *et al.*, 2002; Soltis *et al.*, 2004), could this unusual phylogenetic repartition be rationalized through some ecological and/or phenotypic explanations? Some of these questions will be answered once more extensive knowledge about ecological and phenotypic relationships, and larger genomic collections are available especially for plants belonging to early-diverging angiosperms and Asteranae.

The vastly expanded XIP subfamily is a unique feature of Populus *species*

Of the embryophytes analysed, poplar is unique in that is is the sequenced land plant that to date contains the highest amount and degree of diversity of XIP copies. The *P. trichocarpa* XIP subfamily (*Pt*XIPs) is composed of nine sequences: among which are six full-length coding sequences (CDS) [leaving aside two pseudogenes and one truncated

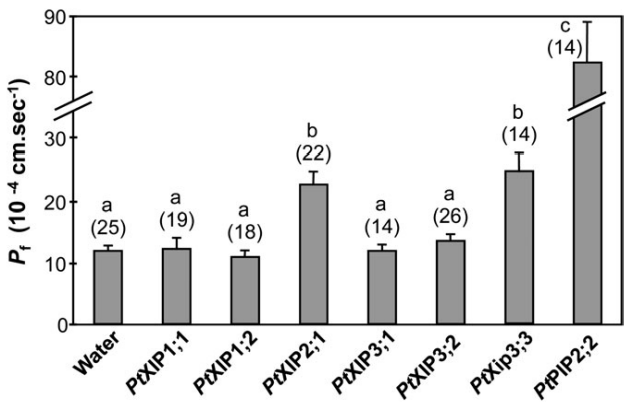

Fig. 7. Osmotic water permeability (P_f) of oocytes expressing aquaporin isoforms. P_f (± SE, with number of cells in parentheses) was measured in oocytes, injected either with water or with cRNAs encoding the indicated aquaporins. Data are from two representative experiments with different oocyte batches and cRNA preparations. Different letters above each bar represent statistically significant differences ($P < 0.05$; one-way ANOVA, Newman–Keuls test).

related product sequence (*Pt*XIP3;1b)]. A fine analysis of the *Pt*XIP subfamily indicated that its members have phylogeneticaly diverged into three branches: *Pt*XIP1 (*Pt*XIP1;1 and *Pt*XIP1;2), *Pt*XIP2 (*Pt*XIP2;1), and *Pt*XIP3 (*Pt*XIP3;1, *Pt*XIP3;2, and *Pt*XIP3;3).

An interesting outcome was revealed during AQP sequence compilation from the two JGI assembly versions: *Pt*XIPs present a significant degree of polymorphism, contrasting with other subfamilies that showed less variation (Supplementary Table S2 at *JXB* online). As previously observed, XIP loci may result from high haplotype variations (Kelleher *et al.*, 2007). Moreover, such amino acid substitutions can reveal potential adaptive evolutionary events, which generally come about with related pressure selection modalities (purifying, neutral, or positive/diversifying). Because the genetic code is redundant, any mutation may or may not be synonymous. Despite a limited number of *Populus* XIP-related ESTs (13 partial sequences phylogenetically homologous to *Pt*XIP2;1 and four partial sequences homologous to *Pt*XIP3;1), the ratio of non-synonymous versus synonymous substitutions was calculated ($\omega = dN/dS$) which is an indicator of the history of selection acting on a gene. Although expressed *Pt*XIPs had high ω values (*Pt*XIP2;1=0.42 and *Pt*XIP3;2=0.37) compared with *Pt*PIPs (*Pt*PIP1s=0.11 and *Pt*PIP2s=0.05), they remained <1. This suggests that in the course of their evolution, expressed *PtXIP* genes underwent a purifying pressure selection, thus illustrating their functional role in the *Populus* genus. A last argument in favour of such purifying pressure concerns the cluster organization of this XIP subfamily. Seven of the nine *Pt*XIP sequences are arranged head-to-tail on chromosome IX. Gene organization typically leads either to a tandem array of reiterated units (e.g. *PtPIP2;5*/*PtPIP2;6*) or to a cluster (such as *PtXIP* genes) when conversion and divergence events occurred (Graham 1995). Such a clustering feature is considered to facilitate the expansion in gene quantity through recombination, and may reflect an adaptive mechanism originating in genome-selective pressure and selection. However, following gene duplication events, paralogous genes can take on alternative fates (Conant and Wolfe, 2008). Within this *Pt*XIP cluster, the duplicated sequences *PtXIP3;1* (expressed in *P. tremula* and *P. tomentiglandulosa*) and *PtXIP3;1b* (non-expressed) are an interesting case study of formation of a gene family in which paralogous copies differentially evolved. Indeed, rather than an acquisition of new adaptive functions through 'positive' mutation (neo-/subfunctionalization), *PtXIP3;1b* may be incapacitated by the occurrence of a deleterious premature stop codon insertion (non-functionalization signature), and then becomes a functionless pseudogene.

A literature review highlights genetic redundancy as a salient feature of living organisms, and gene duplication events are considered as a primary driving force, providing raw material for evolutionary novelty (Taylor and Raes, 2004; Freeling, 2009; Kafri *et al.*, 2009). However, besides the evidence that overlapping functions between duplicate genes manifest as synthetic aggravating interactions between paralogues, they could lead to major repercussions on related steady-state mRNA and/or protein pools and potentially on the regulatory mechanisms controlling various physiological processes, with far-reaching phenotypic effects (Gu *et al.*, 2003; DeLuna *et al.*, 2008). In the light of these data, it is intuitive to note that high non-synonymous variations and major mutations such as premature stop codons may reflect a significant excess of polymorphisms that substantially affect XIP protein structure and function. In other words, this supports and extends these evolutionary results showing that the *Pt*XIP loci and the plant XIP subfamily as a whole could be under a strong selection force associated with duplication and significant differentiations.

PtXIP gene expression and related protein function assessments

Previous works have shown that, when over-represented in tandemly duplicated arrays, plant genes usually respond to environmental constraints (Hanada *et al.*, 2008). Despite poplar *XIP* divergence and expansion, the expressed *XIP* genes are under-represented in poplar databases, with only 17 ESTs, and because most sequences were isolated from pooled tissues no general conclusion could be drawn regarding their expression pattern. *XIP* expression was evaluated first using microarray databases available in public repositories (Gupta and Sankararamakrishnan, 2009). Although microarray methods provide an unprecedented capacity for whole genome profiling, their limits are well characterized, and accurate normalization through quantitative PCR (qPCR) remains a somewhat unavoidable step for obtaining reliable and conclusive results. This is particularly true for the Affymetrix poplar genome array with only five *XIP* genes represented and for which related probesets data should be interpreted with substantial precaution. Here, *XIP* expression was reappraised *in planta* using qPCR. In addition, ISH was performed to determine cell-specific *PtXIP* gene expression patterns. In accordance with expressed sequences

databases, only two members (*PtXIP2;1* and *PtXIP3;2*) were found to be expressed in *P. trichocarpa* 101-74. Surprisingly, they differ substantially from each other by their own accumulative patterns. *PtXIP2;1* was one of the most expressed poplar *MIP* genes. It was ubiquitously expressed in all vegetative tissues with a distinct developmental gradient. It peaked in leaves, with a marked cellular expression in vascular tissues, spongy parenchyma, and epidermis. To a lesser extent, *PtXIP2;1* accumulated in wood, was uniformly distributed in bark and phloem, but was absent in the cambial region where cells have not reached a high level of specialization. As regards *PtXIP3;2*, it preferentially exhibited transcript accumulation in wood, and, although sublocalized in all part of stems (vessel-associated cells, xylem rays, bark, and phloem), its expression reached a maximum in xylem. Similarly, *PtXIP2;1* and *PtXIP3;2* were also expressed differently in challenged plants, where *PtXIP2;1* showed the most contrasted transcript accumulation. A drastic down-regulation of *PtXIP2;1* expression was observed under severe drought stress, whereas *PtXIP2;1* was transiently up-regulated by SA and wounding. Furthermore, the oocyte expression experiments clearly revealed that *Pt*XIP2;1 promotes a significant water channel activity. Considering that the plasma membrane localization of Solanales XIP could be extrapolated to *Pt*XIP, these data may suggest different roles for XIPs in membrane transport at specific plant sublocalizations, and under stable or fluctuating environmental conditions. *Pt*XIP2;1 could play a leading role in this, and, as suggested for *Pt*PIPs and MIPs from various plant species (Heinen *et al.*, 2009; Secchi and Zwieniecki, 2010; Almeida-Rodriguez *et al.*, 2010; this study), *Pt*XIP2;1 can be reasonably considered as a physiological co-actor contributing to regulate the cellular osmotic equilibrium.

Whereas the oocyte expression experiments did not allow any definitive conclusion about the putative transport activity of *Pt*XIP1s, *Pt*XIP3;1, and *Pt*XIP3;2, this approach revealed a significant water permeability for *Pt*XIP2;1 and *Pt*XIP3;3. Previous studies have shown that several sequence regions within XIPs present notable differences compared with typical AQPs. Some of these concern substitutions in the ar/R selectivity filter, forming a quite hydrophobic pore environment predominantly allocated to the conduction of hydrophobic and bulky solutes (Bienert *et al.*, 2011). In the present assays and in line with its water transport functionality, only *Pt*XIP2;1 clearly differs in sequence from the other *Pt*XIPs, with a particular ar/R selectivity filter and canonical NPA boxes. This is also relevant comparing *Pt*XIP2;1 with XIPs of other land plants. A significant water channel activity for *Pt*XIP3;3 was also observed. This ability is quite puzzling as it was not possible to link it with any singular structural motif. Indeed, *Pt*XIP3;3 harboured ar/R residues and NPA motifs similar to those of*Pt*XIP1 and of other members of the *Pt*XIP3 clade for which no water transport capacity was observed. These observations suggested that the transport water ability of *Pt*XIP3;3 is not simply controlled by NPA motifs and the ar/R selectivity filter, and that other structural features could also be involved in this control. Further studies are needed to identify the residue(s) beyond those in the ar/R and NPA regions which are important for this water permeability. As for *Pt*XIP1s, *Pt*XIP3;1 and *Pt*XIP3;2 were apparently devoid of water transport, and they exhibited several ar/R residue similarities with Solanales XIPs which suggested probable common channel activities. Their solute specificity will have to be established.

To conclude, XIP-related data illustrate the potential transport of alternative solutes between members from an MIP subclass, suggesting differential but complementary functional specialization in plant environmental adaptive responses. To conclude definitively on the water and solute transport functions of *Pt*XIPs and their physiological relevance in a plant's life processes, suppression of *XIP* gene function will have to be addressed in future experiments. Moreover, further studies are needed to determine the role, if any, of structural motifs in *Pt*XIP-related functions and those involved in this XIP water permeability.

Supplementary data

Supplementary data are available at *JXB* online.

Figure S1. Phylogenetic trees of all the full-length members of the major membrane intrinsic AQP protein family of *Populus trichocarpa* cv. Nisqually.

Figure S2. Sequence alignment of all the full-length members of the major membrane intrinsic AQP protein family of *Populus trichocarpa* cv. Nisqually.

Figure S3. Protein sequence alignment of the 50 Viridiplantae XIPs.

Figure S4. *In situ* localization of *PoptrXIP3;2* mRNA in leaves.

Table S1. List of the non-redundant representative Viridiplantae *XIP* gene sequences used in this work.

Table S2. Excel spreadsheet of the *Populus trichocarpa* cv. Nisqually *MIP* gene family including all available genomic annotations from JGI.

Table S3. Primers used for qPCR, *in situ* hybridization, and oocyte experiments.

References

Agre P, Sasaki S, Chrispeels MJ. 1993. Aquaporins: a family of water channel proteins. *American Journal of Physiology* **265,** F461.

Almeida-Rodriguez A, Cooke JEK, Yeh F, Zwiazek JJ. 2010. Functional characterization of drought-responsive aquaporins in *Populus balsamifera* and *Populus simonii×balsamifera* clones with different drought resistance strategies. *Physiologia Plantarum* **140,** 321–333.

Altschul S, Madden T, Schaffer A, Zhang J, Zhang Z, Miller W, Lipman D. 1997. Gapped BLASt and PSI-BLAST: a new generation of protein database search programs. *Nucleic Acids Research* **25,** 3389–3401.

Beitz E, Wu B, Holm LM, Schultz JE, Zeuthen T. 2006. Point mutations in the aromatic/arginine region in aquaporin 1 allows

passage of urea, glycerol, ammonia, and protons. *Proceedings of the National Academy of Sciences, USA* **103,** 269–274.

Bienert GP, Bienert MD, Jahn TP, Boutry M, Chaumont F. 2011. *Solanaceae* XIPs are plasma membrane aquaporins that facilitate the transport of many uncharged substrates. *The Plant Journal* **66,** 306–317.

Chang S, Puryear J, Cairney J. 1993. A simple and efficient method for isolating RNA from pine trees. *Plant Molecular Biology Reporter* **11,** 113–116.

Chaumont F, Barrieu F, Wojcik E, Chrispeels MJ, Jung R. 2001. Aquaporins constitute a large and highly divergent protein family in maize. *Plant Physiology* **125,** 1206–1215.

Chaumont F, Moshelion M, Daniels MJ. 2005. Regulation of plant aquaporin activity. *Biology of the Cell* **97,** 749–764.

Chase MW, Reveal JL. 2009. A phylogenetic classification of the land plants to accompany APG III. *Botanical Journal of the Linnean Society* **161,** 122–127.

Chevenet F, Brun C, Banuls AL, Jacq B, Chisten R. 2006. TreeDyn: towards dynamic graphics and annotations for analyses of trees. *BMC Bioinformatics* **7,** 439.

Clamp M, Cuff J, Searle SM, Barton GJ. 2004. The Jalview Java alignment editor. *Bioinformatics* **20,** 426–427.

Conant GC, Wolfe KH. 2008. Turning a hobby into a job: how duplicated genes find new functions. *Nature Reviews Genetics* **9,** 938–950.

Czechowski T, Stitt M, Altmann T, Udvardi MK, Scheible WR. 2005. Genome-wide identification and testing of superior reference genes for transcript normalization in *Arabidopsis*. *Plant Physiology* **139,** 5–17.

Danielson JAH, Johanson U. 2008. Unexpected complexity of the aquaporin gene family in the moss *Physcomitrella patens*. *BMC Plant Biology* **8,** 45.

De Luna A, Vetsigian K, Shoresh N, *et al.* 2008. Exposing the fitness contribution of duplicated genes. *Nature Genetics* **40,** 676–681.

Engel A, Stahlberg H. 2002. Aquaglyceroporins: channel proteins with a conserved core, multiple functions, and variable surfaces. *International Review of Cytology* **215,** 75–104.

Freeling M. 2009. Bias in plant gene content following different sorts of duplication: tandem, whole-genome, segmental, or by transposition. *Annual Review of Plant Biology* **60,** 433–453.

Graham GJ. 1995. Tandem genes and clustered genes. *Journal of Theoretical Biology* **175,** 71–87.

Gu ZL, Steinmetz LM, Gu X, *et al.* 2003. Role of duplicate genes in genetic robustness against null mutations. *Nature* **421,** 63–66.

Guindon S, Gascuel O. 2003. A simple, fast, and accurate algorithm to estimate large phylogenies by maximum likelihood. *Systematic Biology* **52,** 696–704.

Gupta AB, Sankararamakrishnan R. 2009. Genome-wide analysis of major intrinsic proteins in the tree plant *Populus trichocarpa*: characterization of XIP subfamily of aquaporins from evolutionary perspective. *BMC Plant Biology* **20,** 134.

Gustavsson S, Lebrun A-S, Norden K, Chaumont F, Johanson U. 2005. A novel plant major intrinsic protein in *Physcomitrella patens* most similar to bacterial glycerol channels. *Plant Physiology* **139,** 287–295.

Hanada K, Zou C, Lehti-Shiu MD, Shinozaki K, Shiu SH. 2008. Importance of lineage-specific expansion of plant tandem duplicates in the adaptive response to environmental stimuli. *Plant Physiology* **148,** 993–1003.

Heinen RB, Ye Q, Chaumont F. 2009. Role of aquaporins in leaf physiology. *Journal of Experimental Botany* **60,** 2971–2985.

Johanson U, Karlsson M, Johansson I, Gustavsson S, Slovall S, Fraysse L, Weig AR, Kjellbom P. 2001. The complete set of genes encoding major intrinsic proteins in Arabidopsis provides a framework for a new nomenclature for major intrinsic proteins in plants. *Plant Physiology* **126,** 1358–1369.

Judd WS, Campbell CS, Kellogg EA, Stevens PF, Donoghue MJ. 2002. *Plant systematics: a phylogenetic approach*. Sunderland, MA: Sinauer Associates.

Kaldenhoff R, Fischer M. 2006. Functional aquaporin diversity in plants. *Biochimica and Biophysica Acta* **1758,** 1134–1141.

Kafri R, Springer M, Pilpel Y. 2009. Genetic redundancy: new tricks for old genes. *Cell* **136,** 389–392.

Kelleher CT, Chiu R, Shin H, *et al.* 2007. A physical map of the highly heterozygous *Populus* genome: integration with the genome sequence and genetic map and analysis of haplotype variation. *The Plant Journal* **50,** 1063–1078.

Kjellbom P, Larson C, Johansson I, Karlsson M, Johanson U. 1999. Aquaporins and water homeostasis in plants. *Trends in Plant Sciences* **4,** 308–314.

Leblanc-Fournier N, Coutand C, Crouzet J, Brunel N, Lenne C, Moulia B, Julien JL. 2008. Jr-ZFP2, encoding a Cys2/His2-type transcription factor, is involved in the early stages of the mechano-perception pathway and specifically expressed in mechanically stimulated tissues in woody plants. *Plant, Cell and Environment* **31,** 715–726.

Maurel C. 2007. Plant aquaporins: novel functions and regulation properties. *FEBS Letters* **581,** 2227–2236.

Maurel C, Reizer J, Schroeder JI, Chrispeels MJ. 1993. The vacuolar membrane protein γ-TIP creates water specific channels in *Xenopus* oocytes. *EMBO Journal* **12,** 2241–2247.

Maurel C, Santoni V, Luu DT, Wudick MM, Verdoucq L. 2009. The cellular dynamics of plant aquaporin expression and functions. *Current Opinion in Plant Biology* **12,** 690–698.

Mitani-Ueno N, Yamaji N, Zhao FJ, Ma JF. 2011. The aromatic/arginine selectivity filter of NIP aquaporins plays a critical role in substrate selectivity for silicon, boron, and arsenic. *Journal of Experimental Botany* **62,** 4391–4398.

Park W, Scheffler BE, Bauer PJ, Campbell BT. 2010. Identification of the family of aquaporin genes and their expression in upland cotton (*Gossypium hirsutum* L.). *BMC Plant Biology* **10,** 142.

Pfaffl MW. 2001. A new mathematical model for relative quantification in real-time RT-PCR. *Nucleic Acids Research* **29,** 2003–2007.

Pfaffl MW, Tichopad A, Prgomet C, Neuvians TP. 2004. Determination of stable housekeeping genes, differentially regulated target genes and sample integrity: *BestKeeper*—Excel-based tool using pair-wise correlations. *Biotechnology Letters* **26,** 509–515.

Rozen S, Skaletsky HJ. 2000. Primer3 on the WWW for general users and for biologist programmers. *Methods in Molecular Biology* **132,** 365–386.

Sade N, Vinocur BJ, Diber A, Shatil A, Ronen G, Nissan H, Wallach R, Karchi H, Moshelion M. 2009. Improving plant stress tolerance and yield production: is the tonoplast aquaporin SlTIP2;2 a key to isohydric to anisohydric conversion? *New Phytologist* **181,** 651–661.

Sakurai J, Ishikawa F, Yamlaguchi T, Uemura M, Maeshima M. 2005. Identification of 33 rice aquaporin genes and analysis of their expression and function. *Plant and Cell Physiology* **46,** 1568–1577.

Secchi F, Maciver B, Zeidel ML, Zwieniecki MA. 2009. Functional analysis of putative genes encoding the PIP2 water channel subfamily *Populus trichocarpa*. *Tree Physiology* **29,** 1467–1477.

Secchi F, Zwieniecki MA. 2010. Patterns of PIP gene expression in *Populus trichocarpa* during recovery from xylem embolism suggest a major role for the PIP1 aquaporin subfamily as moderators of refilling process. *Plant, Cell and Environment* **33,** 1285–1297.

Shelden MC, Howitt SM, Kaiser BN, Tyerman SD. 2009. Identification and functional characterization of aquaporins in the grapevine, *Vitis vinifera*. *Functional Plant Biology* **36,** 1065–1078.

Simossis VA, Heringa J. 2005. PRALINE: a multiple sequence alignment toolbox that integrates homology-extended and secondary structure information. *Nucleic Acids Research* **33,** W289–W294.

Soltis PS, Soltis DE, Chase MW, Endress PK, Crane PR. 2004. The diversification of flowering plants. In: Cracraft J, Donoghue MJ, eds. *The tree of life*. Oxford: Oxford University Press, 154–167.

Taylor JS, Raes J. 2004. Duplication and divergence: the evolution of new genes and old ideas. *Annual Review of Genetics* **38,** 615–643.

Tornroth-Horsefield S, Wang Y, Hedfalk K, Johanson U, Karlsson M, Tajkhorshid E, Neutze R, Kjellbom P. 2006. Structural mechanism of plant aquaporin gating. *Nature* **439,** 688–694.

Tuskan GA, DiFazio S, Jansson S, *et al.* 2006. The genome of black cottonwood, *Populus trichocarpa* (Torr. & Gray). *Science* **313,** 1596–1604.

Wallace IS, Roberts DM. 2004. Homology modelling of representative subfamilies of Arabidopsis major intrinsic proteins. Classification based on the aromatic/arginine selectivity filter. *Plant Physiology* **135,** 1059–1068.

Xu M, Zhang B, Su X, Zhang S, Huang M. 2011. Reference gene selection for quantitative real-time polymerase chain reaction in Populus. *Analytical Biochemistry* **408,** 337–339.

Supplemental Table S1. Selection of the non-redundant representative *Viridiplantae XIP* gene sequences used in this work

Plant organism	Protein Id	resource web
Aquilegia cærula	AcoGoldSmith_v1.018398m AcoGoldSmith_v1.020066m	Phytozome v7.0 Phytozome v7.0
Carica papaya	evm.model.supercontig_37.203 evm.model.supercontig_37.204	Phytozome v7.0 Phytozome v7.0
Casuarina glauca	CO038695	NCBI
Centaurea solstitialis	EH762170	NCBI
Cichorium endivia	EL356401	NCBI
Cichorium intybus	EH690282	NCBI
Citrus trifoliata	Contig CV704404 / CV704403	NCBI
Citrus sinensis	Contig CF838129 / CX049224	NCBI
Citrus clementina	Contig DY275505 / DY262747	NCBI
Coffea arabica	Contig CA00_XX_FB1_055_B03_JF.F / CA00_XX_FR2_085_D04_AC.F Contig CA00_XX_RM1_025_G11_UT.F / CA00_XX_RX1_097_B09_EB.F	Coffee Genome Project Coffee Genome Project
Cucumis sativus	cusca.169290	NCBI
Eucalyptus grandis	Egrandis_v1_0.019688m	Eucalyptusdb
Euphorbia esula	Contig DV129605 / DV132047	NCBI
Glycine max	Glyma11g10360.1 Glyma12g02640.1	Phytozome v7.0 Phytozome v7.0
Gossypium hirsutum	Contig DV849518 / CO092422	NCBI
Guizotia abyssinica	GE552915	NCBI
Helianthus argophyllus	EE625751	NCBI
Ipomoea nil	Contig CJ764230 / CJ745852 ADO66668	NCBI NCBI
Lactuca serriola	DW109345	NCBI
Liriodendron tulipifera	Contig DT600377 / FD501811	NCBI
Lotus japonicus	Contig GO005163 / GO019235	NCBI
Lycopersicon esculentum	SGN-U579905 SGN-U580338	Sol Genomics Network (NCBI) Sol Genomics Network (NCBI)
Mimulus guttatus	mgv1a009528m	Phytozome v7.0
Malus domestica	MDP0000163334 MDP0000171154	Genome Database for Rosacae Genome Database for Rosacae
Manihot esculenta	cassava4.1_012566m cassava4.1_029070m cassava4.1_028389m cassava4.1_031007m	Phytozome v7.0 Phytozome v7.0 Phytozome v7.0 Phytozome v7.0
Nicotiana tabacum	SGN_U495710 (FG645431)	Sol Genomics Network (NCBI)
Nicotiana benthamiana	SGN_U435101(ADO66675)	Sol Genomics Network (NCBI)
Nicotiana sylvestris	SGN_U512663 (ADO66676)	Sol Genomics Network (NCBI)
Petunia axillaris	FN015029	NCBI
Prunus persica	ppa025096m ppb013496m	Genome Database for Rosacae Genome Database for Rosacae
Solanum Tuberosum	ADO66669 SGN-U278472 (ADO66670)	NCBI Sol Genomics Network (NCBI)
Ricinus communis	28846.m000048 28846.m000049 28929.m000055 28747.m000131	Phytozome v7.0 Phytozome v7.0 Phytozome v7.0 Phytozome v7.0
Triphysaria pusilla	Contig EY137515 / EY137516	NCBI
Vitis vinifera	GSVIVT01024113001 GSVIVT01024115001	Genoscope Genoscope
Selaginella moellendorffii	DN837617 fgenesh2_pg.C_scaffold_1000216 e_gw1.1.90.1	NCBI Phytozome v7.0 Phytozome v7.0
Physcomitrella pattens	Pp1s31_73V6.1 Pp1s32_353V6.1	Phytozome v7.0 Phytozome v7.0

Coffee Genome Project	http://www.lge.ibi.unicamp.br/cafe/
Eucalyptusdb	http://eucalyptusdb.bi.up.ac.za/
Genome Database for Rosacae	http://www.rosaceae.org/
Genoscope	http://www.genoscope.cns.fr
NCBI	http://www.ncbi.nlm.nih.gov
Phytozome v7.0	http://www.phytozome.net
Sol Genomics Network	http://solgenomics.net

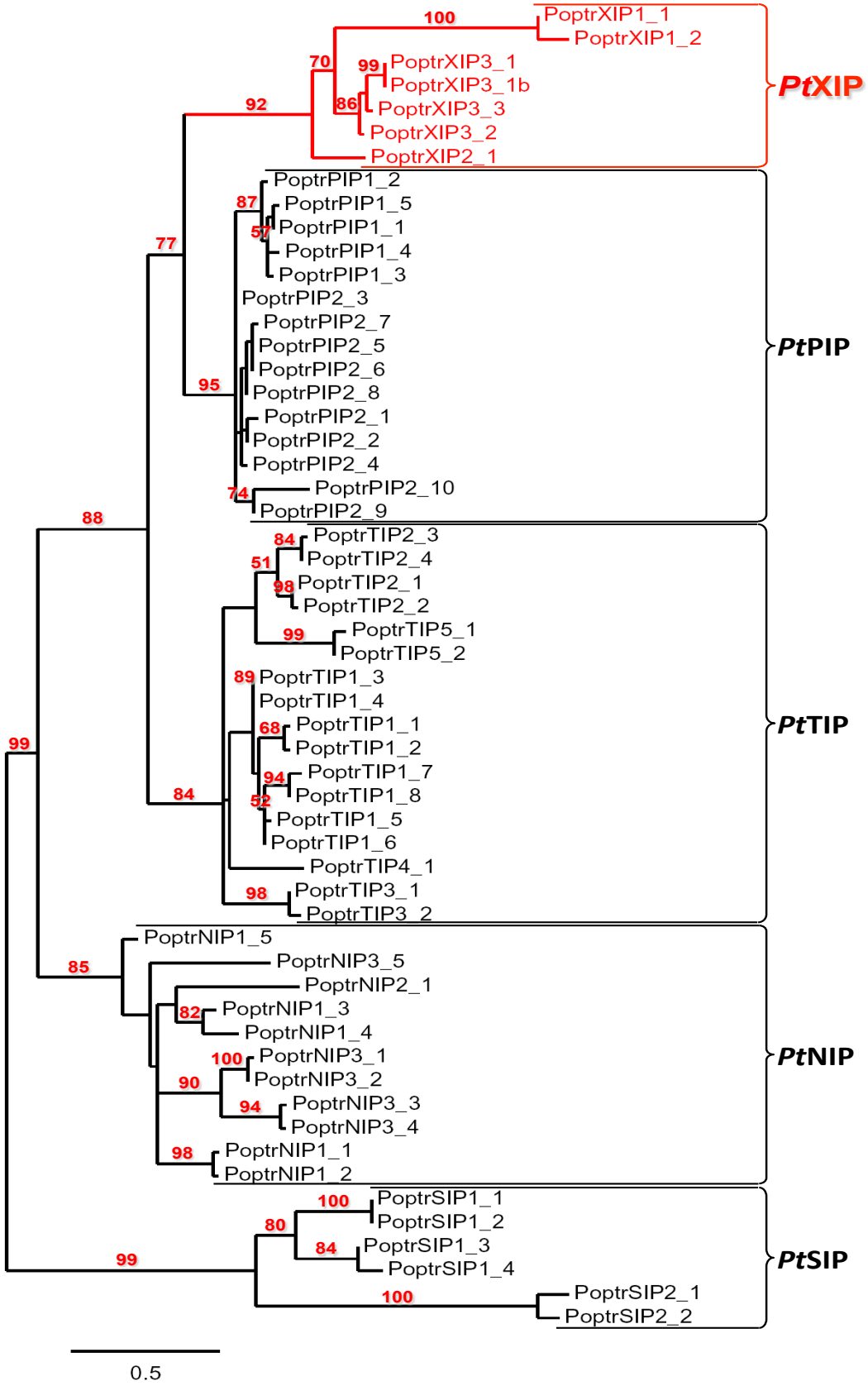

Supplemental Fig. S1. Phylogenetic trees of all Major membrane Intrinsic AQP Proteins family of *Populus trichocarpa cv.* nisqualy. Only the truncated sequence *PtXIP3;1b*-829126 was included in the analysis. Others truncated and pseudogenes related protein sequences were discarded of the analysis. The unrooted phylogeny of the XIP protein sequence was inferred using maximum likelihood. The tree was produced using PhyML with a genetic distance calculated by the JTT model of amino acids change. The numbers at the nodes represent percent of bootstrap values (above 50%) based on 1000 replicates.

Supplemental Fig. S2. Sequence alignment of the 55 full length aquaporins out of *Populus trichocarpa cv. nisqually*. Five sub-families are compared. The score reaches 34% sequence identity. XIP members show an interesting sequence insertion consisting in a slightly longer loop in between helix 3 and helix 4. To manage to do such a comparison PRALINE-PSI was used and involved a 5 psiblast iteration search (with an e-value cut-off of 0.01) within the non-redundant database. Jalview was used with the clustal-x color code to illustrate this result.

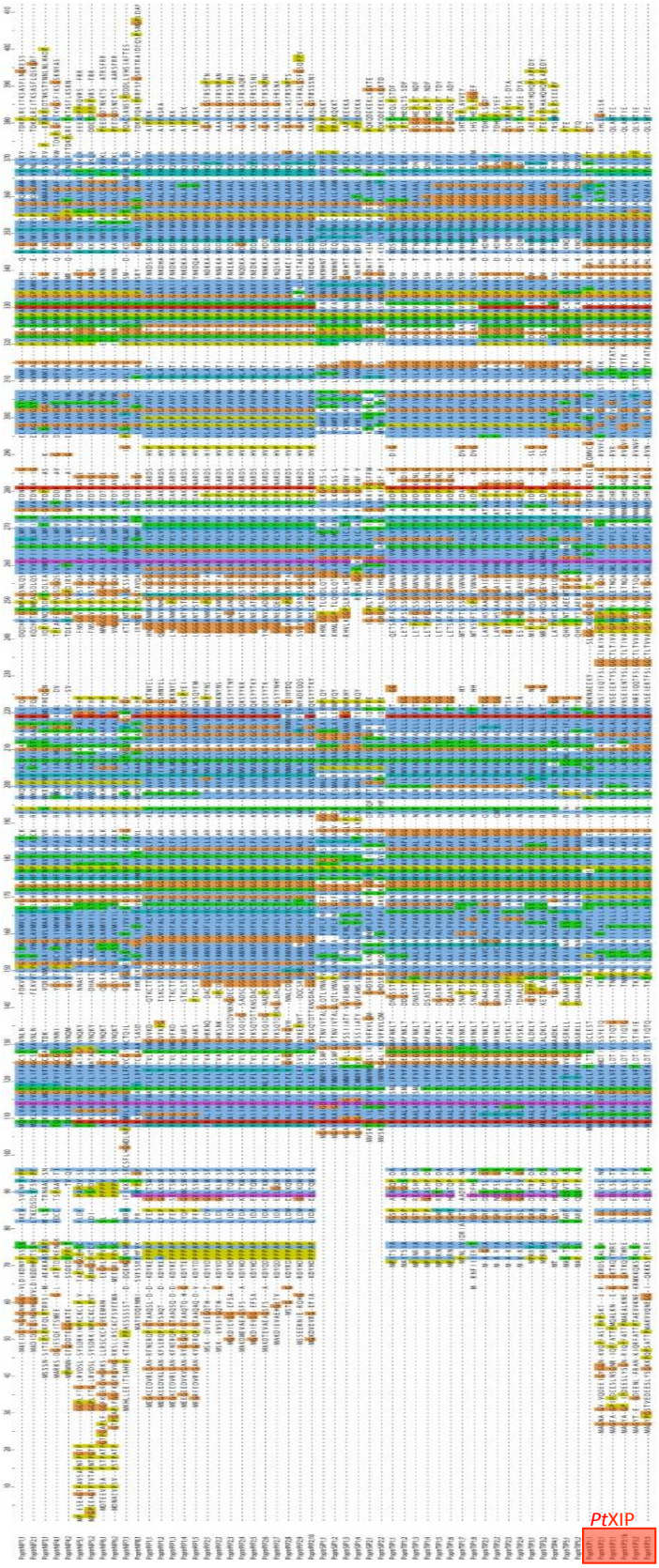

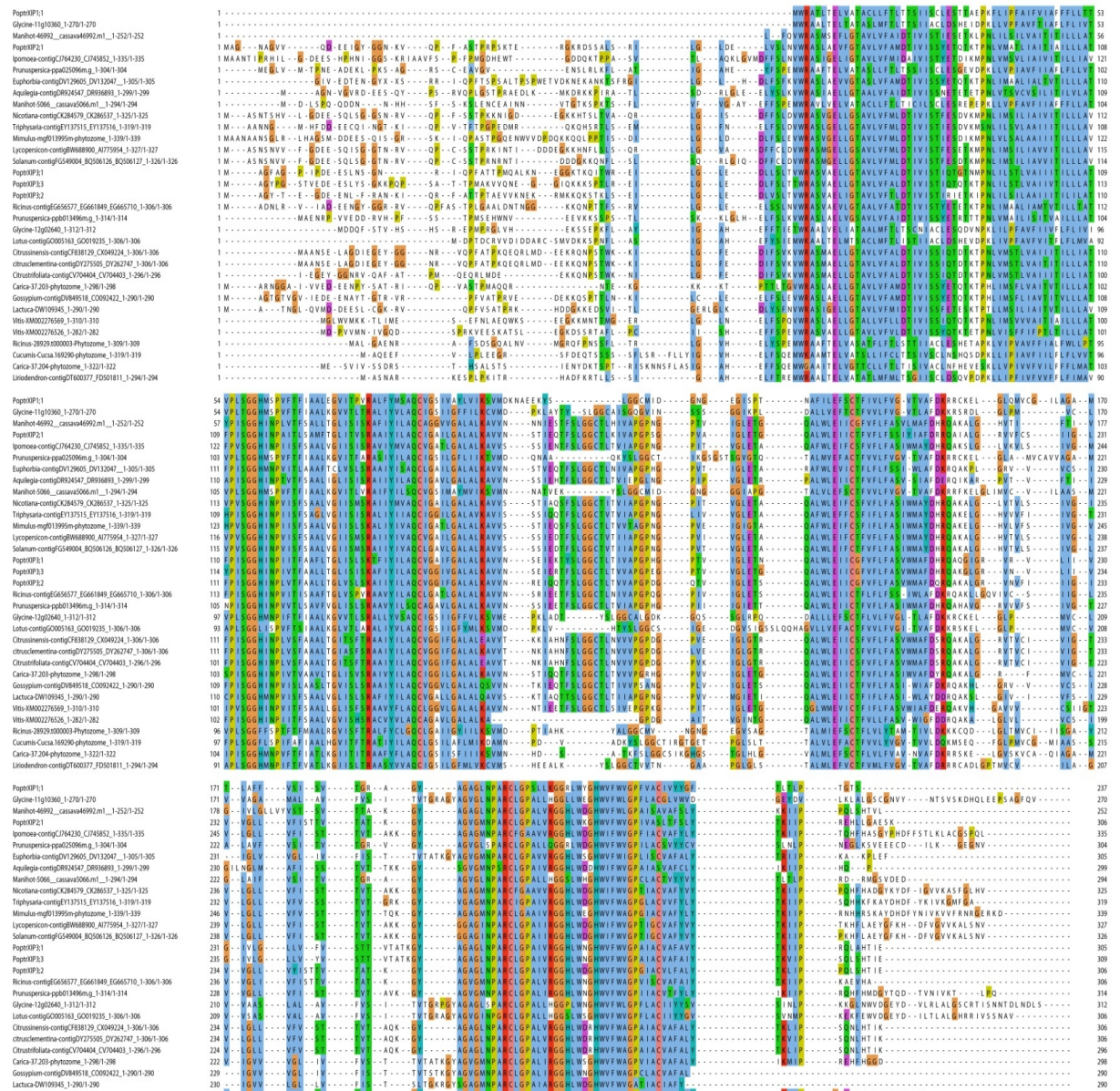

Supplemental Fig. S3. Sequence alignment of the XIPs from the Phylum of the Dicotyledons. The score reaches 49% sequence identity. Out of this sample of sequences few remarkable conserved motifs are highlighted and could constitute a hallmark to identify quickly more XIP members : for instance, both taken together -for the first so-called NPA motif- P-ψ-S/T-G-G-H/F-ψ-N/S-P-ψ/T and G-ψ-G-ψ-N/S-P-A/S-R-C-ψ -for the second NPA motif- (where ψ is typically an hydrophobic residue) seem a unique feature of the XIPs among the aquaporin family. Polymorphism is mostly found at the amino-terminal end of the protein. To manage to do such a comparison PRALINE-PSI was used and involved a 5 psiblast iteration search (with an e-value cut-off of 0.01) within the non-redundant database. Jalview was used with the clustal-x color code to illustrate this result.

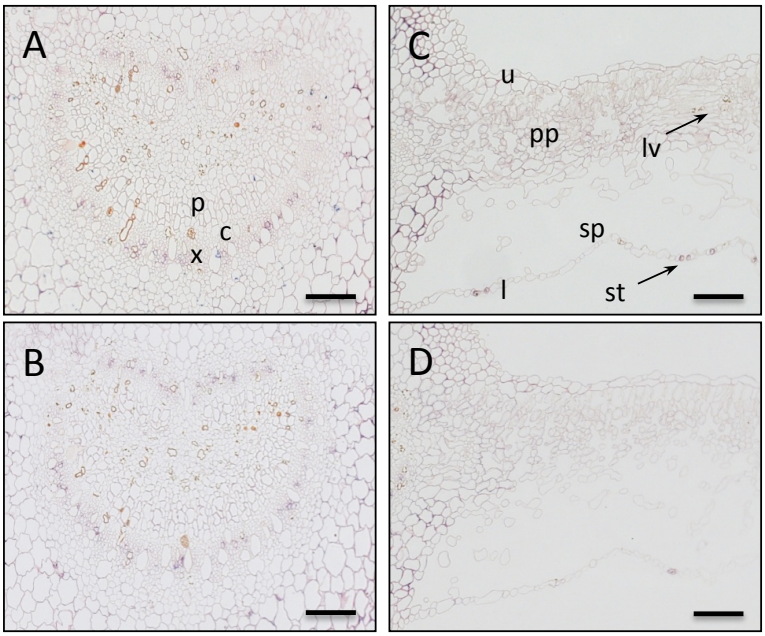

Supplemental Fig. S4. *In situ* localization of *Poptr*XIP3;2 mRNA in leaves (A to D)
Methacrylate-embedded *Populus trichocarpa* leaf samples transversal sections hybridized with specific antisense probes (positive) A and C ; or with sense probes as negative controls (B and D). p phloem; c cambium; x xylem vessels; u upper epidermis; pp palisade parenchyma; lv lateral vein; sp spongy parenchyma; st stomata; l lower epidermis. Positive hybridization signals are visualized by violet staining using a DIG-labeled RNA immunodetection system as described in material and methods. Arrows indicates alkaline phosphatase staining. Bar indicates 100 µm.

Supplemental Table S3. Primers used for qPCR amplification, *in situ* hybridization and oocytes experiments

Primers used for the gene expression study using quantitative polymerase chain reaction (qPCR) reaction

	Locus name [JGIv2.2]	**Primer sequences** [5' to 3' ; Forward / Reverse]	**Amplicon length**
PtActine 1	POPTR_0001s31700	GAAGTGCTTCTAAGTTCTACAAG / CTCAATAAATTCTCCATATCAACC	120 pb
PtSAND	POPTR_0009s01980	CATGATAAAGGCAACGGGGCG / CTGTGTTACAAGATATTTTTGGG	118 pb
PtTIP41-like	POPTR_0001s30580	TAGTGATAGTGCAAATCCTGTCA / CTTACAAGTTACTGTGGACCAC	178 pb
PtXIP2;1	POPTR_0009s13110	ATGATTCCACGGGAACACCT / CATCCCCCTTAACTACATAAC	141 pb
PtXIP3;2	POPTR_0009s13070	CACAATAGAATAGACTAAAACTAT / AGTTAAGGACGACGACTCTACATC	156 pb
PtPIP1;2	POPTR_0008s06580	CAAGAAGTGATGATTGTGATGC / ACGTCACTGTTATAGCACGC	144 pb
PtPIP2;2	POPTR_0004s18240	CAACCCCGCCAACTAAAGAGG / GTGACGGAGTGAGTAAAAGAGTG	105 pb

Primers used for the *XIP* transcript tissues location using *in situ* hybridization experiment

	Primer sequences [5' to 3' ; Forward / Reverse]	**Amplicon length**
***Pt*XIP2;1**	GGTTGGGCCTGTAGTTGCCA / GCAACAAGCAACGAGTTATTAATAAA	229 pb
***Pt*XIP3;2**	CACAATAGAATAGACTAAAACTAT / CTAACTGCTTGCATGGCTTCAA	206 pb

Primers used for the XIP protein function assay using *Xenopus leavis* oocytes system

***Pt*XIP1;1**	CGTGTGCCTTCATTTTTCCAGATGTGG / CATCTCCCCTCATCATGACGTCC
***Pt*XIP1;2**	TTCCAGATATGGAGGGCAACCCC / GTAGGCAAGGTCAGGGTGAATCT
***Pt*XIP2;1**	GAAGTGCTTCTAAGTTCTACAAG / SP6 primer
***Pt*XIP3;1**	GAGTTCAAAGAGGAGACATGCAAA / ATGGTGATCTTATTACATCAATCG
***Pt*XIP3;2**	CGATATCCAGATCTCTGGCTG / CATATTATTACTAGTCCACTC
***Pt*XIP3;3**	GGAGCCTTGAAAACATACGAAAACG / CAAACTTGAACATAACTTTATGCCC
***Pt*PIP2;2**	ACACAGTTACAAGCCGAGAGAG / GTGACGGAGTGAGTAAAAGAGTGAAG

Supplemental Table S2. *MIPs* gene family in *Populus trichocarpa* cv. Nisqualy

Putative subfamily[a]	Nomenclature used for this paper[b]	ProteinID DbXref JGI[c]	JGI v2.2 annotation of the v2 assembly name[c]	Scaffold position	JGI v1.1 annotation JGI sequence name[c]	JGI v2.2 annotation Amino-acids sequence	JGI v1.1 annotation Amino-acids sequence
XIP	***Poptr*XIP1;1**	557138	POPTR_0009s13090	10508627 - 10509502	eugene3.00090398	MWRATLTELVATACLLFTLT	MWRATLTELVATTLTTCLL
	***Poptr*XIP1;2**	nd	POPTR_0009s13105	10524036 - 10525007	nd	MMIWRATPTELVATTLT	nd
	***Poptr*XIP2;1**	821124	POPTR_0009s13110	10526083 - 10527458	estExt_fgenesh4_pg.C_LG_IX0381	MAGNAGVVQDEEIGYGGN	MAGNAGVVQDEEIGYGGN
	Poptr*XIP3;1	557139	POPTR_0009s13080	10505897 - 10507454	eugene3.00090399	MAGFAGPIPDEESLNSGNI	MAGYAGLIPDEESLYSGNI
	***Poptr*XIP3;2**	767334	POPTR_0009s13070	10499641 - 10500432	fgenesh4_pg.C_LG_IX000385	MAGYTEGDEENLFRANKI	-
	***Poptr*XIP3;3**	759781	POPTR_0004s17430	17627914 - 17629082	fgenesh4_pg.C_LG_IV001409	MAGYPGSTVEDEESLYSG	MAGYPGSTVEDEESLYSG
	Poptr*XIP3.1b	829126	POPTR_0009s13100	10522189 - 10523510	estExt_fgenesh4_pg.C_36020001	MAG#YAGPIPDEESLYSGN	MAG#AGPIPDEESLYSGN
	***Poptr*XIP-579750**	579750	POPTR_1606s00200	1555 - 1855	eugene3.111150001	MPSIPRELKLGSASQDQHI	-
	***Poptr*XIP-nd**	nd	nd	10525867 - 10526066	nd	*HAQQAGRAPQHPRELEL	nd
PIP1	***Poptr*PIP1;1**	724520	POPTR_0010s19930	17692707 - 17694253	estExt_Genewise1_v1.C_LG_X1818	MEGKEEDVRLGANKFNEF	-
	***Poptr*PIP1;2**	656216	POPTR_0008s06580	3917339 - 3918994	grail3.0049030302	MEGKEEDVRLGANRFNEF	-
	***Poptr*PIP1;3**	711735	POPTR_0003s12870	13317757 - 13320631	estExt_Genewise1_v1.C_LG_III0271	MEGKEEDVKLGANKFSER	-
	***Poptr*PIP1;4**	831918	POPTR_0006s09920	7347864 - 7349618	estExt_fgenesh4_pm.C_LG_VI0336	MEEGEEDVKVGANRYGE	-
	***Poptr*PIP1;5**	835561	POPTR_0016s12070	11340137 - 11341291	estExt_fgenesh4_pm.C_LG_XVI0408	MEGREEDVRVGANKYGE	MEGREEDVRVGANKYGE
	***Poptr*PIP1**	417298	POPTR_0006s09910	7330105 - 7330477	gw1.VI.1671.1	MEGREEDARVGQNRYRE	-
PIP2	***Poptr*PIP2;1**	821084	POPTR_0009s13890	10978294 - 10980012	estExt_fgenesh4_pg.C_LG_IX0306	MSKDVIEEGQTHTKDYVD	-
	***Poptr*PIP2;2**	648808	POPTR_0004s18240	18205023 - 18206765	grail3.0045020302	MSKEVSEVGQTHGKDYVD	-
	***Poptr*PIP2;3**	567607	POPTR_0010s22950	19653002 - 19656217	eugene3.00102165	MAKDMEVAEAGSFSAKDY	-
	***Poptr*PIP2;4**	563742	POPTR_0008s03950	2177146 - 2180969	eugene3.00080337	MAKDTEVAEAGSFSAKDY	-
	***Poptr*PIP2;5**	826419	POPTR_0006s12980	10229864 - 10231351	estExt_fgenesh4_pg.C_280159	MGKDIEVGGEFSAKDYHD	-
	***Poptr*PIP2;6**	-	POPTR_0006s13000	10235527 - 10237354	-	MGKDVEVRGEFIAKDYHD	-
	***Poptr*PIP2;7**	735495	POPTR_0016s09090	6990270 - 6992229	estExt_Genewise1_v1.C_LG_XVI2799	MGKDIEVGGEFSAKDYHD	-
	***Poptr*PIP2;8**	821627	POPTR_0009s01940	2408174 - 2409914	estExt_fgenesh4_pg.C_LG_IX1411	MAKDIEVAEHGETVKDYQ	-
	***Poptr*PIP2;9**	836572	POPTR_0005s11110	8046008 - 8048999	estExt_fgenesh4_pm.C_570016	MSTGGKDYRDPPPAPLLD	-
	***Poptr*PIP2;10**	796664	POPTR_0005s11100	8041914 - 8043619	fgenesh4_pg.C_scaffold_57000043	MSSEERNIERQHGRDYHD	-
	***Poptr*PIP2**	206485	scaffold_5	24506012 - 24506927	gw1.V.1886.1	nd	WSFYRAITANLICIXFSSSV
TIP	***Poptr*TIP1;1**	549212	POPTR_0001s24200	23556947 - 23558126	eugene3.00011653	MPITSIAFGSPAEAGQPDA	-
	***Poptr*TIP1;2**	833283	POPTR_0009s03230	3921492 - 3922937	estExt_fgenesh4_pm.C_LG_IX0624	MAITSIAFGSPAEVGQSDA	-
	***Poptr*TIP1;3**	822504	POPTR_0010s21700	18878920 - 18880497	estExt_fgenesh4_pg.C_LG_X1886	MPINRIAFGTPREASHPDA	-
	***Poptr*TIP1;4**	656044	POPTR_0008s05050	2933717 - 2935006	grail3.0049017002	MPINRIAVGTPGEASHPDS	-
	***Poptr*TIP1;5**	667870	POPTR_0016s10780	9145049 - 9146358	grail3.0025002201	MPIRNIAVGHYRETTQPDA	-
	***Poptr*TIP1;6**	589502	POPTR_0006s12350	9512816 - 9514266	eugene3.00280238	MPIRNIAVGHYHEATQPDA	-
	***Poptr*TIP1;7**	558321	POPTR_0009s01070	1207538 - 1208555	eugene3.00091581	MPNLIVIDRIAIGTVAADFH	MPNLIVIDRIAIGTVAADFH
	***Poptr*TIP1;8**	828458	POPTR_0004s22600	21469032 - 21470077	estExt_fgenesh4_pg.C_1630021	MRNFIIIERITIGRVEDDFHS	-
	***Poptr*TIP2;1**	548890	POPTR_0001s18730	15867375 - 15869029	eugene3.00011331/grail3.7684000101	MAGIAFGRFDDSFSLGSFH	-
	***Poptr*TIP2;2**	645978	POPTR_0003s04930	6025673 - 6027262	grail3.0037015101	MARIAFGRFNDSFSLGSLK	-
	***Poptr*TIP2;3**	817166	POPTR_0003s07550	9120443 - 9122482	estExt_fgenesh4_pg.C_LG_III0571	MAKIAFGSLGDSFSLASIK	MAKIAFGSLGDSFSLASLK
	***Poptr*TIP2;4**	676397	POPTR_0001s15700	12514892 - 12516210	grail3.0029005501	MVKIAFGSLGDSFSVGSLK	-
	***Poptr*TIP3;1**	584517	POPTR_0018s14910	14923713 - 14925022	eugene3.01640006	MPRRYAFGKADEATRPDA	-
	***Poptr*TIP3;2**	811826	POPTR_0017s03540	2567193 - 2568238	fgenesh4_pm.C_scaffold_184000008	MPRRHAFGRADEATHPDS	-
	***Poptr*TIP4;1**	561759	POPTR_0006s25620	23994648 - 23996456	eugene3.00061718	MTKIALGSRHEAAQPDCLH	-
	Poptr*TIP5;1	414059	POPTR_0003s10800	11684799 - 11686082	gw1.III.1162.1	MASTSLTARFKQSVTPASL	-
	Poptr*TIP5;2	423803	POPTR_0001s00690	571477 - 572852	gw1.29.315.1	MAPTSLTARFQQSVTPASL	-
	***Poptr*TIP**	562841	POPTR_0007s07950	6443104 - 6443436	eugene3.00070779	MKNVVVGHCHEATRLDAL	MKNVVVGHYHEATRLDAL
	***Poptr*TIP**	567478	POPTR_0010s21700	18878281 - 18878590	eugene3.00102036	MRKSNFTSKSHLTMLELVS	-
NIP	***Poptr*NIP1;1***	197507	POPTR_0004s06160	4879260 - 4881826	gw1.IV.2596.1	MAEIDGTNGNGNHGGVVI	-
	Poptr*NIP1;2	235172	POPTR_0011s06770	7424915 - 7426964	gw1.XI.3152.1	MADIDGTGSNGNHGGVVL	-
	***Poptr*NIP1;3**	566501	POPTR_0010s12330	12362213 - 12363646	eugene3.00101059	MPWNNEFGDDTEGGKKT	-
	***Poptr*NIP1;4**	756079	POPTR_0017s03060	2220350 - 2222392	fgenesh4_pg.C_LG_II002259	MARKSDGIESQEITSMEEG	-
	***Poptr*NIP1;5**	754717	POPTR_0002s09740	6977811 - 6979557	fgenesh4_pg.C_LG_II000897	MSSSNSITEPSPKFQLPTR	-
	***Poptr*NIP2;1**	577637	POPTR_0017s11960	12049497 - 12052785	eugene3.00170379	MATVDQEMNISVESSRFH	-
	***Poptr*NIP3;1**	757987	POPTR_0003s17930	17164650 - 17167051	fgenesh4_pg.C_LG_III001529	MDNAEVPSVPSTPATPGTI	-
	***Poptr*NIP3;2**	797136	POPTR_0001s14850	11665838 - 11668761	fgenesh4_pm.C_LG_I000139	MDTEEVPSAPSTPATPGTI	MDNEEVPSAPSTPATPGT
	***Poptr*NIP3;3**	708017	POPTR_0001s45920	46424317 - 46429237	estExt_Genewise1_v1.C_LG_I5715	MPESEAGTPAVSAPNTPG	-
	***Poptr*NIP3;4**	823094	POPTR_0011s14990	17199025 - 17201090	estExt_fgenesh4_pg.C_LG_XI1253	MPGPEEAGTPTVTAPNTP	-
	***Poptr*NIP3;5**	803915	POPTR_0008s20750	14728756 - 14731183	fgenesh4_pm.C_LG_VIII000870	MKHLLEEITSAHVPKTAVLF	-
	***Poptr*NIP**	263239	POPTR_0011s06770	7425042 - 7425881	gw1.10499.5.1 (1605 pb)	nd	AAGTIRLIFQGKQDHFTGT
	***Poptr*NIP**	590872	*Ralstonia metallidurans*	Genbank ABF12564.1	eugene3.33970001	-	-
SIP	***Poptr*SIP1;1**	729942	POPTR_0013s05030	3548929 - 3551903	estExt_Genewise1_v1.C_LG_XIII1897	MGAVKAAIGDAVFTFMWV	MGAVKAAIGDAVFTFMWV
	***Poptr*SIP1;2**	665418	POPTR_0019s04640	4809520 - 4813983	grail3.0065000501	MGAIKAASGDAVLTFMWV	-
	***Poptr*SIP1;3**	755885	POPTR_0002s21410	17878246 - 17879218	fgenesh4_pg.C_LG_II002065	MGAIKGAIVDGILTAMWVF	MGAIKGAIVDGILTAMWVF
	***Poptr*SIP1;4**	572968	POPTR_0014s15250	11321732 - 11322456	eugene3.00141013	MGAIKGAIVDGILTCMWVF	MGAIKGAIVDGILTCMWVF
	***Poptr*SIP2;1**	734665	POPTR_0016s02560	1263110 - 1265592	estExt_Genewise1_v1.C_LG_XVI1012	MVSKTRLILSDFVVSLMWV	-
	***Poptr*SIP2;2**	652505	POPTR_0006s02800	1769199 - 1771278	grail3.0024017601	MVSKTRLIVSDFIVSIIWVV	-
	***Poptr*SIP**	587423	scaffold_35	81619 - 81798	eugene3.02120008	MNTPNNRLCFNFNQPTTS	-

[a] According to literature nomenclature

[b] PoptrXIP: revisited classification by authors according data from the study ; PoptrPIP: according to Secchi *et al*. classification's ;
PoptrNIP, PoptrTIP and PoptrSIP: according to Gupta et al. classification's

[c] Protein ID number and JGI sequence name according to JGI database v1.1 *(Populus trichocarpa* v1.1 annotation of the v1.1 assembly)

Cell shaded in red predicted putative pseudogene or related truncated protein product

Cell shaded in green predicted putative splicing variant : Dark green splicing variant validated with Populus EST ;
Light green splicing variant no validated with Populus EST

Cell shaded in yellow predicted a sequence from JGI v1.1 annotation of the v1 assembly now assigned to a linkage group in the JGI v2.2 annotation of v2.2 assembly

- : Sequence 100% similar between JGI database v1.1 and v2.2

* Sequences longer than those presented in the JGI database, to which an extension in N- and C-terminus has been predicted because of their similarity to
Populus EST collections and full-lenght counterpart, and Arabidopsis sequences.

stop codon emplacement

Annexe 3

Modulation de la survie du bourgeon chez *Populus nigra* en réponse à l'embolie induite par le stress hydrique

Modulation of bud survival in *Populus nigra* sprouts in response to water stress-induced embolism

TETE SEVERIEN BARIGAH[1,2*a], MARC BONHOMME[1,2a], **DAVID LOPEZ[1,2]**, AMIDOU TRAORE[3], MARIE DOURIS[1,2], JEAN-STEPHANE VENISSE[1,2], HERVE COCHARD[1,2] and ERIC BADEL[1,2a]

[1] INRA, UMR547 PIAF, F-63100 Clermont-Ferrand, France
[2] Clermont Université, Université Blaise-Pascal, UMR547 PIAF, BP 10448, F-63000 Clermont-Ferrand, France
[3] INRA, UR 0370 QuaPA, F-63122 Saint-Genès-Champanelle, France

[a] These authors contributed equally to the work
* Corresponding author: Têtè Sévérien BARIGAH
Email address: tete.barigah@clermont.inra.fr
INRA PIAF, 5 chemin de Beaulieu, 63039 Clermont-Ferrand Cedex 02, France
Tel: + 33.4.73.62.44.72 - Fax: + 33.4.73.62.44.54

Running head: BUD SURVIVAL DURING WATER STRESS-INDUCED EMBOLISM

Summary

Understanding drought tolerance mechanisms requires knowledge about the induced weakness that leads to tree death. Bud survival is vital to sustain tree growth across seasons. We hypothesized that the hydraulic connection of the bud to stem xylem structures was critical for its survival. During an artificial drastic water stress, we carried out a census of bud metabolic activity of young *Populus nigra* trees by microcalorimetry. We monitored transcript expression of aquaporins (AQP; PIPs, XIPs and TIPs) and measured local water status within the bud and tissues in the bearer shoot node by nuclear magnetic resonance (NMR) imaging. We found that bud respiration rate was closely correlated to its water content and decreased concomitantly in buds and their surrounding bearer tissues. At the molecular level, we observed modulation patterns of aquaporins (PIP, TIP and XIP subfamilies) linked

to water movements in living cells. However, aquaporin functions remain to be investigated. Both bud and tree died beyond a threshold water content and respiration rate. NMR images provided relevant local information about the various water reservoirs of the stem, their dynamics and their interconnections. Comparison of pith, xylem and cambium tissues showed that the hydraulic connection between the bud and saturated parenchyma cells around the pith allowed the bud to stay wet for a long time. At the tree death date, NMR images showed that the cambium tissues remained largely hydrated. Overall, respiration rate (Rco_2) and a few aquaporins isoforms were found to be two suitable, complementary criteria to assess bud metabolic activity and ability to survive a severe drought spell. Bud moisture content could be a key factor in determining the capacity of poplar to recover from water stress.

Introduction

Global climate changes are expected to exacerbate the negative effects of water deficiency by increasing temperatures worldwide and changing rainfall patterns (IPCC 2007). Among predicted effects, increasing frequency and intensity of extreme climatic events such as drought are expected to impact trees and forests. Drought stress leads to numerous physiological effects on several traits related to water transport in trees, such as stomatal behaviour (Sperry et al. 1998; Hacke 2000; Domec et al. 2006), photosynthetic capacity (Brodribb and Feild 2000), turgor loss point of leaf cells (Alder et al. 1996; Brodribb et al. 2003) and water transport efficiency of the xylem (Tyree and Zimmermann 2002; Holbrook and Zwieniecki 2005). Because of the tensions under which it operates, the xylem is potentially sensitive to water deficit and the danger of cavitation. Xylem cavitation is a physical phenomenon that causes to the embolism of the hydraulic system. Xylem conduits become air-filled and lose their functionality in water conduction conduits (Sperry et al. 1996; Tyree and Zimmermann 2002). As a direct consequence, the hydraulic system can no longer supply water properly to leaves and other tissues, including the meristematic zones. Within these zones, aquaporins may play major roles in cell membrane regulation of water permeability (Kaldenhoff et al. 2008).

Temperate trees develop terminal and axillary buds during the summer to protect the meristematic zone and leaf primordia against unfavourable winter conditions and allow the production of new shoots in spring. The success of new organ development depends on the firm establishment of efficient pathways for the supply of carbon, water and mineral nutrients which are delivered to the growing tissues through the phloem and xylem (Wardlaw 1990). The production of such structures is controlled by growth regulators (Ye 2002).

Consequently, any adverse factor that impairs bud vitality may be life-threatening for the tree.

Bud break quality is strongly dependent on the previous year's environmental conditions (Herter et al. 1988; Escobedo and Crabbe 1989; Egea and Burgos 1994; Cook and Jacobs 2000). Thus drought stress, which affects the development of buds may impact their survival capacity (Marks 1975; Lavender 1991). Brodribb and Cochard (2009) demonstrate the major roles that stem and leaf hydraulics play in determining the drought tolerance of conifers, but they did not consider the fate of buds during and after water deprivation. Bud connections with the xylem network have rarely been addressed in trees and hydraulic conductance data at the base of buds are limited. A recent study on *Fagus sylvatica* showed a positive correlation between the number of leaf primordia in the bud before budburst and the hydraulic conductance of the xylem vascular system connected to this bud (Cochard et al. 2005) without establishing the nature of the bud water feeding pathway. We still lack detailed information on how the buds are supplied with minerals and water from the bearer stem and on the impact of drought on bud survival.

Although buds are fed through connections with the stem, they are generally considered as relatively independent appendages because their vascular connections to the xylem are non-functional until near bud break (Aloni 1987; Bartolini and Giorgelli 1994), and because the symplasmic pathway is blocked during winter (van der Schoot and Rinne 1999). The recent review on vascular development by Ye (2002) introduced molecular approaches in plant models. Works on *Arabidopsis* improved knowledge on the dynamics of this development and location of connections (Berleth et al. 2000; Grbic and Bleecker 2000; Kang et al. 2003), the role of auxin produced by leaf primordia in the bud (Bennett et al. 2006), the role of auxin sink strength of the stem (Ongaro et al. 2008), and the role of cytokinin (Aloni et al. 2005). Yet there are few specific studies on the buds of trees. In particular, the mechanisms of water storage and water transport that may be involved in their drought resistance through apoplastic and cell-to-cell pathways are poorly documented (Rinne et al. 1994; Bréda et al. 2006).

At the cellular level, aquaporins play a central physiological role in the regulation of the plant-water relations because of their biological membrane location and their functional involvement in the water transport across these membranes (Kaldenhoff et al. 2008). The aquaporins belong to the ubiquitous superfamily of major intrinsic proteins (Maurel et al. 2008). In plants, they fall into four mean homology subfamilies, of which plasma membrane intrinsic proteins (PIPs) and tonoplastic membrane intrinsic proteins (TIPs) are the most abundant in the plasma membrane and tonoplastic membrane respectively. Recently, a fifth

uncategorized subfamily, designated X intrinsic proteins (XIP) was characterized in some plant species (Danielson and Johanson 2008). *Populus* encompasses this subfamily, with nine members. Knowledge of the XIPs remains partial; some XIP members are located in the plasma membrane and show water transport capacity (Danielson and Johanson 2008; Bienert et al. 2011; Lopez et al. 2012). Because biological membranes are potential barriers to passive transcellular water flow, PIPs and TIPs (and possibly XIPs) can control a large part of the cell water permeability and tissue hydraulic conductivity (Kaldenhoff et al. 2008). Their activity is finely regulated at the transcriptional and translational levels (Maurel et al. 2009), particularly in response to environmental factors, such as water deficit (Maherali et al. 2004; Alexandersson et al. 2005; Lopez et al. 2012). The steady-state level of aquaporin transcripts offers a suitable marker for monitoring any tissue-water relations involved in the cell-to-cell pathway. However, the functional roles of aquaporins in water transport toward the buds are still poorly documented.

Here, we hypothesized that bud behaviour was a key factor for tree survival during a drastic water stress. We investigated the behaviour of the buds during a drastic water stress of poplars for several weeks. We hypothesized that the rapid xylem embolism would break the hydraulic connections to the buds and that this process would lead to the interruption of the water and nutrient supply to the buds. These buds would rapidly become isolated, dry and die, preventing the tree from sprouting again. Assuming that a bud respiration decrease would be one of the first indicators predicting plant death, we investigated whether this loss of vitality might be related to the lack of availability of water for the bud. Thus we monitored the axillary bud metabolic activity by measuring respiration rate by microcalorimetry. We investigated the local water distribution and status in buds and other surrounding bearer tissues using nuclear magnetic resonance (NMR) imaging. We also assessed the responses of buds and surrounding tissues in terms of water permeability by studying the expression and modulation of PIP, XIP and TIP aquaporin transcripts using RT-qPCR.

Materials and methods

Plant material, growth conditions and experimental design

We chose poplar (*Populus nigra*) as a model tree because of its fast growth rate and pronounced responses to environmental conditions, notably drought and other abiotic factors, and its worldwide research status (Bradshaw et al. 2000). We planted a single cutting of *Populus nigra* per pot in a total of 64 black plastic 20-litre pots in a glasshouse at Blaise-

Pascal University (Clermont-Ferrand, France) on November 13, 2009. We filled the pots with a 2:1 v/v mixture of homogenized clay loamy soil and peat. We watered the plants to field water capacity every day for 3 months with tap water using a timer-controlled drip irrigation. We then split the trees into eight groups of six individuals each plus a single set of 16 control plants. From February to April 2010 we stopped watering the plants in the eight groups selected for the treatment to induce a drastic water stress, and we continued to water the control plants every day as before to field water capacity throughout the experiment.

Every 30 minutes we recorded night and day air temperatures (20 °C/ 22 °C) and relative humidity in the glasshouse. Night-time air relative humidity was high (up to 94%) but it could decrease to 55% when lights came on at about 4 a.m. Diurnal photosynthetically active radiation (PAR) in the glasshouse was about 1000 µmol m^{-2} s^{-1} over the waveband 400–700 nm and was provided by 400 W Master son-T Pia Hg Free lamps (Philips lighting France, Suresnes, FRA). The photoperiod was 8/16 hours night and day. We measured PAR every 5 seconds (Li-190SA quantum sensor, Li-Cor Inc., Lincoln, Ne, USA), and stored 10 min. average values in a 21X data logger (Campbell Scientific, Shepshed, Leics, UK).

Experimental protocol during water stress

During the period of water deprivation we conducted eight samplings 0, 14, 18, 21, 25, 28, 32 and 61 days after the start of treatment. At each date, we focused on a set of six water-stressed plants and two control plants. We measured the predawn leaf water potential and then harvested the sprouts from the sampled trees. We cut the stem at 50 mm above the soil and divided it into four parts. From the proximal to the distal end, we used a first 20 mm-long segment, which bore one bud, for NMR observations, a second 20-mm-long segment, which bore also one bud, for molecular analyses, a third segment with 10 to 15 buds, which was 200 mm long, for heat flow and respiration rate measurements, and a last 50 mm-long segment to evaluate the percent conductivity loss. Finally, we re-watered the stumps of the sampled trees to field capacity every day. Four weeks after the sampling date we evaluated the total tree survival rate as the number of stumps from stressed trees that were still able to re-sprout.

Predawn water potential measurements

We measured predawn leaf water potential for fully exposed healthy undamaged leaves borne on sprouts. We used a Scholander-type pressure chamber (PMS, Corvallis, Oregon, USA) to assess plant water status (Scholander et al. 1965; Hinckley et al. 1992). We collected two bagged leaves per stressed and control tree to determine their predawn leaf

water potential (Y_p). We wrapped these leaves in aluminium foil and sealed them in a plastic bag the evening before sampling to prevent transpiration and promote water tension equilibrium between the sprout axis and root zone overnight. At the sampling time we removed the bagged leaf from the sprout and promptly placed it in the pressure chamber without removing the plastic bag (Turner 1988; Ameglio et al. 1999). We completed Y_p measurements every sampling date until the plants had shed almost all their leaves in 3 to 4 weeks.

NMR imaging

We wrapped both end-cuts of each sampled stem segment in Parafilm©, placed them in a sealed NMR tube to prevent sample water loss, and took them immediately to the NMR facility (INRA, Clermont-Ferrand/Theix, France). We performed proton magnetic resonance imaging (MRI) experiments at 400 MHz in a 9.4 tesla vertical wide-bore (89 mm diameter) spectrometer equipped with Micro2.5® micro-imaging accessories (Bruker Biospin Ettlingen, Germany). We used a 15 mm ^{1}H-imaging birdcage coil in the imaging probe for the radio frequency (RF) transmission and signal reception. To reduce transpiration during the imaging process, we wrapped the sample a few centimetres beyond its proximal end with plastic film. We then inserted the bud in the 13 mm diameter NMR tube. For calibration purposes we inserted a 0.5 mm glass capillary filled with 500 µmol l^{-1} $MnCl_2$-doped water (allowing a water proton T2 relaxation time of 40 ms at 400 MHz) into the NMR tube close to the sample. We centred each sprout in the RF coil using foam supports. We performed all the experiments at room temperature (~21°C).

We applied two kinds of imaging sequence to map the local water distribution in different tissues and collect information about the degree of binding of water. We acquired T2-weighted images using a multi-spin echo multi-echo (MSME) pulse sequence on a volume of 10 contiguous slices, 0.75 mm thick, centred on the bud location to generate the map of the T2 relaxation times (T2 parametric map). For each slice, we recorded six echo times (TE) ranging from 11 to 66 ms; 11 ms with the following parameters: time to repetition (TR) 2000 ms, field of view (FOV) 10 mm and matrix size 256 x 256 allowing an in-plane resolution of 39 mm^2. We performed these acquisitions on both transverse and longitudinal planes for a total acquisition time of 13 min.

For structure analysis, we selected a region of interest of 101010 mm for 3D anatomical imaging that covered the bud and its surroundings. We used a 3D proton density rapid acquisition with relaxation time enhancement (RARE) pulse sequence with the following

parameters: TR/TE 1300/9 ms, acceleration factor (AF) 4. The final volume image was 256256256 voxels with a resulting isotropic voxel resolution of 39 mm^3. We performed two scans per sample and averaged the data.

We carried out NMR measurements on two individuals per sampling date: 0, 21, 28, 32 and 61 days after water stress onset (total 10 individuals). We computed the parametric images (proton density and T2 maps) by fitting the decay of the signal intensity (S) with echo time (TE) to $\ln(S) = -TE/T2$ using linear regression. The local proton density (signal intensity extrapolated for TE=0 ms) and the T2 maps were then processed by image analysis using ImageJ software (Rasband 1997-2009) on radial-tangential cross sections, and on radial-longitudinal sections. We calibrated the proton density images using the glass capillary content as reference. Diametrical 540 µm (15 pixels) thick profiles were then plotted in the middle plane, which included the centre of the bud. We used these profiles to extract the variations in bark, xylem, cambium (which includes here the living cells of xylem), pith (for convenience, we use the term "pith" for the central part, which comprises the pith and its surrounding parenchyma cells) and bud proton densities. Finally, we extracted maximum and mean values of proton density. In the same way, we extracted the maximum and mean of the characteristic relaxation time of the water from the T2 parametric image. For these T2 measurements, we focused on exactly the same regions of interest as for proton images.

Native state embolism measurements

Native state embolism refers to the percent loss of conductivity (PLC) that occurs as a consequence of the water stress experienced by an intact plant in situ. We measured the native state percent embolism with a xylem embolism meter (XYL'EM, Bronkhorst, Montigny-les-Cormeilles, France) on the specimens and control plants. We collected the sprouts in the morning put them in wet black plastic bags, and brought them immediately to the laboratory for hydraulic conductance measurements. We cut the 5 cm stem segments under water from the sprouts and fitted them to water-filled tubing. We connected one end to a tank of a de-gassed, filtered (0.2 µm) solution containing 100 mmol KCl l^{-1} and 10 mmol $CaCl_2$ l^{-1}. We recorded the flux of this solution through a stem segment section under low pressure (6 kPa) as initial hydraulic conductance (k_{ini}). We then perfused the stem segments at least twice with the same filtered solution at 0.2 MPa for 2 minutes to remove air from embolized vessels and determined maximum hydraulic conductance (k_{max}). Percent loss of conductivity (PLC) was determined for each stem segment as $PLC = 100\ (1 - k_{ini} / k_{max})$.

Bud metabolic heat rate and respiration rate measurements

Plant calorimetry offers an approach for assessing the metabolic activity of living tissues (Hansen et al. 1997; Llamas et al. 2000; Hansen et al. 2004). We used this approach to carry out a census of dry-down impacts on bud ability to burst in re-watering stressed plants. For each sampling date, we measured the metabolic heat rate (Rq) and respiration rate (Rco_2) of buds at 20 °C. We collected ten to fifteen buds depending on their size, as a minimum of fresh matter is required to run the micro-calorimeter. We measured their fresh weight and inserted them into a 1 cm^3 micro-calorimeter cell. The measurements were made with differential scanning calorimeters (micro DSC VII, SETARAM, France). Micro-calorimetric procedures are described in Criddle et al. (1991). Briefly, the operating method involved three steps. Firstly, a heat flow was generated in the cell (continuously recorded) until a steady state (q1) was reached in roughly 20 minutes. Secondly, we inserted a small capsule with 20 µl of 1N NaOH into the measurement cell. The NaOH reacts with the CO_2 released by the respiration of the tissues. This reaction resulted in an additional heat flow, which led to a new steady state (q2). Thirdly, we removed the capsule and the heat flow decreased to a new steady state (q3; equal or close to q1 if no alteration of the living system occurred during the measurement process). Lastly, we estimated the metabolic heat flow as the mean values of q1 and q3, and the respiration flow as the difference between q2 and the metabolic heat flow value.

We retrieved, dried at 70 °C for 24 hours and weighed the samples to determine their dry masses (Dw). Finally, we calculated the metabolic heat rate and respiration rate according to Hansen et al. (1989) and Hansen and Criddle (1990). Metabolic heat rate corresponding to the metabolic heat flow per unit dry mass (Eq.2) was expressed in µW mg^{-1}, and the respiration rate as the flow of CO_2 per second and per dry mass unit and expressed in nmol CO_2 g^{-1} s^{-1} (Eq. 3):

$$Rq = (q1+q3) / (2\ Dw), \quad (2)$$

$$Rco_2 = (q2 / Dw - Rq) / 108.5 \quad (3)$$

We carried out five replicates at each sampling date and we recorded the mean values. We also measured the bud moisture content as weight of water divided by dry mass.

Total RNA isolation, cDNA synthesis and amplification

We performed molecular investigations at Day 28. We extracted the total RNA from buds, bark (including phloem and cambium tissues) and wood (i.e. xylem without cambium) at the intermediate part of the stem using CTAB extraction buffer according to Chang et al. (1993). First-strand cDNA was synthesized from 1 µg of total RNA using SuperScript III (Invitrogen, Carlsbad, CA, USA) following the manufacturer's instructions. We performed the real-time PCR amplification using a MyiQ thermocycler (Bio-Rad, Hercules, CA, USA) with MESA GREEN qPCR MasterMix Plus (Eurogentec, Seraing, Belgium) containing 2 µL of 40-fold diluted cDNA according to the manufacturer's protocol. The thermal profile of the reaction was: 94 °C for 3 min, 40 cycles (94 °C for 20 s, 54 °C to 58 °C for 20 s, and 72 °C for 20 s). We verified the specificity of amplicons by melting curve analysis, and checked them by gel electrophoresis. We deduced PCR efficiencies for each gene from series of diluted cDNA (Pfaffl 2001). The crossing cycle number (C_t) was automatically determined for each reaction by the iCycler iQ v2.0 software with default parameters. Normalization of the target gene abundance was achieved using the geometric mean of three reference genes (*18SrRNA*, *EF1α*, *SAND* for a final geometric mean of C_t ± standard deviation = 18.02±0.83). We chose these candidates from different protein families to reduce the possibility of co-regulation. We assessed the MIP transcript steady-state levels in each vegetative tissue by comparison of their mean of C_t after normalization with the geometric mean of the reference gene C_t. Expression levels were graphically represented after distribution and scoring on an arbitrary range between 0 and 100. A C_t of 20 was assigned an arbitrary value of 100 (corresponding to the highest MIP expression level in our condition, here *PIP1;2*); a C_t of 40 was given an arbitrary value of 0 (no expressed gene). We then assigned all the other C_t values between 0 and 100, scaled based on their relative distributions. For the evaluation of the differential expression of MIP transcript in response to stresses in each tissue, we computed the relative changes using the equation $\log_2(2^{-\Delta\Delta Ct})$ equation according to the procedure of Pfaffl (2001). The mean C_t value was determined from two independent biological replicates for each sample, and every PCR reaction was carried out in triplicate. All the primers used for this study were designed with Primer3plus application (http://www.bioinformatics.nl/primer3plus; (Rozen and Skaletsky 2000) and are listed in the Supplemental Data (Table 1).

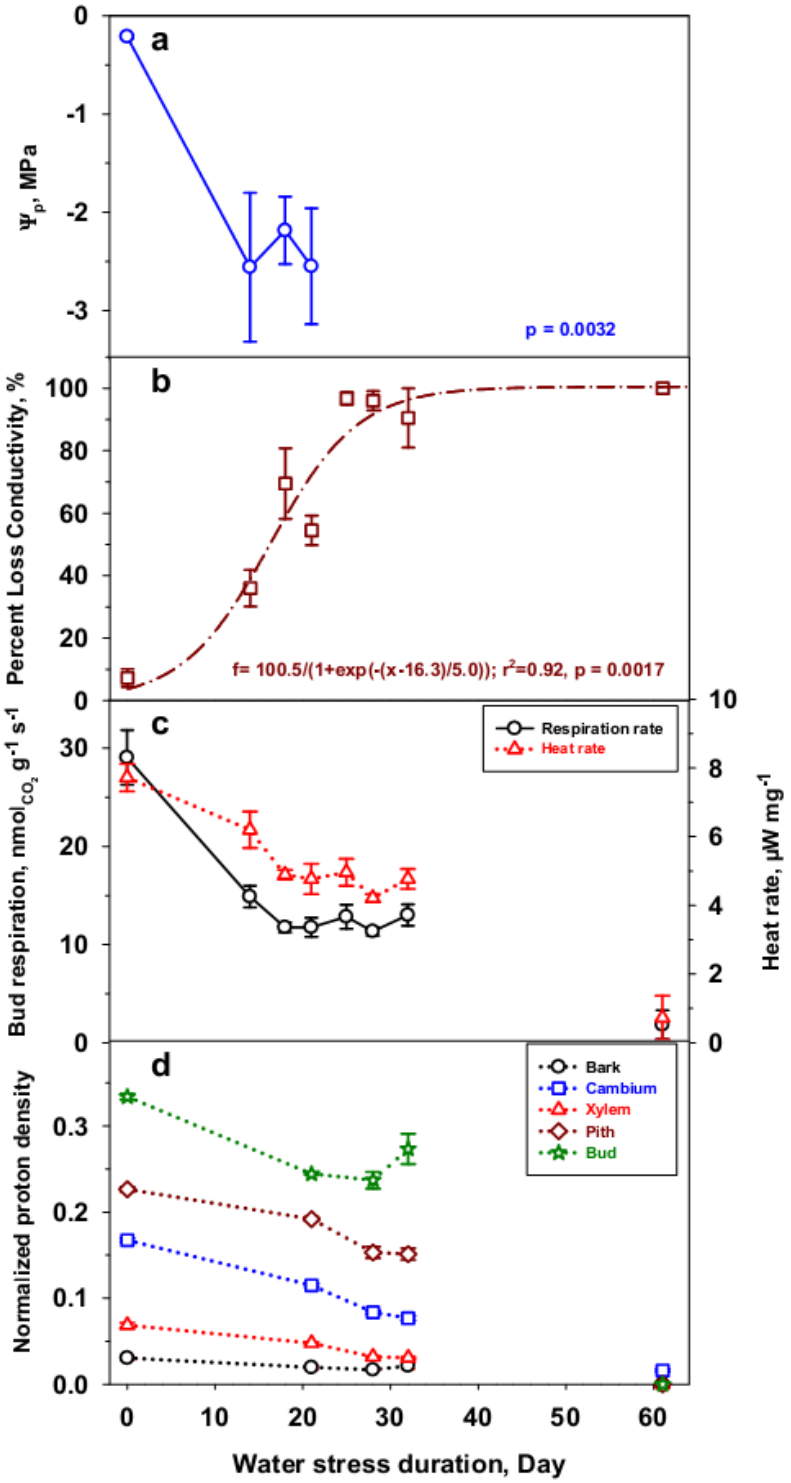

Figure 1. Patterns of predawn leaf water potential (a), percent loss of conductivity of the stem (b), bud heat rate and respiration rate (c) and normalized proton density (d) over the sampling periods of time. Error bars represent standard errors (n=5) at each sampling date. Leaf water potential was not available after the leaves had fallen. Values of control plants are merged in the 0 date.

Data analysis

Aquaporin steady-state levels for each biological assay were computed by one-way ANOVA followed by a Tukey HSD post hoc test ($p<0.05$). Data of heat flows and respiration rates are given as mean ± standard error (SE). The comparisons of predawn water potential of the plants, bud heat flows and respiration rates over time were computed with the repeated data collected on each sampling date using the non-parametric test of Kruskall-Wallis. We computed ANOVA and the non-parametric tests using the R software package and made non-linear curve fittings using the SigmaPlot 9.0.1 software package (SigmaPlot, Systat Software Inc., Point Richmond, CA, USA).

Results

Variation in predawn leaf water potential, PLC, bud respiration rate, proton density and bud moisture content during water stress

The predawn leaf water potential Yp decreased significantly ($p = 0.003$) within the first 14 days after the onset of water deprivation (Figure 1a). In a second phase, Yp kept a stable value for 7 days. The stem segments then lost their water transport ability and the plants shed almost all their leaves about 3 weeks after water stress inception. Consequently, no further measurement of the predawn leaf water potential was possible. Stem segment PLC increased with time in a sigmoid pattern from the start of the water stress treatment (Figure 1b). The loss of conductivity reached 50% after 16 days of water stress and 90% after 4 weeks of water deprivation. Bud metabolic heat and respiration rates showed similar patterns (Figure 1c). They decreased significantly ($p = 0.009$) during the first 18 days respectively from 29.1± 2.8 (SE) nmol CO_2 g^{-1} s^{-1} to 11.8 ± 0.5 nmol CO_2 g^{-1} $s^{-1}$for bud respiration and from 7.7 ± 0.4 µW mg^{-1} to 4.9 ± 0.1 µW $mg^{-1}$for metabolic heat rate. This weak respiration rate remained at a steady state ($p = 0.46$) for at least 14 days before decreasing to 1.8 ± 1.5 nmol CO_2 g^{-1} s^{-1}. Measurements on NMR images showed that the proton density could reliably discriminate among the different components of the stem segment at the bud level (Figure 1d and Figure 2). Proton density was higher in bud tissues than in pith, cambium, xylem and bark. For all the tissues studied, a decrease in proton densities occurred over time: the decrease was very low for both the bark and the xylem, but was marked for the bud, pith and cambium. The bud moisture content ranged from 0.4 ± 0.3 to 2.1 ± 0.1. However, the moisture content of most of the buds was close to 1.3. We found a close relationship between bud moisture contents and respiration rates (Figure 3a) and also between proton density values (Figure 3b).

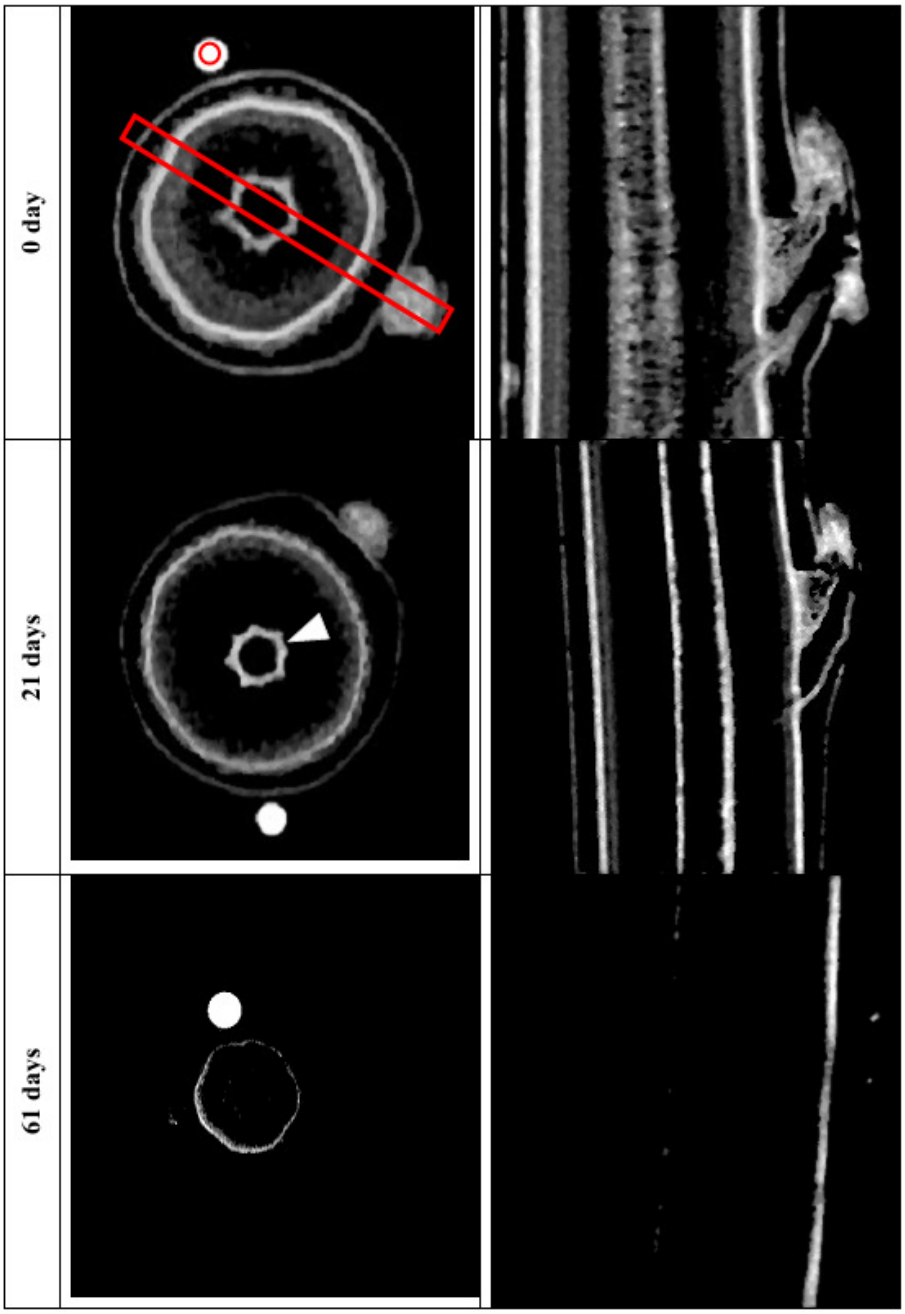

Figure 2. 3D MRI mapping of the shoot segments containing the bud. Grey levels show the normalized proton density that reflects the water content. Bright discs show the capillary glass filled with doped water that allows the calibration for each pixel of the grey levels. Radial-tangential plane (left) and radial-longitudinal plane (right) were used for proton density measurements of tissues. The parenchyma tissues close to the pith and the cambium areas showed very high moisture contents. At the last step, the cambium remained hydrated while the bud was already dry and dead. Spatial resolution is 39 µm.

After watering for 4 weeks, all the stumps recovered from their dry-down episode (data not shown). Only the trees that had experienced 61 days of water stress died.

Local water availability and its distribution in bud and shoot bearer

Three weeks after the inception of the water stress treatment, the xylem tissues were largely embolized (Figure 2) while all the other stem tissues remained consistently hydrated. In the next steps, proton imaging showed that the bud remained highly hydrated despite the almost complete embolism of the xylem. The base of the bud seemed hydraulically connected to the cambial zone, which showed the highest proton density. Similarly, the base of the bud was hydraulically connected to the pith (Figure 4, white arrow). This connection crossed the xylem, even when parts were fully embolized. The central part of the pith appeared water-free, but a layer of surrounding tissue was strongly hydrated (Figure 2, grey arrow).

The maximum proton density was found in the peripheral zone of the stem where the living cells are located. This zone includes the cambium area where the cells divisions occur. This area also showed the highest values for T2 (Table 1) at more than 30 ms, indicating a low degree of binding of water, which was therefore easily movable and usable. The pith area was also highly hydrated. Nevertheless, it showed a lower T2 than cambium area (about 20 ms). Thus although water was present, it seemed to be less movable and so less usable by surrounding tissues. Other tissues such as bud and xylem showed lower moisture content. Even though all the tissues of stressed plants remained highly hydrated compared with the control (Figure 1), their proton density clearly decreased during the first 3 weeks of the treatment. They then remained stable for at least 12 days. Finally, the proton density decreased to zero from Day 32 to Day 61. It reached zero in the bud and in the pith areas. However, water remained in the peripheral tissues of the stem, including the cambium and bark tissues, which were the last to keep water.

Whether we used the mean or the maximum value (data not shown), the patterns of proton density and T2 curves over time were similar. The high value of the relaxation time in the cambium area decreased steadily over time. The value of the T2 became very low (10 ms), and three times lower than before the water stress treatment. The T2 value was initially lower for the bud than in the cambium area, but it remained fairly stable (14 ms) until Day 32, i.e. for 4 to 5 weeks under water-stressed conditions. At the end of the experiment, the T2 value of bud decreased to a very low value of around 4 ms. This value needs careful analysis because the proton density was close to zero in this area. In the pith, the relaxation time remained stable (between 15 and 19 ms) until Day 32 and then decreased to zero on the last

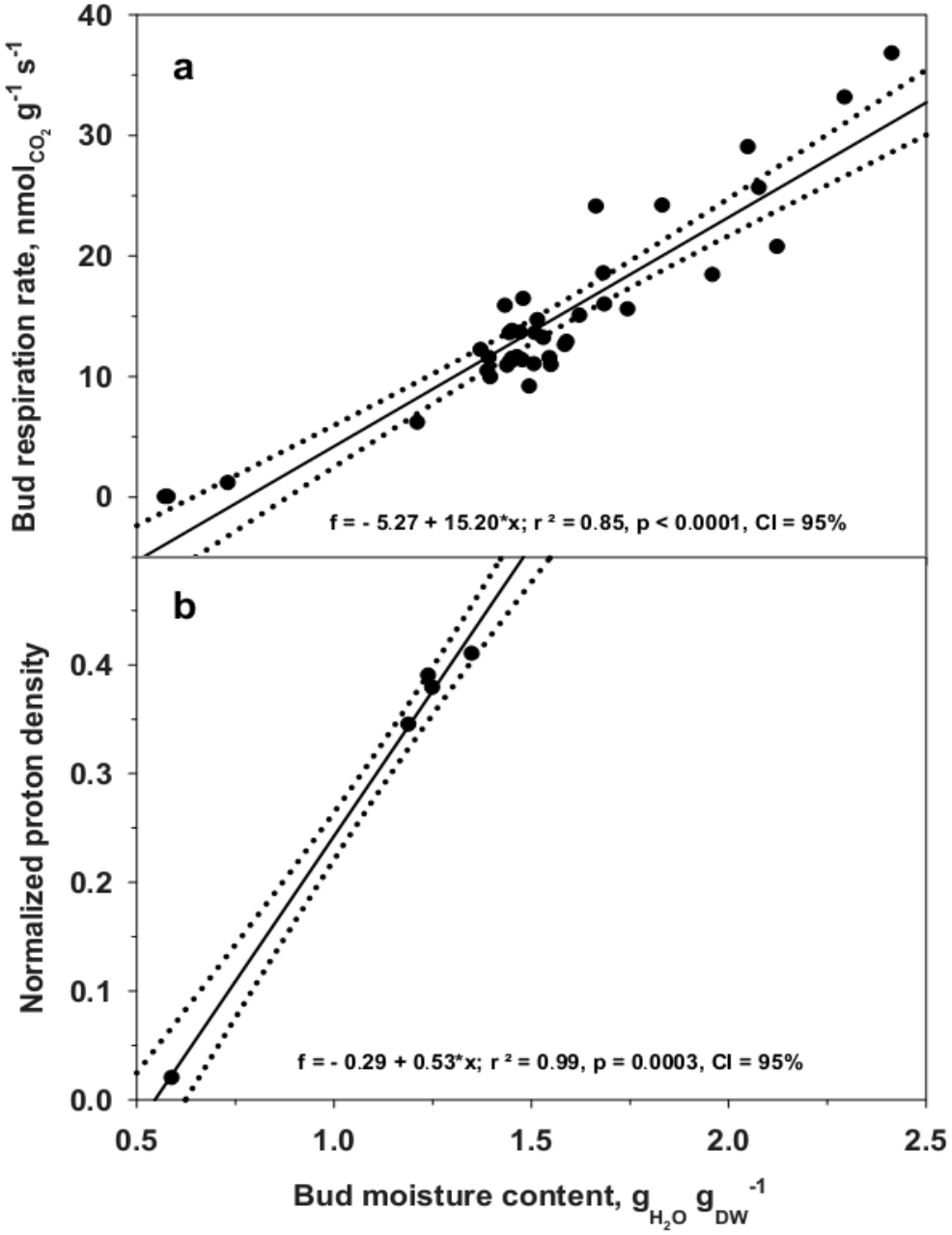

Figure 3. Relationship between bud moisture content, bud respiration rate and normalized proton density in *Populus nigra* sprouts. Solid and dotted lines represent regression line and confidence interval at 95% of sprouts (a, b) and buds (c).

date. At this date, the proton density also became nil. In the bark, the time course was quite similar, showing a first stable plateau until Day 32 followed by a decrease to zero at the end of the experiment.

Expression pattern of aquaporin transcripts

The steady-state levels of transcript accumulation for the PIP, XIP and TIP subfamilies were simultaneously traced in the axillary buds and their immediate stem surroundings in wood (including xylem and pith) and bark (including phloem) from plants either well-watered or exposed to 28 days of the described drastic water stress constraint (Figure 5). Of the 15 PIP, 9 XIP and 17 TIP members observed in the *Populus* genus (Lopez et al. 2012), all *PIPs*, 3 *XIPs* and 14 *TIPs* showed detectable expression in *P. nigra*. No *XIP1s*, *XIP3*;*3*, *TIP1*;*2*, *TIP 5*;*1* and *TIP5*;*2*, transcripts were detected (data not shown). With the exception of *XIP3*;*1* and *XIP3*;*2*, which were exclusively expressed in wood, all the other AQPs were ubiquitously expressed in buds, wood and bark in both control and stressed plants. However, no clear organ specificity expression emerged, except for *PIP2*;*5* and *PIP2*;*8,* which were preferentially expressed in wood and bud respectively. Compared with the most constitutively expressed AQP (*PIP2*;*1*, *PIP1*;*2*), 7 *PIP2s* (*PIP2;1*, *PIP2;2*, *PIP2;3*, *PIP2;4*, *PIP2;6*, *PIP2;7*, *PIP2;10*), all *PIP1s* and 7 *TIPs* (*TIP1;3*, *TIP1;5*, *TIP1;6*, *TIP1;7*, *TIP2;1*, *TIP2;2*, *TIP4;1*) could be considered as highly accumulated (>50%). Conversely, 4 AQPs (*TIP1*;*1*, *TIP1*;*8*, *TIP3*;*1* and *TIP3*;*2*) were marginally accumulated (<25%). The XIP subfamily showed the most sharply contrasted accumulations between organs where *XIP2*;*1* and *XIP3*;*2* were notably expressed in buds and wood respectively, whereas *XIP3*;*1* remained marginally expressed.

Among all the AQP members we monitored, only *PIP1*;*1* remained constant whatever the organs, whereas all the other members presented differential accumulation when plants were under water stress constraint. Overall, bark tissue presented the strongest response to water stress, with the significant modulation of 23 AQPs, among which 7 AQPs were upregulated (*PIP2*;*1*, *PIP2*;*9*, *TIP1*;*1*, *TIP1*;*6*, *TIP2*;*3*, *TIP3s*) and 15 AQPs were downregulated. Wood tissue encompassed 13 modulated AQPs with two upregulations (*PIP1*;*3* and *TIP1*;*5*) and 11 downregulations, including the tissue-specific AQP, *XIP3*;*2*. For bud tissue, 15 AQPs were modulated: eight were upregulated and seven were downregulated. All were distributed over the three MIP subfamilies.

	Elapsed time (days)	0	21	28	32	61
Pith (ms)		**21.5±0.9**	**18.3±0.7**	**15.3±0.7**	**17.5±0.7**	**0.0±0.0**
Cambium (ms)		**33.0±0.9**	**31.0±0.6**	**22.5±0.9**	**19.5±0.8**	**11.0±1.0**
Bud (ms)		**18.5±0.8**	**14.6±0.8**	**13.5±0.5**	**14.2±0.6**	**4.1±0.7**

Table 1. Relaxation time T2 obtained by NRM imaging using a multi-spin multi-echo (MSME) pulse sequence. Values are expressed in milliseconds and reflect locally the degree of binding of water in the tissues. Values of control plants are merged in the 0 column.

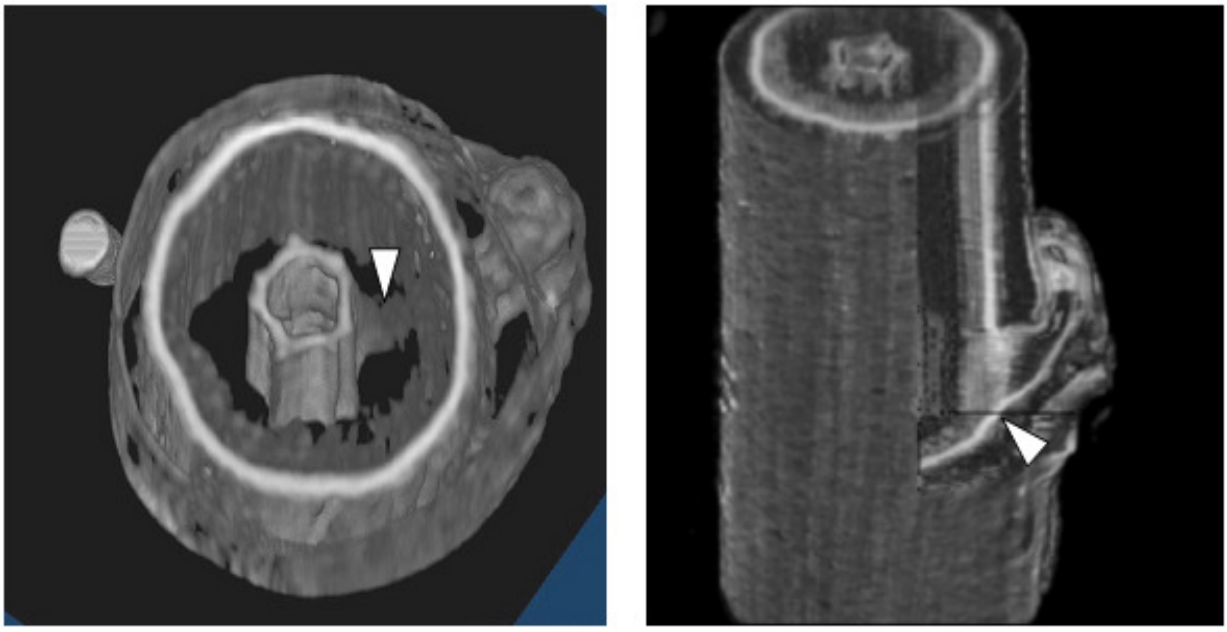

Figure 4. 3D visualisation of the normalized proton density (MRI measurements) in the bud and the stem of poplar (*Populus nigra*) during a water stress event (4 weeks). The proton density reflects the quantity of water contained in the tissues. This shows the large hydraulic connection between the bud and the parenchyma tissue (white arrow) that surrounds the pith (left) and the connection of the bud with the cambial area (right). The cambium was the most highly hydrated tissue, as the xylem area was almost fully embolized: remaining water was 839 concentrated around its peripheral zone, close to the cambium where living cells are located.

Discussion

Water stress impacts on plant water status and bud respiration rate

Severe water stress (8 weeks without watering) generated changes in some physiological processes for our juvenile poplar plants: predawn water potential, reduction in stem conductance or in respiration rate were observed and were typical responses for progressive stages of water stress (Figures 1a, 1b, 1c).

We found that the trees displayed an ability to keep their Y_p relatively constant for at least 2 weeks after a substantial drop, which occurred during the first 14 days after the inception of the water stress. This stabilization of Y_p may be under stomata control (Schulze 1993; Flexas et al. 2004; Thapa et al. 2011). Our physiological observations are in line with those of Braatne et al. (1992), Hinckley et al. (1992) and Rood et al. (2000) who underlined the substantial vulnerability of black poplars to prolonged drought. Our trees shed their leaves within 3 weeks after water stress inception. This could be due to the inability of the stomatal closure to maintain a favourable water balance, as leaf abscission is an effective, rapid reaction to temporary drought (Kozlowski and Pallardy 1997; Taiz and Zeiger 1998). In our case, leaf shedding seemed to delay fatal desiccation, as only plants deprived of water for more than 4 weeks failed to recover after re-watering.

The widespread embolism that occurred within the sprouts in a sigmoid-like pattern towards 100% water conductivity loss was expected (Tyree and Sperry 1988; Rood et al. 2000). Meanwhile, total loss of conductivity coincided with total leaf abscission in the study plants. This suggests a close relationship between embolism and leaf abscission and might be analysed as a physiological strategy of the plant to reduce the transpiration process. Reducing water loss may preserve the internal tissues, particularly the meristematic ones, from excessive desiccation (Blum 2009) and cessation of cellular metabolism.

According to de Faÿ et al. (2000) and Monserrat-Marti et al. (2009), water stress alters bud formation, growth and burst. However, we did not observe any severe water stress effect on bud survival in this study except for the trees that experienced more than 32 days of water shortage. Therefore, we suggest that there is a specific safety mechanism that allows the trees to slow down the lethal desiccation of their buds during a water shortage period by preserving part of their available water for vital living tissues including buds. The NMR images (Figure 2) provide new insights into a compartmentalization of the available water in the different tissues. They reveal that buds contained high free water density while xylem tissue became rapidly embolized during the water stress. NMR images and conductivity

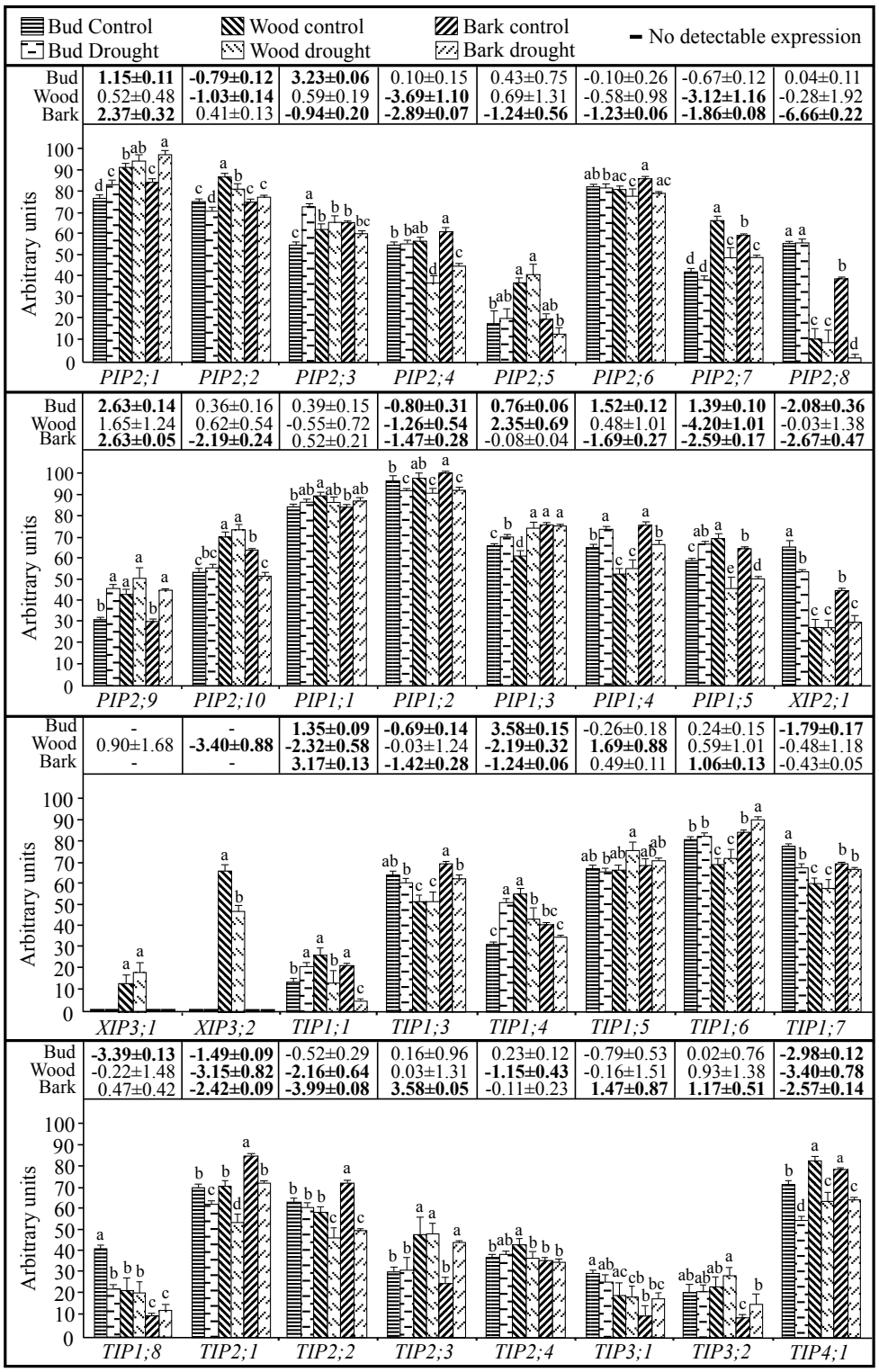

Figure 5. Expression patterns of *PIP*, *TIP* and *XIPs* isoforms in bud, wood and bark of *Populus nigra* after 28 days of water stress exposure. Changes in expression levels for the three tissues are presented as expression ratio (water stressed *vs* well-watered control). Steady-state level representation for each biological assay is given in Materials and methods. Transcript expression levels were determined by real-time quantitative RT-PCR using specific primer sets for each isoform. The geometric mean of three reference genes was used as endogenous control. Data correspond to means of three technical replicates from two independent biological experiments, and bars represent standard error (n=2). Three plants were pooled per biological sample. Change data in boldface are to be interpreted as being significant. Levels not sharing the same letters are significantly different (Tukey HSD, $p<0.05$).

measurement (PLC) were consistent with this finding (Figure 1b). The inner part of the xylem became rapidly non-conductive, while the peripheral zone still contained water for 4 weeks. In addition, the hydraulic connections of buds with highly hydrated tissues suggest possible mutual water exchanges. In particular, the bud seems to be hydraulically connected to the cambium area and to a ring of parenchyma cells located around the pith (Figure 2 and Figure 4). Both areas are fully saturated with water. Also, the moisture content of the cambium and pith areas decreases in the same way as the bud. Again, this supports the hypothesis of functional hydraulic connections between them even during a water stress event. These areas remain hydrated at least as long as the buds. We therefore hypothesize that they may act as internal safety water reservoirs. Our observations are consistent with the diffusion-weighted images of poplar buds reported by Kalcsits et al. (2009). Cytological observations (Figure 6) show that a large bundle of parenchyma cells, mainly oriented along the radial direction. This anatomical structure may allow an efficient radial transfer pathway of water between an inner reservoir and the bud. These results invalidate our initial hypothesis that the xylem embolism would lead to the rapid desiccation and death of the bud.

From Figures 1b and 1c, the embolism expansion pattern in the sprouts appears closely related to bud respiration rate limitation. We also found that bud respiration rate was closely correlated (R^2 = 0.85, $p<0.0001$) to water content (Figure 3). Thus we suggest that bud respiration rate and their water content are strongly coupled and not independent as previously reported by Huang et al. (1975), who underlined a rapid decline of respiration rate as a consequence of a developing water stress event. For Amthor (1994) and Gibon et al. (2009), the decrease in respiration was a result of reduced resource availability and substrate protein content. It has been reported that metabolic heat rate and respiration rate rely on tissue metabolic activity (Hansen et al. 1997; Llamas et al. 2000; Hansen et al. 2004) and on bud growth capacity (Trejo-Martinez et al. 2009).

The steady-state pattern we observed for the respiration rate two weeks after the water stress inception could reflect the 'maintenance' cost of a basic bud metabolism. Thus we can reasonably hypothesize that any failure in sustaining the basic bud metabolism requirement will lead to vanishing bud metabolic heat and respiration rates and ensuing bud death. To our knowledge, there is no reported data in the literature on bud maintenance respiration rate. Matheson et al. (2004) reported values ranging between 20 and 30 nmol CO_2 g^{-1} s^{-1} for shoots of *Verbascum thapsus*, *Convolvulus arvensis*, *Helianthus tuberosus* and *Avena sativa* seedlings. These values are closely correlated to the number of living cells in their samples. It was therefore likely that the low value we find in our work (12.2 nmol CO_2 g^{-1} s^{-1}) for the bud

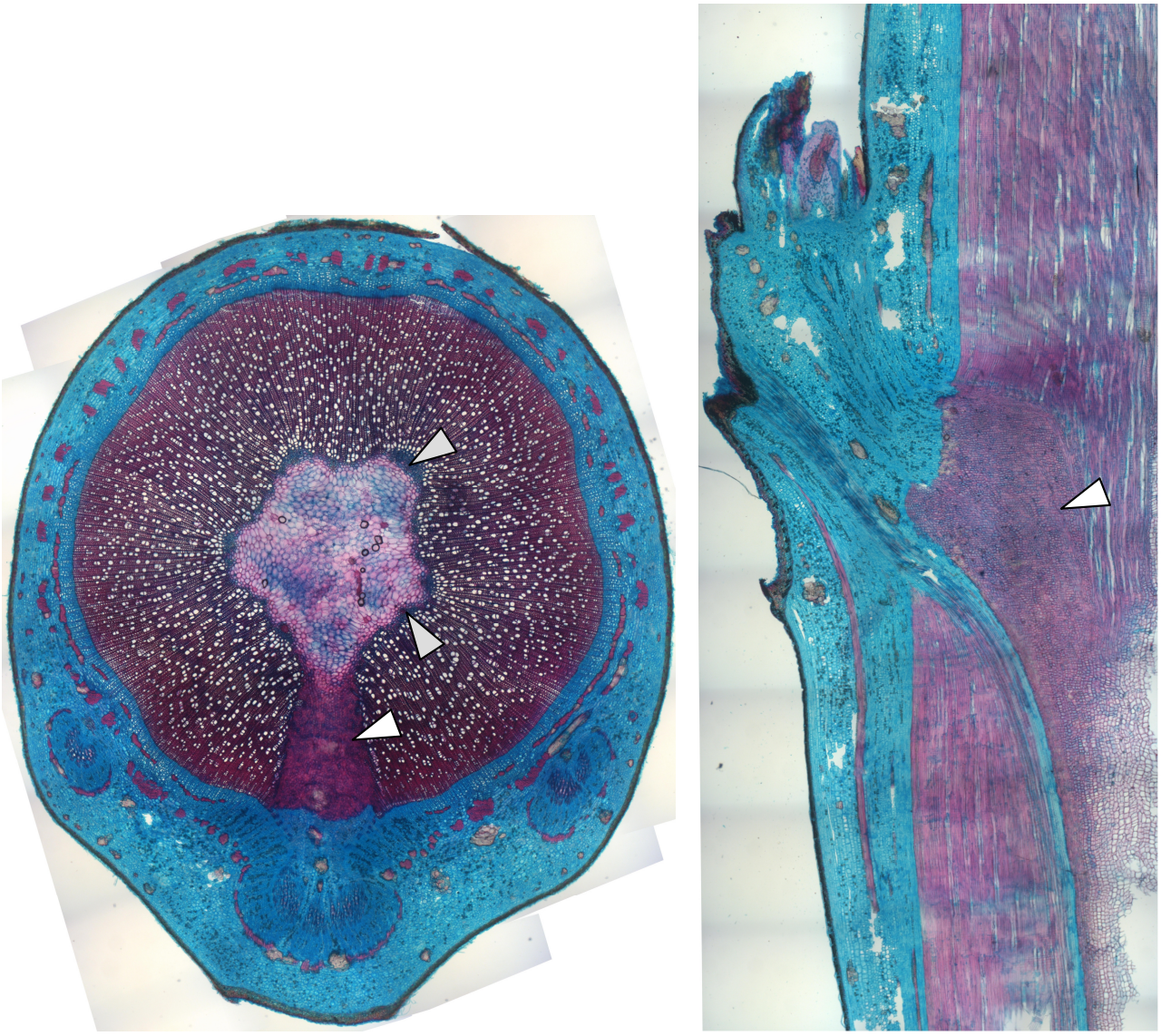

Figure 6. Cytological observations of the stem anatomy. Transversal slice (25 µm thick) shows the large connection between the bud and parenchyma tissue that surrounds the pith. The connection is made of a large bundle of parenchyma cells (white arrow) and allows a radial transfer of water between an inner reservoir (grey arrow) and the bud. The double staining method with safranin/astra blue was applied on microscopic sections. Safranin staining (red) is the indicator for lignin. Astra blue (blue) tints cellulose.

maintenance respiration rate could result from the presence of the protective scales, which are composed of a tiny amount of living tissue. In addition, the associated metabolic heat rate (4.7 µW mg^{-1}) we record for poplar buds is close to that of dormant *Larix laricina* buds (Hansen et al. 1989) and *Vitis vinifera* buds (Gardea et al. 1994). Atkin and Macherel (2009) show how the dark respiration maintenance plays a major role in plant survival under water stress conditions and its rapid recovery of productivity after re-watering. Flexas et al. (2005) report that photosynthesis can stop completely in severe water shortage, while the respiration rate may either increase or decrease under stress, but never becomes totally impaired. Our results also show a close correlation between bud respiration rate and water content. Several mechanisms are probably involved in the maintenance of a minimum threshold level of bud moisture content to ensure a minimal activity and a maintenance respiration rate to keep the bud alive during increasing water stress duration. The survival of the meristematic cells is strongly dependent on the capacity to use carbohydrates to produce energy and the capacity to maintain minimally sufficient hydration in this structure (McDowell 2011). This capacity depends not only on the overall response of the plant through stomatal regulation, but also, at a lower scale, to the compartmentalization of the bud and the functional integrity of vascular connections between other tissues of the stem and the bud.

Aquaporin expressions and water transport

Aquaporin expression patterns can be linked to our physiological and NMR imaging data. Xylem was the first embolized area and showed the lowest reactive molecular responses. Hence living cells within the xylem seem unable to preserve their hydraulic reservoir. Conversely bark, and to a lesser extent buds, show the most marked molecular response together with the greatest number and magnitude of modulated aquaporin isoforms. This is consistent with the hypothesis that bark (as a reservoir) and bud (as a vital organ) both need to react to maintain their moisture content.

The *Populus* genus encodes 15 PIP, 9 XIP and 17 TIP members (Lopez et al. 2012). Although these isoforms are numerous, most of them are constitutively expressed and modulated in our experiment (Figure 5). It would nevertheless be unsafe to make any functional interpretations of each isoform pattern in the different biological assays. However, an overall reading of PIP2s and PIP1s may offer us some physiological insight. PIP1s and PIP2s were predominantly upregulated or slightly modulated in buds, whereas both were essentially downregulated in the bark. This might reflect their respective capacity to draw water upward and hold water. We still know very little about the physiological function of

PIPs in woody plants: PIP1 isoforms are thought to have weaker water channel activities than PIP2s isoforms, but PIP1s probably ensure a substantial role in controlling water permeability, since coexpression of PIP1 with PIP2 isoforms potentiate water transport (Fetter et al. 2004; Secchi and Zwieniecki 2010). However, little information is available about the functions of TIP subfamily members which are known to attenuate plant susceptibility to water stress (Wang et al. 2011). Our results show that most modulated TIPs are downregulated during water stress, although some isoforms are upregulated, but in tissue-specific ways. TIPs also provide osmotic potential equilibrium for the cytoplasm by exchanging water with the vacuole. Thus the apparently conflicting patterns we observed could be explained by the different locations in which the isoforms are expressed. However, further investigation is still needed to clarify aquaporin involvement in these physiological processes. This investigation could be done using mutants or transgenic resources in which the expression of specific aquaporins is silenced or upregulated (Kaldenhoff et al. 2008).

Local water availability and its distribution in bud and shoot bearer

At the tree scale, Vilagrosa et al. (2003) found on Mediterranean shrubs that higher resistance to cavitation was not necessarily correlated with higher survival behaviour under field conditions. This result is in line with our observations since all the trees were able to re-sprout after more than 4 weeks of water shortage, even if the xylem became completely embolized. Hence we can conclude that a temporary total embolism of the xylem does not necessarily imply immediate death of the plant. Moreover, we suggest that cavitation events in the xylem can be a mechanism that would allow availability of free water for vital tissues like buds. This mechanism can contribute to the maintenance of the bud moisture content that is necessary to ensure a minimal metabolic activity during water stress events.

Comparison between microcalorimetry and MRI measurements showed similar patterns (Figures 1c and 1d): both are quite sensitive and show a slight increase in their parameters between Day 28 and Day 32. Moreover, the proton density and the relaxation time T2 followed the same pattern (Table 1). This demonstrates that the free water is extracted first when water is removed (Bottemley et al. 1986). It is commonly accepted that the lower water content leads to higher proportion of bound water and a decrease in mean T2.

Since the cambium area contains meristematic cells we can assume that it is a key compartment that must be protected from drying to ensure the tree survival. The cambium proton density is high and shows high T2 values. This observation suggests that the water

contained in this area is movable and could be usable locally or by surrounding connected tissues. However, at the end of the experiment, this area was still partly hydrated, since the bud became completely dehydrated and died. Nevertheless, the T2 values became low, this being a typical feature of bonded water that is not movable or usable. At this date, no tree has been able to recover after re-watering. We conclude that the hydration of the secondary meristem is not a sufficient condition for tree survival.

Conclusion

The present study presents a quantitative evaluation of *Populus nigra* tree bud survival during a severe water stress event. We followed the evolution of bud behaviour and that of close surrounding tissues by combining 3D imaging, molecular tools and physiological measurements. The results reveal that the bud is a very resistant organ able to withstand several weeks of prolonged water deprivation. We find a close correlation between bud respiration rate, water content and proton density. Bud moisture content can be taken as a bud mortality tipping point even in leafless trees, instead of assessing bud respiration measurements, which is difficult. Moreover, 3D RMN imaging shows that this resistance of bud to water stress could be due to large hydraulic connections with highly hydrated tissues located in the stem and around the pith. Furthermore, the NMR images help to establish a lack of direct hydraulic connection of the bud to the vascular system of the bearer stem. This is probably one of the reasons why the bud is not rapidly and irreversibly impacted by the large embolism of the stem xylem system. Another reason may be the role of the aquaporin isoforms, which probably help to maintain a higher water status in the buds and the cambium than in the other tissues.

Overall, this study provides the first insights into a possible water distribution between connected tissues within water stressed plants, hydraulic trade-offs between the meristematic zone integrity, and the hydration of the bud and its surrounding tissues. It also reveals the implication of molecular actors during water stress events. Combining 3D NMR imaging, molecular tools and physiological measurements opens up new perspectives to help understand the roles played by each tissue and their interactions in plant drought resistance.

Acknowledgements

We thank N. Lajoinie, C. Bodet, C. Serre, P. Conchon, P. Chaleil and A. Faure for plant care and handling, and for their field assistance. We also thank the anonymous reviewers for evaluating this manuscript and for their comments, and N. Boirie and ATT for

language editing.

References

Alder, N.N., J.S. Sperry and W.T. Pockman. 1996. Root and stem xylem embolism, stomatal conductance and leaf turgor in *Acer grandidentatum* populations along a soil moisture gradient. Oecologia. 105:293-301.

Alexandersson, E., L. Fraysse, S. Sjövall-Larsen, S. Gustavsson, M. Fellert, M. Karlsson, U. Johanson and P. Kjellbom. 2005. Whole gene family expression and drought stress regulation of aquaporins. Plant Molecular Biology Reporter. 59:469-484.

Aloni, R. 1987. Differentiation of vascular tissues. Annual review of plant physiology. 38:179-204.

Aloni, R., M. Langhans, E. Aloni, E. Dreieicher and C.I. Ullrich. 2005. Root-synthesized cytokinin in Arabidopsis is distributed in the shoot by the transpiration stream. Journal of Experimental Botany. 56:1535-1544.

Ameglio, T., P. Archer, M. Cohen, C. Valancogne, F.A. Daudet, S. Dayau and P. Cruiziat. 1999. Significance and limits in the use of predawn leaf water potential for tree irrigation. Plant and Soil. 207:155-167.

Amthor, J.S. 1994. Plant respiratory responses to the environment and their effects on the carbon balance. *In* Plant-Environment Interactions Ed. R.E. Wilkinson. Marcel Dekker, New York.

Atkin, O.K. and D. Macherel. 2009. The crucial role of plant mitochondria in orchestrating drought tolerance. Annals of Botany. 103:581-597.

Bartolini, S. and F. Giorgelli. 1994. Observations on development of vascular connections in two apricot cultivars. Advances in Horticultural Science. 8:97-100.

Bennett, T., T. Sieberer, B. Willett, J. Booker, C. Luschnig and O. Leyser. 2006. The Arabidopsis MAX pathway controls shoot branching by regulating auxin transport. Current Biology. 16:553-563.

Berleth, T., J. Mattsson and C.S. Hardtke. 2000. Vascular continuity and auxin signals. Trends in Plant Science. 5:387-393.

Bienert, G.P., M.D. Bienert, T.P. Jahn, M. Boutry and F. Chaumont. 2011. *Solanaceae* XIPs are plasma membrane aquaporins that facilitate the transport of many uncharged substrates. Plant Journal. 66:306-317.

Blum, A. 2009. Effective use of water (EUW) and not water-use efficiency (WUE) is the target of crop yield improvement under drought stress. Field Crops Research. 112:119-123.

Bottemley, P.A., H.H. Rogers and T.H. Foster. 1986. NMR imaging shows water distribution and transport in plant-root systems in situ. Proceedings of National Academy of Sciences of the United States of America. 83:87-89.

Braatne, J.H., T.M. Hinckley and R.F. Stettler. 1992. Influence of soil water on the physiological and morphological components of plant water balance in *Populus trichocarpa*, *Populus deltoides* and their F1 hybrids. Tree Physiology 11:325-339.

Bradshaw, H.D., R. Ceulemans, J. Davis and R. Stettler. 2000. Emerging model systems in plant biology: poplar (*Populus*) as a model forest tree. Journal of Plant Growth Regulation. 19:306-313.

Bréda, N., R. Huc, A. Granier and E. Dreyer. 2006. Temperate forest trees and stands under severe drought: a review of ecophysiological responses, adaptation processes and long-term consequences. Annals of Forest Science. 63:625–644.

Brodribb, T.J. and H. Cochard. 2009. Hydraulic failure defines the recovery and point of death in water-stressed conifers. Plant Physiology. 149:575-584.

Brodribb, T.J. and T.S. Feild. 2000. Stem hydraulic supply is linked to leaf photosynthetic capacity: evidence from New Caledonian and Tasmanian rainforests. Plant, Cell and Environment. 23:1381-1388.

Brodribb, T.J., N.M. Holbrook, E.J. Edwards and M.V. Gutierrez. 2003. Relations between stomatal closure, leaf turgor and xylem vulnerability in eight tropical dry forest trees. Plant Cell and Environment. 26:443-450.

Chang, S., J. Puryear and J. Cairney. 1993. A simple and efficient method for isolating RNA from pine trees. Plant Molecular Biology Reporter. 11:113-116.

Cochard, H., S. Coste, B. Chanson, J.M. Guehl and E. Nicolini. 2005. Hydraulic architecture correlates with bud organogenesis and primary shoot growth in beech (*Fagus sylvatica*). Tree Physiology. 25:1545-1552.

Cook, N.C. and G. Jacobs. 2000. Progression of apple (Malus x domestica Borkh.) bud dormancy in two mild winter climates. Journal of Horticultural Science and Biotechnology. 75:233-236.

Criddle, R.S., A.J. Fontana, D.R. Rank, D. Paige, L.D. Hansen and R.W. Breidenbach. 1991. Simultaneous measurement of metabolic heat rate, CO_2 production and O_2 consumption by microcalorimetry. Analytical Biochemistry. 194 413-417.

Danielson, J.A.H. and U. Johanson. 2008. Unexpected complexity of the aquaporin gene family in the moss *Physcomitrella patens*. BMC Plant Biology. 8

de Faÿ, E., V. Vacher and F. Humbert. 2000. Water-related phenomena in winter buds and twigs of *Picea abies* L. (Karst.) until bud-burst: A biological, histological and NMR study. Annals of Botany. 86:1097-1107.

Domec, J.C., F.G. Scholz, S.J. Bucci, F.C. Meinzer, G. Goldstein and R. Villalobos-Vega. 2006. Diurnal and seasonal variation in root xylem embolism in neotropical savanna woody species: impact on stomatal control of plant water status. Plant Cell and Environment. 29:26-35.

Egea, J. and L. Burgos. 1994. CLIMA and double kerneled fruits in almond. Acta Horticulturae. 373:219-224.

Escobedo, J. and J. Crabbe. 1989. Correlative control of early stages of flower bud initiation in "bourse" shoots of apple (*Malus* x *domestica* Borkh., cv. Golden Delicious). Annales Des Sciences Forestieres. 46:44s-46s.

Fetter, K., V. Van Wilder, M. Moschelion and C. F. 2004. Interaction between plasma membrane aquaporins modulate their water channel activity. Plant Cell. 16:215-228.

Flexas, J., J. Bota, F. Loreto, G. Cornic and T.D. Sharkey. 2004. Diffusive and metabolic limitations to photosynthesis under drought and salinity in C(3) plants. Plant Biology. 6:269-279.

Flexas, J., J. Galmes, M. Ribas-Carbo and H. Medrano. 2005. The effects of drought in plant respiration. *In* Plant Respiration: from Cell to Ecosystem Eds. H. Lambers and M. Ribas-Carbo. Kluwer Academic Publishers, Dordrecht, pp 85–94.

Gardea, A.A., Y.M. Moreno, A.N. Azarenko, P.B. Lombard, L.S. Daley and R.S. Criddle. 1994. Changes in the metabolic properties of grape buds during development. Journal of the American Society for Horticultural Science. 119:756-760.

Gibon, Y., E.T. Pyl, R. Sulpice, J.E. Lunn, M. Höhne, M. Günther and M. Stitt. 2009. Adjustment of growth, starch turnover, protein content and central metabolism to a decrease of the carbon supply when *Arabidopsis* is grown in very short photoperiods. Plant Cell and Environment. 32:859-874.

Grbic, V. and A.B. Bleecker. 2000. Axillary meristem development in *Arabidopsis thaliana*. Plant Journal. 21:215-223.

Hacke, U.G. 2000. Drought experience and cavitation resistance in six shrubs from the Great Basin, Utah. Basic and Applied Ecology. 1:31-41.

Hansen, L.D. and R.S. Criddle. 1990. Determination of phase changes and metabolic rates in plant tissues as a function of temperature by heat conduction DSC. Thermochimica

Acta. 160:173-192.

Hansen, L.D., M.S. Hopkin and R.S. Criddle. 1997. Plant calorimetry: A window to plant physiology and ecology. Thermochimica Acta. 300:183-197.

Hansen, L.D., E.A. Lewis, D.J. Eatough, D.P. Fowler and R.S. Criddle. 1989. Prediction of long-term growth rates of larch clones by calorimetric measurement of metabolic heat rates. Canadian Journal of Forest Research. 19:609-611.

Hansen, L.D., C. Macfarlane, N. McKinnon, B.N. Smith and R.S. Criddle. 2004. Use of calorespirometric ratios, heat per CO_2 and heat per O_2, to quantify metabolic paths and energetics of growing cells. Thermochimica Acta. 422:55-61.

Herter, F.G., N.L. Finardi and J.C. Mauget. 1988. Dormancy development in apple trees cvs Gala, Golden and Fuji in Pelotas, RS. Acta Horticulturae. 232:109-115.

Hinckley, T.M., J.H. Braatne, R. Ceulemans, P. Clum, J. Dunlap, D. Newman, B. Smit, G. Scarascia-Mugnozza and E. van Volkenburgh. 1992. Growth dynamics and canopy structure of fast growing trees. *In* Ecophysiology of short rotation forest crop Eds. P.K. Mitchell, L. Sennerby-Forsee and T.M. Hinckley. Elsevier, London, pp 1–34.

Holbrook, N.M. and M.A. Zwieniecki. 2005. Vascular transport in plants. Physiological Ecology, First Edn. Elsevier/Academic, Oxford. 564 p.

Huang, C.Y., J.S. Boyer and L.N. Vanderhoef. 1975. Acetylene reduction (nitrogen fixation) and metabolic activities of soybean having various leaf and nodule water potentials. Plant Physiology. 56:222-227.

IPCC. 2007. Climate change 2007. The physical science basis: contribution of working group I to the fourth assessment report of the Intergovernmental Panel on Climate Change, 2007. Cambridge University Press, Cambridge, United Kingdom and New York, NY, USA. 996 p.

Kalcsits, L.A., S. Silim and K. Tanino. 2009. Warm temperature accelerates short photoperiod-induced growth cessation and dormancy induction in hybrid poplar (*Populus* x spp.). Trees-Structure and Function. 23:971-979.

Kaldenhoff, R., M. Ribas-Carbo, J. Flexas, C. Lovisolo, M. Heckwolf and N. Uehlein. 2008. Aquaporins and plant water balance. Plant Cell and Environment. 31:658-666.

Kang, J., J. Tang, P. Donnelly and N. Dengler. 2003. Primary vascular pattern and expression of ATHB-8 in shoots of *Arabidopsis*. New Phytologist. 158:443-454.

Kozlowski, T.T. and S.G. Pallardy. 1997. Physiology of woody plants, 2nd Edn. Academic Press, San Diego. 411 p.

Lavender, D.P. 1991. Measuring phenology and dormancy. *In* Techniques and approaches in forest tree ecophysiology Eds. J.P. Lassoie and T.M. Hinckley. CRC Press, Boca Raton, pp 403–422.

Llamas, J., E. Carvajal-Millan, A. Rascon-Chu, J.A. Orozco and A.A. Gardea. 2000. Microcalorimetry: an accurate tool for expedite determinations of plant tissue metabolism. *In* 6th International Symposium on Temperate Fruit Growing in the Tropics and Subtropics Location Eds. S. Perez-Gonzalez, F. Dennis, C. Mondragon and C. Byrne. Acta Horticulturae, International Society Horticultural Science, PO Box 500, 3001 Leuven 1, Belgium Queretaro Mexico, pp 79-85.

Lopez, D., G. Bronner, N. Brunel, D. Auguin, S. Bourgerie, F. Brignolas, S. Carpin, C. Tournaire-Roux, C. Maurel, B. Fumanal, F. Martin, S. Sakr, P. Label, J.-L. Julien, A. Gousset-Dupont and J.-S. Venisse. 2012. Insights into *Populus* XIP aquaporins: evolutionary expansion, protein functionality, and environmental regulation. Journal of Experimental Botany. 63:2217–2230.

Maherali, H., W.T. Pockman and R.B. Jackson. 2004. Adaptive variation in the vulnerability of woody plants to xylem cavitation. Ecology. 85:2184-2199.

Marks, P.L. 1975. On the relation between extension growth and successional status of deciduous trees of the Northeastern United States. Bull Torrey Botan Club. 102:172-177.

Matheson, S., D.J. Ellingson, V.W. McCarlie, B.N. Smith, R.S. Criddle, L. Rodier and L.D. Hansen. 2004. Determination of growth and maintenance coefficients by calorespirometry. Functional Plant Biology. 31:929-939.

Maurel, C., V. Santoni, D.-T. Luu, M.M. Wudick and L. Verdoucq. 2009. The cellular dynamics of plant aquaporin expression and functions. Current Opinion in Plant Biology. 12:690-698.

Maurel, C., L. Verdoucq, D.-T. Luu and V. Santoni. 2008. Plant aquaporins: Membrane channels with multiple integrated functions. *In* Annual Review of Plant Biology, pp 595-624.

McDowell, N.G. 2011. Mechanisms linking drought, hydraulics, carbon metabolism, and vegetation mortality. Plant Physiology. 155:1051-1059.

Monserrat-Marti, G., J.J. Camarero, S. Palacio, C. Pérez-Rontomé, R. Milla, J. Albuixech and M. Maestro. 2009. Summer-drought constrains the phenology and growth of two co-existing Mediterranean oaks with contrasting leaf habit: implications for their

persistence and reproduction. Trees-Structure and Function. 23:787-799.

Ongaro, V., K. Bainbridge, L. Williamson and O. Leyser. 2008. Interactions between axillary branches of *Arabidopsis*. Molecular Plant. 1:388-400.

Pfaffl, M.W. 2001. A new mathematical model for relative quantification in real-time RT-PCR. Nucleic Acids Research. 29:2003-2007.

Rasband, W.S. 1997-2009. ImageJ. U. S. National Institutes of Health, Bethesda, Maryland, USA.

Rinne, P., H. Tuominen and O. Junttila. 1994. Seasonal changes in bud dormancy in relation to bud morphology, water and starch content, and abscisic acid concentration in adult trees of *Betula pubescens*. Tree Physiology. 14:549-561.

Rood, S., S. Patino, K. Coombs and M. Tyree. 2000. Branch sacrifice: cavitation-associated drought adaptation of riparian cottonwoods. Trees - Structure and Function 14:248-257.

Rozen, S. and H. Skaletsky. 2000. Primer3 on the WWW for general users and for biologist programmers. Methods Molecular Biology. 132:365-386.

Scholander, P.F., H.T. Hammel, E.D. Bradstreet and E.A. Hemmongsen. 1965. Sap pressure in vascular plants. Science. 148:339-346.

Schulze, E.D. 1993. Soil water deficits and atmospheric humidity as environmental signals. *In* Water deficits: plant responses from cell to community Eds. J.A.C. Smith and H. Griffiths. BIOS Scientific publishers limited, Oxford, UK, pp 129-145.

Secchi, F. and M.A. Zwieniecki. 2010. Patterns of PIP gene expression in *Populus trichocarpa* during recovery from xylem embolism suggest a major role for the PIP1 aquaporin subfamily as moderators of refilling process. Plant Cell Environment. 33:1285-1297.

Sperry, J.S., F.R. Adler, G.S. Campbell and J.P. Comstock. 1998. Limitation of plant water use by rhizosphere and xylem conductance: results from a model. Plant, Cell and Environment. 21:347-359.

Sperry, J.S., N.Z. Saliendra, W.T. Pockman, H. Cochard and P. Cruiziat. 1996. New evidence for large negative xylem pressures and their measurement by the pressure chamber method. Plant, Cell and Environment. 19:427-436.

Taiz, L. and E. Zeiger. 1998. Plant physiology, 2nd Edn. Sinauer Associates Inc, Massachusetts. 792 p.

Thapa, G., M. Dey, L. Sahoo and S.K. Panda. 2011. An insight into the drought stress induced alterations in plants. Biologia Plantarum. 55:603-613.

Trejo-Martinez, M.A., J.A. Orozco, G. Almaguer-Vargas, E. Carvajal-Millan and A.A. Gardea. 2009. Metabolic activity of low chilling grapevine buds forced to break. Thermochimica Acta. 481:28-31.

Turner, N.C. 1988. Measurement of plant water status by the pressure chamber technique. Irrigation Research. 9:289-308.

Tyree, M.T. and J.S. Sperry. 1988. Do woody plantsoperate near the point of catastrophic xylem dysfunction caused by dynamic water stress? Plant Physiology. 88:574-580.

Tyree, M.T. and M.H. Zimmermann. 2002. Xylem structure and the ascent of sap. Springer series in wood science, 2nd Edn. Springer-Verlag, Berlin. 283 p.

Van der Schoot, C. and P.L.H. Rinne. 1999. Networks for shoot design. Trends in Plant Science. 4:31-37.

Vilagrosa, A., J. Cortina, E. Gil-Pelegrin and J. Bellot. 2003. Suitability of drought-preconditioning techniques in Mediterranean climate. Restoration Ecology. 11:208-216.

Wang, X., Y. Li, W. Ji, X. Bai, L.J. Chen and Y.M. Zhu. 2011. A novel glycine soja tonoplast intrinsic protein gene responds to abiotic stress and depresses salt and dehydration tolerance in transgenic *Arabidopsis thaliana*. Journal of Plant Physiology. 168:1241-1248.

Wardlaw, I.F. 1990. The control of carbon partitioning in plants. New Phytologist. 116:341-381.

Ye, Z.H. 2002. Vascular tissue differentiation and pattern formation in plants. Annual Review of Plant Biology. 53:183-202.

Supplemental data:
Table 1 List of primers used for PCR experiments

	PopDraft	Forward primer	Reverse primer
PtPIP1;1	POPTR_0008s06580	CAAGAAGTGATGAYTGTGATGC	ACGTCACTGTTATAGCACGC
PtPIP1;2	POPTR_0003s12870	TTCAAGAGCAGAGCTTAATTTC	TTCAAAAAGCTAGATAATTTACAC
PtPIP1;3	POPTR_0010s19930	AAGAAGTGATTATTATGATTATGG	GATTTGAAGAAACACGTATTGCTA
PtPIP1;4	POPTR_0006s09920	GACAGAAAACAAGGTTCTTTAGA	GAGTAATTTACATAAATGGAACC
PtPIP1;5	POPTR_0016s12070	TCGTTCCCAATCRATGGATGTT	AAGAATTCACTGAGAGGGAATA
PtPIP2;1	POPTR_0009s13890	TGCTAACATGGTGGCTCCC	GATCATCCCAGGCTTTCTTATC
PtPIP2;2	POPTR_0004s18240	TGGTACACTTGGCCACAATC	GCTAATGCTCCCACAAATGG
PtPIP2;3	POPTR_0016s09090	ATTCAGTTATGGAACGTACGC	AGCTCACAACCATGACATAAC
PtPIP2;4	POPTR_0010s22950	CCAACGGTTTTAAATCTCGGTTC	ACCGAAAGGGATAATAAAGGG
PtPIP2;5	POPTR_0006s12980	TGTGTACATTATGGTGTCGTG	CAAAGAAGCAGCACTACCTGAGAC
PtPIP2;6	POPTR_0008s03950	ATCCCAATCACAGGAACTGG	CTATGGCTGCACCAATGAAG
PtPIP2;7	POPTR_0009s01940	ATGACCATTGGCTCTTCTGG	GGCTTTAAGCATTGCTCCTG
PtPIP2;8	POPTR_0005s11110	GCAATCCTACTAGCTAAGGC	ACCCACATATCAAGTTGAGAC
PtPIP2;9	POPTR_0005s11100	ACTGGAACTGGCATCAATCC	CCAACCCAGAAAATCCACAG
PtPIP2;10	POPTR_0006s13000	CACAGTCGTGGTCAAGATGTC	ACTAGTTGATTATGAGATAGGGAG
PtXIP2;1	POPTR_0009s13110	ATGATTCCACGGGAACACCT	CATCCCCCTTAACTACATAAC
PtXIP3;1	POPTR_0009s13080	AACTATAATTCGTTATTCTACT	AACTATAATTCGTTATTCTACT
PtXIP3;2	POPTR_0009s13070	CACAATAGAATAGACTAAAACTAT	AGTTAAGGACGACGACTCTACATC
PtTIP1;1	POPTR_0001s24200	TGCTGCCATTGTCTACGAGGTCAT	CACCACCACAGACGTGTCTTC
PtTIP1;2	POPTR_0009s03230	TGCTGCCATTGTCTACGAGGTCTG	AACAACACCAACATCATCCAAACC
PtTIP1;3	POPTR_0010s21700	GATTGGAAACTCCAGCTTTTGGAT	AATTTCCCTTCTTTGGATCCACT
PtTIP1;4	POPTR_0008s05050	ATTGGAAACACCAGCTTTTGGGC	AATTTCCCTTCTTCGGATCCACC
PtTIP1;5	POPTR_0016s10780	ATTGTGGGTGCTAACATTCTAGTC	CCACCAACCAGTGGTCCGGC
PtTIP1;6	POPTR_0006s12350	CAACCACTGGGTCTACTGGGCA	GAAAGAAAAAGCCGCGGCACTG
PtTIP1;7	POPTR_0009s01070	CGAGTTAATCTTCATCAGCCACAC	GGAAAAAATTCAACGTAGTCTTAAAC
PtTIP1;8	POPTR_0004s22600	AGCTTATCTTCATGAGCCACAGTAC	ACGAATCCAACGTAGTCCAAACG
PtTIP2;1	POPTR_0001s18730	TCTACTGGGCTGGGCCTCTTG	CAAGTGAAGTTATTAGAAGTCTCC
PtTIP2;2	POPTR_0003s04930	TCTACTGGGTTGGGCCTCTTA	ATTTTAGACTGACTTAGAACTCATA
PtTIP2;3	POPTR_0003s07550	TTGCTTCAGGGATGAGTGCTATC	TTCAGAAACTGGGGCAGGCGC
PtTIP2;4	POPTR_0001s15700	TCGCTTCAGGGATGAGTGCTGTT	TTCGGAAACTGGGGCAGCGGT
PtTIP3;1	POPTR_0018s14910	GAGCATTTGGGCCTGCTCTAG	GGTGAGCTACTGGCTCTGCTG
PtTIP3;2	POPTR_0017s03540	GAGCTTTTGGGCCTGCTTTAA	GGCGAGGTACTGGCTCTGTGG
PtTIP4;1	POPTR_0006s25620	ATGGGCTAGGTCCAATGCTGAC	GAAGAGGACGATGAGATCTTGTG

Pt18SrRNA	AY652861.1	GCGATTTGTCTGGTTAATTCCG	GGCCAAGGCTATAGACTCG
PtEF1α	EF146300.1	GTCTGTTGAGATGCACCACG	CAATGTGACAGGTGTGGCAG
PtSand	POPTR_0009s01980	CATGATAAAGGCAACGGGGCG	CTGTGTTACAAGATATTTTTGGG

Résumé

Les modèles actuels de changements climatiques prédisent une réduction globale des précipitations, limitant ainsi la disponibilité en eau des plantes et induisant une augmentation de la fréquence des stress hydriques. Un stress hydrique modéré peut conduire à la fermeture des stomates ce qui diminue l'activité photosynthétique des plantes, et dans les cas les plus extrêmes, induit l'embolie du xylème causée par la rupture de la colonne d'eau. Afin de limiter ces effets délétères, les plantes ajustent en permanence leurs résistances hydrauliques. Les feuilles sont considérées comme la principale résistance aux flux d'eau. La compréhension des mécanismes de régulation de la résistance hydraulique foliaire est donc un enjeu fondamental. Parmi les facteurs influençant potentiellement la résistance hydraulique foliaire, les aquaporines (AQPs) pourraient jouer un rôle prépondérant. Les membres de la famille des PIP (Plasma membrane Intrinsic Protein) sont des AQPs agissant comme des pores permettant un passage sélectif de l'eau au travers du plasmalemme. Ce travail visait à caractériser la conductance hydraulique foliaire (K_{leaf} l'inverse de la résistance) et à étudier la contribution potentielle des PIP dans cinq espèces tempérées ainsi que chez l'arbre modèle: le peuplier. Les espèces pionnières ont des valeurs de K_{leaf} élevées, mais l'augmentation de K_{leaf} en réponse à la lumière est beaucoup plus faible que chez les espèces non-pionnières. Chez le Noyer (*Juglans regia*), la lumière bleue est responsable de la plupart de l'augmentation de K_{leaf} et de la modulation transcriptionnelle des PIP. En situation de disponibilité en eau et de lumière non limitante, la K_{leaf} du peuplier augmente au cours de la journée pour atteindre son maximum à midi. Cette augmentation de K_{leaf} se produit simultanément avec la transcription et l'accumulation de protéines PIP en réponse à l'éclairement. Cependant, l'expression des gènes PIP est en partie sous influence d'une régulation endogène circadienne. L'influence des AQPs dans la valeur élevée de K_{leaf} est démontrée par son inhibition en présence d'$HgCl_2$.

Abstract

Climate changes models predict a global reduction of rainfalls hence limiting plants water availability and increase water stress occurrence. A moderate water stress can lead to stomata closure thereby decreasing the plants photosynthetic activity and in extreme cases, xylem embolism due to the water column breakage. In order to limit such detrimental effects, plants permanently adjust their hydraulic resistances. Leaves are considered as the main bottleneck in plants water fluxes, thus understanding leaf resistance to water flux regulation is fundamental. Within known factors that can potentially influence leaf hydraulic resistance, the aquaporins (AQPs) might have a central role. Plasma membrane Intrinsic Protein (PIP) family members are AQPs acting as pores that selectively allow water to flow through cell membranes. This work aimed at characterizing leaf hydraulic conductance (K_{leaf} the inverse of resistance) and investigate the potential contribution of PIPs in five temperate tree species and in tree model: Poplar. Pioneer species have high K_{leaf} values, but the K_{leaf} increase in response to light is much lower than for non-pioneer ones. In walnut (*Juglans regia*) blue light is responsible of most of the K_{leaf} increase and PIP transcript modulation. Under non-limiting light and water availability, poplar leaf hydraulic conductance increases diurnally with a maximum reached at midday. This increase of K_{leaf} occurs in parallel with PIP transcript and protein accumulation in response to high irradiance. PIP gene expression is also under endogenous circadian regulation to some extent. The involvement of AQPs is demonstrated by the reduction of K_{leaf} using $HgCl_2$.